# THE UNIVERSITY *of* EDINBURGH

| Title | ErbB receptor regulation of growth in ovarian cancer |
|---|---|
| Author | Gilmour, Lynn M.R. |
| Qualification | PhD |
| Year | 2002 |

Thesis scanned from best copy available: may contain faint or blurred text, and/or cropped or missing pages.

**Digitisation Notes:**

Page 34 missing in original document

# ErbB Receptor Regulation of Growth in Ovarian Cancer

Lynn M. R. Gilmour

PhD

The University of Edinburgh

2000-2001

## Declaration

In accordance with the regulations of the University of Edinburgh, I declare that the material described in this theis is composed by myself entirely, except where acknowledgement has been made in the text. This work has not been submitted for any other degree or qualification.

Lynn Gilmour

## Acknowledgements

## Abstract

The erbB receptor family consists of the EGF receptor (erbB1), erbB2, erbB3 and erbB4 . In conjunction with the EGF and neuregulin (NRG) family of growth factors, this ligand-receptor signalling network controls a variety of cellular processes including proliferation and differentiation. Deregulation of this network is a significant factor in the growth and progression of many human cancers including ovarian cancer. The EGF receptor and erbB2 have previously been associated with a poor prognosis in ovarian cancer, however little is known of the roles of the erbB3 and erbB4 receptors. These observations have generated much interest in acquiring information on the mechanisms underlying this network and how disruption of this presents itself as the biological effects seen in malignancy.

This project aimed to assess the relative roles of the different receptors in the growth regulation of ovarian cancer. The associations between levels of erbB receptor expression and type and magnitude of growth response to the activating ligands were investigated. Several of the intracellular signalling pathways activated by these receptors were then studied. Finally the roles of erbB3 and erbB4 along with their activating ligand NRG were assessed in more detail as their functionality in this disease has not previously been explored.

Expression levels of the erbB receptors were measured in a panel of 16 ovarian cancer cell lines using Western blot analysis. While EGF receptor, erbB2 and erbB3 were found in over 90% of cell lines, erbB4 receptor protein was only detected in half. Upon treatment with the ligands, 5/14 cell lines were growth stimulated by NRG1$\alpha$, 7 by NRG1$\beta$ and 8 by TGF$\alpha$. In addition, one cell line was growth inhibited by treatment with either NRG1$\beta$ or TGF$\alpha$. A trend was observed in the magnitude of growth response to ligand and was of the order NRG1$\beta$ > TGF$\alpha$ > NRG1$\alpha$. Furthermore, a significant association between erbB2 receptor expression and magnitude of growth response to the NRG's was detected within the panel of cell lines and is consistent with erbB2 being the preferred hetero-dimerization partner. Expression of NRG mRNA was detected in the majority of cell lines tested and also in the majority of human ovarian carcinomas within a panel consisting of 14 serous, 5 endometrioid and 5 clear cell adenocarcinomas. This would suggest that this growth factor could potentially act in an autocrine manner to stimulate cell growth.

Multiple erbB4 isoforms that differ in sequence in the juxtamembrane (JM) and cytoplasmic (CT) domains have previously been identified in other tissue types and demonstrated to possess differing functionalities. Investigation of the erbB4 receptor isoforms in a panel of 10 cell lines detected expression of the JM-a isoform (which is susceptible to proteolytic cleavage) in half, whilst expression of isoforms resistant to this type of cleavage was not detected. Expression of both the erbB4 receptor CT-a isoform (that is able to couple to PI3K and may promote cell survival) and the CT-b isoform (that is unable to bind PI3K) were detected in the same 5 cell lines. Similarly, expression of JM-a was detected in 18/24 human ovarian tumours whilst both CT-a and CT-b expression were detected in 22/24.

A small panel of the cell lines were further investigated for erbB receptor phosphorylation and activation of the molecules Shc and Erk1/Erk2 to determine if cell growth in response to ligand was reflected in intracellular signalling through the Erk kinase cascade. Trends were observed between the magnitude of growth stimulation and the extent and duration of intracellular signalling.

Anti-erbB3 and anti-erbB4 receptor antibodies were then used to investigate the roles of these receptors in the regulation of cell growth and suggested that the erbB3 receptor was involved in promoting proliferation whilst the erbB4 receptor produced negative growth regulation in cell lines growth stimulated by NRG.

These studies have demonstrated that ovarian cancer cell lines express multiple erbB receptors and reflect the expression patterns found in primary ovarian cancers. NRG, acting via erbB3, appears to be as potent a mitogen as TGFα and could act in an autocrine manner in ovarian cancer cells. Heterodimerization via erbB2 is associated with the magnitude of growth response and intracellular signalling involves the Shc and Erk pathways. ErbB4 appears to play a growth inhibitory role in these cells.

## Abbreviations

| | |
|---|---|
| aa | amino acid |
| BSA | Bovine serum albumin |
| °C | degrees celsius |
| $CO_2$ | Carbon dioxide |
| CT | Cytoplasmic isoform (ErbB4) |
| cDNA | complementary deoxyribonucleic acid |
| DNA | deoxyribonucleic acid |
| EGF | epidermal growth factor |
| FCS | Fetal calf serum |
| $H_2O$ | Water |
| JM | Juxtamembrane isoform (ErbB4) |
| kb | kilobases |
| kDa | kilodaltons |
| μg | micrograms |
| μl | microlitres |
| M | molar concentration |
| mRNA | messenger RNA |
| NRG | Neuregulin (or heregulin) |
| PBS | phosphate buffered saline |
| PCR | polymerase chain reaction |
| TGFα | transforming growth factor alpha |

# Contents

**Chapter 7 General discussion and suggestion for future studies**

## List of Tables

## List of Figures

## Chapter 1 Introduction

1.1 Ovarian Cancer

1.1.1 Incidence and epidemiology

Ovarian cancer is the most common cause of cancer death from gynaecological malignancy with approximately 5000 cases annually in the U.K. (reviewed in Gabra H, 1997). It is the fifth most common cause of cancer death in women after breast, lung, colon and stomach cancer and is responsible for some 3500 deaths per annum. The high mortality rate has been attributed to the late presentation of the disease, which is often at an advanced stage. This translates into one woman in 70 developing ovarian cancer and 1 in 100 will die from this disease. The incidence of ovarian cancer increases with age; it is less common in those under 45 (less than 15 cases per 100,000 per annum) and is most common in women in their $7^{th}$ or $8^{th}$ decades (55 per 100,000 per annum). A slight improvement in the overall five-year survival rate has been observed over the past two decades which has been attributed to improved treatment regimes and multimodality therapies. However, the overall five-year survival still remains poor at approximately 30%, largely due to the late presentation of the disease.

1.1.2 Etiology

Approximately 95% of all patients with ovarian cancer have no family history of the disease which suggests that almost all cases are attributed to spontaneous or environmentally induced carcinogenesis. Published epidemiological studies have been conflicting and therefore this area remains opaque. Potential candidate carcinogens such as inhaled tobacco, talc, asbestos and alcohol have been examined and do not seem to confer excess risk (Whittemore AS, 1988), while dietary factors such as coffee ingestion may be associated with a slightly increased risk of ovarian cancer (Byers T, 1983). More importantly, the consumption of animal fat has been associated with an increased risk (Cramer DW, 1984); a case / control study suggested that every 10g of ingested saturated animal fat per day increased the risk of ovarian cancer by 20%, whilst the same ingested weight of vegetable fibre reduced the risk by 37% (Risch HA, 1994). As this study was virtually unique and has not been confirmed these results should be treated cautiously. However, since the role of estrogens and other steroid hormones, that are often present in saturated animal fat, also play key roles in the ovarian cycle, this may suggest some relevance. The etiology of ovarian cancer

1

may be considered as endocrine related; the ovary is the main site of synthesis of estrogen and progesterone and is also a target for these hormones (through receptors that act as nuclear transcription factors) that may influence cell proliferation or differentiation.
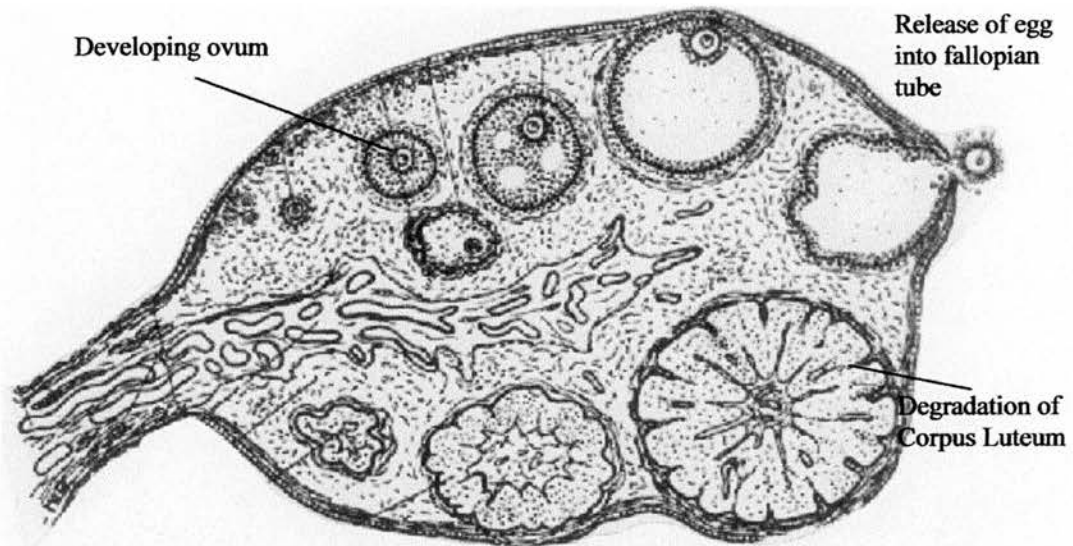


Fig 1.1 Schematic diagram of the ovary depicting the development and release of the ovum, followed by the breakdown of the corpus luteum. These processes take place through each ovarian cycle, causing torsional stress on the epithelial surface of the ovary. The proliferative repair process of the ovarian epithelial surface is thought to accumulate genetic damage and results in over 90% of ovarian cancers being of epithelial origin.

In 1971, Fathalla proposed the hypothesis of "incessant ovulation" in which 'incessant ovulation results in repeated proliferative repair cycles of the ovarian surface epithelium, where the epithelial cells acquire genetic damage during proliferative repair and the cumulative damage due to repeated ovulatory cycles predisposes to the development of ovarian cancer' (Fig 1.1) (Fathalla, 1971). This would suggest that any factor that reduces the number of ovulatory cycles would reduced the risk of ovarian cancer development. Consistent with this, nulliparity and a low mean number of pregnancies have been associated with an increased risk, whilst childbirth, increased total pregnancy and lactation time, confer a protective effect and are reflected in an estimated 30-60% reduction in risk for women with 2 or more pregnancies (Cramer DW, 1983) (Weiss NS, 1981). Similarly, the use of oral contraceptives also decreases the risk of ovarian cancer by 30-60% (Weiss NS, 1981) (Cramer DW, 1982). It has been reported that the use of fertility drugs may present an increased risk of developing ovarian cancer by 2½-3 fold (Rossing MA, 1994),

2

Chapter 1 Introduction

although these findings cannot be regarded as conclusive since nulliparity in itself confers an intrinsic increased risk.

### 1.1.3 Inherited Predisposition

Clearly defined predisposition to ovarian cancer accounts for only about 5% of patients with ovarian cancer. Women with one affected first degree relative run a 5% lifetime ovarian cancer risk (1 in 20), whilst those with two or more first degree relatives affected have a 7% risk (1 in 15) (Gabra H, 1997). Those with autosomal dominant syndromes run a much higher risk (40-50%), but these individuals constitute a mere 3% of women with two affected first degree relatives.

There are three hereditary syndromes; hereditary site-specific ovarian cancer; hereditary breast / ovarian cancer and Lynch syndrome II. Patients with these tend to be younger, usually 10 years below the median and present with bilateral and multifocal tumours. Hereditary site-specific ovarian cancer is rare and usually linked to mutation or disruption of the BRCA1 tumour suppressor gene that encodes a transcription factor (Miki Y, 1994). Similarly, the majority of hereditary breast / ovarian cancers is linked to mutations of the BRCA1 tumour suppressor gene. Although a second tumour suppressor gene has been associated with this disease, BRCA2, this does not account for all non-BRCA1 linked cases (Wooster R, 1994). Lynch syndrome II is an integrated syndrome that incorporates hereditary non-polyposis colorectal cancer with gastrointestinal, gynaecological and urological or breast cancer (Lynch HT, 1985). Lynch syndrome II is linked to disruptions in a family of mismatch repair genes; hMSH2, hMLH1, hPMS1 and hPMS2.

### 1.1.4 Tumour Histology, Grade and Stage

Neoplasms of the ovary may be categorized as benign, borderline or tumours of low malignant potential in addition to being malignant and exhibit a range of histological subtypes including serous, endometrioid and mucinous differentiation. Of these approximately 42% EOC's are serous, 15% mucinous, 15% endometrioid and 17% undifferentiated (reviewed in Neijt, 1990). The classification adopted by the World Health Organization (WHO) is summarized in Table 1.1.

3

Chapter 1 Introduction

Table 1.1 Summary of the World Health Organization classification of malignant ovarian tumours

I  Common epithelial tumours

|   |   |   |   |
|---|---|---|---|
| A. | Serous | E. | Brenner |
| B. | Mucinous | F. | Mixed Epithelial |
| C. | Endometrioid | G. | Undifferentiated |
| D. | Clear cell | H. | Unclassified |

II  Sex cord stromal tumours

III  Lipoid cell tumours

IV  Germ cell tumours

Tumour cell type has little influence on prognosis and is independent of the extent of the disease and histological grade. Patients having tumours of mucinous or endometrioid histology may have a slightly better prognosis than those with serous or undifferentiated cancer and may be due to the disease being less advanced at presentation. The degree of anaplasia of histological grade is of more important prognostic significance where the grading is based on the percentage of undifferentiated cells: 0-25% is defined as grade 1, 25-50% as grade 2, 50-75% as grade 3 and 75-100% as grade 4 (Neijt, 1990). Those with low grade tumours (1&2) have a better prognosis in terms of response to chemotherapy and overall 5 year survival in comparison to those with high grade tumours (3&4). For example, among 296 patients treated in the Mayo clinic, those with grade 1 tumours had an overall 5 year survival rate of 22%, compared with 3% for those with grade 3 or 4 tumours (Neijt, 1990). It seems that grade is particularly important for serous carcinomas and less so for other cell types. Anatomical spread of the cancer is also of prognostic importance and is common due to the continuity of the ovary into the peritoneal cavity. The extent of the disease upon clinical examination and surgical evaluation determines the stage of the disease and the most appropriate mode of action. The most widely used classification of staging is that described by the International Federation of Gynaecology and obstetrics (FIGO) shown in Table 1.2 below (Committee, 1979).

4

Table    1.2 FIGO stages for primary carcinoma of the ovary

Stage    Definition

| Stage | Definition |
| --- | --- |
| I | Growth limited to the ovaries |
| IA | Growth limited to one ovary; no ascites; no tumour on external surface; capsule |
| IB | Growth limited to both ovaries; no ascites; no tumour on external surface; capsule intact |
| IC* | Tumour either Stage IA or IB, but with tumour on surface of one or both ovaries; or with capsule ruptured; or with ascites present containing malignant cells or with positive peritoneal washings |
| II | Growth involving one or both ovaries with pelvic extension |
| IIA | Extension and/or metastases to uterus and/or tubes |
| IIB | Extension to other pelvic tissues |
| IIC* | Tumour either stage IIA or IIB but with tumour on surface of one or both ovaries; or with capsule ruptured; or with ascites present containing malignant cells or with positive peritoneal washings |
| III | Tumour involving one or both ovaries with peritoneal implants outside pelvis and/or positive retroperitoneal or inguinal nodes; superficial liver metastases; tumour is limited to the true pelvis but with histologically proven malignant extension to small bowel or omentum. |
| IIIA | Tumour grossly limited to the true pelvis with negative nodes but with histologically confirmed microscopic seeding of the abdominal peritoneal surfaces |
| IIIB | Tumour involving one or both ovaries with histologically confirmed implants of abdominal peritoneal surfaces none exceeding 2cm in diameter; nodes are negative |
| IIIC | Abdominal implants greater than 2cm in diameter and/or positive retroperitoneal or inguinal nodes |
| IV | Growth involving one or both ovaries with distant metastases. If pleural effusion present, there must be positive cytology to assign a case to Stage IV; parenchymal liver metastases |

* To assess the impact on prognosis of the different criteria for assigning cases to Stage IC or IIC it is of value to know if the source of malignant cells is from (i) peritoneal washings (ii) ascites and whether rupture of the capsule was spontaneous or caused by surgeon.

Predictably increased stage relates to a poor prognosis and in a cohort of approximately 5000 patients the 5 year survival rates according to stage were as follows: 72% in stage IA; 62.5% in IB; 57.4% in IC; 52.2% in IIA; 37.5% in IIB and IIC; 10.8% in III and 4.6% in stage IV (Committee, 1979). Staging and treatment options are assessed at initial laparotomy. In general, removal of the tumour, total hysterectomy, a bilateral salpingo-oophorectomy and omentectomy are carried out.

5

Chapter 1 Introduction

Cytological examination of ascitic fluid and peritoneal washings in conjunction with histological examination of the omentum provides more accurate staging of tumour spread. Cytoreductive surgery or debulking surgery of residual tumour metastases to under 2cm diameter is important to achieve a better response and increased survival with subsequent chemo- or radio-therapy. For example, patients with tumour masses <2cm postoperatively have a median survival of 45 months which is reduced to 16 months for those with tumour masses >2cm. Similarly, the number of residual masses may also be prognostically important.

1.1.5 CA-125 tumour marker

At present CA-125 is the most widely utilized marker for monitoring ovarian cancer. CA-125 is a high molecular weight mucin glycoprotein expressed on the surface of mesothelium lining the pleura, pericardium, peritoneal cavity and produced by cells of the fallopian tubes, endometrium, and endocervix (Kabawat SE, 1983). CA-125 may be expressed on the surface of both benign and malignant ovarian tumours where cell death or turnover increases the release of CA-125 into the bloodstream (Niloff JM, 1984a). The level of circulating CA-125 is increased in 80% of ovarian cancers (Bast R, 1983). Although CA-125 is not specific for ovarian cancer, in that it may be elevated in other cancers including those of the breast, colon, pancreas, lung, lymphoma and also during inflammatory processes, it is currently used to monitor response to therapy and detecting relapse for ovarian cancer (Niloff JM, 1984b). Fall in CA-125 levels with treatment correlates well with response to therapy, it provides a sensitive index for sub clinical relapse preceding disease recurrence by 3 months on average (Niloff JM, 1986).

1.1.6 Treatment

Primary treatment for the majority of ovarian cancers involves surgical removal (as above) followed by adjuvant therapy to eradicate micrometastatic disease. Only in early stage disease (stage Ia/b) with good prognostic indicators (well differentiated histology) would surgery alone be considered adequate without the need for further adjuvant therapy. Adjuvant therapy is most frequently chemotherapy. Previously, standard chemotherapy consisted of platinum containing regimens with an alkylating agent and is administered as six cycles, three weekly.

6

Platinum analogues such as cisplatinum and carboplatin function as cytotoxic agents by binding to the amino or hydroxyl groups of nucleoside bases and therefore cause the formation of DNA intrastrand and interstrand crosslinks in the cell nucleus. This ultimately interferes with cellular replication/repair mechanisms. The choice of platinum agent has been studied; overall findings show that carboplatin appears to be tolerated better with a reduction in gastrointestinal, neurological and renal toxicity whilst cisplatinum exhibits reduced myelosupression (Ozols, 2000) (Thigpen, 2000). Comparison of the two compounds has shown similar median survival times whilst there is some evidence suggesting cisplatin based regimens are more effective than those of carboplatin (Thigpen, 2000). On the whole, significant survival advantages have been detected for platinum based regimens over combinations that did not contain platinum and, for platinum combinations over single agent platinum (Neijt, 1990) (Langdon SP, 1997).

## 1.7 Taxol

Taxol (Paclitaxel) a natural diterpenoid was discovered in 1971 when it was isolated from the bark of the western yew tree. Taxol was found to an active therapeutic agent induces mitotic arrest by causing tubulin polymerization and preventing depolymerization of microtubules. An American randomized study has shown that complete and partial response rates were significantly increased from 2 to 3 years for patients with suboptimally debulked ovarian cancer that received first line treatment with taxol / cisplatin compared to those who received cisplatin / cyclophosphamide (McGuire WP, 1995). Platinum / taxol based regimens are the 'gold standard' in the USA and are now the standard treatment regime in the U.K. Phase II clinical studies of taxol and taxotere previously demonstrated a 30-35% response rate in patients that have previously been treated with other cytotoxic agents (Einzig AI, 1992) (Kavanagh JJ, 1993) (Thigpen JT, 1994). European studies are currently comparing taxol based regimens used in primary treatment for ovarian cancer.

7

Chapter 1 Introduction

1.1.8 Drug Resistance

It has generally been accepted that chemotherapy fails to eradicate cancer due to intrinsic and acquired drug resistance. Cancer cells are those that have acquired genetic damage that results in their escape from normal growth regulation. Treatment with drugs that act to control cell growth evokes mechanisms in cancer cells to escape this regulation and is collectively termed as drug resistance. Such mechanisms include limiting drug accumulation by influx pump inhibition or efflux pump augmentation (expression of the multi drug resistant p-glycoprotein); inactivation of drug ie by antioxidants such as glutathione; de-regulation of tumour suppressor genes such as p53 allowing cells to be tolerant to cytotoxic agents (Fracasso., 2001) (Tai, 2000) (Yazlovitskaya EM, 2001) (Mayr D, 2000). Similarly, disruption in the expression or activity of molecules involved in the induction of apoptosis and those involved in DNA repair mechanisms may contribute to resistance to cytotoxic drugs (Branch P, 2000) (Van Hattum AH, 2000).

8

## 1.21 NRG

The NRG gene is the most extensively spliced growth factor gene to date and is localized to chromosome 8p21-p12 in the human genome. NRG is a member of the epidermal growth factor (EGF) family of ligands, which possess a conserved EGF-like domain that is comprised of 6 cysteine and 2 glycine residues that form 3 disulphide bridges in a 3 loop structure. NRG ligands are mostly produced as transmembrane 'proforms' that undergo proteolytic cleavage to release soluble growth factor, although the transmembrane bound forms have also been shown to have activity with adjacent cells. NRG was first isolated as a prospective ligand for erbB2/HER2 or neu (neu being the same proto-oncogene receptor identified in rat neuroblastomas) and was called NDF (Neu differentiation factor) for its ability to promote differentiation in a breast cancer cell line (Mudge, 1993) (Wen D, 1992). Isolation of the human form revealed that it caused phosphorylation of erbB2/HER2 and induced cell proliferation in a breast cancer cell line and was named heregulin (regulator of HER2). The ligand was subsequently shown to bind to the erbB3 and erbB4 receptors, causing phosphorylation of erbB2 solely through hetero-dimerization (Carraway KL, 1994) (Plowman GD, 1993). Around the same period, the homologous ligands ARIA (Acetyl choline receptor inducing activity) and GGFII (Glial growth factor II) were identified in tissues of neural descent and gave rise to the present family name of 'Neuregulins'. The NRG family of ligands are similar to that of the EGF family in that they possess the characteristic 'EGF motif', although they are dissimilar in that they also contain an immunoglobulin-like domain (Ig-like domain) which also classifies them as members of the immunoglobulin superfamily (Fig 1.3).

13

The erbB receptor network or module, is comprised of the binding ligands, erbB receptors and the intracellular signalling cascades they stimulate upon ligand activation. The following sections will discuss the ligands neuregulin (NRG) and TGFα, the erbB receptor family and intracellular signalling within the mitogen activated protein kinase (MAPK) cascade, in more detail.

12

Whilst TGFα is associated with cell mitogenesis and binds to the EGF receptor, it is primarily associated with causing EGF receptor-erbB2 hetero-dimerization, although EGF receptor homodimers, EGF receptor-erbB3 and EGF receptor-erbB4 hetero-dimerizations have also been reported (Alroy I, 1997). In contrast, NRG1β may bind to either erbB3 or erbB4 and has been shown to induce stabilization and phosphorylation of erbB3-erbB2 and erbB4-erbB2 heterodimers predominantly. However hetero-dimerization between erbB3-EGF receptor and erbB4-EGF receptor has been frequently observed, yet erbB3-erbB4 and erbB4 homodimers are less common, but have been identified in some cellular systems (Alroy I, 1997) (Gamet DC, 1997). NRG induced interactions are under current investigation and while there is some speculation on the overall biological response (which is ultimately determined by the cellular system or cell line model used), there is a general consensus that NRG induced erbB3-erbB2 dimerization may be the most potent mitogenic signalling combination (Slikowski MX, 1994) (Fitzpatrick VD, 1998), whilst other receptor dimerisations have been shown to influence cell survival, proliferation or produce a nil response (Riese DJ, 1998) (Alroy I, 1997).
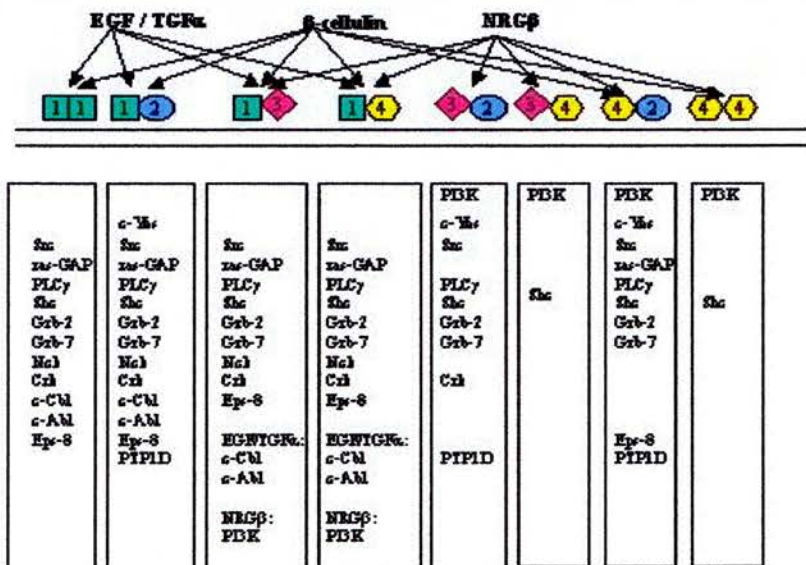


Fig 1.2 Diagrammatic representation of ligand-receptor interactions and the recruitment of intracellular signalling molecules that are associated with specific receptor dimerisation. This diagram was reproduced from Alroy I, 1997.

11

Chapter 1 Introduction

serve as docking sites for specific SH2 containing proteins. Therefore each receptor dimer funnels signalling through a unique set of pathways (Burden S, 1997). To add to this complexity, erbB2 is the preferred heterodimerization partner for all of the other erbB receptors by enhancing their affinity for ligand and therefore introduces a hierarchy of receptor dimerizations within the network (Graus-Porta D, 1997) (Graus-Porta et al., 1995). Although erbB2 does not bind any of the above mentioned ligands, through heterodimerization, it plays the role of a 'master co-ordinator or regulator' by increasing coupling to the mitogen-activated protein kinase cascade and amplifying signal by delaying ligand dissociation in conjunction with impeding the rate of receptor down-regulation (Pinkas-Kramarski R, 1997a) (Klapper LN, 2000a) (Carraway KL, 2001) (Sweeney C, 2000). In addition, erbB receptor tyrosine kinase domains are highly conserved except in the case of the erbB3 receptor, where differences in residues within this domain render the receptor almost devoid of catalytic activity. Although it may bind ATP, it is dependent on heterodimerization with other erbB receptors for efficient signal transduction (Alroy I, 1997) (Beerli et al., 1995) (Fitzpatrick VD, 1998) (Slikowski MX, 1994).

The following examples are known interactions and aim to simplify receptor dimerization and hierarchy; for instance EGF binds to the EGF receptor and is principally associated with the formation of EGF receptor homodimers or EGF receptor-erbB2 heterodimers, whilst EGF receptor heterodimerization with erbB3 and erbB4 are less common or have been detected in over-expression systems (Riese DJ, 1998). The biological response elicited by these specific interactions may reflect the efficiency of receptor dimer coupling to intracellular signalling cascades and have been most easily identified in recombinant expression systems; EGF receptor homodimers and EGF receptor–erbB3 heterodimers confer increased cell survival, whilst EGF receptor heterodimerization with either erbB2 or erbB4 results in cell proliferation (Riese DJ, 1998).

Chapter 1 Introduction

1.2 Introduction to the ErbB receptor family network

The erbB receptor family of type I receptor tyrosine kinases consists of the EGF receptor (erbB1 or HER1), erbB2 (HER2 or Neu), erbB3 (HER3) and erbB4 (HER4) receptors. For clarity, the term Neu for erbB2 is used when referring to the rat gene or cDNA, whereas the human and mouse homologs are referred to as erbB2. Expression of the EGF receptor and similarly erbB2 has been associated with poor prognosis in many diseases including ovarian carcinoma (Bartlett et al., 1996) (Slamon DJ, 1989). In contrast, relatively little is known of the role or function of the erbB3 and erbB4 receptors, although multiple erbB receptor expression is significantly higher in malignant tumours than benign or borderline tumours (Simpson et al., 1995a). The erbB receptor family is now regarded as a ligand-receptor network (Fig 1.2) within which a family of 'epidermal growth factor-like' ligands that possess a characteristic 'EGF-like' domain (a sequence that includes 6 conserved cysteine residues forming 3 peptide loops (Prigent SA, 1992) (Groenen LC, 1994)) bind to one or more erbB receptors to initiate intracellular signalling (Alroy I, 1997) (Pinkas-Kramarski R, 1998). Ligand binding to a specific erbB transmembrane receptor is accompanied by receptor dimerization, rapid phosphorylation in the receptor carboxyl termini and recruitment of cytoplasmic signalling molecules that bind to phosphorylated receptor tyrosine residues and initiate a cascade of signalling events (Pinkas-Kramarski R, 1996). Growth factors that bind to the erbB family of receptors can be divided into 4 subgroups depending on their receptor binding specificities. Ligands that bind (i) EGF receptor, include EGF, transforming growth factor alpha (TGFα) and amphiregulin; (ii) EGF receptor and erbB4, comprise betacellulin (BTC), heparin-binding EGF-like growth factor and epiregulin; (iii) erbB4 alone, involves neuregulin3 (NRG3); (iv) erbB3 and erbB4, consists of neuregulin (NRG) family members including the heregulins/neu differentiation factors such as NRG1α and NRG1β, sensory and motor neurone-derived factor (SMDF) and NRG2 (Sundaresan et al., 1998). The receptor dimerizations that are dependent on binding ligand (Tzahar E, 1996), generate a diverse plethora of biological messages and are distinguished at 3 levels; firstly, a range of ligands bind in a receptor specific manner, secondly each ligand has a different preference for stabilizing distinct receptor dimers, and thirdly, each receptor dimer has a different set of    tyrosine autophosphorylation sites that

9

Chapter 1 Introduction
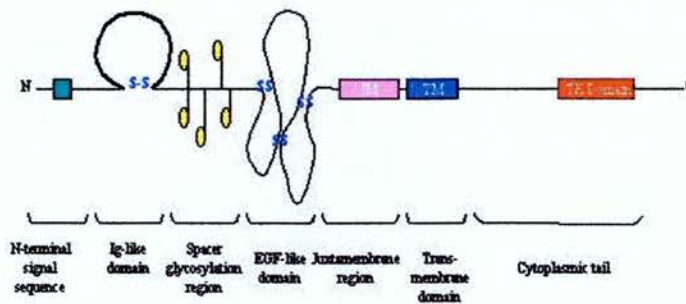
Fig1.3 Schematic representation depicting the structure of the NRG family of ligands. NRG family members are processed as transmembrane precursors and cleaved to release the soluble ecto-domain ligand. Variants arise from spicing of the gene that codes for 7 domains; an N-terminal signal peptide, an immunoglobulin-like domain (Ig-like), a glycosylated domain, the EGF-like domain that binds ligand, a juxtamembrane and transmembrane domain and a cytoplasmic region. NRG isoforms are distinct from the EGF family of growth factors in that they possess an immunoglobulin-like domain.

Although the 'standard' NRG molecule consists of 6 domains, the pro-form transmembrane glycoprotein consists of 7 domains; an N-terminal region, an immunoglobulin-like domain, a spacer segment (for carbohydrate attachment), an EGF-like domain, a highly variable juxtamembrane segment, a transmembrane segment and a cytoplasmic tail of variable-length. Isoforms are identified by differences in the EGF-like domain, the juxtamembrane segment and the cytoplasmic tail (Wen D, 1994). The α and β isoforms arise from differences in the third loop (cysteines 5 & 6) of the EGF-like domain and the next 9-12 amino acids in the following manner; when the stretch in this region from cysteine 5 contains 21 amino acids the molecule is designated an α isoform whilst if this region contains 18 amino acids it is designated the β form. These isoforms have low amino acid identity over this stretch and translates into the β isoforms having a higher receptor binding affinity than the α isoforms (Wen D, 1994) and is reflected by the β isoforms being more effective than the α isoforms at inducing DNA synthesis resulting in mitogenesis (Lu HS, 1995).

14

NRG isoforms also differ in the number of amino acids within the juxtamembrane segment and give rise to a further 5 subtypes; type 1 isoforms contain 9 amino acids, type 2 contain only 1 amino acid, type 3 contain 11 amino acids, type 4 have 27 amino acids and type 5 have 14 amino acids in this segment. All NRG variants are produced as transmembrane molecules except that of the type 3 isoforms, which terminate after the 11th residue and are either secreted or retained within the cell. Further classification arises from the length of the carboxyl terminal which is designated type a, b and c, if the region contains 374, 194 or 157 amino acids respectively. However, most NRG's that are available commercially are classified as the secreted molecule (that arises from proteolytic cleavage after the juxtamembrane domain) and posess only the EGF-like domain and juxtamembrane region designations, for example; NRG1α.

The NRG isotypes 1-4 have distinct expression patterns and biological activities. NRG1 plays an essential role in the normal development of heart, cardiac muscle, the Schwann cells and cranial ganglia of the central nervous system (Meyer D, 1995). NRG deficient embryos die during embryogenesis with heart malformations. In this context, NRG has been shown to act in a local and paracrine manner in tissues that locally express either erbB3 or erbB4. Similarly, expression of erbB4 is essential for differentiation of cardiac muscle and normal axon formation in the central nervous system, whilst mice lacking erbB4 die during mid-embryogenesis (Gassmann M, 1995). In the peripheral nervous system, NRG1 acts to promote end-stage differentiation of muscle cells, stimulates proliferation in developing nerves, which in turn promotes proliferation, survival and differentiation of Schwann cells (Carraway KL, 1997).

NRG1 is the most extensively studied NRG to date and various reports have implicated its involvement in a variety of cellular processes including cell proliferation, growth inhibition, differentiation, chemotaxis and metastasis. The wide variation of cellular effects may in part be to differences in expression of the erbB receptors in different cell types, for example co-expression of NRG and erbB3 is associated with the proliferation of neural cells, whilst expression with erbB4 is associated with differentiation of the same neural cells (Pinkas-Kramarski R, 1997b).

More importantly, differences in spatial location of the NRG receptors and co-expression of NRG is also important for maintaining regulation of these various processes during development; reciprocal fluctation of erbB3 and erbB4, in conjunction with the expression of NRG occurs through different stages of development of the cerebullum (Pinkas-Kramarski R, 1997b). In transgenic mice, expression of NRG in the mammary gland resulted in an inhibition of normal differentiation of terminal end buds and resulted in adenocarcinoma, whilst expression of NRG in mammary tumours in nude mice promoted metastasis (Krane IM, 1996) (Meiners S, 1998).

NRG has been shown to be growth stimulatory for the majority of both normal human and malignant breast and ovarian epithelial cells (Aguilar Z, 1999) (Lewis GD, 1996). Whilst the extent of growth stimulation in response to NRG1 has been attributed to the level of expression of erbB2 co-expressed with either erbB3 or erbB4 (Daly JM, 1997)(Xu F, 1999), cells over-expressing erbB2 are either growth inhibited or undergo mitotic arrest and differentiation or apoptosis (Sepp-Lorenzino L, 1996) (Bacus SS, 1992) (Daly JM, 1999).

Expression of NRG2 was found to be highest in the cerebellum and olfactory bulb with a low level of expression in the liver (Chang H, 1997). Complementary to that of NRG1, which is expressed at high levels in the ventricular endothelium and weakly in the atrial endothelium, NRG2 transcripts were also detected in the heart with the highest level of expression in the atrium and a lower level of expression in the ventricle (Carraway KL, 1997). Although both isotypes bind erbB3 and erbB4 they elicit different activities in that NRG1 is more effective at stimulating erbB2 phosphorylation through hetero-dimerization, whilst NRG2 is more effective at stimulating EGF receptor phosphorylation through receptor hetero-dimerization. Similarly, morphological changes observed in breast cancer cell lines in response to NRG1 were dramatically reduced when cells were treated with NRG2.

16

Expression of the more recently identified NRG3 is restricted to the developing and adult nervous system and whilst this ligand has been shown to bind erbB4 it induces phosphorylation of all the erbB receptor family members (Zhang D, 1997). More importantly, NRG3 has been shown to alter the growth rates of breast cancer cell lines and is produced by breast cancer cell lines indicating that this ligand may be a potential regulator of normal and malignant mammary epithelial cells (Hijazi MM, 1998).

NRG4 expression was identified in the pancreas and in muscle tissue but was undetectable in other tissues (Harari D, 1999). This isotype displays a strict specificity for binding to erbB4 and may displace NRG1 bound to erbB4. The strict expression pattern of this most recently identified NRG and specificity of binding to erbB4 suggests a distinct physiological role from that of the other NRG family members.

Chapter 1 Introduction

## 1.2.2 TGFα

TGFα is a member of the EGF superfamily of growth factors possessing the characteristic EGF-like binding motif. Similarly, TGFα is processed as a membrane bound precursor and is then cleaved to release a soluble ectodomain that acts as a growth factor by binding to the EGF receptor (Prigent SA, 1992). TGFα does not bind erbB2 but may induce phosphorylation of erbB2 by receptor hetero-dimerisation. It has been identified in ovarian adenocarcinomas and cultured ovarian carcinoma cells and is reported to be present in 50-100% of ovarian tumours (Stromberg K, 1994) (Morishige K, 1991). TGFα stimulates the growth of ovarian cancer cell lines in vitro, whilst antibodies directed against TGFα can inhibit the proliferation of ovarian cancer cells that produce TGFα and possess the EGF receptor (Crew AJ, 1992) (Morishige K, 1991) (Kurachi H, 1991). This is consistent with a mechanism of autocrine growth stimulation. In addition, TGFα is angiogenic (Groenen LC, 1994) and it has been suggested development of an antagonist may inhibit tumour angiogenesis and progression to a more advanced stage.

Chapter 1 Introduction

### 1.2.3 EGF receptor

The EGF receptor was the first member of the family to be identified and was isolated from the squamous carcinoma cell line A431 in which it was over-expressed (Wrann MM, 1979). The EGF receptor is a 170 kDa glycoprotein consisting of three domains; an extracellular domain responsible for ligand recognition (621 amino acids), a 23 amino acid hydrophobic transmembrane region and a 542 amino acid intracellular portion that contains a highly conserved tyrosine kinase domain (Fig 4). The tyrosine kinase domain is responsible for propagating cytoplasmic signalling upon ligand binding and causes tyrosine phosphorylation of a number of residues in the cytoplasmic tail enabling recruitment of a repertoire of signalling molecules.

| Sub-Domain | EGFR/ErbB2 | EGFR/ErbB3 | EGFR/ErbB4 |
|---|---|---|---|
| I | 42 | 40 | 48 |
| II | 46 | 46 | 53 |
| III | 45 | 46 | 43 |
| IV | 41 | 50 | 44 |
| TK | 82 | 60 | 73 |
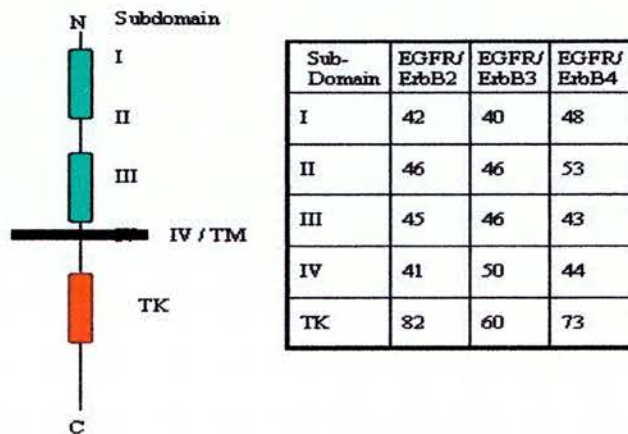
Fig 1.4 Diagrammatic representation of the sequence similarities of EGF receptor (EGFr) domains with erbB2, erbB3 and erbB4. The data indicates percentage of amino acid sequence identity of the region with that of the EGF receptor.

19

Phosphorylation of cytoplasmic signalling molecules may initiate activation of a number of cascades including the MAP kinase cascade which is associated with cell growth and proliferation. The erbB receptors are thought to play a leading role in the activation of this cascade and are therefore regarded as potential mediators in oncogenesis and disease progression.

Unlike the other members of the erbB receptor family the EGF receptor has the ability to recruit the secondary signalling molecule c-Cbl as a consequence of ligand activation. Phosphorylation of c-Cbl ubiquitin ligase elevates receptor ubiquitination and therefore targets the EGF receptor for proteosomal / lysosomal degradation in late endocytic compartments. This is alternatively known as 'de-sensitization' and may be responsible for a 'short-lived response' in receptor activated signalling pathways.

The EGF receptor has been associated with poor prognosis and reduced survival in many cancers including carcinoma of the breast and ovary (Sainsbury JRC, 1987) (Scambia G, 1992) (Bauknecht T, 1990) (Bartlett et al., 1996). In ovarian cancer, expression of the EGF receptor has been identified in 48-98% of human ovarian carcinomas with over-expression found in 19-50% of cases (Scambia G, 1992) (Owens OJ, 1992) (Stromberg K, 1994). Expression has been positively associated with tumours of serous histology (Bartlett et al., 1996). Similarly, EGF receptor positivity has been associated with disease progression in both primary and advanced ovarian tumours (Van der Burg ME, 1993) (Scambia G, 1992). More importantly, co-expression of EGF receptor with EGF or EGF-like ligands has been identified in ovarian carcinomas and increased expression of growth factor has been associated with reduced survival (Bauknecht T, 1989a) (Bauknecht T, 1989b). In addition, the presence of EGF receptor has been correlated with expression of TGFα in malignant tumours (Bartlett et al., 1996) and in adenocarcinomas of high grade or stage (Stromberg K, 1994). In contrast, EGF receptor positivity has been associated with a better response to chemotherapy (Bauknecht T, 1991) (Bauknecht T, 1988) although this did not seem to influence overall survival (Bauknecht T, 1990).

Chapter 1 Introduction

More recently, identification of products that arise from splicing of the EGF receptor gene has introduced greater complexity within the network. Firstly, a truncated EGF receptor (VIII) which has a deletion of 801 bases coding for 267 amino acids in the receptors extracellular domain has been identified (Ekstrand et al., 1994). This gives rise to a product of between 100 kDa and 140 kDa depending on the extent of glycosylation. Presence of this truncated receptor has been frequently identified in human glioblastoma, medulloblastoma, cancer of the breast and in 73% of primary ovarian carcinomas (Moscatello DK, 1995). Although this truncated receptor is proposed to be incapable of binding ligand, it has been identified as a constitutively active tyrosine kinase that promotes cell growth and may induce transformation (Ekstrand et al., 1994). Secondly, identification of a soluble secreted product from the EGF receptor gene that is composed of the extracellular domains I, II and the amino terminal half of subdomain III has been implicated as being a negative regulator of the full length p170 EGF receptor (Reiter JL, 1996). This 60 kDa soluble form resembles that of the secreted receptor product encoded by the avian c-erbB1 transcript (Flickinger TW, 1992). It is proposed to exert its regulatory effect by either competing with full length p170 EGF receptor for binding ligand (sequesters available ligand) or by forming inactive hetero-dimers with cell surface EGF receptor (Reiter JL, 1996).

21

1.2.4 ErbB2 receptor

ErbB2 is a 185 kDa transmembrane receptor which has 42%, 46%, 45% and 41% homology with domains I-IV respectively of the EGF receptor (Fig4) and 82% homology with its tyrosine kinase domain (YamamotoT, 1986). It is known as the 'orphan receptor' as it has no known binding ligand to date and therefore requires hetero-dimerization with other erbB receptors to transduce a ligand-stimulated signal. ErbB2 is therefore regarded as a pan-erbB receptor as it may hetero-dimerize with all other erbB receptors and more importantly, it is the preferential hetero-dimerization partner (Karunagaran D, 1996) (Graus-Porta D, 1997) (Klapper LN, 1999). It forms high affinity receptor complexes for NRG through dimerization with erbB3 and erbB4, and for EGF through dimerization with the EGF receptor (Karunagaran D, 1996). The erbB2 receptor contains a sequence in the carboxyl terminal, an autophosphorylation site (Y1253) that enables coupling to the MAP kinase cascade and also confers the oncogenic, transforming ability of this receptor (Ben-Levy et al., 1994). In breast cancer, expression of erbB2 alongside that of NRG increased expression of cell adhesion molecules and promoted a more motile invasive phenotype (Xu FJ, 1997). More recently erbB2 has been regarded as the 'master regulator of the erbB signalling network' that drives epithelial cell proliferation by acting on several levels; by delaying ligand dissociation from receptor complex, it enhances coupling the MAP kinase signalling pathway and it impedes the rate of receptor down-regulation (Klapper LN, 2000b).

Similar to that found in breast cancer, increased expression of the erbB2 receptor has been reported in 24-30% of ovarian carcinomas and there is an excellent correlation between gene amplification and over-expression (Slamon DJ, 1989) (Singleton TP, 1994) (Reese DM, 1997). Increased expression of erbB2 in approximately 20% of early epithelial ovarian cancers or tumours of low malignant potential does not appear to be a strong prognostic marker nor does it relate to survival. However, increased expression in advanced ovarian cancer is of prognostic significance; erbB2 receptor expression is significantly higher in invasive ovarian cancer than benign tumours (Kim YT, 1998) and significantly increased in patients with recurrent / persistent disease after chemotherapy than at initial presentation (Van Dam PA, 1994).

22

Chapter 1 Introduction

Similarly, Slamon et al (1989 #93) have reported a negative relationship between increased erbB2 receptor expression and survival. In addition, it has been suggested that the increased expression of topoisomerase IIα that is associated with over-expression of erbB2, contributes to the correlation of erbB2 with poor prognosis and poor response to chemotherapy (Hengstler JG, 1999).

More recently, the availability of phosphorylation–state-specific antibodies showed erbB2 over-signalling in up to two thirds of breast cancers in comparison to the previous conservative reports of erbB2 over-expression in 20-35% by immunohistochemistry (Ouyang X, 1999). This is consistent with reports depicting erbB2 as having an intrinsic tyrosine kinase activity and it has been suggested that this is a consequence of spontaneous erbB2 dimerization in cancer cells over-expressing the receptor (Lonardo F, 1990) (Akiyama T, 1991) (Ben-Levy et al., 1994). In support of this, human breast and ovarian cancer cells over-expressing erbB2 have high levels of receptor tyrosine phosphorylation (DiGiovanna MP, 1995). Taken together, these suggest that the phosphorylation state of erbB2 may be a more important prognostic indicator than the level of expression. Further studies into erbB2 phosphorylation may more accurately depict the involvement of the receptor in the growth and progression of ovarian cancer and perhaps reflect the view that erbB2 is more likely to be involved in the pathogenesis of disease rather than solely at an advanced stage (Slamon DJ, 1989).

With the current advances in immuno-therapy, production of an anti-erbB2 receptor antibody called trastuzumab or herceptin® (Genentech Inc., California) that binds with high affinity and specificity to the erbB2 receptor promoting inhibition of cell proliferation, has proved valuable in the treatment of erbB2 over-expressing breast cancers (Goldenberg, 1999). Herceptin is currently in phase III clinical trials in the treatment of breast cancer and has proven to significantly increase response rate, improve the longevity of response and time to progression, when used in combination with standard first line chemotherapy (doxorubicin and cyclophosphamide or taxol) (Beuzeboc P, 1999) (Stebbing J, 2000). Both *in vitro* and *in vivo*, it has been demonstrated that herceptin® in combination with docetaxel produces a true synergistic response and is well tolerated (Burris, 2000).

23

Chapter 1 Introduction

Combination therapy of doxorubicin and cyclophosphamide plus herceptin® has demonstrated increased cardiac toxicity and may be due to the cardio-protective action of erbB2, whereas this was not found when herceptin® was used in conjunction with taxol compounds (Feldman AM, 2000) (Gilewski T, 2000). Moreover, anti-angiogenic effects have also been attributed to treatment with herceptin which may also lead to minimal host toxicity and acquired drug resistance (Kerbel RS, 2000). These results have called for erbB2 receptor status testing for all patients with metastatic breast cancer and a similar trial for herceptin® in the treatment of ovarian cancer. There are currently phase II trials underway in the USA using herceptin® in combination with paclitaxel in the treatment of patients with progressive/metastatic breast or ovarian cancer that over-expresses the erbB2 receptor (NCI-99-C-0121/NCI-T98-0087).

### 1.2.5 ErbB3 receptor

The erbB3 receptor is a 180 kDa transmembrane receptor and unlike the other members of the erbB family, it has a defective tyrosine kinase domain that is devoid of catalytic activity (Guy PM, 1994). The erbB3 receptor tyrosine kinase domain shares the least homology with the other erbB receptors (Fig1.4) and differences in residues in this region are thought to give rise to the impaired kinase activity (Carraway KL, 1994) (Gullick, 1996). Although erbB3 binds NRG with low affinity, coupling to erbB2 reconstitutes a high affinity receptor for NRG and is proposed to be the most potent mitogenic signalling complex within the erbB receptor family to date (Waterman et al., 1999)(Fitzpatrick VD, 1998)(Slikowski MX, 1994). ErbB3 receptor dimerization and phosphorylation leads to recruitment of a repertoire of signaling molecules in which Shc and PI3K predominate, this results in activation of the MAP kinase cascade and activation of pathways associated with increased cell survival respectively (Soltoff SP, 1994) (Alroy I, 1997). The mitogenic superiority of the erbB3 receptor is proposed to be attributed to the carboxy terminal tail of the receptor which shunts the receptor complex into a characteristic erbB3 recycling pathway back to the membrane instead of being down-regulated through lysosomal / proteasomal

Chapter 1 Introduction

degradation (Waterman et al., 1999). The recycling pathway allows prolonged signalling through an erbB3 specific compliment of molecules that propagate the potent mitogenic ability of the receptor. It has been suggested that the kinase domain of erbB3 has lost catalytic activity in order to restrain this potent signalling capability of the carboxyl terminal tail (Waterman et al., 1999).

More importantly, erbB3 has been implicated as playing an essential role within the erbB network since knockout of the gene results in severe defects in the sympathetic nervous system. Similarly erbB3 in conjunction with erbB2 has been implicated in the development of keratinocytes, Schwann cell precursors, oligodendrocytes and the neuromuscular synapse. The co-operation of erbB3 with erbB2 is significant in epithelial cancers, which often display increased expression of erbB2 alongside that of moderate to high erbB3 receptor expression (Klapper LN, 2000b).

Investigation of erbB3 receptor expression in normal adult tissues detected strong immunoreactivity in the primordial follicle and granulosa cells of the ovary yet staining was not apparent in the surface epithelium or stroma (Prigent et al., 1992). Similarly, weak expression of erbB2 has also been detected in the normal ovary. In contrast, erbB3 expression has been detected in 85-100% of human ovarian carcinomas (Simpson et al., 1995b) (Simpson et al., 1995a) (Scoccia B, 1998). The incidence of erbB3 receptor positivity was found to be less in benign tumours than overtly malignant tumours, although a more intense staining pattern was observed in borderline specimens than malignant cases (Simpson et al., 1995b). ErbB3 expression did not appear to be associated with age at diagnosis, stage or degree of differentiation, although early stage malignant tumours were more likely to display increased expression than late stage tumours. Similarly, in a study investigating expression of the EGF receptor, erbB2 and erbB3, multiple receptor expression was highest in overtly malignant tumours and positive associations were detected between expression of erbB3 with EGF receptor and erbB3 with erbB2 (Simpson et al., 1995a) (Scoccia B, 1998). Similar expression profiles have been detected in colorectal carcinoma; where an increase in erbB2 expression (over that found in normal colon tissue) was accompanied by over-expression of the erbB3 receptor as detected by

25

Chapter 1 Introduction

immunohistochemistry and Northern blot analysis (Maurer CA, 1998). In contrast, increased co-expression of erbB3 and erbB4 in breast cancer has been associated with a prognostically favourable sub-group that is likely to benefit from endocrine therapy (Knowlden JM, 1998). However, the findings for ovarian cancer to date, would implicate that the erbB3 receptor is involved in growth and progression to a more malignant phenotype and is most commonly accompanied with increased expression of erbB2.

Five alternate erbB3 receptor transcripts that arise from read-through of an intron have been identified in normal human tissues and ovarian cancer cell lines (Lee H, 1998). In contrast to the 6.2kb transcript that encodes the full length transmembrane receptor, the transcripts of 1.4kb, 1.6kb, 1.7kb, 2.1kb and 2.3kb are proposed to encode soluble secreted products and may correspond to a 90kDa product previously detected by anti-erbB3 receptor antibody in the culture medium of ovarian cancer cells. Other products that have arisen from intron read-through within the erbB receptor family have been shown to have potent growth regulatory effects (Flickinger TW, 1992) and are proposed to act by either binding ligand and sequestering ligand availability or by interacting with receptor to prevent dimerization. In addition, the synthesis of these transcripts may also provide a mechanism for regulating full-length erbB3 receptor expression at the level of transcription. This is reinforced by the finding that the ratio of the 1.4kb product to that of the full length 6.2 kb transcript is high in cells expressing low levels of erbB3 and low in erbB3 over-expressing cell lines. Recently, identification of an erbB3 binding protein, ebp1, which translocates from the cytoplasm to the nucleus following treatment with NRG, has been shown to have a growth inhibitory effect and promotes differentiation of human breast cancer cell lines (Lessor TJ, 2000). This, along with production of an anti-erbB3 receptor antibody that is to be conjugated to a pro-drug delivery system marks a new era for therapeutic intervention for erbB3 over-expressing cancers (Rajkumar T, 1994).

26

1.2.6 ErbB4 receptor

The erbB4 receptor is the most recently identified member of the erbB family. It was first identified as a 180 kDa high affinity receptor for neuregulin (NRG) and shares extensive homology with erbB3 in its extracellular domain (Plowman GD, 1993). ErbB4 has been shown to be expressed in many adult and foetal tissues including the lining epithelia of the gastrointestinal, urinary, reproductive and respiratory tracts, as well as skin, skeletal muscle, circulatory, endocrine and nervous systems (Srinivasan R, 1998). The adult ovarian surface epithelium is weakly positive whereas the stroma is non-reactive (Srinivasan R, 1998).

To date, the roles of the erbB4 receptor are variable in different tumour types and include promoting cell growth and proliferation, differentiation and chemotaxis. For instance, in breast cancer, stimulation of erbB4 has been shown to result in cell proliferation (Cohen BD, 1998) (Weis FU, 1997) which could be inhibited by hammerhead ribozymes targeted to erbB4 mRNA that additionally reduced anchorage-independent colony formation (Tang et al., 1998). Another group have shown that stimulation of erbB4 by heparin binding EGF (HbEGF) results in chemotaxis of breast cancer cells (Elenius et al., 1997b) whilst expression of erbB4, erbB2 and NRG confers a more aggressive invasive phenotype that is resistant to treatment with anti-estrogens (Lupu R, 1996). In stark contrast, erbB4 has also been associated with differentiation of neuronal cells (Pinkas-Kramarski R, 1997b) and similarly associated with differentiated tissues, whilst loss of expression has been noted in 40-80% of a variety of adenocarcinomas (Srinivasan R, 1998) and may suggest that in some cases, loss of expression may be oncogenic. ErbB4 receptor stimulation with NRG has also been shown to induce differentiation of breast tumour cells (Chen X, 1996). Additionally, a significant inverse correlation was detected for erbB4 receptor expression and histological grade in breast cancer, where increased levels of erbB4 was associated with a more differentiated phenotype, although expression was unable to be associated with the disease-free interval or survival (Kew TY, 2000).

27

Chapter 1 Introduction

In a manner similar to that observed for the erbB3 receptor, erbB4 undergoes receptor recycling as opposed to the receptor down-regulation exhibited by the EGF receptor (Lenferink et al., 1998) (Vecchi M, 1997). Receptor recycling involves the activated receptor being recruited into endocytic vesicles in the cytoplasm before being returned to the membrane and is therefore associated with the diffuse cytoplasmic staining seen by immunohistochemistry (McCaig, 1998). This pathway allows receptor signalling to continue and results in prolonged stimulation of signalling molecules such as Erk and PI3K (Vecchi M, 1997).

More recently, splice variants of erbB4 have been identified and encode sequence differences in the juxtamembrane (JM) and cytoplasmic (CT) regions (Fig1.5). The JM isoforms arise through differential splicing of 2 regions, 'a' and 'b', in the juxtamembrane domain giving rise to 4 isoforms designated as follows: JM-a encodes for the 'a' region only containing 23 amino acids, JM-b for the 'b' region only containing 13 amino acids, whereas Jm-d encodes for both 'a' and 'b' sequences and JM-c does not contain either sequence (Elenius et al., 1997a) (Gilbertson RJ, 1999). The JM-a and JM-b isoforms have been shown to be expressed in a tissue specific manner with for example, expression of both isoforms being found in neural tissues whereas kidney expresses JM-a only and heart expresses only the JM-b isoform (Elenius et al., 1997a). More importantly, the JM-a isoform is susceptible to cleavage by matrix metalloproteases that are released in response to stimuli activating Protein Kinase C (PKC). This yields an 80 kDa cytoplasmic fragment and 120 kDa ectodomain fragment (Vecchi M, 1996). The 80 kDa fragment becomes ubiquitinated and destined for degradation in the proteosome; this mechanism of degradation or regulation of expression is unique to the erbB4 receptor JM-a isoform and is not observed for the EGF receptor, erbB2 or erbB3 (Vecchi M, 1997). Expression of the JM-c and JM-d isoforms have only recently been identified in childhood medulloblastoma and it has been proposed that the JM-d isoform will be susceptible to cleavage like JM-a, since it contains the 'a' sequence (Gilbertson RJ, 1999). Although JM-a expression is regulated by matrix metalloproteases and JM-b is not, both receptors are capable of being activated to the same extent by treatment with NRG1β or Beta-cellulin (Elenius et al., 1997a).

28

Alternate splicing of a region in the cytoplasmic domain gives rise to another 2 isoforms CT-a and CT-b (Sawyer et al., 1998) (Elenius et al., 1999), also known as CYT-1 and CYT-2 (Kainulainen V, 2000). The CT-a isoform encodes a sequence of 48 nucleotides that includes the single erbB4 PI3K binding site while the CT-b isoform is deficient in this region and therefore is unable to bind PI3K. Both the CT-a and CT-b isoforms are able to be stimulated by NRG1β and characteristically phosphorylate Shc and Erk although significant differences have been observed in the two isoforms consequence to the ability to bind PI3K. The CT-a isoform is able to protect cells from starvation induced apoptosis through phosphorylation of Akt (a signalling molecule known to mediate cell survival) and NRG1β may stimulate chemotaxis and membrane ruffling in cells expressing CT-a, whereas the CT-b isoform is unable to mediate either of these functions (Kainulainen V, 2000).
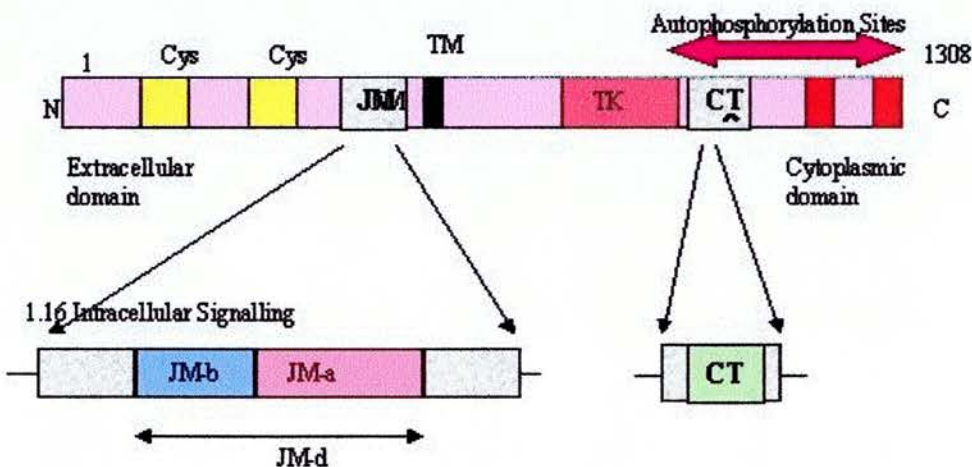


Fig1.5 Diagrammatic representation of the erbB4 receptor and the regions where alternate splicing gives rise to the erbB4 receptor isoforms. Alternate splicing of 2 sequences in the juxtamembrane domain gives rise to 4 isoforms; possessing either the JM-a or JM-b sequence, possessing both sequences JM-d, or neither sequence JM-c. Alternate splicing of a sequence in the cytoplasmic tail gives rise to 2 isoforms; possessing a sequence coding for a PI3-kinase binding site CT-a, or lacking this sequence CT-b.

29

Chapter 1 Introduction

1.2.7 ErbB receptor dimerization

Ligand-induced dimerization of these receptors is essential for transmembrane signalling which enables receptor autophosphorylation in the cytoplasmic domain. This simultaneously generates docking sites for recruitment of a repertoire of cytoplasmic signalling molecules. Although ligand-induced dimerization was first reported for the EGF receptor (Yarden Y, 1987b), (Yarden Y, 1987a), the exact mechanism by which dimerization occurs is still unknown. At present, there have been 3 models of association proposed. In the first, a single ligand molecule binds to each receptor monomer and promotes dimerization by allosterically altering the shape of the receptor extracellular domain which stabilizes dimer formation (this model assumes ligand does not interact with more than one receptor surface). Alternatively, a single ligand might bind to one receptor and then form a ternary complex with a second receptor (in this case a single ligand interacts simultaneously with both receptors). In the third, a more complex version, two ligands form bridges between the receptor pair. However, receptor hetero-dimerization is preferential to that of receptor homo-dimerization and since each receptor has docking sites for a particular repertoire of intracellular signalling molecules, hetero-dimerization is thought to diversify the nature of intracellular signalling (Pinkas-Kramarski R, 1996) (Alroy I, 1997).

The erbB family is unique among other subgroups of the receptor-type I tyrosine kinases in that one receptor, erbB2, has been named the 'orphan-receptor' since a direct binding ligand has not been identified to date and another receptor erbB3 has an impaired kinase activity. None the less, erbB2 has been characterized by having a constitutively active kinase domain (Lonardo F, 1990) and has been proposed to act as a pan-erbB receptor that enhances intracellular signalling by decelerating the rate of ligand dissociation. In addition, although the erbB3 receptor is regarded to be 'kinase-defective', once dimerized with erbB2, it has been reported to be the most potent signalling complex within the family of erbB receptors (Fitzpatrick VD, 1998) (Slikowski MX, 1994). Moreover, the complexity within the network increases since intracellular signalling induced by the erbB3 and erbB4 receptors is prolonged in

30

comparison to that of the EGF receptor which is down-regulated as a consequence to binding the signalling molecule c-cbl (Levkowitz G, 1998) (Waterman et al., 1999).

## 1.2.8 Receptor phosphorylation leads to initiation of intracellular signalling pathways including that of the MAPK cascade

Ligand stimulation of the erbB receptors results in receptor dimerization and autophosphorylation of the receptor C-terminal tail. This enables a repertoire of cytoplasmic signalling molecules to bind and initiates signalling through a number of pathways including the mitogen activated protein kinase (MAPK) cascade that is associated with cell proliferation. This pathway may be initiated by the binding of Shc or Grb2-mSos to the activated receptor (Fig 1.6) and results in phosphorylation of Erk1/2. Erk may then translocate to the nucleus to initiate gene transcription and cell cycle progression (Marshall, 1995).
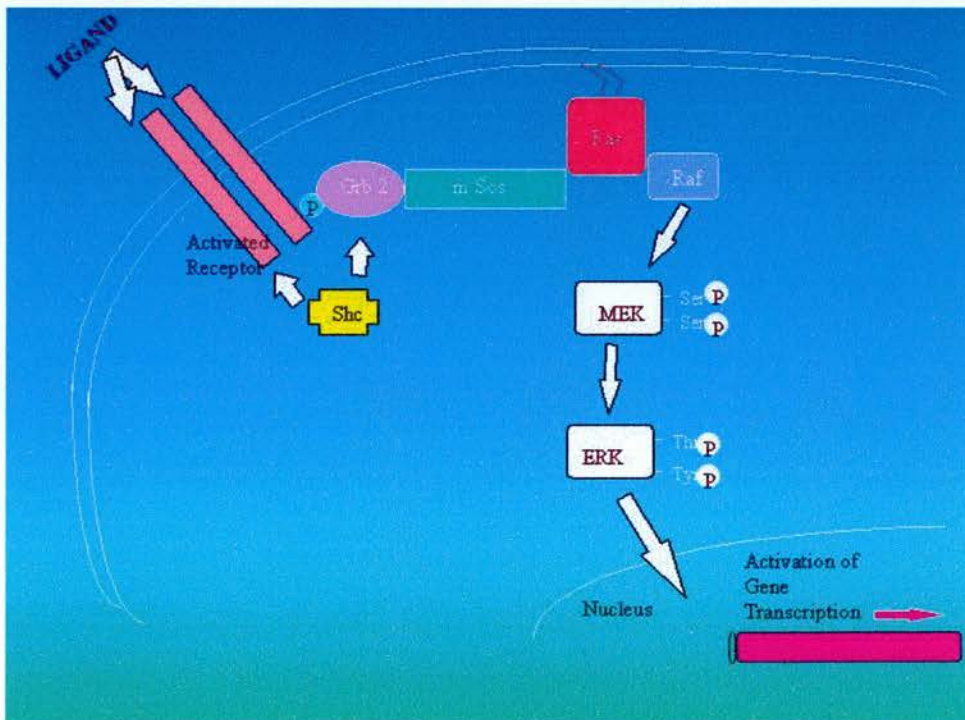


Fig1.6 Schematic diagram representing activation of the MAP/ERK kinase cascade that is associated with cell proliferation. Ligand binding to receptor stimulates receptor dimerisation and autophosphorylation inducing the recruitment of a number of cytoplasmic signalling molecules including Grb2 and Shc to the carboxyl tail. This initiates signalling through the cascade by Ras, Raf, MEKK and ERK which may translocate to the nucleus to activate gene transcription.

31

Chapter 1 Introduction

1.2.9 Shc

The molecule Shc (Fig1.7) can bind to all four erbB receptors to initiate signalling within the MAPK cascade.
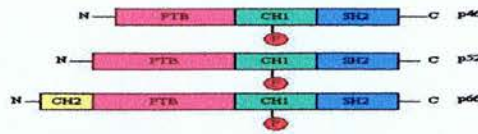


Fig 1.7 Schematic diagram of Shc structure. Shc signalling proteins are characterized by an amino terminal phosphotyrosine binding domain (PTB), a central proline / glycine rich region (CH1) containing the unique Grb2 binding site and a carboxyl terminal SH2 domain. Three isoforms have been identified; p46 and p52 that arise from differential translation initiation at two proximal sites while p66 is a splicing isoform that contains the p52 sequences and an additional amino terminal glycine / proline rich (CH2) domain.

To date, 3 Shc isoforms p46, p52 and p66 (Shc A) (Fig1.7) and the related molecules p47, p52 (both Shc B), p54 (Shc C) have been identified (Pelicci G, 1996). Although expression of the Shc A molecules is ubiquitous, expression of Shc C is limited to brain whilst Shc B is also expressed in the salivary gland, uterus, ovary and testis. The Shc molecules are structurally similar sharing a carboxyl terminal SH2 domain, a central glycine and a proline rich region (CH1) and an amino terminal phosphotyrosine binding domain (PTB). Upon cell stimulation with EGF, Shc molecules are released from the endoplasmic reticulum as a result of an EGF-stimulated rise in intracellular calcium($Ca^{2+}$) and recruited to the plasma membrane in close proximity for binding to activated receptors (Lotti LV, 1996). The SH2 and PTB domains are involved in membrane localization and binding to specific phosphorylated tyrosine residues located within the carboxyl terminal tail of activated receptors. The tyrosine residue within the CH1 domain (Tyr$^{317}$) is responsible for binding to the SH2 domain of Grb2, whilst the CH1 and CH2 domains are involved in additional interactions with molecules possessing an SH3 domain such as eps8, PLCγ and p120GAP (Van der Geer P, 1996) (Ravichandran KS, 1997). The Shc molecules are involved in transmission of signal from        activated or phosphorylated receptor

32

Chapter 1 Introduction

tyrosine kinase to Ras; Shc phosphorylation correlates with its recruitment to the plasma membrane and forms a stable complex with Grb2 (Pelicci G, 1992)(Ravichandran KS, 1997) (Lotti LV, 1996).

Increased expression of p46/p52 Shc increases the proliferative response and activation of Erk by EGF. Similarly, these Shc isoforms are able to transform NIH3T3 fibroblasts or induce terminal differentiation in PC12 cells (Pelicci G, 1992) (Rozakis-Adcock M, 1992). More importantly, the transforming ability of both erbB2 and genetically engineered mutants of erbB2, has been correlated to their ability to bind Shc and Grb2 (Dankort DL, 1997).

In direct contrast, the p66 isoform has differing biological properties to that of p46/p52, which have been proposed to be due to the addition of the amino terminal CH2 domain. Whilst p46 and p52 Shc isoforms transduce the active signal from receptor to Ras, the p66 isoform is proposed to function as a negative regulatory component in this pathway. Over-expression of the p66 isoform (unlike that observed for p46 or p52) does not induce cell transformation and whilst p66 forms a stable complex with Grb2, its expression markedly reduces the extent of Erk phosphorylation and inhibits the early gene 'fos' promoter activation, post-stimulation with EGF (Migliaccio E, 1997). Moreover, it has been demonstrated that the p66 isoform competes with p46/p52 for binding to a limited pool of Grb2 proteins (Okada S, 1997). Treatment of CHO cells (Chinese Hamster Ovary cells) with EGF or NIH3T3 fibroblasts with phorbol ester, resulted in an additional serine and threonine phosphorylation of p66 Shc, which translated into a decrease in mobility by polyacrylamide gel electrophoresis (Okada S, 1997) (Mahmoud YM, 1997a). The serine/threonine phosphorylated p66 was exclusively associated with Grb2 whilst the non-serine/threonine phosphorylated form was associated with the receptor. This has led to the proposal that the p66 isoform reduces Erk activation by sequestering Grb2 from coupling with Ras. In addition, insulin has been shown to increase the serine/threonine phosphorylation of p66 by an Erk dependent pathway implying that p66 may be stimulated as a result of Erk activation and forms a negative feedback loop (Kao AW, 1997) (Migliaccio E, 1997). Similarly, increased expression of erbB2 and the level of erbB2 phosphorylation has been correlated with the level of p46 and

Chapter 1 Introduction

p52 tyrosine phosphorylation, whilst the amount of p66 was inversely correlated to the level of erbB2 expression in breast cancer cells (Stevenson LE, 1998).

34

1.2.10 Erk

In eukaryotic cells, activation of ubiquitous mitogen-activated protein kinases (MAPK) contributes to cell-type and ligand specific responses. MAP kinase cascades (or MAP kinase modules) are comprised of a core of enzymes that consist of a serine threonine protein kinase (MAPKKK) that phosphorylates and activates a dual-specificity kinase, MAP kinase kinase (MAPKK) or MEK, which in turn phosphorylates and activates another serine/threonine protein kinase, MAP kinase. The most well characterized MAP kinase module contains the Raf isoforms (corresponding to MAPKKK), MEK (corresponding to MAPKK) and p44 Erk1 and p42 Erk2 (corresponding to MAPK). Signalling through this pathway results in serine and threonine phosphorylation (or dual phosphorylation) of Erk1 and Erk2 and has been associated with cell proliferation or differentiation in different cell types. Studies investigating the duration of Erk phosphorylation and outcome of Erk translocating into the nucleus to initiate cell transcription or remaining cytoplasmic, has established a model for determining different cellular responses (Marshall, 1995). The model is based upon responses determined in PC12 cells where sustained activation led to translocation of Erk to the nucleus whereas transient activation of Erk does not lead to nuclear accumulation. The duration of Erk activation will therefore have very different consequences since nuclear accumulation will result in phosphorylation of transcription factors. In the PC12 cell line, sustained activation of Erk produced cell differentiation whilst transient activation resulted in cell proliferation. However, it is not a requirement of this model that sustained Erk phosphorylation invariably leads to cell differentiation and transient activation always leads to proliferation, but that the compliment of transcription factors in any given cell type, that are activated by nuclear Erk localization will determine the biological response. For example, in other cell types the converse is true; sustained activation of Erk in fibroblasts is associated with cell proliferation. Similarly, whilst nuclear localization of Erk is required for mitogen-induced gene expression and entry to the cell cycle in fibroblasts (Brunet A, 1999b), nuclear localization of Erk is required to induce neurite extension in PC12 cells (Robinson MJ, 1998). The important feature of the model is that cells utilize transient and sustained activation of Erk to determine different cellular responses. More importantly, constitutive activation of Erk has been detected in a variety of tumour

derived cell lines and was tissue specific with lines derived from the pancreas, colon, lung, kidney and ovary displaying a high frequency of constitutively active Erk as well as a high degree of activation (Hoshino R, 1999). Erk activation was associated with activation of Raf, MEK or point mutation of Ras, indicating that the constitutive activation of the cascade was not due to disorder of MEK or Erk, but deregulation of Raf, Ras or signalling upstream of this.

More recently, stimulation of ovarian cancer cell lines with EGF or NRG showed that although transient activation of Erk correlated with induction of proliferation, only sustained activation would actually result in cell proliferation (Campiglio M, 1999).

1.3 Scopes and objectives of this study

The aims of this study were to address the following:
i) To investigate erbB receptor expression within the panel of human ovarian cancer cell lines and establish if expression of a single erbB receptor could determine a growth response to NRG or TGFα.
ii) To compare the relative mitogenic effects of NRG with that of known response to TGFα.
iii) To investigate expression of NRG in a panel of human ovarian cancer cell lines and tumours to determine if the ligand could be involved in the disease.
iv) To explore intracellular signalling associated with a growth response to NRG in comparison to TGFα.
v) To further elucidate the role(s) of the erbB3 and erbB4 receptors in the regulation of cell growth.

This thesis examines the expression and potential roles of the erbB receptors and the ligands NRG and TGFα in ovarian cancer. Study of the ligand NRG was chosen to establish the role(s) of its binding receptors, erbB3 and erbB4, whilst TGFα was used for to compare the effects of a ligand that in contrast binds to the EGF receptor. ErbB receptor expression was investigated through a panel of ovarian cancer cell lines by Western blot analysis and cell growth assays were employed to determine growth responses to the ligands. These techniques were used to identify relationships

between receptor expression and a growth response. RT-PCR was used to investigate NRG expression in both human ovarian cancer cell lines and tumours, to determine if NRG could have a potential role in this disease. Assessment of the cellular growth in response to the ligands was further investigated by examining subsequent receptor phosphorylation and intracellular signalling within the Erk kinase cascade. Activation of the molecules Shc and Erk1/2 were studied by Western blot analysis, to monitor mitogenic signalling downstream of ligand-receptor activation/phosphorylation. Elucidation of the potential growth regulatory role(s) of the erbB3 and erbB4 receptors was established by using anti-receptor antibodies that inhibit ligand binding to the receptor.

This project was designed to investigate the erbB receptor - growth factor network at several levels, these pathways are illustrated in Fig 1.8.
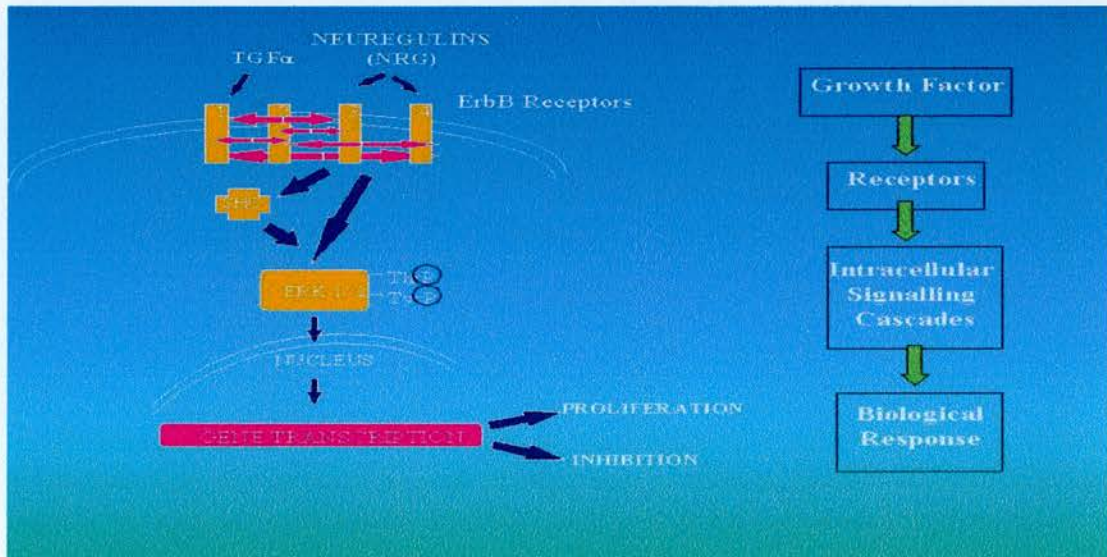


Fig 1.8 ErbB receptor - growth factor network. The erbB receptor - growth factor network may be structured into components; the binding ligand, expression of the erbB receptors, intracellular signalling which may lead to a change in cellular growth.

## Chapter 2 Materials and Methods

2.1 Cell lines

The PEO1, PEO1$^{CDDP}$, PEO4, PEO6, PEO14 and PEO16 cell lines were developed at the Edinburgh Medical Oncology Unit. The OVCAR3, OVCAR4 and OVCAR5 cell lines were kindly donated by Dr T Hamilton (Fox Chase Institute, PA). The 41M, OAW42, 59M and A2780 cell lines were obtained from the European Tissue Collection (Porton Down, UK). The SKOV3, CAOV3 and SW626 cell lines were obtained from the American Type Culture Collection (Mannassas, VA).

2.2 Ovarian Tumours

Fresh primary ovarian tissue was obtained from 24 patients with epithelial ovarian cancer at initial debulking surgery, transferred to liquid nitrogen. RNA was extracted using TRI-reagent™ as described below for RT-PCR (all reagents were obtained from Sigma, Poole, UK).

2.3 Materials and methods

The following materials and methods were used to obtain the results generated in this thesis

2.4 Cell culture materials
Bovine Serum Albumin (BSA) (Sigma, Poole, UK)
Charcoal (Sigma, Poole, UK)
Dextran T-70 (Sigma, Poole, UK)
DMSO (Sigma, Poole, UK)
EDTA (Sigma, Poole, UK)
Fetal calf serum (FCS, Gibco BRL, Life Technologies, Paisley, UK)
Glutamine (Sigma, Poole, UK)
NRG1α (Heregulin1α, Sigma, Poole, UK.)
NRG1β (Heregulin1β, Neomarkers, Fremont CA.)
Phosphate buffered saline (PBS, Gibco BRL, Life Technologies, Paisley, UK)
Penicillin (Gibco BRL, Life Technologies, Paisley, UK)
RPMI 1640 Medium (Gibco BRL, Life Technologies, Paisley, UK)
Sodium chloride, NaCl (Sigma, Poole, UK)
Streptomycin (Gibco BRL, Life Technologies, Paisley, UK)
TGFα (Transforming Growth Factor alpha), Boehringer Mannheim, East Sussex,UK.)
Sulphatase (Sigma, Poole, UK)
Tissue culture flasks & 24 well plates (Nuncleon, Life Technologies, Paisley, UK)

## 2.5 Routine Culture of Cell Lines

All cell lines were routinely cultured in RPMI 1640 at 37°C in an atmosphere of 5% $CO_2$ in a humidified incubator. The media was supplemented with penicillin (100 IU ml$^{-1}$) and 10% fetal calf serum (FCS), which had been heat-inactivated by incubation at 56°C for 1h.

## 2.6 Cell Harvesting

Routinely cells were grown to 70% confluence in 75 or 175 cm$^2$ flasks and fed fresh media every 2-3 days. Cells were usually harvested once weekly which involved removing the media, washing twice with phosphate buffered saline (PBS) pH7.3 to remove traces of FCS. Cells were detached from the plastic by incubation with a 1:1 solution of trypsin (0.25% [w / v] in Gibco solution A) and versene (1mM EDTA in PBS, 0.5% [v / v]phenol red), for 5-10 min at 37 °C. The trypsin was inactivated by the addition of medium (RPMI 1640+ 10% FCS), cells were pelleted at 2000rpm for 2min and resuspended in a small volume of medium. The cells were passed through a 1.5 gauge needle to produce a single cell suspension.

## 2.7 Cryopreservation and recovery of cells from liquid nitrogen

Cells to be stored were harvested as described above to produce a single cell suspension. The cells were then re-pelleted and suspended in ice cold freezing mixture (10% [v / v] dimethyl sulphoxide [DMSO] in newborn calf serum). Aliquots were transferred to cryotubes and stored in liquid nitrogen.

Cells were recovered from liquid nitrogen by being thawed and washed with media (RPMI1640 + 10%FCS), pelleted to remove traces of DMSO and resuspended in media and transferred to 25cm3 flasks. Cells were allowed to attach overnight at 37°C before media was changed to remove dead cells and fresh media added.

2.8 Charcoal stripping of FCS

FCS was heat inactivated at 56°C for 1h and allowed to cool before being incubated with 200U sulphatase per 100ml at 37°C for 2h. The pH of the serum was adjusted to 4.2 before the addition of 5g charcoal and 25mg dextran T-70 per litre. The mixture was stirred overnight at 4°C, the charcoal was then removed by centrifugation. The stripping process was repeated before the pH of the serum was readjusted to 7.2, filter sterilized and stored at -20°C until use.

2.9 Preparation and storage of growth factors

Human recombinant NRG1α was purchased lyophilized and reconstituted to a concentration of 20μM solution with 0.1% BSA in PBS. The solution was then aliquoted and stored at -20°C until further use. NRG1β was purchased as a 10μgml$^{-1}$ solution which was aliquoted and stored at -40°C. Lyophilized TGFα was reconstituted with sterile PBS to achieve a concentration of 10μM, aliquoted and stored at -40°C until use.

2.10 Cell Counting

To estimate cell numbers for setting up experiments cells were counted using a haemocytometer. Counting of cells from experimental conditions in 24 well trays was done by a ZF Coulter Counter. The media was removed from the wells, the wells were washed twice with PBS pH7.3 and cells were incubated at 37°C with 250μl of 1:1 trypsin/versene solution to detach cells from the plastic. Once cells were detached the plate was placed on ice and aliquots of 200μl of cell suspension from each well were removed and added to 9.8ml of NaCl (0.9%). Each suspension was counted in duplicate, the average multiplied by the dilution factor (x25) to estimate cell numbers per well.

## 2.11 Growth Assays

Exponentially growing cells were harvested by trypsinisation and plated in 24-well plates at a density of $5 \times 10^4$ cells per well in RPMI 1640 medium containing 10% fetal calf serum. After 24h to allow for attachment, the medium was removed, cells were washed twice with PBS and the following experimental medium was used: RPMI 1640 medium without phenol red but containing 5% double charcoal stripped fetal calf serum. After a further 24h, this medium was removed and replaced with experimental medium with or without growth factor ($10^{-9}$M), this was designated Day 0. In experiments where anti-receptor antibodies were used (anti-erbB4 receptor antibody Ab72/H4.72.8, anti-erbB3 receptor antibody Ab105/H3.105.5), these were added 30 min prior to the addition of NRG1β. Media with or without growth factor and /or antibody was replaced on Day 2. Cells were harvested from wells by trypsinisation on Days 0, 2 and 5 and counted on a Coulter counter. Details of the antibodies used are listed in Table 2.1.

2.12 Protein Extraction and Immune-precipitation

Cells were grown to approximately 60% confluence in $75cm^2$ flasks in the presence of RPMI 1640 containing 10% FCS. Cells were washed twice with PBS and experimental medium was replaced (above). After 24h, the medium was removed and replaced with experimental medium, experimental medium containing growth factor and/or anti-receptor antibody. Cells were harvested at 15min, 1h, 8h, and 24h which involved 2 washes with ice cold PBS before addition of the following lysis buffer: 50mM Tris (pH7.5), 5mM EGTA (pH8.5), 150mM NaCl, 1% Triton X-100, 2mM Sodium orthovanadate, 50mM Sodium Flouride, 20µM Phenylarsine oxide, 1mM Phenylmethyl-sulphonylfluoride (PMSF), $10µgml^{-1}$Leupeptin,$10 µgml^{-1}$ Aprotinin, 10mM Sodium Molybdate (all obtained from Sigma, Poole, UK). Cells were allowed to lyse for 10min on ice, the lysate was spun at 12000rpm for 10 min and the protein supernatant removed. Protein content was estimated by a colorimetric assay (Bio-Rad Protein Assay, Bio-Rad, UK) which is an adaptation from that used by Bradford (Bradford, 1976). 100µl of sample was incubated with 5ml of protein assay reagent for 5min at room temperature. A 200µl aliquot was then transferred to a microtitre plate and protein concentration estimated by sample absorbance at 595nm in comparison to that of a linear gradient of BSA standards .

Immune-precipitation reactions were carried out using 1mg of cell lysate, which was incubated with 1µg of antibody at 4°C for 2h. Protein A/G Agarose (Santa Cruz Biotechnology Inc, USA) (20µl) was added and incubated at 4°C for a further 2h, spun at 2500rpm at 4°C for 5min to pellet the immune-precipitate complex, washed 3 times with lysis buffer (above) and finally washed in TNE (50mM Tris HCl, 140mM NaCl, 5mM EDTA, obtained from Sigma, Poole, UK). The pellet was then resuspended in sample loading buffer and incubated at 95°C for 10 min, spun at 2500rpm for 5min and the supernatant loaded onto the gel (5% and 12% polyacrylamide gels were used to detect the erbB receptors and intracellular signalling molecules (Shc and Erk1/2) respectively. Details of the antibodies used are listed in Table 2.1.

2.13 Western Blot Analysis

Polyacrylamide gel electrophoresis (BioRad,UK) was carried out and proteins were transferred onto an Immobilon ™ membrane using a BioRad Semi-Dry blotting apparatus at 30 volts overnight. Membranes were blocked in Tris buffered saline pH 7.4, containing 0.05% Tween (Sigma, Poole, UK), 5% ovalbumin (Sigma, Poole, UK), and 10% normal sheep serum (Dako,UK). Antibodies were incubated either overnight at 4°C or for 1h at room temperature. Expression was detected using an enhanced chemiluminescence kit (ECL – Boehringer Mannheim, East Sussex, UK) and scored as positive when protein was detected at the correct molecular weight against the 'color markers' molecular weight standards (Sigma, Poole, UK). Integrated optical density values were obtained using a gel scanner (UVP Life Sciences, Cambridge, UK) and analysed by the Labworks gel analysis software (UVP).

2.14 Reverse Transcription Polymerase Chain Reaction (RT-PCR)

Total cellular RNA was extracted from cells in log phase growth using TRI reagent™ (Sigma, Poole, UK). Samples were treated with 20 U / 50µl DNAse I (Boehringer Mannheim, East Sussex, UK) to remove any genomic DNA contamination. RNA was then re-extracted using a phenol-chloroform protocol (Sigma, Poole,UK). Reverse transcription was performed using oligo dT primers and the first strand cDNA synthesis kit (Boehringer Mannheim East Sussex, UK). 1µg of RNA yielded 20µl of cDNA, of which 5µl was used for each subsequent PCR reaction, with each primer pair. PCR reactions were were carried out for optimization varying the annealing temperature, $MgCl_2$ concentration and cycle number. Subsequently, the reactions were carried out containing the following components in a 50µl reaction volume: 1X PCR buffer, 1.5mM $MgCl_2$, 0.2mM dNTP mixture, 2.5U TAQ polymerase, 400mM each primer (TAQ polymerase and primers were obtained from ICRF, Clare Hall, UK; all other components were from Boehringer Mannheim, East Sussex, UK). Amplification was performed over 35 cycles using the following parameters: step 1, 1 min at 93°C; step 2, 1 min at 61°C for the erbB4 primers, 1 min at 51°C for the NRG primers, 1 min at 57°C for the γ-actin primers; step 3, 1 min at 72°C. A final step of 72°C for 5 min was undertaken to ensure all transcripts were full length. PCR products were visualized after electrophoresis on polyacrylamide gels and

staining with ethidium bromide. DEPC treated water was used as a control to check for the presence of contamination in both the reverse transcription and PCR reactions (Diethyl pyrocarbonate (DEPC) obtained from Analar, UK). Cell lines and tumours were scored as positive for the erbB4 receptor or NRG ligand when a PCR product of the correct size, against a 100 bp ladder (Gibco, Life Technologies, UK), was amplified and identified after electrophoresis. Products amplified by the erbB4 receptor primers were excised and sequenced to confirm identity. Primer sequences are listed in Table 2.2.

2.15 Sequencing

PCR products were purified using Sea-plaque agarose (Sigma, Poole, UK) made up to a 1.5% gel, extracted and purified by Wizard PCR miniprep column (Promega, Southampton, UK). The cDNA product was ligated, inserted into a p-Gem-T Easy Vector™ (vector and cells obtained from Promega, Southampton, UK) and grown in JM109 cells plated on agar. Transformed colonies were checked for product by PCR. PCR products were sequenced using a dRhodamine Terminator Cycle sequencing kit (Applied Biosystems, Warrington, UK) and run on a PE Biosystems 377 Automatic Sequencer.

Table 2.1 Antibodies used

| Antibody | Ig Isotype | Technique | Supplier | Dilution / Concentration | Details |
|---|---|---|---|---|---|
| Anti-EGF receptor (Ab7 / clone H11+11E8) | IgG$_1$ + IgG$_{2a}$ | Western blotting | Neomarkers Genzyme | 1.5µgml$^1$ | Antibody raised to clone H11 microsomal membranes and recombinant human EGFR-HpE fusion protein generated from the cytoplasmic domain (clone11E8) |
| Anti-EGF receptor (Ab13 / clone 528+199.12) | IgG$_{2a}$ + IgG$_{2a}$ | Immune-precipitation | Neomarkers Genzyme | 10µlmg$^{-1}$ protein lysate | Partially purified EGFR from A431 cells (clone528) and ECD of recombinant human EGFR protein (clone199.12) |
| Anti-EGF receptor (Ab12 / cocktail R19 / 48) | IgG$_1$ + IgG$_{2a}$ | Western blotting | Neomarkers Genzyme | 1 / 500 | Antibody raised to ECD and cytoplasmic domains of recombinant human EGFR protein |
| Anti-erbB2 receptor NCL-CB11 | IgG$_1$ | Western blotting | Novocastra | 1 / 40 | Clone CB11 raised to cytoplasmic domain of the erbB2 receptor |
| Anti-erbB2 receptor NCL-CBE1 | IgG$_{2a}$ | Immune-precipitation | Novocastra | 1/200 | Raised to a synthetic peptide corresponding to a site on the ECD of the erbB2 protein |
| Anti-erbB3 receptor (RTJ-2) | IgG$_1$ | Western blotting | Santa Cruz Biotech. | 1/200 | Raised to a peptide mapping within the cytoplasmic domain of human erbB3 oncoprotein |
| Anti-erbB3 receptor (Ab90 / clone H3.90.6) | IgG$_{2a}$ | Immune-precipitation | Neomarkers Genzyme | 10µlmg$^{-1}$ protein lysate | Raised to an extracellular fragment of recombinant human erbB3 oncoprotein |
| Anti-erbB3 receptor (Ab105 / clone H3.105.5) | IgG$_1$ | Inhibition of Neuregulin Binding (Growth Assays) | Neomarkers Genzyme | 10µgml$^{-1}$ | Raised to a portion of the ECD of the human erbB3 oncoprotein |
| Anti-erbB4 receptor (Ab2) | Rabbit poly-clonal IgG | Western blotting | Neomarkers Genzyme | 1 / 400 | Raised to a synthetic peptide from the cytoplasmic domain of the human erbB4 oncoprotein |
| Anti-erbB4 receptor (HFR-1) | Mouse mono-clonal | Western blotting | Courtesy of Prof. WJ Gullick | 3µgml$^{-1}$ | Raised to peptide 96.4 from the cytoplasmic domain of the erbB4 receptor |
| Anti-erbB4 receptor (clone H4.77.16) | IgG$_1$ | Immune-precipitation | Neomarkers Genzyme | 10µlmg$^{-1}$ cell lysate | Raised to an extracellular fragment of recombinant human erbB4 oncoprotein |

| Antibody | Ig Isotype | Technique | Supplier | Dilution / Concentration | Details |
|---|---|---|---|---|---|
| Anti-erbB4 receptor (Ab72 / cloneH4.72.8) | IgG$_{2a}$ | Inhibition of Neuregulin Binding (Growth Assays) | Neomarkers Genzyme | 10µgml$^{-1}$ | Raised to a portion of the ECD of the human erbB4 oncoprotein |
| Anti-phosphotyrosine (PY20) | IgG$_{2b}$ | Western blotting / Immune-precipitation | Santa Cruz Biotech. | 1µgml$^{-1}$ (WB)/ 1µgmg$^{-1}$ cell lysate (IP) | Derived by fusion of PA1 mouse myeloma cells with spleen cells from a BALB/C moouse immunized with phosphotyrosine coupled to keyhole limpet hemocyanin |
| Anti-phosphotyrosine (PY99) | IgG$_{2b}$ | Immune-precipitation | Santa Cruz Biotech. | 1µgmg$^{-1}$ cell lysate (IP) | Derived by fusion of PA1 mouse myeloma cells with spleen cells from a BALB/C moouse immunized with phosphotyrosine coupled to KLH |
| Anti-Shc (S14630) | Rabbit poly-clonal | Western blotting | Transduction Laboratories | 1 / 1000 | Raised to a portion of the carboxyl terminal of the Shc protein that encompasses the SH2 domain |
| Anti-phospho p44 / p42 MAPkinase | IgG Rabbit poly-clonal | Western blotting | New England Biolabs | 1 / 1000 | Raised to a synthetic phopshothreonine-tyrosine peptide (KLH coupled) corresponding to res.198-211 of human p44 MAPkinase |

Table 2.2 Primers used for RT-PCR

| Target mRNA | Primers |
|---|---|
| ErbB4 JM isoforms | f5'CAGTGTGAGAAGATGGAAGATG3' |
| | r5'CTTTTTGATGATCTTCCTTCTAAC3' |
| ErbB4 CT isoforms | f5'ATCTCTTGGATGAAGAGGATTTGG3' |
| | r5'GTCATCAAAAATCTCAGCAGTAGC3' |
| NRG | f5'TCCAATCTGTTAGCAATGTG3' |
| | r5'GACCTCTACTTCTCGTGACA3' |
| γ-actin | f5'ATGGCATCGTCACCAACTGG3' |
| | r5'ATGACAATGCCAGTGGTGCG3' |

All primers were obtained from ICRF, Clare Hall, South Mimms, UK

## Chapter 3

### 3.1 Expression of the ErbB Receptors and Neuregulin in ovarian cancer cell lines

The following section describes the results of experiments that assessed the expression of the different erbB receptors in a panel of ovarian cancer cell lines. Levels of erbB receptor expression were evaluated using Western blot analysis with chemiluminescent detection. The ovarian cancer cell lines used were as follows;

| Cell Line | Histology | Source | Prior Treatment |
|---|---|---|---|
| PEO1 | P.D. Serous adenocarcinoma | Ascites | P/FU/CHL |
| PEO1$^{CDDP}$ | P.D. Serous adenocarcinoma | Ascites | P/FU/CHL |
| PEO4 | P.D. Serous adenocarcinoma | Ascites | P/FU/CHL |
| PEO6 | P.D. Serous adenocarcinoma | Ascites | P/FU/CHL |
| PEO14 | W.D. Serous adenocarcinoma | Ascites | None |
| PEO16 | P.D. Serous adenocarcinoma | Ascites | Radiotherapy |
| OVCAR3 | P.D. papillary adenocarcinoma | Ascites | P/Cy/Adr |
| OVCAR4 | Adenocarcinoma | Ascites | P/Cy/Adr |
| OVCAR5 | Adenocarcinoma | Ascites | None |
| SW626 | Adenocarcinoma | — | — |
| 41M | Adenocarcinoma | Ascites | None |
| 59M | Endometrioid adenocarcinoma | Ascites | None |
| OAW42 | Serous adenocarcinoma | Ascites | P |
| A2780 | Adenocarcinoma | — | None |
| CAOV3 | Adenocarcinoma | Tumour | Cy/Adr/FU |
| SKOV3 | Adenocarcinoma | Ascites | T |

P=cisplatin; FU=5-fluorouracil; CHL=chlorambucil; T=thiotepa;
Cy=cyclophosphamide; Adr=adriamycin

Initial studies identified optimal conditions for use of the antibodies. Conditions for use of the anti-erbB2 receptor antibody were already available in our laboratory. Optimization of conditions for the anti-EGF receptor, anti-erbB3 and anti-erbB4 receptor antibodies were carried out as follows using the anti-erbB4 receptor antibody (Ab2; Neomarkers) as an example.

## 3.1 Optimization of Western blotting technology

This method involved the use of antibodies to detect levels of receptor protein in whole cell lysates. With variation in antibody affinity and the amount of receptor protein between samples it was necessary to optimize both protein loading and antibody concentration to achieve a chemiluminescent signal which when captured on Hyperfilm™ was within a linear range of optical densities to enable quantitation. Lysates were prepared as described in Materials and Methods and analysed by SDS-PAGE on a 5% polyacrylamide gel to achieve enhanced resolution at the erbB receptor positions.

## 3.1a Determination of antibody dilution

Three cell lines were chosen to determine conditions for use of the anti-erbB4 receptor antibody (Ab2; Neomarkers); PEO1 ovarian cancer cells which from preliminary RT-PCR experiments were thought to express very low levels of erbB4 receptor and OVCAR3 ovarian cancer cells and MCF7 breast cancer cells, which were both reported to express the erbB4 receptor to different extents (Beerli, 1995). A standard amount of protein (75 μg) of each of the cell lysates was loaded onto a 5% polyacrylamide gel in triplicate sets and separated by lanes containing molecular weight markers. The Western blot obtained was cut into three sections and probed with dilutions of Ab2 antibody varying from 1 / 500 to 1 / 300 according to the supplier's recommended guidelines. Fig3.1 shows a major band at 180 kDa consistent with the p180 erbB4 receptor in the MCF7 and OVCAR3 cell lines. The MCF7 cell line expressed a greater amount of p180 erbB4 receptor protein than the OVCAR3 cell line. An obvious band was not detected at the p180 position in the PEO1 cell line. Banding was detected both at higher and lower molecular weights relative to the p180 position in all three cell lines and will be discussed in further detail in section 3.1.1. Optical density was dependent on antibody dilution; the strongest signal was obtained with the 1 / 300 dilution and weakest signal with the 1 / 500 dilution. Differences in

Western blot quality were also observed with respect to antibody dilution; the 1 / 300 antibody dilution resulted in a higher background signal while the 1 / 500 antibody dilution achieved a weaker signal at the p180 erbB4 position. The intermediate dilution of 1 / 400 was chosen for further experimentation since this resulted in a clear signal at the p180 erbB4 position with relatively little interference from background.
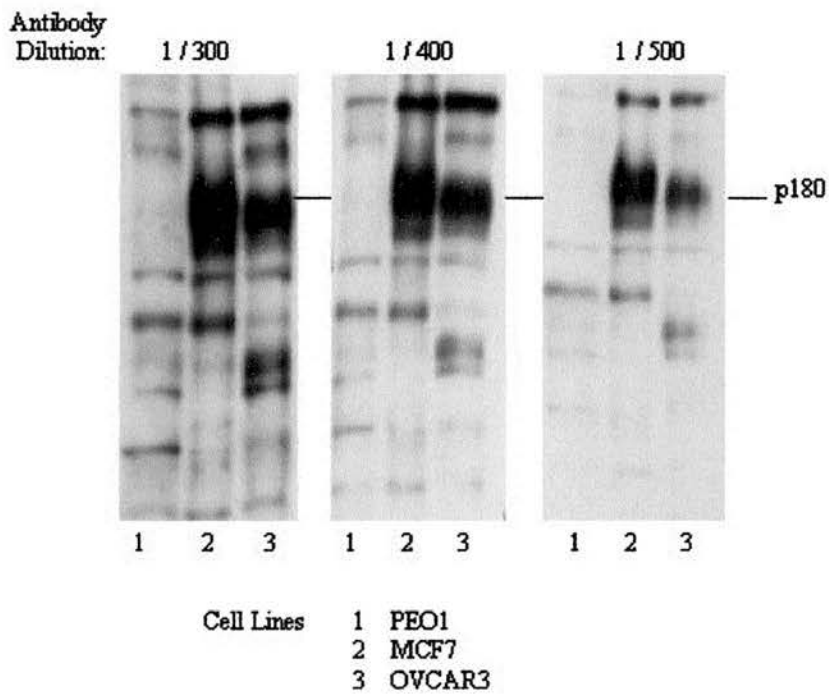


Fig 3.1 Determination of optimal antibody concentration for Western Blot analysis using anti-erbB4 Ab2 (Neomarkers). p180 erbB4 receptor was detected in MCF7 and OVCAR3 cell lines at all dilutions of antibody tested. p180 erbB4 was not clearly expressed in the PEO1 cell line although bands at higher and lower molecular weights were observed.

3.1b Optimization of protein loading

PEO1, MCF7 and OVCAR3 cell lines were used to assess optimal protein loading. This involved increased protein loading of the PEO1 cell line to determine if a signal could be detected at the p180 erbB4 position. The strong p180 erbB4 signal from the MCF7 breast cancer cell line was used to assess the density of signal achieved loading 50μg through to 125μg and determine if these signals could be visualized simultaneously with a much weaker p180 signal, if detected in the PEO1 cell line. The anti-erbB4 receptor antibody Ab2 (Neomarkers) was used at a dilution of 1 / 400 as previously determined (section 3.1a). The resulting blot (Fig 3.2) indicated that p180 erbB4 receptor protein could not be detected in the PEO1 cell line even with increased protein load of 125μg, although weak bands were still apparent above and below this position. Conversely, the increase in protein load of 100μg (lane 6) and 125μg (lane 8) of the MCF7 cell line resulted in distortion at the edges of the p180 erbB4 receptor band. Decreased protein loading of the MCF7 sample (50μg) produced a weaker signal.



Lanes:
| 1 | PEO1 50μg | 5 | PEO1 100μg |
| 2 | MCF7 50μg | 6 | MCF7 100μg |
| 3 | PEO1 75μg | 7 | PEO1 125μg |
| 4 | MCF7 75μg | 8 | MCF7 125μg |
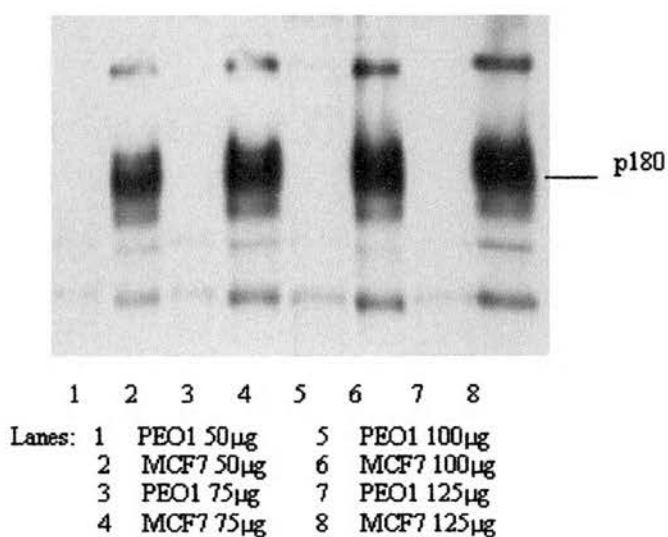
Fig 3.2 Determination of optimal protein loading using anti-erbB4 Ab2 (Neomarkers). 50-125μg of protein from the PEO1 ovarian cancer cell line and MCF7 breast cancer cell line were loaded. p180 erbB4 receptor was not detected in the PEO1 cell line even with increased loading. The p180 signal increased with increasing protein load for the MCF7 cell line.

The OVCAR3 cell line was used to investigate protein loading onto the gel and obtain signals which reflect p180 erbB4 receptor expression levels in an ovarian cancer cell line. The optical density of the p180 erbB4 band increased with amount of protein loaded through the range of 25-125µg (Fig 3.3). The band density was calibrated against a step tablet to obtain an integrated optical density value (IOD) using the *Labworks* (UVP) gel analysis package. When IOD value was plotted against amount of protein loaded (Fig3.4) the graph obtained was linear through the series 50 – 100µg loading for the OVCAR3 cell line. Again, in the OVCAR3 cell line at increased protein loading of 100µg and 125µg, the p180 erbB4 receptor band tends to become less well defined at the edges and may be due to increased background noise as a consequence of higher protein loading in the lane. The 75µg protein loading was chosen to allow for increased or decreased expression of the erbB4 receptor within the larger panel of cell lines.



| Protein load | 25µg | 50µg | 75µg | 100µg | 125µg |
|---|---|---|---|---|---|
| IOD values | 102.32 | 244.38 | 357.21 | 441.95 | 534.15 |
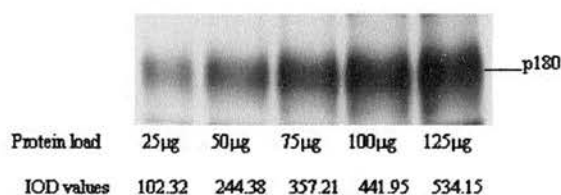
Fig 3.3 Optimal protein loading using the OVCAR3 ovarian cancer cell line. Signal optical density increased with protein loaded in the OVCAR3 cell line.
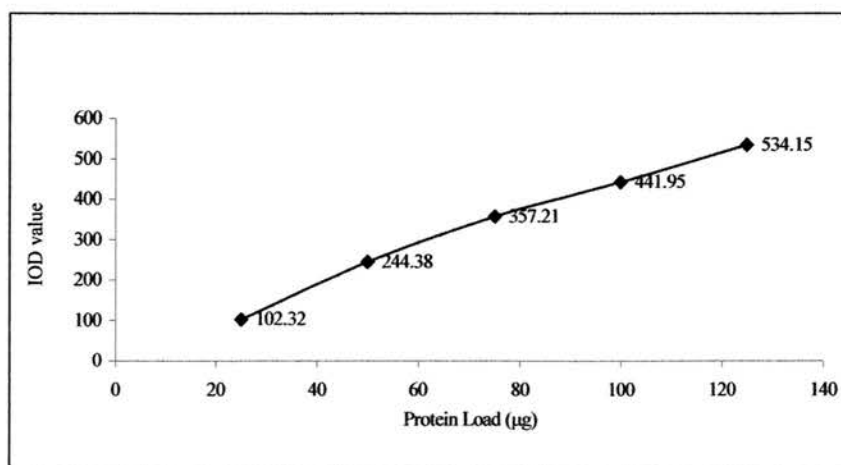


Fig3.4 Graph to show integrated optical density values vs Protein loaded (µg) for the OVCAR3 ovarian cancer cell line. Optical density is linear within the range 50-100µg protein loading for the OVCAR3 cell line.

3.1c Comparison of anti-erbB4 receptor antibodies Ab2 and HFR1

Two antibodies targeted to the erbB4 receptor, HFR1 and Ab2, were compared for detection of erbB4. The majority of antibodies available commercially to detect the erbB receptors by Western blot analysis recognize a portion of the receptor carboxyl terminal. The polyclonal Ab2 and monoclonal HFR1 antibodies were raised to the carboxyl terminal of the erbB4 receptor: HFR1antibody recognizes a peptide corresponding to amino acids 1249-1264 while Ab2 recognizes a peptide corresponding to amino acids 1285-1308 of the erbB4 receptor; both these sites are located in the carboxyl terminal autophosphorylation region (Fig 3.5).
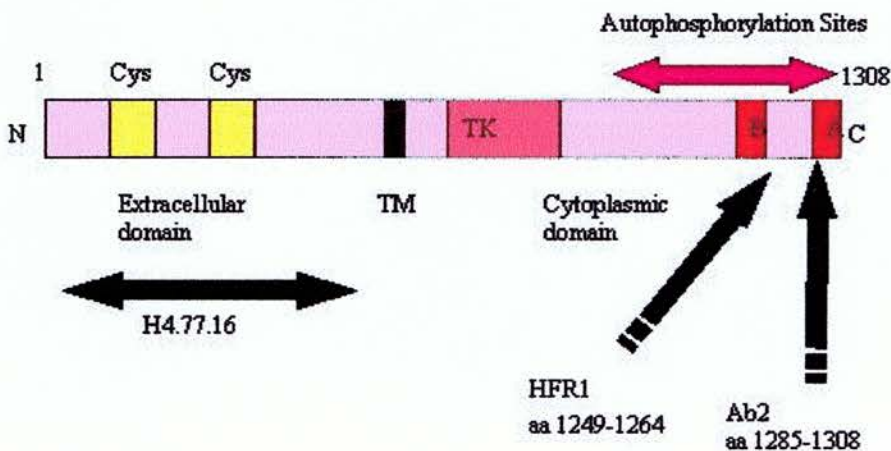


Fig 3.5 Structure of the anti-erbB4 receptor and sites to which antibodies have been targeted. Anti-erbB4 receptor antibodies HFR1 and Ab2 were raised to peptide sequences in the carboxyl terminal autophosphorylation region of the erbB4 receptor. Antibody H4.77.16 was raised to the extracellular portion of the erbB4 receptor.

The peptide 96.4 (the immunogen for HFR1) was used to investigate non-specific binding resulting in artefactual bands which may be incurred with the use of antibodies. The antibody HFR1 was used at the recommended concentration of $3\mu gml^{-1}$ with or without the peptide 96.4 ($6\mu gml^{-1}$). Antibody Ab2 was used at a dilution of 1 / 400 and the cell lines tested were PEO1, MCF7, and OVCAR3. The p180 erbB4 receptor was detected as the major band using the antibody Ab2 (Neomarkers) along with the characteristic higher and lower molecular weight bands (Fig 3.6 (i)). The corresponding blot probed with HFR1 antibody detected a band at the p180 position which was consistent with the main band detected with the Ab2 antibody, although the band density was significantly reduced (Fig 3.6 (ii)). Bands surrounding the p180 erbB4 position were observed using the HFR1 antibody and are similar to those

detected with Ab2. The blot probed with HFR1 antibody that had been pre-incubated with peptide 96.4 showed one clear band, indicating that this band (Fig 3.6 (iii)) directly below the p180 position, was likely to be an artefact and not specific for the erbB4 epitope to which the antibody had been raised. The HFR1 antibody detected 3 bands below the p180 position in the PEO1 cell line (Fig 3.4(ii) lane1). These bands were still apparent in the blot probed with HFR1 antibody pre-incubated with peptide 96.4, which suggests these are artefactual bands in the PEO1 cell line. Overall, the anti-erbB4 receptor antibody Ab2 was superior to antibody HFR1 in detecting expression levels of p180.
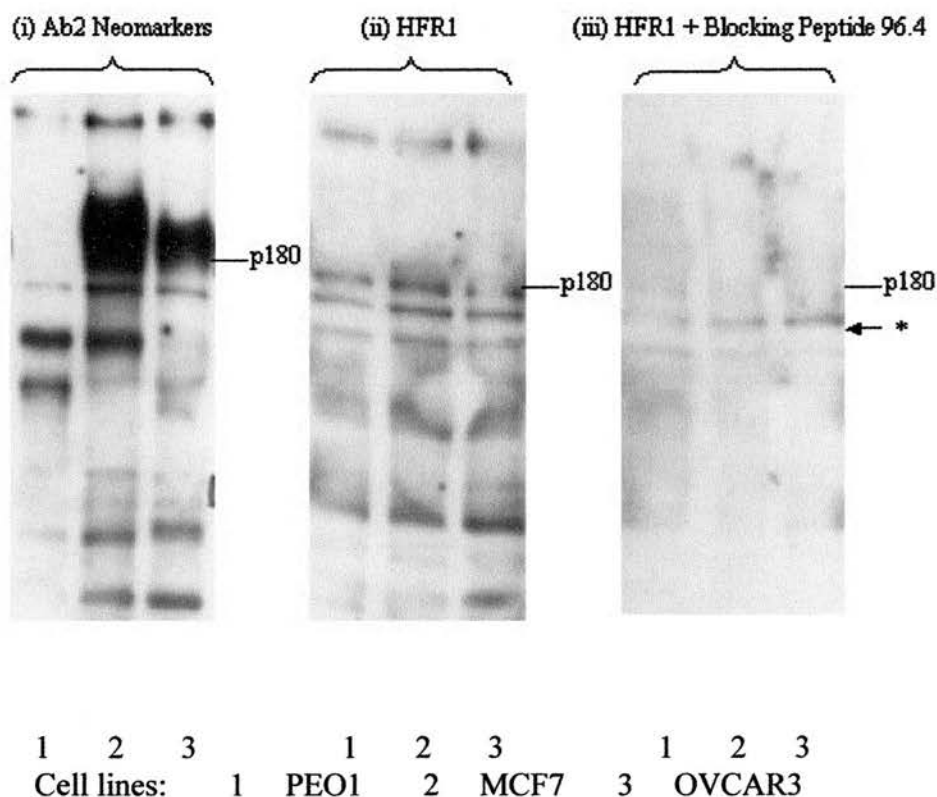


Fig 3.6 Comparison of anti-erbB4 receptor antibodies Ab2 and HFR1.(i) The polyclonal Ab2 antibody detected p180 erbB4 as the main band but also detects higher and lower molecular weight bands. (ii) Monoclonal antibody HFR detects p180 erbB4 as well as lower bands at similar positions to that observed with antibody Ab2. Intensity of the p180 erbB4 band with HFR1 was greatly reduced in comparison to antibody Ab2. (iii) HFR1 pre-incubated with the peptide 96.4 showed a clear band below p180 (*) which is most likely artefactual.

3.1d Immune-precipitation of the erbB4 receptor.

Confirmation of the position of full length erbB4 receptor was achieved by immune-precipitation using the anti-erbB4 receptor antibody H4.77.16 (Neomarkers) which is directed to the extracellular portion of the erbB4 receptor (Fig 3.5) and after separation on a gel the resulting blot probed with anti-erbB4 receptor Ab2. The samples used were PEO6 cells which had not been exposed to ligand (PEO6 control cells) and PEO6 cells which had been treated with NRG1β for 15 min. The immune-precipitated samples were run simultaneously with samples from whole cell lysates, which were blotted with anti-erbB4 receptor antibody Ab2 or anti-phosphotyrosine PY20. The resulting blot showed that full length erbB4 receptor immune-precipitates at the p180 position and that this process eliminates the downstream banding which is observed in the whole cell lysates (Fig 3.7). This is consistent with the view that the downstream banding is due to processes such as receptor degradation or to specific cleavage of erbB4 receptor isoforms (developed further in section 3.1.1). The density of the erbB4 receptor band seems to have reduced upon treatment with NRG1β in the immune-precipitated samples (Fig 3.7 lanes 1&2) although this may be due to irregular efficiency of the immune- precipitation process and is not observed with whole cell lysates (Fig 3.7 lanes 3&4). Immune-precipitation does however distinguish two areas within the p180 erbB4 receptor band (Fig 3.7*) which may correspond to the slight differences in molecular weight of the erbB4 receptor isoforms. It is also possible that this higher band is due to the p185 erbB2 receptor, which may co-precipitate with erbB4 when erbB4-erbB2 heterodimerization has occurred. Alternatively, these bands may distinguish between higher and lower tyrosine phosphorylation states of the erbB4 receptor and may instead suggest a shift to a higher tyrosine phosphorylation state in NRG1β treated cells (Fig 3.7, lane 2). In support of this, the tyrosine phosphorylation signal which is induced at the p180 position upon treatment with NRG1β (Fig 3.7, lane 6) aligns with the higher portion of the erbB4 receptor band. This suggests that erbB4 receptor tyrosine phosphorylation by NRG1β retards receptor migration through the gel and results in a band shift to a higher molecular weight.

Probe:
Anti-erbB4 receptor
antibody Ab2
(Neomarkers)

Probe:
Anti-phosphotyrosine
antibody PY20
(Santa Cruz Biotech.)

1  PEO6 CTRL
2  PEO6 NRG1β 15 min  } Immune-precipitated samples

3  PEO6 CTRL
4  PEO6 NRG1β 15min  } Non immune-precipitated samples

5  PEO6 CTRL
6  PEO6 NRG1β 15min  } Non immune-precipitated samples
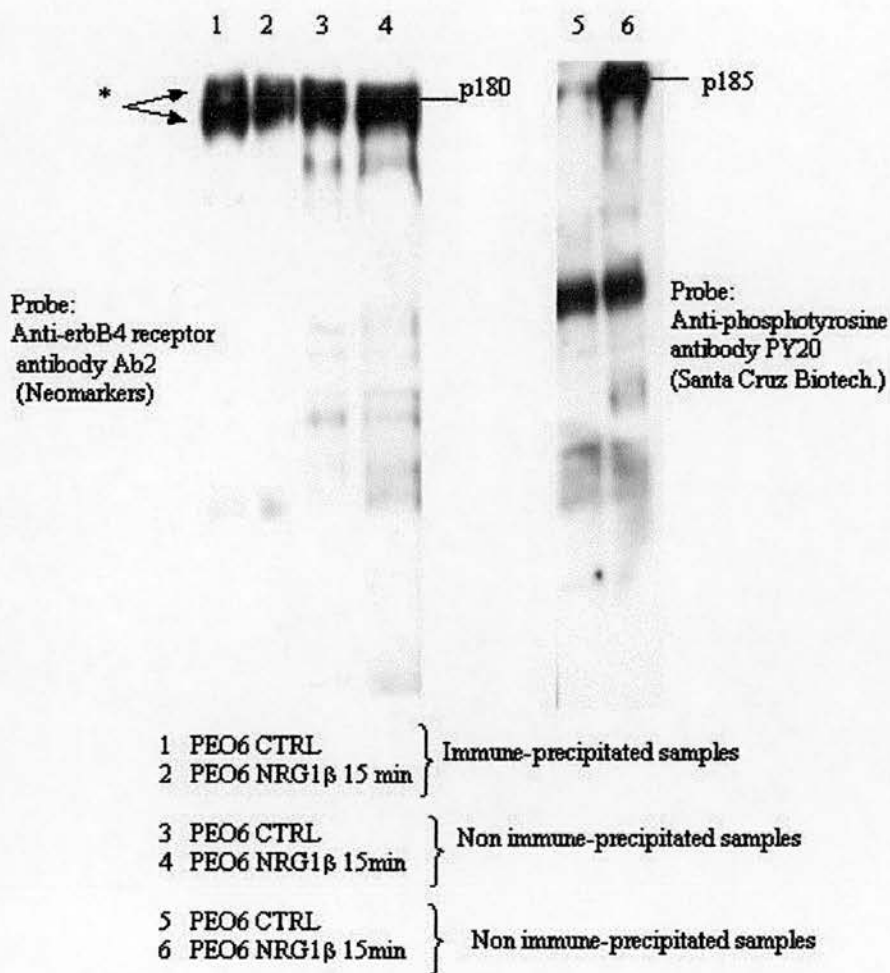
Fig 3.7 Immune-precipitation of the erbB4 receptor. Full length erbB4 immune-precipitates at the p180 position (lanes 1&2) and this process eliminates the lower molecular weight banding (lanes 3&4) previously observed in whole cell lysates. Immune-precipitation distinguishes two positions within the p180 erbB4 receptor band which could be expression of the erbB4 receptor isoforms or alternatively signify different tyrosine phosphorylation states of the erbB4 receptor (arrowed*). The higher portion of the erbB4 receptor band aligns with the p185 erbB2 receptor tyrosine phosphorylation signal and suggests erbB4-erbB2 receptor heterodimerization upon treatment with NRG1β (lane 6).

3.1.1 ErbB4 receptor protein expression

The panel of 16 ovarian cancer cell lines was tested for protein expression of the erbB4 receptor by Western blot analysis using antibody Ab2 (Neomarkers) at a dilution of 1/400 with 75µg of cell lysate. p180 erbB4 receptor expression was detected in only 8 / 16 ovarian cancer cell lines (Fig 3.8) and included PEO4, PEO6, PEO14, OVCAR3, OVCAR4, OAW42, A2780 and SKOV3. Cell lines expressing erbB4 had integrated optical densitometry values (IOD's) ranging from 14.2 (PEO14) to 1260.2 (PEO6). Although half of the cell lines did not express full length p180 erbB4 receptor, the majority possessed distinct bands at lower molecular weights. It has recently emerged that erbB4 has multiple mRNA isoforms which are designated JM-a to JM-d (Elenius, 1997)(Gilbertson RJ, 1999), CT-a and CT-b (Sawyer, 1998). These splice variants of the erbB4 receptor will be discussed in more detail in section 3.3, but it is interesting to note that the JM-a isoform that is expressed in ovarian cancer, is proteolytically cleaved by metalloproteases into two fragments; a soluble ectodomain that can be observed by gel electrophoresis around 120kDa and a membrane localised cytoplasmic tail, observed at approximately 80kDa (Vecchi M, 1997). Activation of the intracellular signalling molecule protein kinase C, enhances this proteolytic processing of the erbB4 receptor and accumulation of the 80kDa fragment intracellularly (Vecchi M, 1996). The lower band with molecular weight of approximately 80kDa (Fig 3.9 *) is consistent with expression of the 80kDa product from this cleavage event and may suggest activation of protein kinase C in these cell lines. The 120kDa product, which is composed of the extracellular domains, would not be detected by Ab2 since this antibody is specific for a region in the carboxyl tail of the erbB4 receptor. Detection of the band at 80kDa may suggest activation of protein kinase C in these cell lines. Alternatively, the lower molecular weight banding could be due to receptor degradation or to non-specific binding of the antibody.

| 1 | 2 | 3 | 4 | 5 | 6 | 7 | 8 | 9 | 10 | 11 | 12 | 13 | 14 | 15 | 16 |

| | | | |
|---|---|---|---|
| 1 PEO1 | 5 PEO14 | 9 OVCAR5 | 13 OAW42 |
| 2 PEOfᴰᴰᴾ | 6 PEO16 | 10 SW626 | 14 A2780 |
| 3 PEO4 | 7 OVCAR3 | 11 41M | 15 CAOV3 |
| 4 PEO6 | 8 OVCAR4 | 12 59 M | 16 SKOV3 |
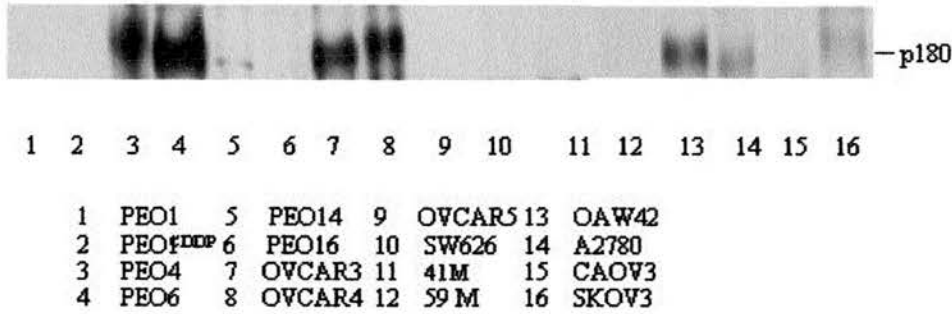
Fig 3.8 ErbB4 receptor protein expression in the panel of human ovarian carcinoma cell lines. Clear expression of the erbB4 receptor was detected in only 8 / 16 cell lines, (including PEO4, PEO6, PEO14, OVCAR3, OVCAR4, OAW42, A2780 and SKOV3) using the anti-erbB4 receptor antibody Ab2.



Cell lines:
1 59M
2 OAW42
3 PEO14
4 PEO16
5 OVCAR3
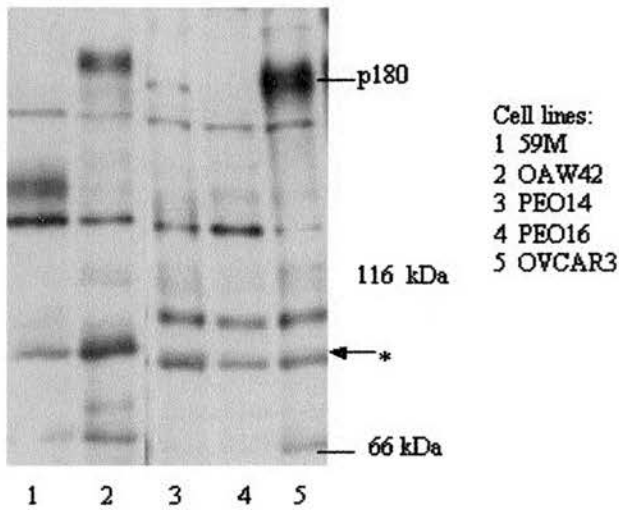
Fig 3.9 An example of full length erbB4 receptor Western blot analysis. ErbB4 receptor (p180) was differentially expressed in the panel of ovarian cancer cell lines although distinct lower banding was detected in the majority of samples. The lower band at 80kDa(*) most likely corresponds to the cytoplasmic cleavage product of the erbB4 JM-a isoform.

3.1.2 EGF receptor protein expression

The panel of 16 cell lines was investigated for expression of the EGF receptor by Western blot analysis using the anti-EGF receptor H11 & 11E8 cocktail of antibodies which recognizes both the extracellular and intracellular domains of the EGF receptor. The antibody cocktail was used at $1.5\mu gml^{-1}$ and detected p170 EGF receptor in 15 / 16 cell lines tested (Fig 3.10). Values obtained by integrated optical densitometry in cell lines expressing EGF receptor ranged from 8.8 (PEO16) to 2888.7 (41M). Only the PEO6 cell line did not test positive by gel analysis, although a weak EGF receptor band may be present but may not have been detected due to the background staining in the lane.



| 1 | PEO1 | 5 | PEO14 | 9 | OVCAR5 | 13 | OAW42 |
|---|------|---|-------|---|--------|----|-------|
| 2 | PEO1$^{CDDP}$ | 6 | PEO16 | 10 | SW626 | 14 | A2780 |
| 3 | PEO4 | 7 | OVCAR3 | 11 | 41M | 15 | CAOV3 |
| 4 | PEO6 | 8 | OVCAR4 | 12 | 59M | 16 | SKOV3 |
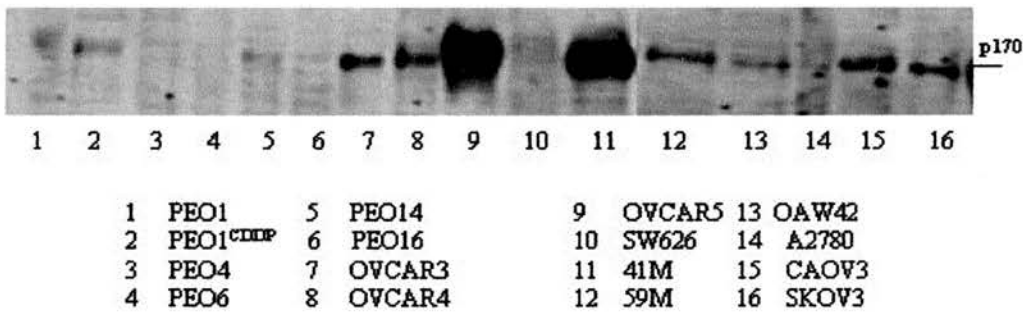
Fig 3.10 EGF receptor protein expression in the panel of human ovarian carcinoma cell lines. Anti-EGF receptor antibody cocktail H11 & 11E8 (Neomarkers), detected p170 EGF receptor expression in 15 / 16 human ovarian cancer cell lines. EGF receptor expression was not detected in the PEO6 cell line by Western blot analysis.

Lower bands were apparent in some of the cell lines, for example the PEO14 and OVCAR3 cell lines (Fig 3.11), expressed a band around 110kDa which is detected by the H11 & 11E8 cocktail. This band could possibly correspond to expression of the truncated EGF receptor vIII (p110) which has been reported to be frequently expressed in ovarian carcinomas (Moscatello DK, 1995). Banding below the p110 position is also apparent in the OVCAR4 and OVCAR5 cell lines which may reflect expression of the soluble form of the EGF receptor (60kDa) (Reiter JL, 1996).
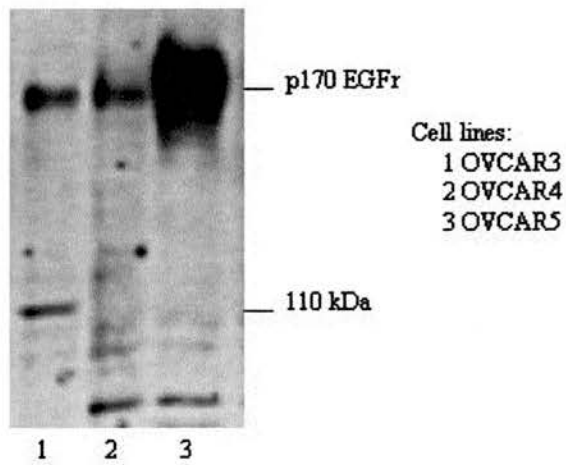
Fig 3.11 An example of full length EGF receptor Western blot analysis. Lower molecular weight banding is observed on the full length EGF receptor Western blot. It is possible that the banding around the 110kDa position is expression of the truncated EGF receptor vIII protein (p110), although a higher molecular weight glycosylated version (p140) is not apparent. It is also possible that the lower banding observed in the OVCAR4 and OVCAR5 cell lines is the soluble form of the EGF receptor (p60).

3.1.3 ErbB2 receptor protein expression

Expression of the erbB2 receptor in the panel of cell lines was investigated by Western blot analysis using the anti-erbB2 receptor antibody CB11. This antibody recognizes a site on the cytoplasmic domain of the erbB2 receptor and was used at a dilution of 1 / 60, loading 50µg cell lysate. The erbB2 receptor appeared as a single band at the p185 position in all of the 16 cell lines tested (Fig 3.12). The IOD values obtained for erbB2 receptor expression ranged from 13.2 (PEO16) to an estimated 5242 (see below for SKOV3). No other bands were observed on the gel using the anti-erbB2 receptor antibody CB11.
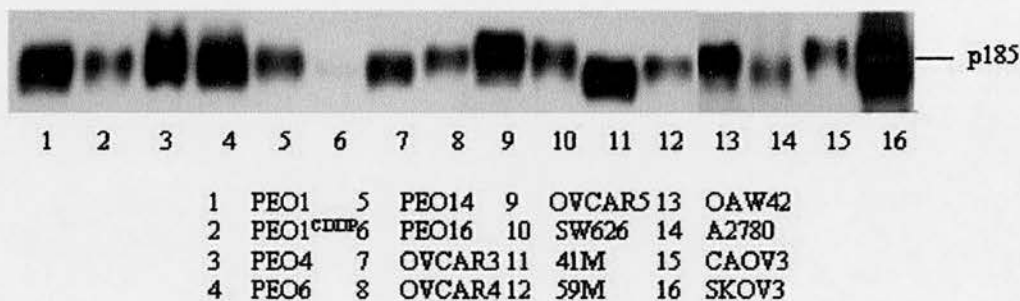


Fig 3.12 ErbB2 receptor protein expression in the panel of human ovarian carcinoma cell lines. Antibody CB11 (Novocastra) detected erbB2 receptor expression in all of the ovarian cancer cell lines. ErbB2 receptor expression varied from IOD values of 13.2 (PEO16) to an estimated 5242 (SKOV3). The SKOV3 cell line had an extremely high protein expression of erbB2 which required 1/5 of the usual protein loading for visualization simultaneously with the other cell lines.

The SKOV3 cell line possessed a high level of expression of the erbB2 receptor and required sample dilution to obtain a signal that could be visualized simultaneously with the other cell lines. Loading 10µg of SKOV3 cell lysate allowed an IOD measurement of 1048.4 to be obtained. Since all other cell lysates were loaded at 50µg per lane, the SKOV3 sample has been given an estimated IOD value of 5242 which is five times the value obtained for the 10µg load. Extrapolating a graph of IOD values obtained for 1, 10 and 20 µg of SKOV3 cell lysate confirmed that an IOD value for 50µg would be in the region of 5242 (not shown).

### 3.1.4 ErbB3 receptor protein expression

Expression of the erbB3 receptor in the panel of cell lines by Western blot analysis was investigated using the anti-erbB3 RTJ2 antibody which is directed to the carboxyl terminus of the receptor. This was used at a concentration of $2\mu gml^{-1}$ with loading a protein content of 125μg cell lysate. Although the erbB3 receptor has a molecular weight of 180 kDa, it characteristically appears as a doublet at 160kDa when analysed by Western blotting. In the panel of 16 ovarian cancer cell lines, erbB3 receptor protein was clearly detected in 15 (Fig 3.13). Only the 59M cell line did not display protein expression of the p160 erbB3 receptor and has been classified as negative. In cell lines expressing p160 erbB3 receptor, IOD values ranged from 6.47 (PEO14) to 396.25 (PEO1$^{CDDP}$). Lower molecular weight banding was detected using the RTJ2 antibody, with band positions of approximately 130, 100 and 60kDa (Fig 3.14). As yet publications referring to protein expression of alternate erbB3 transcripts are only detected by antibodies specific for the extracellular domain of erbB3 and would therefore not be recognized by the RTJ2 antibody. To date, there are no other publications detailing smaller molecular weight species of the erbB3 receptor. Therefore, these bands are likely artefactual and due to non-specific binding of the antibody, or possibly due to receptor degradation.



| | | | | | | | | | | | | | | | |
|1|2|3|4|5|6|7|8|9|10|11|12|13|14|15|16|

| | | | |
|---|---|---|---|
|1 PEO1|5 PEO14|9 OVCAR5|13 OAW42|
|2 PEO1$^{CDDP}$|6 PEO16|10 SW626|14 A2780|
|3 PEO4|7 OVCAR3|11 41M|15 CAOV3|
|4 PEO6|8 OVCAR4|12 59M|16 SKOV3|
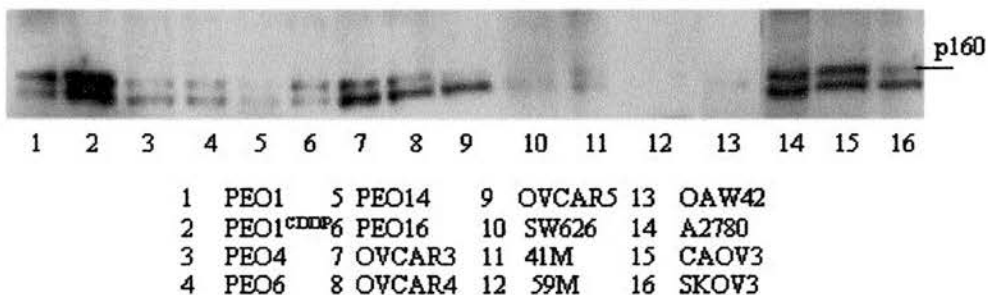
Fig 3.13 ErbB3 receptor protein expression in a panel of human ovarian carcinoma cell lines. Antibody RTJ2 (Neomarkers) detected erbB3 receptor protein in 15 / 16 cancer cell lines. Only the cell line 59M showed no apparent expression of the erbB3 receptor.
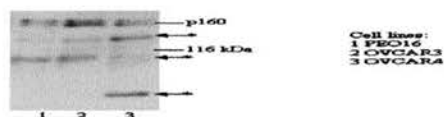
Fig 3.14 An example of full length erbB3 Western blot. Lower molecular weight banding was detected using the antibody RTJ2 (Neomarkers). It is most likely the bands at around 130kDa, 100kDa and 60kDa (*) are due to non-specific binding of the antibody or due to receptor degradation.

## 3.1.5 Summary of erbB receptor expression in the panel ovarian cancer cell lines

ErbB receptor protein expression investigated by Western blot analysis demonstrated that the majority of ovarian cancer cell lines express the EGF receptor, erbB2 and erbB3. The EGF receptor and erbB3 proteins were expressed in 15 of the 16 cell lines and erbB2 was detected in all of the cell lines (Fig 3.15 & Table 3.1). Expression of the erbB4 receptor differed dramatically from the other three receptors; only 8 of the 16 cell lines tested positive for p180 erbB4 receptor protein. This demonstrates that the majority of ovarian cancer cell lines express multiple erbB receptors.
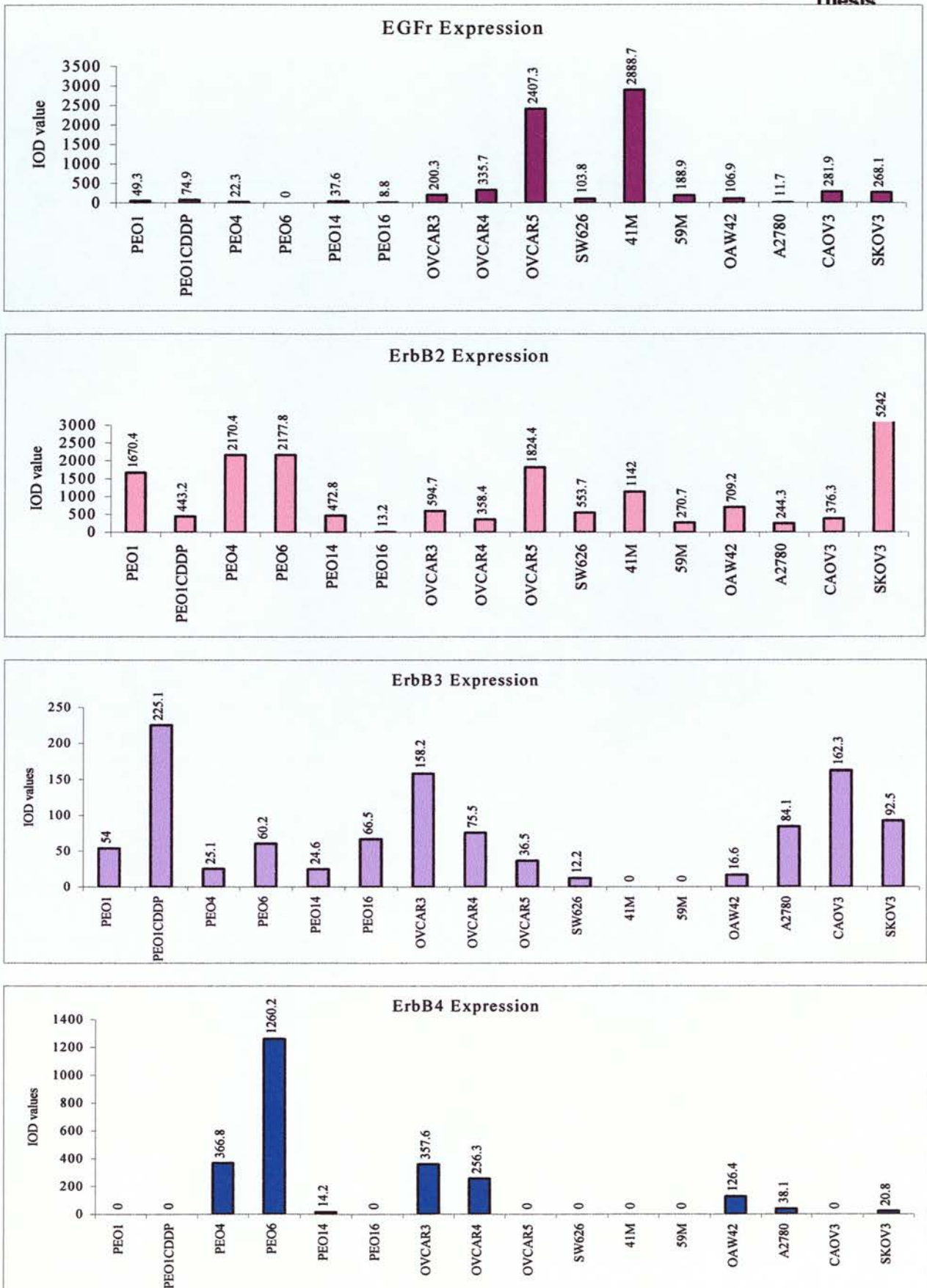
Fig 3.15 Expression of the erbB receptors in ovarian cancer cell lines. The majority of ovarian cancer cell lines express multiple erbB receptors. Expression of the erbB4 receptor protein was less consistent and detected in only 8 / 16 ovarian cancer cell lines investigated. IOD= Integrated Optical Density

Table 3.1 Summary of erbB receptor expression (IOD values) in the panel of 16 ovarian cancer cell lines.

| Cell Line | EGFr | ErbB2 | ErbB3 | ErbB4 |
|-----------|------|-------|-------|-------|
| PEO1 | 49.3 | 1670.4 | 126.0 | — |
| PEO1$^{CDDP}$ | 74.9 | 443.2 | 396.3 | — |
| PEO4 | 22.3 | 2170.4 | 39.4 | 366.8 |
| PEO6 | ± | 2177.8 | 33.1 | 1260.2 |
| PEO14 | 37.6 | 472.8 | 6.5 | 14.2 |
| PEO16 | 8.8 | 13.2 | 41.7 | — |
| OVCAR3 | 200.3 | 594.7 | 184.9 | 357.6 |
| OVCAR4 | 335.7 | 358.4 | 126.5 | 256.3 |
| OVCAR5 | 2407.3 | 1824.4 | 106.2 | — |
| SW626 | 103.8 | 553.7 | 16.7 | — |
| 41M | 2888.7 | 1142.0 | 32.6 | — |
| 59M | 188.9 | 270.7 | — | — |
| OAW42 | 106.9 | 709.2 | 9.1 | 126.4 |
| A2780 | 11.7 | 244.3 | 242.8 | 38.1 |
| CAOV3 | 281.9 | 376.3 | 218.9 | — |
| SKOV3 | 268.1 | >5242.0 | 129.5 | 20.8 |

±   Weak expression
—   expression not detected

## Chapter 3.2 Expression of neuregulin (NRG)

The following section describes investigations of the presence of NRG expression in ovarian cancer cell lines (3.2.1) and human ovarian tumours (3.2.2). Expression of NRG mRNA was determined by Reverse Transcription Polymerase Chain Reaction (RT-PCR) using primers which detect a sequence common to all known NRG isoforms. mRNA's from human ovarian cancer cell lines and tumours were prepared and reverse transcribed enabling primers to amplify a NRG specific cDNA sequence by PCR and yield a product of 255 base pairs. Primers specific for γ-actin were used to control for quality of the mRNA samples and yielded a product of 250 base pairs. DEPC treated water was used as a control to identify the presence of contamination in the reagents.

3.2.1 Expression of NRG in ovarian cancer cell lines

The presence of NRG mRNA was examined in 9 ovarian cancer cell lines (PEO1, PEO4, PEO6, OVCAR5, 41M, SW626, 59M, SKOV3 and PEO1$^{CDDP}$). Of these 9, 8 tested positive for expression of NRG mRNA (Fig 3.16) with clear expression of the product at 255 bp's. The only cell line in which NRG mRNA was not detected was OVCAR5 (Fig 3.13 lane 4) and was classified as negative. All cell lines tested positive for expression of γ-actin mRNA expressing bands at 250 bp's, while a water control sample tested negative. This experiment was repeated and the same result obtained. These results demonstrate that the majority of ovarian cancer cell lines express mRNA for NRG.

67
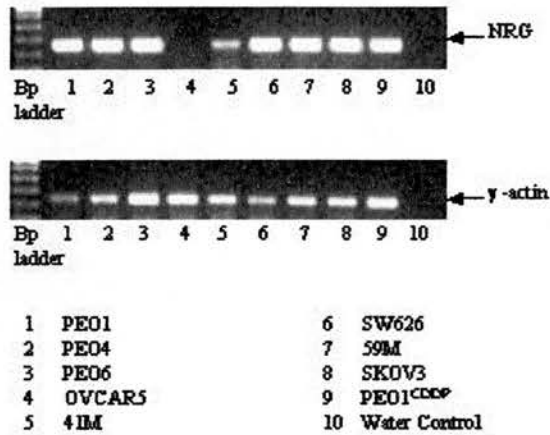
Fig 3.16 mRNA expression of NRG in ovarian cancer cell lines. NRG expression was detected in 8 / 9 ovarian cancer cell lines; only the OVCAR5 cell line (lane4) did not express mRNA for NRG although positivity for γ - actin was detected. The water control samples tested negative.

## 3.2.2 Expression of NRG in human ovarian tumours

A panel of human ovarian tumours of different histological subtypes was assessed for mRNA expression of NRG as detected by RT-PCR. Of the 24 human ovarian carcinomas investigated, 22 were clearly positive for expression of NRG mRNA and 2 tested weakly positive (HOV tumours 77 and 99), with a product band at the appropriate size of 255 bp's (Fig 3.17). All tumour samples tested positive for γ-actin yielding product bands at 250bp's. The tumour sample 12 had a weak signal for γ-actin although mRNA for NRG was still detected. These results are typical of an experiment that was carried out in triplicate. Water control samples tested negative. These results demonstrate that the majority of human ovarian tumours express mRNA for NRG.

Chapter 3
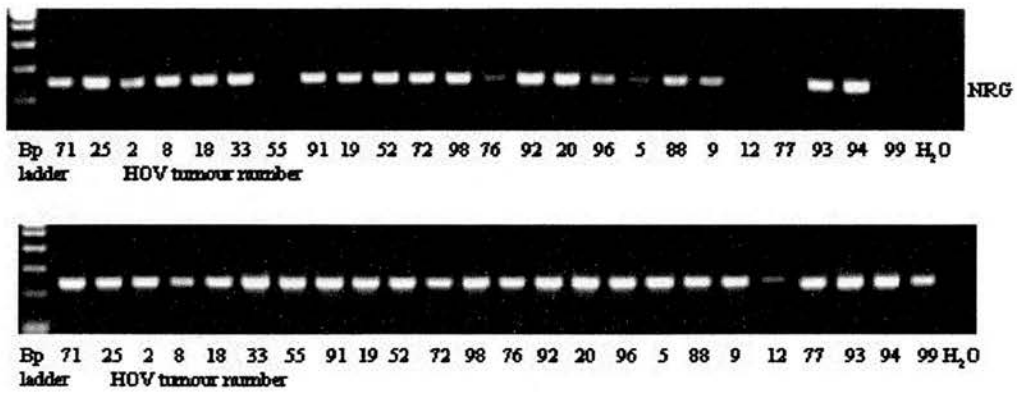
Fig 3.17 mRNA expression of NRG in human ovarian tumours. A panel of 24 human ovarian tumours were tested for mRNA expression of NRG by RT-PCR. 22 / 24 tumours tested positive for NRG mRNA and $\gamma$-actin was used to control for quality of mRNA. This analysis is typical of an experiment which was carried out in triplicate.

69

Chapter 3

Chapter 3

## Chapter 3.3 Expression of the erbB4 receptor isoforms

The following section describes the investigation of expression of the recently identified erbB4 receptor isoforms in ovarian cancer cell lines and human ovarian tumours. To date, several isoforms have been identified and designated JM and CT; JM-a, JM-b (Elenius, 1997), JM-c and JM-d (Gilbertson RJ, 1999) are splice variants of a sequence in the juxtamembrane domain; CT-a and CT-b isoforms (Sawyer, 1998) arise from splicing of a region in the carboxyl terminal encoding the single erbB4 receptor phosphatidyl inositol 3-kinase binding site (See Fig 1.5). Expression of the JM and CT isoforms was investigated by RT-PCR using primers which amplify a sequence spanning these regions. The primers that were used and the sequences which they amplify from the published erbB4 sequence (L07868) are shown in Tables 3.2 (JM isoforms) and 3.3 (CT isoforms).

Table 3.2 Partial sequence of the erbB4 receptor showing the sequence specific to the JM-a isoform.

1701 ccccagtgt gagaagatgg aagatggcct cctcacatgc catggaccgg gtcctgacaa
1761 ctgtacaaag tgctctcatt ttaaagatgg cccaaactgt gtggaaaaat gtccagatgg
1821 cttacagggg gcaaacagtt tcattttcaa gtatgctgat ccagatcggg agtgccaccc
1881 atgccatcca aactgcaccc aagggtg[1908]**taa cggtccccact agtcatgact gcatttacta**
1941 **cccatggacg ggccattcca ctttaccaca acatgc** [1976] taga actcccctga ttgcagctgg
2001 agtaattggt gggctcttca ttctggtcat tgtgggtctg acatttgctg tttatgttag

The JM-a specific sequence is shown in bold and the sequence to which the primers were directed is shown in grey.

The sequence of the JM-a isoform is that of the full length sequence in the Genbank database (L07868). The other JM isoforms differ in the following manner: The JM-b isoform contains [1908] **cataggctcaagtattgaagactgcatcggcctgatgga** , in place of the JM-a specific sequence [1908]**taa cggtccccact agtcatgact gcatttacta cccatggacg ggccattcca ctttaccaca acatgc** [1976]. Alternate splicing of these sequences gives rise to another two isoforms; JM-c has neither sequence while JM-d contains both JM-a and JM-b sequences (Gilbertson RJ, 1999). The expected JM product sizes using the above primers are as follows: JM-a 375 bp's, JM-b 345 bp's, JM-c 306 bp's and JM-d 414 bp's.

71

The sequence for the CT-a isoform is shown in Table3.3.

Table 3.3 Partial sequence of the erbB4 receptor showing the sequence specific for the CT-a isoform.

3041 tctttcagaa tctcttggat gaagaggatt tggaagatat gatggatgct gaggagtact tggtccctca
3111 ggctttcaac atcccacctc ccatctatac ttccagagca agaattgact cgaatagga[3169]g
3171**tgaaattgga cacagccctc ctcctgccta cacccccatg tcaggaa**[3217]acc agtttgtata
3231 ccgagatgga ggttttgctg ctgaacaagg agtgtctgtg ccctacagag ccccaactag cacaattcca
3301 gaagctcctg tggcacaggg tgctactgct gagattttttg atgactcctg ctgtaatggc accctacgca

The CT-a specific sequence is shown in bold and the sequence to which the primers were directed is shown in grey. The CT-b isoform lacks this 48 bp sequence of CT-a.
CT product sizes using the above primers are as follows: CT-a 296 bp's, CT-b 248 bp's.

3.3.1 Optimization of the erbB4 isoform specific PCR

Conditions for the PCR of the erbB4 receptor JM and CT regions were
optimized using cDNA samples from the PEO6 and OAW42 cell lines. The OAW42
cell line had previously been shown to express the JM-a but not the JM-b isoform and
both CT-a and CT-b isoforms (personal communication with Prof. WJ Gullick) and
was used as a control. Preliminary PCR experiments yielded poor results justifying
optimization that involved variation of primer annealing temperature, magnesium
concentration and number of PCR cycles.

3.3.1a Optimization of primer annealing temperature

The calculated annealing temperatures for the primers were 59°C (JM) and
63°C (CT), although preliminary experiments conducted at these temperatures
resulted in poor product yield. A series of less stringent (lower) annealing
temperatures were chosen to enhance primer binding to sequence and increase product
yield (Innis MA, 1990). The annealing temperature was varied from 48°C to 60°C
through increments of 4°C. All other parameters were kept constant and the PCR
reaction was conducted through a series of 35 cycles. Primers specific for γ-actin were
used to control for quality of the RNA. To control for genomic contamination in the
RNA, samples which had been reverse transcribed (+RT) and those which had not
(-RT) were used. DEPC treated water was used to check for contamination in the
reagents.

Chapter 3

The JM primers detected a band around 375bp's consistent with JM-a isoform expression in both the PEO6 and OAW42 cell lines throughout the range of annealing temperatures investigated (Fig 3.18). In the PEO6 cell line an increase in product yield was observed through the series 48-56 °C, before a reduction in product yield at 60°C. Product yield increased with increase in annealing temperature from 48 to 52°C in the OAW42 cell line and was reduced at the higher annealing temperatures of 56 and 60°C. A higher band above 400 bp's was detected in the PEO6 cell line samples when annealing temperatures of 48 and 52°C were used. This higher band was possibly due to expression of the JM-d isoform. Alternatively, this could be a non-specific product as a result of reducing the primer specificity in lowering the annealing temperature. Lower bands corresponding to the erbB4 receptor JM-b and JM-c isoforms were not observed or if present, were below the limit of detection by RT-PCR.

73

Chapter 3
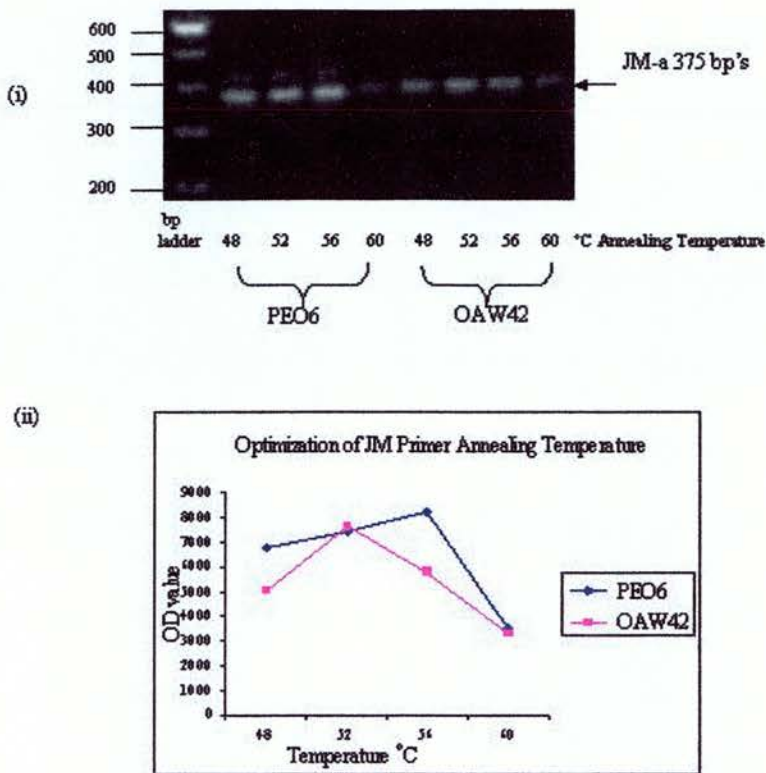
Fig 3.18 Optimization of annealing temperature for the primers specific to the erbB4 receptor JM isoforms. (i)Product yield increased with increasing annealing temperature from 48-56°C for both PEO6 and OAW42 cell lines before a reduction in product yield at 60°C. (ii) Plot of optical density vs annealing temperature demonstrated the PEO6 cell line had greatest product yield at 56°C while the OAW42 cell line had maximum product yield at 52°C.

The CT primers detected two bands in both the PEO6 and OAW42 cell lines (Fig 3.19). The upper band size around 300 bp's was consistent with the CT-a isoform; the lower band size was around 250 bp's consistent with the CT-b isoform. The higher band (CT-a) was of stronger intensity than the lower band (CT-b). Increase in annealing temperature through the series 48-60 °C did not significantly affect product yield in either the PEO6 or OAW42 cell line although a slight increase in yield was observed at 60 °C.

Chapter 3
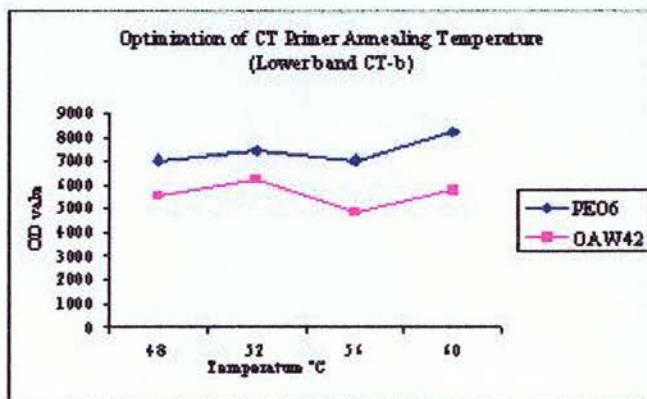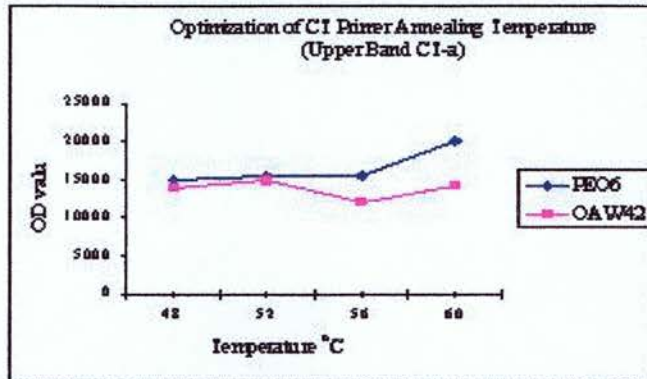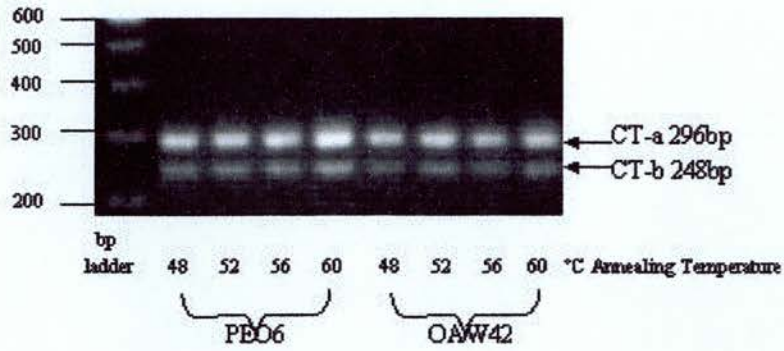
3.19 Optimization of the annealing temperature for the primers specific to the erbB4 receptor CT isoforms.(i) The increase in annealing temperature did not seem to significantly alter product yield of either the CT-a or CT-b isoforms. With gel analysis and plotting optical density against annealing temperature, a slight increase in product yield at 60°C for both the CT-a (ii) and CT-b (iii) isoforms was demonstrated

75

Primers for γ-actin detected a single band at 250 bp's in both PEO6 and OAW42 cell line samples which had been reverse transcribed (Fig 3.20). Samples which had not been reverse transcribed were negative and water control samples were also negative (not shown).

The annealing temperature of 52 °C was chosen for both the JM and CT primers; this temperature resulted in a good yield of product in both the PEO6 and OAW42 cell lines using the JM primers while the annealing temperature had little effect on CT product yield.
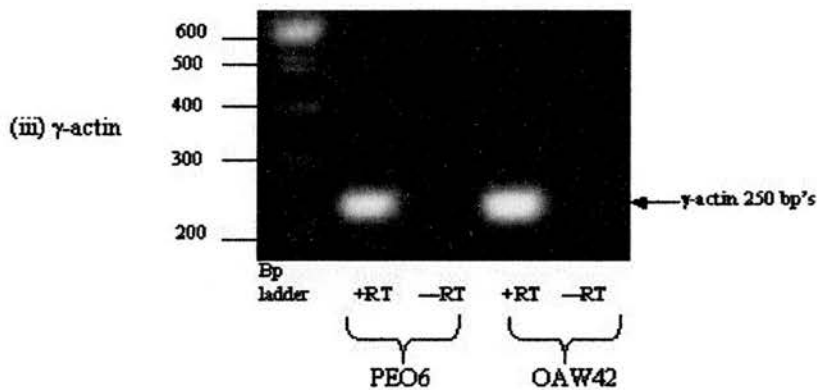


Fig 3.20 Primers specific for γ-actin were used to control for quality of RNA from the PEO6 and OAW42 cell lines. Samples which had been reverse transcribed (+RT) tested positive and those which had not (-RT) were negative for γ-actin expression.

3.3.1b Optimization of magnesium concentration

The PCR reaction for the JM and CT primers used a standard 1.0mM of    Mg $^{2+}$. Optimization involved concentrations of 0.5, 1.0, 1.5, 2.0 and 2.5mM Mg$^{2+}$ in the individual PCR's using cDNA from the OAW42 cell line as a template. Each PCR went through 35 cycles using an annealing temperature of 52°C (section 3.3.1a). Water was used as a control for detecting contamination in the reagents.

A product was not detected with either the JM or CT primers when 0.5mM Mg $^{2+}$ was used in the reaction (Fig 3.21). At higher concentrations JM primers produced a band around 400 bp's with maximum band intensity at 1.5mM Mg $^{2+}$. It is possible that the JM band is composed of two components as previously observed (Fig 3.18), but owing to the decreased                resolution of this gel this is difficult to

Chapter 3

visualize. The CT primers yielded products of around 300 and 250 bp's corresponding to CT-a and CT-b isoform expression respectively (Fig 3.21). Again, individual PCR product bands are less easily visualized due to decreased resolution of this gel. Similarly, CT band intensity was maximal at 1.5mM Mg$^{2+}$ and this was chosen for further analyses with both JM and CT primers. All water control samples tested were negative.
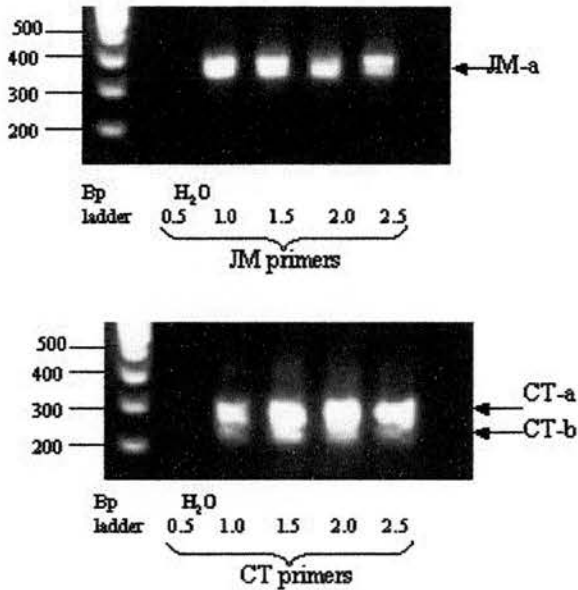


Fig 3.21 Optimization of magnesium concentration for the PCR reaction using the JM and CT primers and cDNA from the OAW42 cell line. Product was not detected using 0.5mM Mg$^2$ for either the JM or CT primers. For both the JM and CT primers, signal intensity corresponding to product formation, increased with increasing Mg$^{2+}$ concentration upto a maximum at 1.5mM Mg$^{2+}$. A reduction in product formation was observed at 2.0 and again at 2.5mM Mg$^{2+}$.

Chapter 3

3.3.1c Optimization of PCR Cycle Number

All reactions thus far had gone through 35 PCR cycles. Optimization of PCR cycles involved cDNA samples from the PEO6 cell line undergoing 25, 30, 35, and 40 cycles with 1.5mM Mg $^{2+}$ per reaction and an annealing temperature of 52 °C. DEPC treated water was used to control for contamination in the reagents.

The JM primers yielded a weak signal below 300 bp's after 25 PCR cycles. The intensity of the signal increased with increasing cycle number (Fig 3.22). The CT primers produced weak bands at 250 and 300 bp's after 25 PCR cycles. Both CT-a and CT-b bands increased with increasing cycle number and the intensity of the upper band (300 bp's CT-a) was greater than that of the lower band (250 bp's CT-b) in all samples. A high cycle number often results in increased amount and complexity of non-specific background products [M A Innis, 1990 #69]. This was observed with the CT primers which had undergone 40 PCR cycles (Fig 3.22 arrowed *). Therefore 35 cycles was chosen for both the JM and CT primers to investigate the expression of the erbB4 receptor isoforms in ovarian cancer cell lines (Section 3.3.2) and human ovarian tumours (Section 3.3.3).

Chapter 3
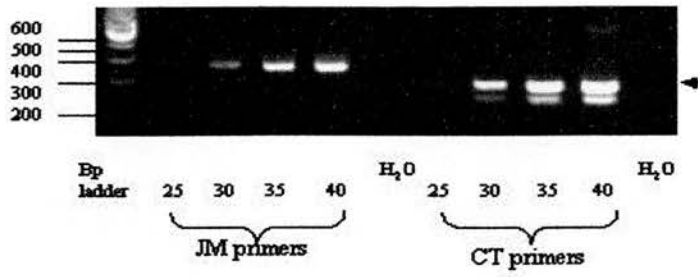
Fig 3.22 Optimization of PCR cycle number. cDNA from the PEO6 cell line was used to assess product formation after 25, 30, 35 and 40 PCR cycles using the JM and CT primers. The intensity of the signal increased with increasing cycle number for both the JM and CT primers. Formation of non-specific background product was detected using the CT primers and 40 PCR cycles *.

79

Chapter 3

### 3.3.2 Expression of the ErbB4 Receptor Isoforms in Ovarian Cancer Cell Lines

mRNA from the following panel of ovarian cancer cell lines were used to investigate expression of the erbB4 receptor JM and CT isoforms by RT-PCR: PEO1, PEO1$^{CDDP}$, PEO6, SKOV3, PEO16, OVCAR3, OVCAR5, SW626, 41M and OAW42.

Primers for γ-actin were used to ensure integrity of the mRNA samples and DEPC treated water was used to check for contamination in the reagents.

The JM primers yielded products in 5 / 10 ovarian cancer cell lines (Fig 3.23 (i)). A band under 400 bp's was detected in 5 cell lines consistent with erbB4 receptor JM-a isoform expression. Cell lines with putative JM-a expression were PEO6, SKOV3, OVCAR3, 41M and OAW42. Another band over 400bp's was detected in the cell lines PEO6, OVCAR3, and OAW42 and is consistent with expression of the JM-d isoform. Intensity of signal for the JM-d isoform was less than that observed for JM-a. Bands corresponding to the JM-b or JM-c isoforms were not observed and if present, were below the limit of detection by RT-PCR.

The CT primers yielded products of 300 and 250 bp's consistent with CT-a and CT-b expression in the same 5 cell lines which tested positive for the JM isoform expression (Fig 3.23 (ii)). A very weak signal at 300 bp's (CT-a position) was also detected for the PEO1 and OVCAR5 cell lines. For the majority of cell lines, which expressed the CT isoforms, the intensity of the CT-a band was greater than that observed for CT-b. The single exception was the SKOV3 cell line which had a more intense signal for CT-b isoform expression than for CT-a. γ-actin tested positive for all cell lines and water control samples were negative (Fig 3.23 (iii)).

80
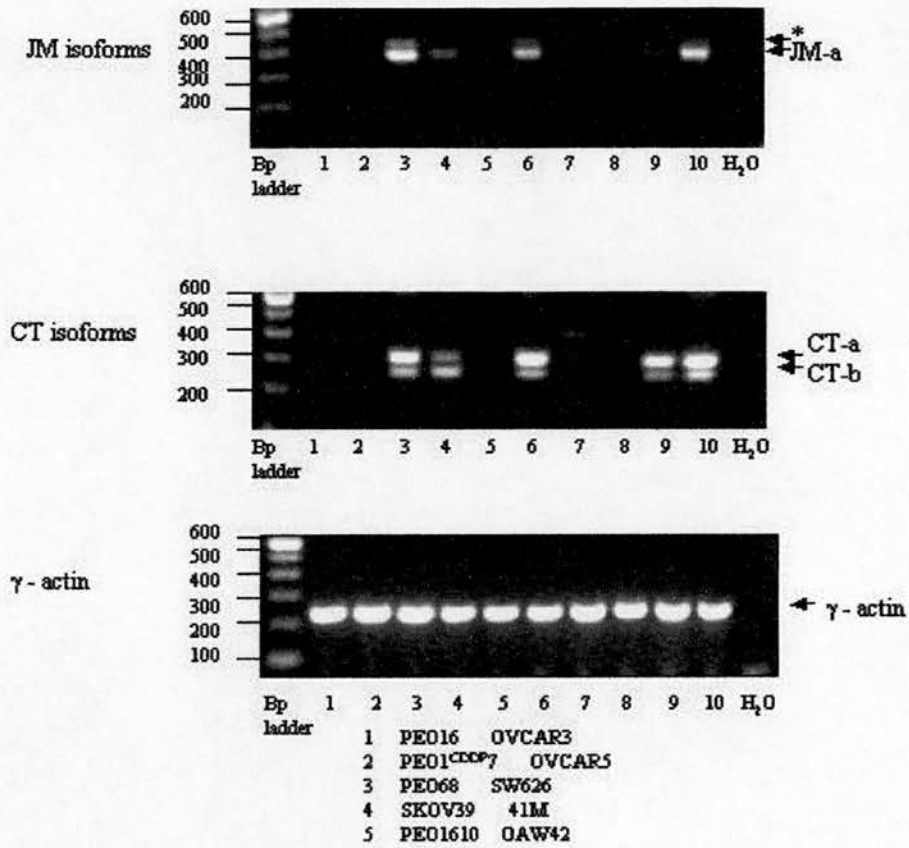
Fig3.23  mRNA expression of the JM and CT erbB4 receptor isoforms in ovarian cancer cell lines
detected by RT-PCR. (i) The JM-a isoform is detected in 5 / 10 of the cell lines,the PEO6 (lane3),
OVCAR3 (lane6) and OAW42 (lane10) cell lines posessed a higher band which is possibly expression
of the JM-d isoform *. Expression of the JM-b or JM-c isoforms was not detected. (ii) Expression of
both CT-a and CT-b isoforms was observed in the same 5 cell lines that were positive for JM-a
expression. (iii) γ - actin was used to control for quality of mRNA and tested positive in all samples.
DEPC treated water was used to control for contamination in the reagents and tested negative.

81

Chapter 3

This experiment was duplicated with products run on a longer 2.5% agarose gel to allow greater resolution between the product bands. The resulting gel was analysed by Labworks (UVP), inverted to ease visualization and calibrated against the base pair ladder to obtain estimated product sizes. The JM-a product sizes ranged from an estimated 383 bp's (PEO6 - lane 3) to 392 bp's (OAW42 - lane10)(Fig 3.24 (ii)). The higher band which was thought to correspond to JM-d isoform expression was found to have estimated sizes of 434 bp's (PEO6), 438 bp's (PEO16) and 441 bp's (OAW42). Gradual increase in product sizes from the left to right side of the gel indicated a small inconsistency in the gel run which may account for the increase in product size, alternatively inaccuracy in calibration against the base pair ladder may also contribute to the error.

The CT isoforms expressed by the cell lines had estimated sizes ranging from 296 bp's (OAW42) to 305 bp's (SKOV3) for the CT-a isoform; and 250 bp's (OAW42) to 256 bp's (SKOV3) for the CT-b isoform (Fig 3.24 (ii)). These product sizes were consistent with that expected for the CT isoforms. An increasing drift in product size was observed across the gel and indicated an inconsistent gel run.

Chapter 3
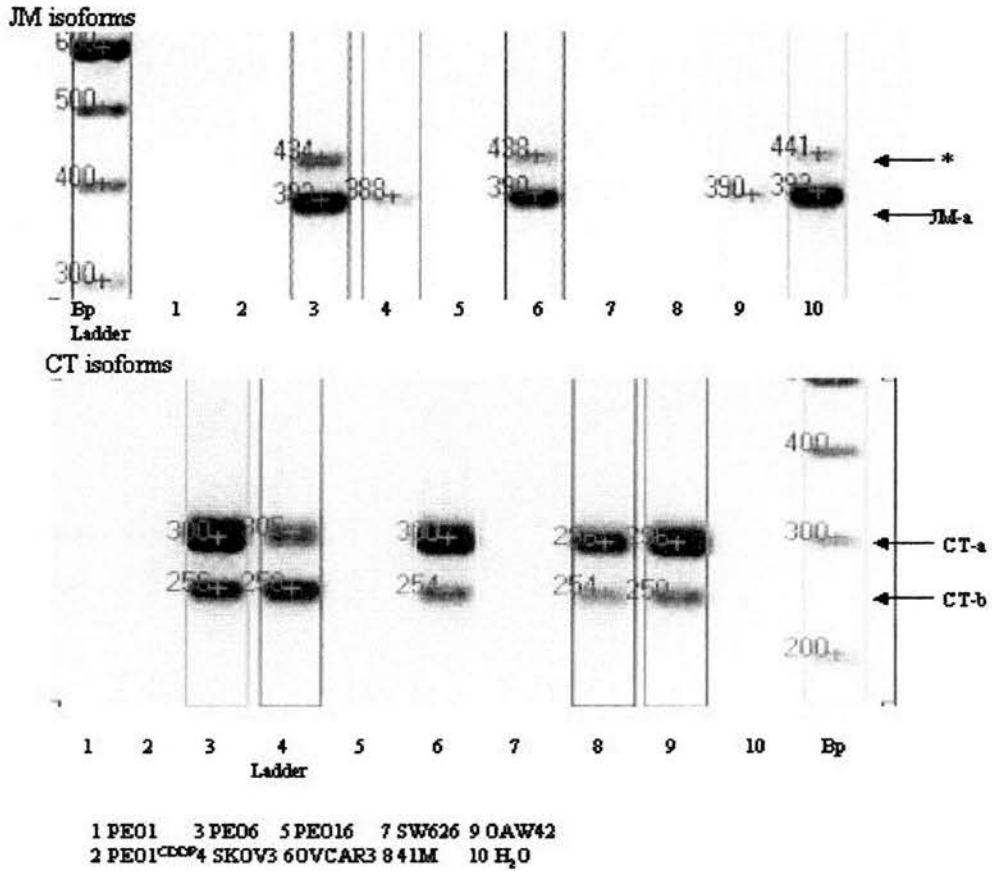
Fig 3.24 The same panel of cell lines from Fig3.20 was run on a longer 2.5% agarose gel to achieve greater resolution of the banding for analysis by Labworks 3.0 (UVP). Calibration against the 100 base pair ladder shows the JM bands run at approximately 390bp's which is consistent with that expected for JM-a (375 bp's) and 440bp's which is most likely the more recently identified JM-d isoform. The CT bands were approximately 300bp's and 250bp's consistent with that expected for CT-a and CT-b respectively.

83

Chapter 3

### 3.3.3 Sequencing of the erbB4 receptor isoforms

PCR products from the PEO6 cell line which were thought to correspond to the JM-a, JM-d, CT-a and CT-b erbB4 receptor isoforms were sequenced to confirm their identity. The PCR products were purified on a Sea-Plaque Agarose gel, extracted and purified by a Wizard Prep. Column. The cDNA product was ligated, inserted into P-Gem-T Easy Vector™ (Fig 3.25) and grown in JM109 cells plated on agar. Transformed colonies were checked for product by PCR. The product was then end labelled with rhodamine for sequencing.
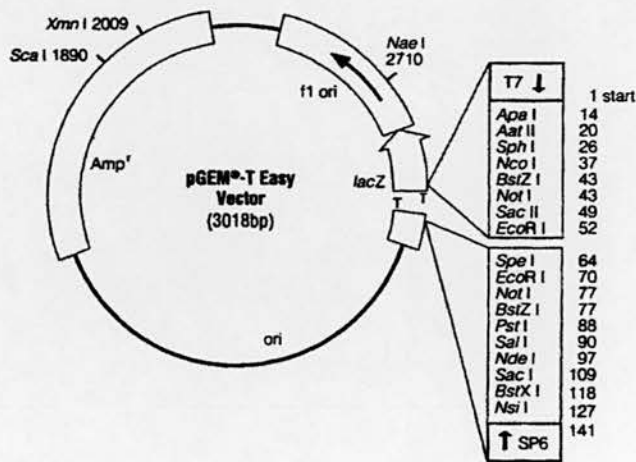


Fig 3.25 Diagrammatic representation of the pGEM™-T Easy Vector used for insertion and amplification of the cDNA product in JM109 cells.

The sequences obtained verified expression of the JM-a, JM-d, CT-a and CT-b erbB4 receptor isoforms in the PEO6 cell line.

The erbB4 receptor JM isoforms sequenced from the PEO6 cell line are shown in Tables 3.4 & 3.5. The isoform specific sequences are shown in bold, the sequence to which the primers were directed is shown in grey and the Eco R1 site (GAATTC) of the pGEM™-T Easy vector is boxed.

Chapter 3

Table 3.4 Sequence obtained for the putative JM-a isoform

**GAATTC**GATTCAGTGTGAGAAGATGGAAGATGGCCTCCTCACATGCCATGGACCG
GGTCCTGACAACTGTACAAAGTGCTCTCATTTTAAAGATGGCCCAAACTGTGTGGA
AAAATGTCCAGATGGCTTACAGGGGGCAAACAGTTTCATTTTCAAGTATGCTGATC
CAGATCGGGAGTGCCACCCATGCCATCCAAACTGCACCCAATGGTG**TAACGGTCC
CACTAAGTCATGNCTGCATTTACTACCCATGNNCGGGCCANTCCACTTTANCACAA
CATGC**NAGAACTCCCCTGANTGCAGCTGNAGTAATTGGTGGGCTCTTCATTCTGG
TCATTGTGGGGTCTGACATTTGCTGTTTATGTTAGAAGGAAGATCATCAAAAAG

Table 3.5 Sequence obtained for the putative JM-d isoform

**GAATTC**GATNCAGTGTGAGAAGATGGAAGATGGCCTCCTCACATGCCATGGAC
CGGGTCCTGACAACTGTACAAAGTGCTCTCATTTTAAAGATGGCCCAAACTGTGT
GGAAAAATGTCCAGATGGCTTACAGGGGGCAAACAGTTTCATTTTCAAGTATGCT
GATCCAGATCGGGAGTGCCACCCATGCCATCCAAACTGCACCCAAGGGTG**CAT
AGGCTCAAGTATTGAAGACTGCATCGGCCTGATGGA**TAGGTGT**AACGGTCCCAC
TAATCATGACTGCATTTACTACCCATGGACGGGCCATTCCACTTTACCACAACAT
GC**TAAAACTCCCCTGATTGCAGCTGGAGTAATTGGTGGGCTCTTCAATCTGGTC
ATTGTGGGGTCTGACATTTGCTGTTTATGTTAGAAGGAAGATCATCAAAAAGAATC
N

This sequence confirms that the JM-d isoform is composed of both JM-a and JM-b
components, which are linked by a six base pair segment TAGGTG. This sequence
demonstrated that the JM-d isoform has a product size of 420 bp's using these primers.

The erbB4 receptor CT isoforms sequenced from the PEO6 cell line are shown in Tables 3.6 & 3.7. The isoform specific sequences are shown in bold, the sequence to which the primers were directed is shown in grey and the Eco R1 site (GAATTC ) of the pGEM™-T Easy vector is boxed.

Table 3.6 Sequence obtained for the putative CT-a isoform

GG**GAATTC**GATT**ATCTCTTGGATGAAGAGGATTTGG**AAGATATGATGGATGCTG
AGGAGTACTTGGNCCCTCAGGCTTTCAANATCCCACCTCCCANCTATACTTCNAN
AGNAAGAATTGACTCGAATAGGA**GTGAAATTGGACANAGCCCTCCTCNTGCCTA
CACCCCCATGTCAGGAA**ACCAGTTTGTATACCGAGATGGAGGTTTTGCTGCTGA
ACAAGGAGTGTCTGTGCCCTACAGAGCCCCANCTAGCACATTTCCAAAAGCTCC
TGTGGCACAGGGTGCTACTGCTGAGATTTTTGATGACAATCACTAAGTGANTTC
G

Table 3.7 Sequence obtained for the putative CT-b isoform

CCGGCCGNTNTGGACGGCCGCGG**GAATTC**GATTATCTCTTGGATGAAGAGGAT
TTGGAAGATATGATGGATGCTGAGGAGTACTTGGTCCCTCAGGCTTTCAACATC
CCACCTCCCATCTATACTTCCAGAGCAAGAATTGACTCGAATAGGA**ACCAGTTT
GTATACCGAGATGGAGGTTTTGCTGCTGAACAAGGAGTGTCTGTGCCCTACAGA
GCCCCAACTAGCACAATTCCAGAAGCTCCTGTGGCACAGGGTGCTACTGCTGA
GATTTTTGATGACAATCACTA

This sequence confirms the CT-b isoform lacks the 48 bp sequence of the CT-a isoform. The region where the CT-b isoform lacks the CT-a specific sequence is shown as **.

These results confirmed that the CT product sizes were 296 and 248 bp's for CT-a and CT-b respectively.

Chapter 3

3.3.4    Expression of the erbB4 isoforms in human ovarian tumours

mRNA's for the panel of 24 human ovarian tumours were used to investigate expression of the erbB4 receptor JM and CT isoforms by RT-PCR. Primers for γ-actin were used to ensure integrity of the mRNA samples, DEPC treated water was used to control for contamination in the reagents.

The JM primers yielded products of 375 bp's in 18 / 24 tumours consistent with erbB4 receptor JM-a isoform expression (Fig 3.26). Tumours 91, 96, 5, 9, 77 and 99 were consistently negative in the experiment that was run in triplicate. A higher band was also detected that was consistent with JM-d isoform expression. The JM-d band was most easily visualized by gel magnification (not shown) and was detected in the tumours 55, 19, 98, 20, 88 and 94. No other bands indicating expression of the JM-b or JM-c isoforms were detected or if present, fall below the level of detection using RT-PCR.

The CT primers yielded PCR products of 300 bp's and 250 bp's corresponding to expression of the erbB4 receptor CT-a and CT-b isoforms (respectively) in 20 / 24 human ovarian tumours. The tumours 91, 96, 5 and 77 that were negative for expression of the JM-a isoform were also negative for expression of the CT isoforms. However, tumours 9 and 99 tested positive for CT isoform expression even though expression of the JM isoform was not detected. This may be due to the JM primers being less sensitive than the CT primers or may suggest expression of a truncated erbB4 receptor at the mRNA level. All tumour mRNA samples tested positive for expression of γ-actin and all water control samples were negative. These results are typical of an experiment that was carried out in triplicate.

These results demonstrate that the majority of human ovarian carcinomas express mRNA for the erbB4 receptor JM-a, CT-a and CT-b isoforms. Expression of the erbB4 receptor isoforms in human ovarian tumours is summarized in Table 3.3.4.

Chapter 3
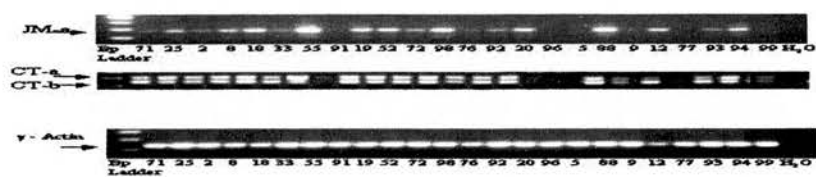
Fig 3.26 The panel of human ovarian tumours was screened for mRNA expression of the JM and CT isoforms of the erbB4 receptor. 18 / 24 tumours tested positive for JM-a expression with both the CT-a and CT-b detected in 20 / 24. Again higher banding was observed in some tumours which expressed JM-a and is consistent with expression of the JM-d isoform. γ - actin was used to ensure viability of the mRNA and tested positive for all tumour samples, the DEPC treated water was used to control for contamination in the reagents and tested negative.

88

Chapter 3

Table 3.3.4 Expression of the erbB4 receptor isoforms and NRG detected by RT-PCR in a panel of human ovarian tumours.

| Histology | HOV Tumour No. | JM-a | JM-d | CT-a | CT-b | NRG |
|---|---|---|---|---|---|---|
| serous | 71 | + | - | + | + | + |
| serous | 25 | + | - | + | + | + |
| serous | 2 | + | - | + | + | + |
| serous | 8 | + | - | + | + | + |
| serous | 18 | + | - | + | + | + |
| serous | 33 | + | - | + | + | + |
| serous | 55 | + | + | + | + | + |
| serous | 91 | - | - | - | - | + |
| serous | 19 | + | + | + | + | + |
| serous | 52 | + | - | + | + | + |
| serous | 72 | + | - | + | + | + |
| serous | 98 | + | + | + | + | + |
| serous | 76 | + | - | + | + | + |
| mixed serous / endometrioid | 92 | + | - | + | + | + |
| endometrioid | 20 | + | + | + | + | + |
| endometrioid | 96 | - | - | - | - | + |
| endometrioid | 5 | - | - | - | - | + |
| endometrioid | 88 | + | - | + | + | + |
| endometrioid | 9 | - | - | + | + | + |
| clear cell | 12 | + | - | + | + | + |
| clear | 77 | - | - | - | - | ± |
| mixed mesodermal | 93 | + | - | + | + | + |
| mixed epithelial / mesodermal | 94 | + | + | + | + | + |
| sexcord stromal | 99 | - | - | + | + | ± |
| | | 18 / 24 | 5 / 24 | 20 / 24 | 20 / 24 | 22 / 24 |

+ tested positive for expression
- expression was not detected or if present, was below the limit of detection
± weak signal detected, which may correspond to expression

Chapter 4 Cell Line Responses to the Neuregulins and TGFα

Chapter 4 Cell Line Responses to the Neuregulins and TGFα

## Chapter 4 Cell Line Responses to the Neuregulins and TGFα

This section describes the growth response of the panel of ovarian cancer cell lines to the ligands NRG1α, NRG1β and TGFα. Response was assessed in growth assays over a five-day period. Cellular response to concentration of ligand was first evaluated using the PEO1 cell line.

4.1 Evaluation of ligand concentration for cellular response

Preliminary experiments were conducted with the PEO1 cell line to evaluate the ligand concentration of the three growth factors that produced the maximal growth response. The PEO1 cell line was treated with concentrations of ligand varying from $1 \times 10^{-10}$M to $5 \times 10^{-9}$M over a period of 5 days. Cell counts were taken on day 0, day 2 and day 5 and medium containing growth factor was replaced on day 2. Cells were counted using a Coulter Counter. Cells not treated with ligand were used as controls to compare growth rates and assigned a 100% value. All other cell counts under experimental conditions were expressed as a percentage relative to the control cell number.

4.1a   PEO1 response to NRG1α

The PEO1 cell line was growth stimulated by NRG1α in a concentration dependent manner. Growth response to NRG1α was evident on day 2 and was more pronounced by day 5. The magnitude of response was greatest on day 5 with $5 \times 10^{-9}$M NRG1α and resulted in a growth stimulation increasing the control cell count by 48%. The growth response had reduced to 5% above the control cell count using $1 \times 10^{-10}$M ligand (Table 4.1). The 50-fold variation of NRG1α concentration resulted in a narrow range of growth responses of 105 through 148% by day 5 (Fig4.1).

91
Chapter 4 Cell Line Responses to the Neuregulins and TGFα

Table 4.1 PEO1 response to NRG1α.

| NRG1α | Control | $1\times10^{-10}$M | $5\times10^{-10}$M | $1\times10^{-9}$M | $5\times10^{-9}$M |
|---|---|---|---|---|---|
| Day 0 | 37580* | 37580 | 37580 | 37580 | 37580 |
| SD | 1602 | 1602 | 1602 | 1602 | 1602 |
| Day 2 | 47461 | 47757 | 52523 | 53138 | 61619 |
| SD | 2631 | 1895 | 1547 | 1457 | 3106 |
| Day 5 | 92876 | 97500 | 103958 | 119577 | 137004 |
| SD | 10383 | 5604 | 5852 | 5444 | 5990 |
| Day 5 % of Control | 100% | 105% | 112% | 129% | 148% |

* cells per well
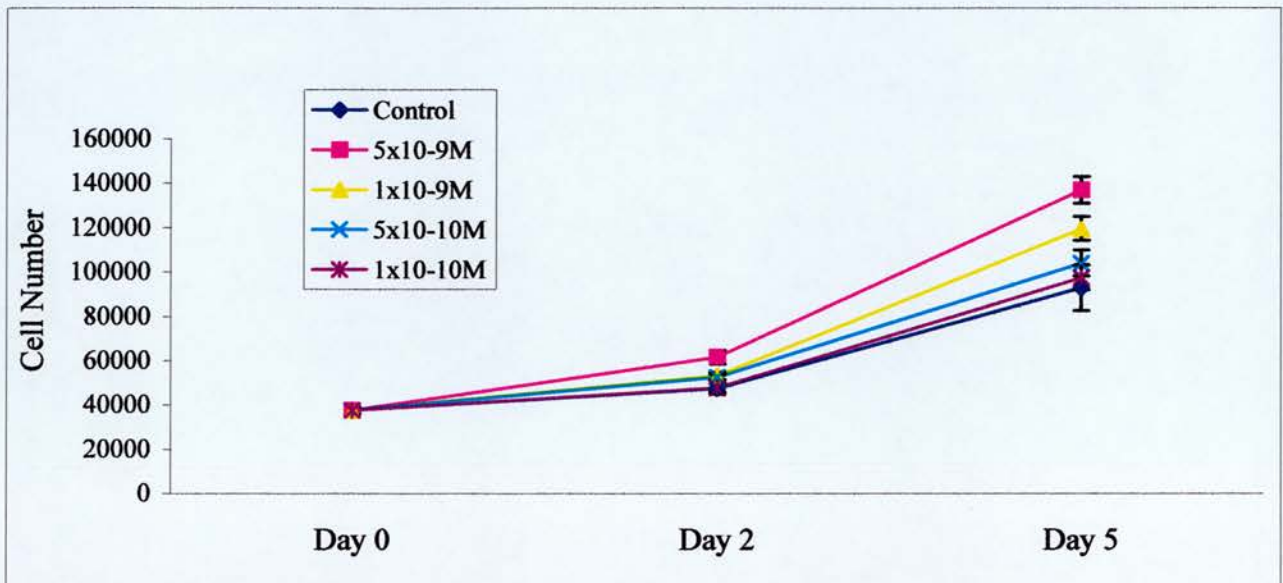


Fig 4.1 PEO1 response to the ligand NRG1α. Cells were grown in phenol red-free medium supplemented with 5%DCSFCS and treated with concentrations of NRG1α indicated over a period of 5 days. Medium or medium containing growth factor was replaced on day 2. Each value represents the mean of quadruplicate samples, error bars denote the standard deviation between the samples which were counted in triplicate by Coulter Counter. The graph shows the result of one experiment and is typical for the experiment that was run in duplicate.

Chapter 4 Cell Line Responses to the Neuregulins and TGFα

### 4.1b PEO1 response to NRG1β

PEO1 cells were stimulated by NRG1β in a concentration dependent manner and the greatest growth stimulation was observed on day 5. The magnitude of growth responses obtained on day 5, ranged from increases of 48% with $1 \times 10^{-10}$M to 95% with $5 \times 10^{-9}$M NRG1β above the control cell count (Table 4.2). The 10-fold increase in ligand concentration from $5 \times 10^{-10}$M to $5 \times 10^{-9}$M produced a narrow range of increased growth (78-95%) above the control cell number (Fig 4.2).

NRG1β produced a mitogenic effect which was superior to that of NRG1α; 95% for NRG1β vs 48% for NRG1α on day 5 using $5 \times 10^{-9}$M ligand. In direct comparison, equivalent growth responses were observed using the highest tested concentration of NRG1α ($5 \times 10^{-9}$ M; 48%) and the lowest tested concentration of NRG1β ($1 \times 10^{-10}$M; 48%) on day 5.

Table 4.2 PEO1 response to NRG1β

| NRG1β | Control | $1 \times 10^{-10}$M | $5 \times 10^{-10}$M | $1 \times 10^{-9}$M | $5 \times 10^{-9}$M |
|---|---|---|---|---|---|
| Day 0 | 37580* | 37580 | 37580 | 37580 | 37580 |
| SD | 1602 | 1602 | 1602 | 1602 | 1602 |
| Day 2 | 44031 | 61211 | 67784 | 73703 | 72553 |
| SD | 2924 | 3278 | 6450 | 2990 | 2076 |
| Day 5 | 99844 | 147411 | 177578 | 184898 | 194388 |
| SD | 9167 | 5238 | 5812 | 8339 | 10542 |
| Day 5 % of Control | 100% | 148% | 178% | 186% | 195% |

*(cells per well)

Chapter 4 Cell Line Responses to the Neuregulins and TGFα
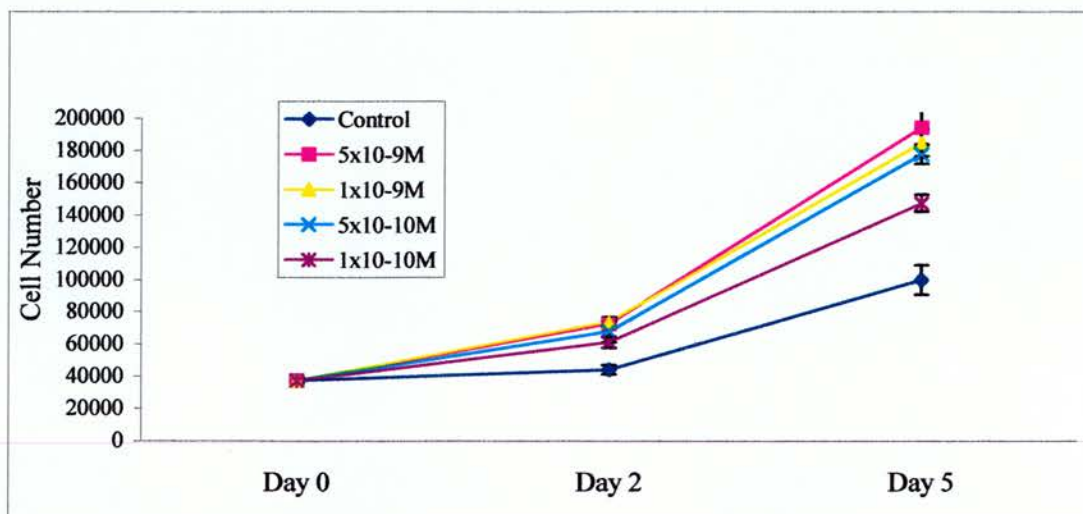
Fig 4.2 PEO1 response to NRG1β. Cells were grown in phenol red-free medium supplemented with 5%DCSFCS and treated with concentrations of NRG1β indicated over a period of 5 days. Medium / medium containing growth factor was replaced on day 2. Each value represents the mean of quadruplicate samples, error bars denote the standard deviation between the samples which were counted in triplicate by Coulter Counter. The graph shows the result of one experiment and is typical for the experiment that was run in duplicate.

### 4.1c    PEO1 response to TGFα

The PEO1 cell line was growth stimulated by TGFα. Growth stimulation was concentration dependent and the greatest effects were observed on day 5. The increase in cell growth above the control cell count ranged from 24% with $1 \times 10^{-10}$M TGFα to 73% with $5 \times 10^{-9}$M TGFα on day 5 (Table 4.3 & Fig 4.3).

The growth stimulation using TGFα at the concentration of $5 \times 10^{-9}$M (73%) was less than that achieved with NRG1β (95%), although greater than NRG1α (48%) at the same concentration by day 5. This trend in the magnitude of growth responses to the three ligands, was consistent through the range of concentrations investigated.

Chapter 4 Cell Line Responses to the Neuregulins and TGFα

Table 4.3 PEO1 response to TGFα

| TGFα | Control | $1 \times 10^{-10}$M | $5 \times 10^{-10}$M | $1 \times 10^{-9}$M | $5 \times 10^{-9}$M |
|---|---|---|---|---|---|
| Day 0 | 37580* | 37580 | 37580 | 37580 | 37580 |
| SD | 1602 | 1602 | 1602 | 1602 | 1602 |
| Day 2 | 50411 | 68671 | 75134 | 78244 | 77470 |
| SD | 3171 | 3226 | 1181 | 4188 | 1798 |
| Day 5 | 96144 | 118652 | 149777 | 155785 | 165891 |
| SD | 9365 | 9234 | 7421 | 4319 | 5665 |
| Day 5 % of Control | 100% | 123% | 156% | 162% | 173% |

*(cells per well)
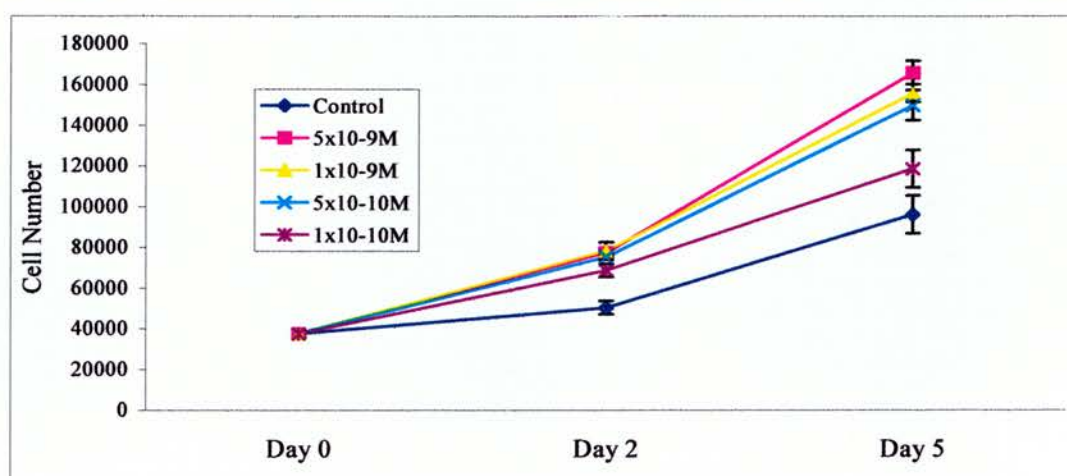


Fig 4.3 PEO1 Response to TGFα. Cells were grown in phenol red-free medium supplemented with 5%DCSFCS and treated with the concentrations of TGFα indicated over a period of 5 days. Medium / medium containing growth factor was replaced on day 2. Each value represents the mean of quadruplicate samples, error bars denote the standard deviation between the samples which were counted in triplicate by Coulter Counter. The graph shows the result of one experiment and is typical for the experiment that was run in duplicate.

The PEO1 cell line was growth responsive to each of the ligands NRG1α, NRG1β and TGFα. Growth responses were observed on day 2 and were more pronounced by day 5. The magnitude of growth response to the ligands was of the order NRG1β > TGFα > NRG1α. The concentration of $5 \times 10^{-9}$M was impractical for growth analysis of the panel of cell lines due to the high cost of the reagents. Consequently, $1 \times 10^{-9}$M was chosen for all three growth factors to allow direct comparisons between the ligands. This concentration produced similar growth effects to those observed for $5 \times 10^{-9}$M using NRG1β and TGFα; the reduction in growth stimulation in response to NRG1α was attributed to the lower affinity of NRG1α for the receptors.

95

Chapter 4 Cell Line Responses to the Neuregulins and TGFα

4.2 Response to the ligands in the panel of ovarian carcinoma cell lines.

A panel of ovarian cancer cell lines was assessed for response to NRG1α, NRG1β and TGFα ($1x10^{-9}$M) over a period of 5 days. Cell counts were measured using a Coulter counter on days 0, 2 and 5, with growth factor and medium being replaced on day 2. Cells not treated with ligand were used as controls to monitor cellular growth and were assigned a 100% value. Change in cell number upon treatment with growth factor is represented as a percentage relative to the control cell count (100%). 24 well trays allowed 6 replicates of each sample population to be analyzed simultaneously, mean values were calculated for each well. The experiments were conducted at least twice and representative results shown.

A response to ligand was arbitrarily regarded as a change of more than 15% from the control cell number. The data was also analyzed for statistical significance to detect small changes in cellular growth upon treatment with ligand. Using the Student t test, p values of <0.05 were regarded as statistically significant.

4.2a Response to NRG1α.

A panel of 14 cell lines was tested for response to NRG1α ($10^{-9}$M). Five cell lines (PEO1, PEO4, PEO6, OVCAR5 and 41M) were growth stimulated by NRG1α with increases in cell growth ranging from 15% (OVCAR5) to 132% (PEO6) above the control cell count (Fig 4.4 & Table 4.4).

Statistical analysis revealed that cell lines OVCAR3 and SKOV3 were also growth stimulated by NRG1α (10% and 6% respectively), whilst the CAOV3 cell line was shown to be significantly growth inhibited (10%) by NRG1α. The other 6 cell lines (PEO1$^{CDDP}$, PEO14, OVCAR4, SW626, 59M and OAW42) were unresponsive to treatment with NRG1α.
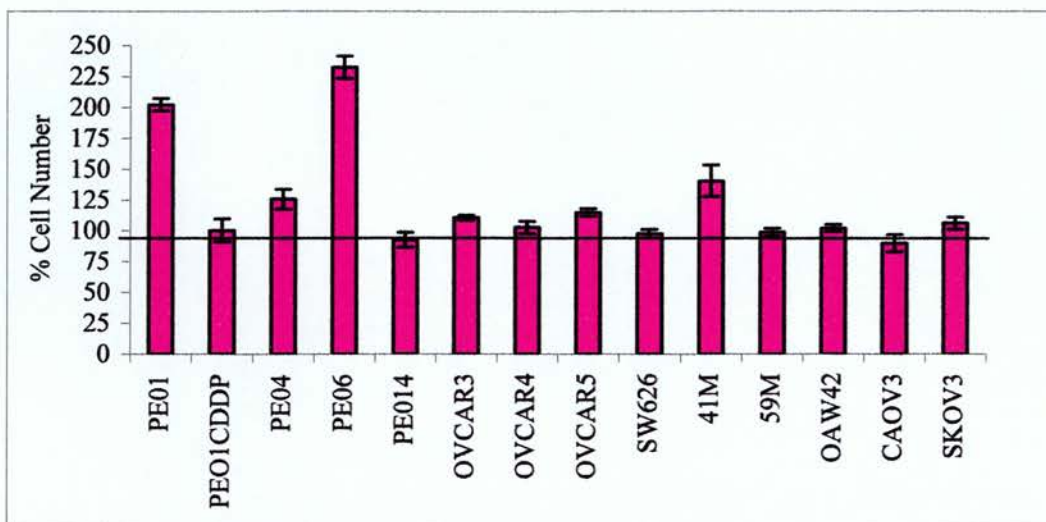
Fig 4.4 Ovarian cancer cell line response to NRG1$\alpha$. Treatment with NRG1$\alpha$ ($10^{-9}$M) in medium supplemented with 5%DCSFCS, stimulated growth in 5 of the 14 cell lines (PEO1, PEO4, PEO6, OVCAR5 and 41M). Statistical analysis revealed that the OVCAR3 and SKOV3 cell lines were also growth stimulated by NRG1$\alpha$, whilst the CAOV3 cell line was growth inhibited.

Chapter 4 Cell Line Responses to the Neuregulins and TGF$\alpha$

Table 4.4 Cell line response to NRG1α.

| Cell Line | % cell number in comparison to control cell number assigned 100% | Standard Deviation | Students T-test P value |
|---|---|---|---|
| PE01 | 202 | 5.0 | <0.0001 |
| PEO1$^{CDDP}$ | 100 | 9.3 | 0.9276 |
| PE04 | 126 | 8.0 | <0.0001 |
| PE06 | 232 | 9.1 | <0.0010 |
| PE014 | 92 | 6.1 | 0.2042 |
| OVCAR3 | 110 | 1.9 | <0.0001 |
| OVCAR4 | 102 | 5.0 | 0.1534 |
| OVCAR5 | 115 | 3.0 | <0.0001 |
| SW626 | 98 | 3.5 | 0.3353 |
| 41M | 141 | 12.9 | <0.0001 |
| 59M | 99 | 2.9 | 0.4369 |
| OAW42 | 102 | 2.8 | 0.1678 |
| CAOV3 | 90 | 7.0 | 0.0009 |
| SKOV3 | 106 | 4.9 | 0.0412 |

Chapter 4 Cell Line Responses to the Neuregulins and TGFα

4.2b Response to NRG1β

A panel of 14 cell lines was assessed for response to NRG1β. Seven cell lines were growth stimulated by NRG1β (by ≥ 15%) and included PEO1, PEO4, PEO6, OVCAR3, OVCAR5, 41M and CAOV3 (Fig 4.5). Growth stimulation ranged from increases of 60% (OVCAR3) to 378% (PEO6) above the control cell count. The cell line PEO1$^{CDDP}$ was growth inhibited by NRG1β and cellular growth decreased to 25% in comparison to the control cell count (100%).

Statistical analysis of the raw data showed that cell lines OVCAR4, SW626 and SKOV3 also had significantly increased growth upon treatment with NRG1β though by < 15%, whilst the 59M cell line had significantly reduced growth in comparison to the control cell count (Table 4.5). Only 2 cell lines were unresponsive to the ligand, PEO14 (5%; p=0.47) and OAW42 (5%; p=0.15).

These results indicated that the majority of ovarian cancer cell lines tested are growth stimulated by NRG1β.
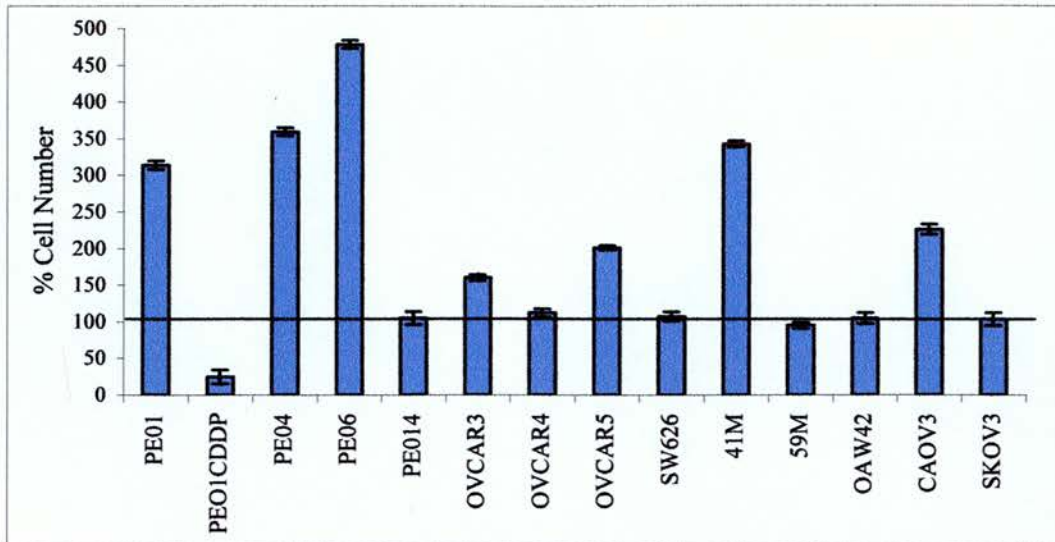
Fig 4.5 Ovarian cancer cell line response to NRG1β. Treatment with NRG1β ($10^{-9}$M) in medium supplemented with 5%DCSFCS, stimulated growth in 8 of the 14 cell lines (PEO1, PEO4, PEO6, OVCAR3, OVCAR4, 41M and CAOV3) of more than 10% above the control cell count. The PEO1[CDDP] cell line was growth inhibited by NRG1β to 25% in comparison to the control cell number (100%). Statistical analysis revealed that SW626 and SKOV3 were growth stimulated by NRG1β, whilst the 59M cell line was growth inhibited.

Table 4.5 Cell line response to NRG1β.

| Cell Line | % Cell number in comparison to control cell number assigned 100% | Standard Deviation | Students T-test P value |
|---|---|---|---|
| PE01 | 314 | 6.0 | <0.0001 |
| PEO1CDDP | 25 | 9.2 | <0.0001 |
| PE04 | 360 | 5.5 | <0.0001 |
| PE06 | 478 | 5.4 | <0.0001 |
| PE014 | 105 | 8.7 | 0.4655 |
| OVCAR3 | 160 | 3.7 | <0.0001 |
| OVCAR4 | 112 | 5.6 | <0.0001 |
| OVCAR5 | 201 | 2.8 | <0.0001 |
| SW626 | 107 | 6.0 | 0.0134 |
| 41M | 343 | 3.9 | <0.0001 |
| 59M | 95 | 3.9 | 0.0025 |
| OAW42 | 105 | 7.2 | 0.1492 |
| CAOV3 | 226 | 6.7 | <0.0001 |
| SKOV3 | 104 | 8.9 | <0.0001 |

Chapter 4 Cell Line Responses to the Neuregulins and TGFα

4.2c Response to TGFα

A panel of 14 cell lines was tested for response to TGFα. Of the panel, 9 cell lines were responsive to the ligand; 8 of which were growth stimulated by TGFα and the PEO1$^{CDDP}$ cell line which was growth inhibited (Fig 4.6). Cell lines that were growth stimulated included PEO1, PEO4, PEO6, OVCAR3, 41M, 59M, CAOV3 and SKOV3. The increase in cell growth above that of the control cell count ranged from 32% (SKOV3) to 322% (PEO6). The PEO1$^{CDDP}$ cell line was growth inhibited to 13% in comparison to the control cell count (100%).

Of the other 5 cell lines, only the OVCAR5 cell line was shown to have significantly increased growth upon treatment with TGFα (10%; p=0.04). The other 4 cell lines (PEO14, OVCAR4, SW626 and OAW42) were unresponsive to this ligand. This data demonstrated that the majority of ovarian cancer cell lines investigated were growth stimulated by TGFα.

Chapter 4 Cell Line Responses to the Neuregulins and TGFα
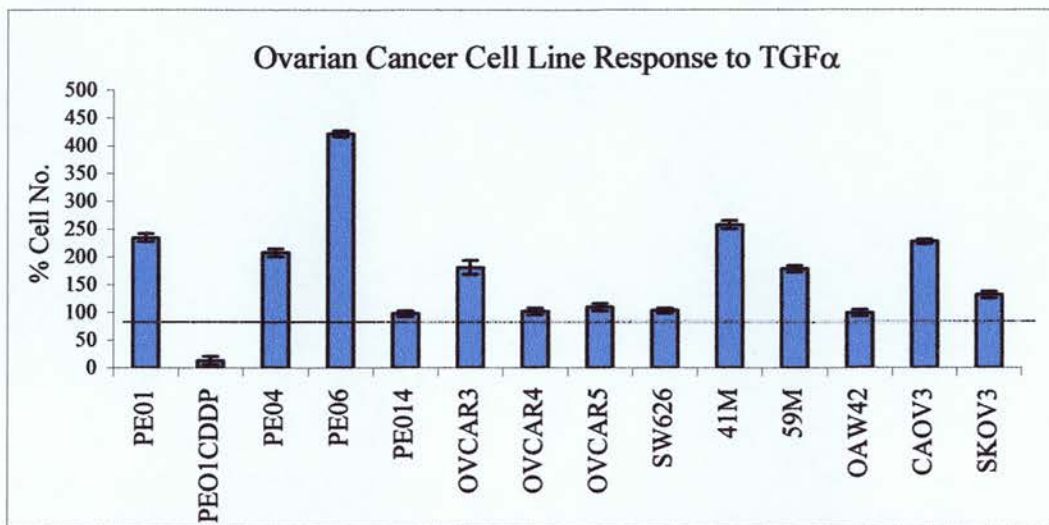
Fig 4.6 Ovarian cancer cell line response to TGFα. Treatment with TGFα ($10^{-9}$M) in medium supplemented with 5%DCSFCS, stimulated an increase in cell growth for 8 of the 14 cell lines (PEO1, PEO4, PEO6, OVCAR3, 41M, 59M, CAOV3 and SKOV3). The PEO1$^{CDDP}$ cell line was growth inhibited by TGFα to 13% of control cell count (100%). Statistical analysis revealed that OVCAR5 was growth stimulated by TGFα.

Table 4.6 Cell line response to TGFα

| Cell Line | % Cell number in comparison to control cell number assigned 100%. | Standard Deviation | Students T-test P value |
|-----------|---------------------------------|--------------------|-------------------------|
| PE01 | 235 | 7.2 | <0.0001 |
| PEO1CDDP | 13 | 7.6 | <0.0001 |
| PE04 | 208 | 6.9 | <0.0001 |
| PE06 | 422 | 5.1 | <0.0001 |
| PE014 | 98 | 5.3 | 0.6920 |
| OVCAR3 | 181 | 12.6 | <0.0001 |
| OVCAR4 | 102 | 6.2 | 0.5841 |
| OVCAR5 | 110 | 6.2 | 0.0378 |
| SW626 | 103 | 4.3 | 0.1016 |
| 41M | 258 | 7.7 | <0.0001 |
| 59M | 179 | 5.8 | <0.0001 |
| OAW42 | 100 | 5.8 | 0.8171 |
| CAOV3 | 228 | 4.1 | <0.0001 |
| SKOV3 | 132 | 5.8 | <0.0001 |

Chapter 4 Cell Line Responses to the Neuregulins and TGFα

4.2d Discussion

Of the cell lines tested, half were growth stimulated by NRG1$\alpha$ and the majority of cell lines were growth responsive to NRG1$\beta$ and TGF. The magnitude of growth stimulation in the PEO1 cell line by the ligands was of the order NRG1$\beta$ > TGF$\alpha$ > NRG1$\alpha$ (each at $10^{-9}$M) (Fig4.7). This trend is apparent in cell lines which were responsive to all three ligands ( PEO1, PEO4, PEO6 and 41M).

It is plausible that using higher concentrations of NRG1$\alpha$ may achieve similar growth effects to $10^{-9}$M NRG1$\beta$ since $5 \times 10^{-9}$M NRG1$\alpha$ produces an effect similar to $1 \times 10^{-10}$M NRG1$\beta$ in the PEO1 cell line. It has also been reported that NRG1$\alpha$ can only bind to the high affinity erbB4 receptor whereas NRG1$\beta$ can bind to either erbB3 or erbB4 receptors. This is conflicting with the response observed with the PEO1 cell line where erbB4 receptor expression was unable to be detected at the protein level, yet the cell line was growth stimulated by this ligand.

It was apparent that the majority of cell lines stimulated by NRG1$\beta$ were also stimulated by TGF$\alpha$ (exceptions being OVCAR5 and 59M). This is suggestive of crosstalk either at the receptor level or integration of intracellular signalling. A certain subset of cell lines (PEO14, SW626, OAW42), was not greatly influenced by these ligands and the growth of these cells is likely to be regulated by other growth factors or hormones.
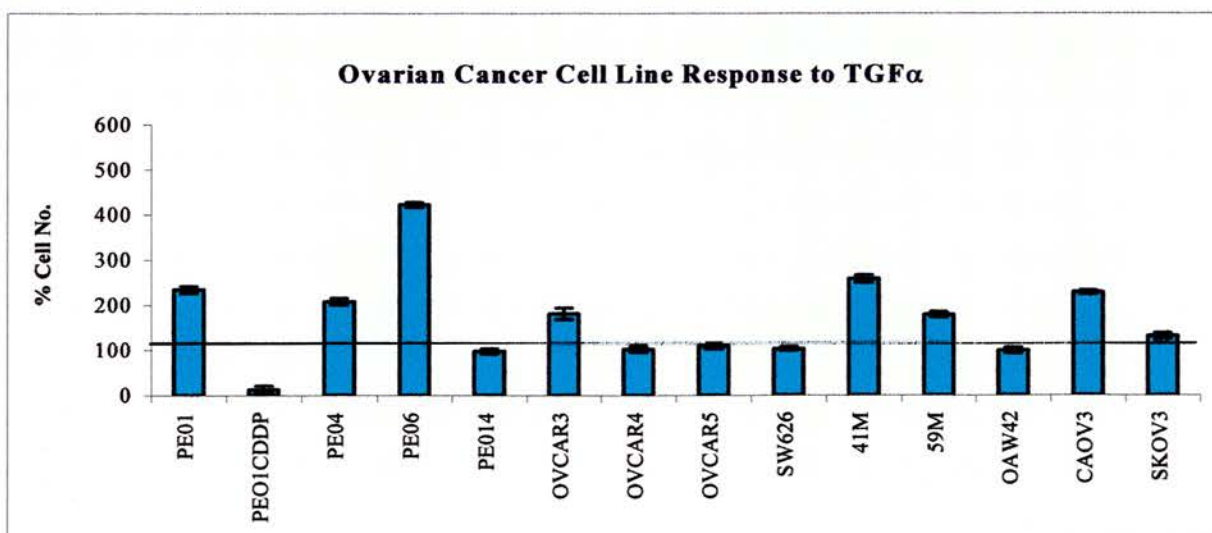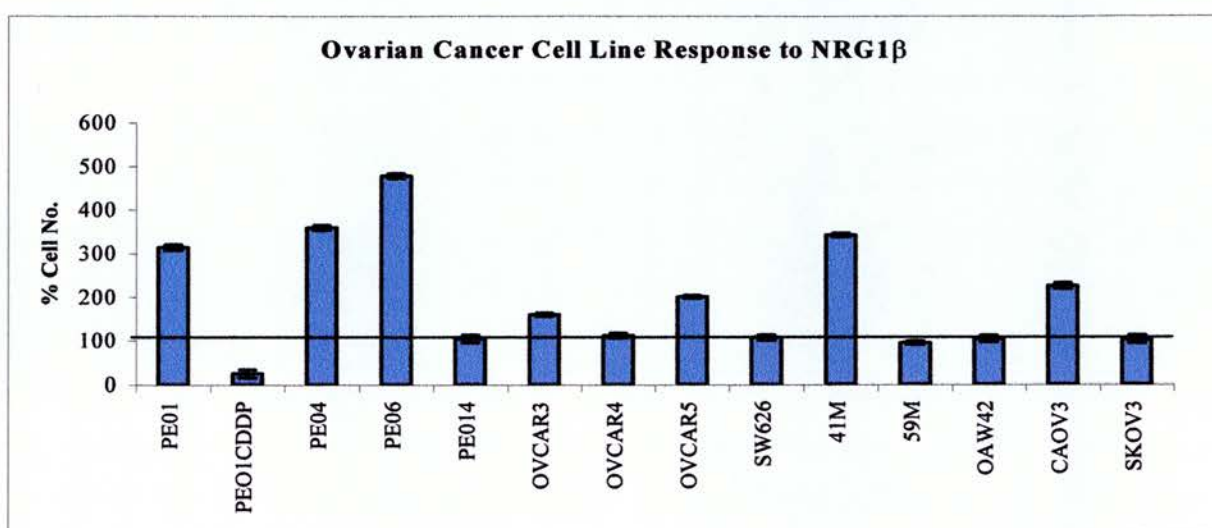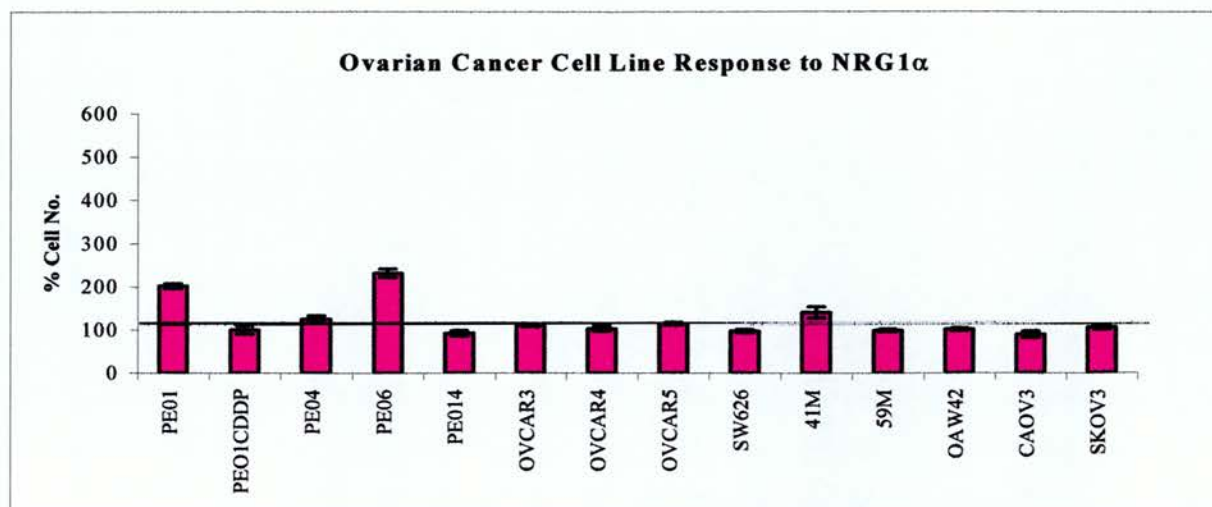
Fig 4.7 Ovarian cancer cell line response    to the ligands NRG1α, NRG1β and TGFα.

Chapter 4 Cell Line Responses to the Neuregulins and TGFα

4.2 Correlating Receptor Expression to Cellular Response

The association between erbB receptor expression and cellular response to NRG1α, NRG1β and TGFα was then explored

. An erbB receptor expression profile was generated for the panel of cell lines from the data in chapter 3 to identify patterns of erbB receptor expression and co-expression. The integrated optical densitometry values which represent the level of expression of the receptor were used to assign a + / ++ / +++ scoring system in the following manner:

EGF receptor IOD values ranged from 11.7 to 2888.7 and scoring was assigned (+) for IOD values from 0 – 1000; (++) for IOD values 1000.1 – 2000 and (+++) for IOD values > 2000. ErbB2 receptor IOD values ranged from 13.2 to > 5240 and scoring was assigned (+) for IOD values 0 – 1500; (++) for IOD values 1500.1 – 3000 and (+++) for IOD values > 3000.1. ErbB3 receptor IOD values ranged from 6.5 to 397 and scoring was assigned (+) for IOD values 0 – 150; (++) for IOD values 150.1 – 300; (+++) for IOD values > 300.1. ErbB4 receptor IOD values ranged from 14.2 to 1260 and scoring was assigned (+) for IOD values 0 – 400; (++) for IOD values 400.1 – 800 and (+++) for IOD values > 800.1. Response to ligand was regarded as a change in cellular growth of at least 15% in comparison to the control cell count (Table 4.7).

Table 4.7 ErbB receptor expression and response to ligand in the panel of ovarian cancer cell lines

| Cell Line | EGFR | ERBB2 | ERBB3 | ERBB4 | NRG1α | NRG1β | TGFα |
|---|---|---|---|---|---|---|---|
| PEO1 | + | ++ | + | — | ↑ | ↑ | ↑ |
| PEO1$^{CDDP}$ | + | + | +++ | — | - | ↓ | ↓ |
| PEO4 | + | ++ | + | + | ↑ | ↑ | ↑ |
| PEO6 | — | ++ | + | +++ | ↑ | ↑ | ↑ |
| PEO14 | + | + | + | + | - | - | - |
| PEO16 | + | + | + | — | ND | ND | ND |
| OVCAR3 | + | + | ++ | + | - | ↑ | ↑ |
| OVCAR4 | + | + | + | + | - | - | - |
| OVCAR5 | +++ | ++ | + | — | ↑ | ↑ | - |
| SW626 | + | + | + | — | - | - | - |
| 41M | +++ | + | + | — | ↑ | ↑ | ↑ |
| 59M | + | + | — | — | - | - | ↑ |
| OAW42 | + | + | + | + | - | - | - |
| A2780 | + | + | ++ | + | ND | ND | ND |
| CAOV3 | + | + | ++ | — |  | ↑ | ↑ |
| SKOV3 | + | +++ | + | + | - | - | ↑ |

   —     Expression not detected by Western Blotting
   +     Low level of expression
   ++    Intermediate level of expression
   +++ High level of expression
   ↑     Growth stimulated response > 15%
   ↓     Growth inhibited response > 15%
   -      Change in growth <15% from control cell count
   ND  Not Determined

Association between the magnitude of growth response to ligand and the level of expression of individual erbB receptors was first assessed using the Spearman rank correlation. Since the SKOV3 cell line expressed a very high level of erbB2 receptor protein in comparison to the rest of the panel of cell lines, analyses were conducted with and without the SKOV3 cell line data.

Chapter 4 Cell Line Responses to the Neuregulins and TGFα

A positive association was detected for the magnitude of growth response to NRG1α and the level of erbB2 receptor expressed p=0.0022 when the SKOV3 cell line data was included (Table 4.8 & Fig 4.8). The statistical significance of this association was increased by excluding the SKOV3 cell line data from the analysis (p=0.0009). Associations between expression of the EGF receptor, erbB3 or erbB4 receptors and response to NRG1α were not detected.

Table 4.8 ErbB receptor expression levels investigated by Spearman rank correlation to find association with response to NRG1α.

| Level of erbB receptor investigated | P value |
| --- | --- |
| EGF receptor | 0.7081 |
| ErbB2 (incl. SKOV3 data) | 0.0022* |
| ErbB2 (excl. SKOV3 data) | 0.0009* |
| ErbB3 | 0.8456 |
| ErbB4 | 0.2100 |

* Statistically significant association.
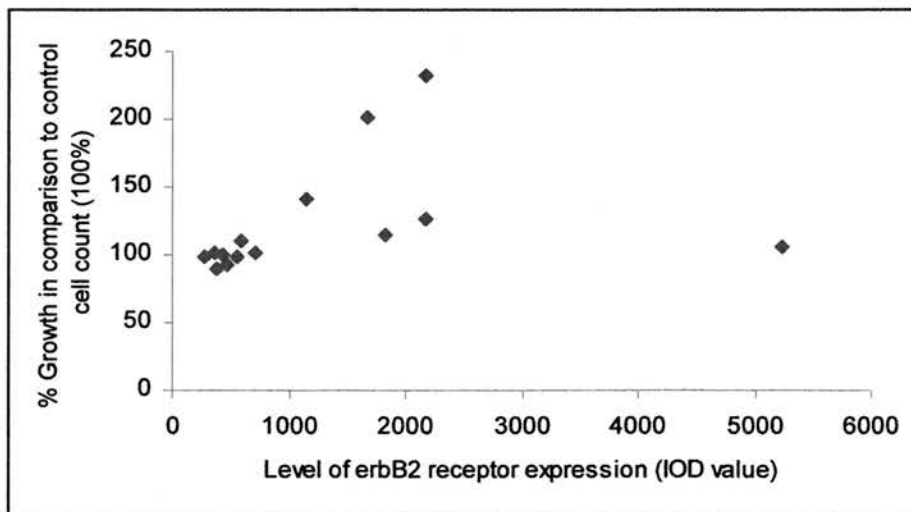


Fig 4.8 Percentage increase in cell growth in response to NRG1α vs level of expression of the erbB2 receptor for the panel of ovarian cancer cell lines. A significant association was detected for increasing level of expression of the erbB2 receptor and greater magnitude of growth response to NRG1α p= 0.0022 using the Spearman rank correlation. The significance of the association was increased by excluding data for the SKOV3 cell line (p=0.0009).

107

Chapter 4 Cell Line Responses to the Neuregulins and TGFα

A trend was observed for increasing expression of the erbB2 receptor and greater magnitude of response to NRG1β (p=0.0795) using data from the panel of cell lines that included the SKOV3 cell line (Table 4.9& Fig 4.9). Exclusion of the data from the high erbB2 receptor expressing cell line SKOV3, showed a significant association for increased erbB2 receptor expression and response to NRG1β for the remaining cell lines (p=0.0047).

Table 4.9 ErbB receptor expression levels investigated by Spearman rank correlation to find association with response to NRG1β.

| Level of erbB receptor investigated | P value |
| --- | --- |
| EGF receptor | 0.7591 |
| ErbB2 (incl. SKOV3 data) | 0.0795 |
| ErbB2 (excl. SKOV3 data) | 0.0047* |
| ErbB3 | 0.8310 |
| ErbB4 | 0.3081 |

* Statistically significant association.
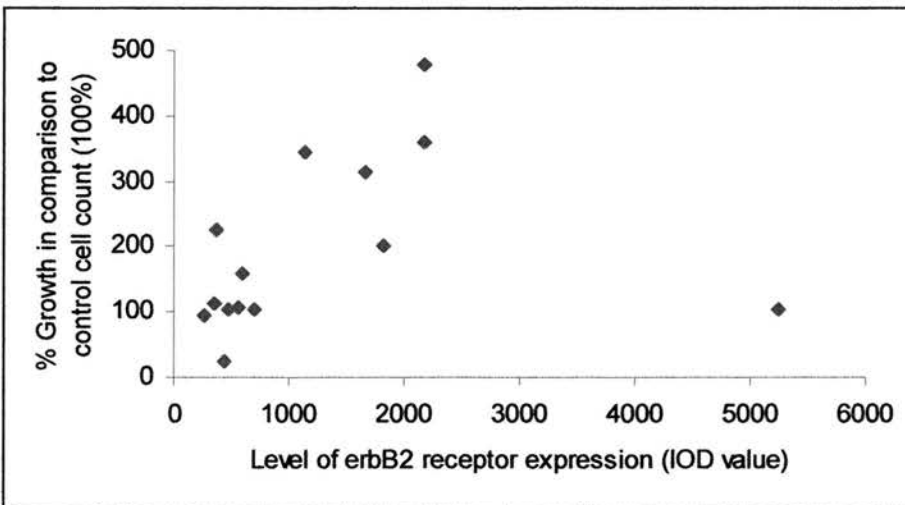


Fig 4.9 Percentage increase in cell growth in response to NRG1β vs level of expression of the erbB2 receptor for the panel of ovarian cancer cell lines. Spearman rank correlation detected a trend approaching significance for increasing level of expression of the erbB2 receptor and greater magnitude of growth response to NRG1β for the panel of cell lines. The association was statistically significant when data for the high erbB2 expressing cell line SKOV3 was excluded (p= 0.0047).

Chapter 4 Cell Line Responses to the Neuregulins and TGFα

However, the Spearman rank correlation did not reveal any significant relationship between the level of expression of the EGF receptor, erbB2, erbB3 or erbB4 with response to TGFα (Table 4.10).

Table 4.10 ErbB receptor expression levels investigated by Spearman rank correlation to find association with response to TGFα.

| Level of erbB receptor investigated | P value |
|---|---|
| EGF receptor | 0.9940 |
| ErbB2 (incl. SKOV3 data) | 0.1351 |
| ErbB2 (excl. SKOV3 data) | 0.0743 |
| ErbB3 | 0.7992 |
| ErbB4 | 0.7074 |

110

Chapter 4 Cell Line Responses to the Neuregulins and TGFα

## CH5 Intracellular responses to Neuregulin and TGF alpha

This section describes the intracellular responses elicited in four cell lines by NRG1$\alpha$, NRG1$\beta$ and TGF$\alpha$. The cell lines exhibited growth stimulation, inhibition or no response to the ligands and were chosen for comparison of intracellular signalling. The PEO1 and PEO6 cell lines were growth stimulated by all three ligands, PEO1$^{CDDP}$ was growth inhibited by NRG1$\beta$ and TGF$\alpha$ and yet unresponsive to NRG1$\alpha$, while the SKOV3 cell line was responsive only to TGF$\alpha$ which stimulated growth.

ErbB receptor activation by ligand leads to tyrosine autophosphorylation and results in association of the receptor with cytoplasmic target proteins that contain SH2 domains and phosphotyrosine binding domains, such as Shc and Grb2. This triggers activation of the Erk kinase cascade that leads to phosphorylation of nuclear proteins involved in transcriptional control. This pathway was monitored by tyrosine phosphorylation of the erbB receptors, band shifts associated with increased phosphorylation of the secondary signalling molecule Shc and phosphorylation of Erk1 and Erk2.

5.1 ErbB receptor tyrosine phosphorylation

Response to ligand was investigated by measuring tyrosine phosphorylation of the erbB receptors using Western blot analysis. The gel positions of tyrosine phosphorylated EGF receptor and erbB2 receptor were first determined using immune-precipitation (section 5.1.1). ErbB receptor tyrosine phosphorylation was evaluated in the four cell lines at 15min, 1h, 8h and 24h in response to ligand (10$^{-9}$M) using the anti-phosphotyrosine antibody PY20 (Santa Cruz Biotech.) at a dilution of 1/1000. The optical density of the signal was evaluated using Labworks 3.0.

5.1.1 Immune-precipitation of the EGF receptor and erbB2

The EGF receptor and erbB2 receptor positions were evaluated by Western blot analysis. EGF receptor was immune-precipitated from PEO1 cells that had been treated with TGFα (15min) using the anti-EGF receptor antibody Ab7 (Neomarkers) and run simultaneously with an un-precipitated sample. Phosphorylated EGF receptor was detected using the anti-phosphotyrosine antibody PY20.

The phosphotyrosine activity induced by TGFα in PEO1 cells spanned a region of approximately 20kDa (Fig 5.1 (i)) which had previously been shown to be composed of 2 bands (Fig 5.2 (iii)). Due to the increased density of this signal, resolution between the bands was not achieved. However, immune-precipitation of the EGF receptor demonstrated that tyrosine phosphorylated EGF receptor co-migrated with the tyrosine phosphorylation signal induced by TGFα. Phosphorylated EGF receptor migrated to a molecular weight of approximately 170 kDa that was within the lower range of molecular weights encompassed by the phosphotyrosine signal stimulated by TGFα.

Tyrosine phosphorylated erbB2 receptor was immune-precipitated from PEO1 cells treated with NRG1β (15min) using the more sensitive anti-phosphotyrosine antibody PY99 (Santa Cruz Biotech.). A sample that had been immune-precipitated was run simultaneously with an un-precipitated sample and erbB2 receptor was detected using the anti-erbB2 receptor antibody CB11. Tyrosine phosphorylated erbB2 receptor co-migrated with the erbB2 receptor position to a molecular weight of approximately 185 kDa (Fig 5.1 (ii)).

(i) EGF receptor
IP Ab: None    EGF receptor
Blot :  PY20    PY20

(ii) erbB2 receptor
IP Ab:  PY99    None
Blot:   ErbB2   ErbB2



(i)                                    (ii)

←p185
←p170

←p185

PEO1      PEO1
TGFα      TGFα

PEO1      PEO1
NRG1β    NRG1β
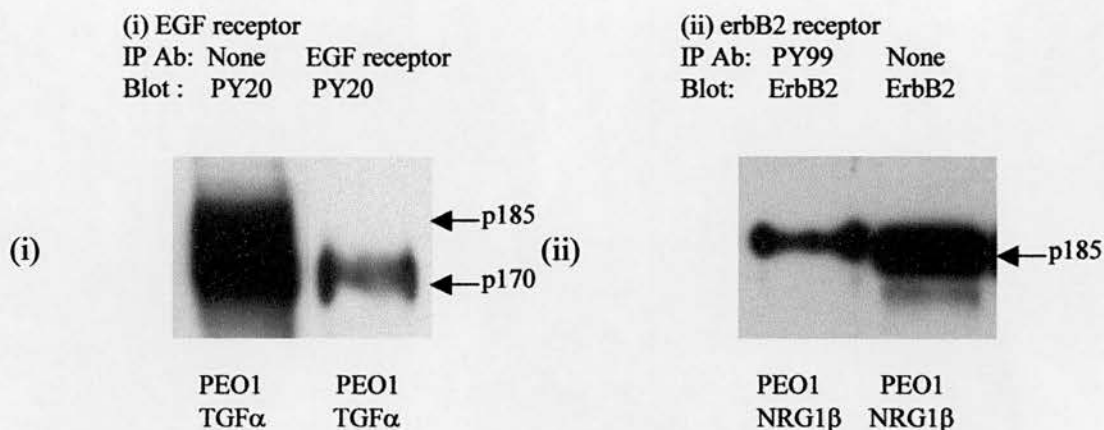
Fig 5.1 Immune-precipitation of the EGF receptor and erbB2 receptor in the PEO1 cell line. (i) Tyrosine phosphorylated EGF receptor was immune-precipitated from PEO1 cells treated with TGFα. The EGF receptor migrated to a molecular weight of approximately 170 kDa and aligned with the phosphotyrosine signal induced by TGFα. (ii) Tyrosine phosphorylated erbB2 receptor was immune-precipitated from PEO1 cells that had been treated with NRG1β and co-migrated with the erbB2 receptor position of 185 kDa.

### 5.1.2 ErbB receptor tyrosine phosphorylation in the PEO1 cell line

A single band of tyrosine phosphorylation was detected in PEO1 control cells at the p185 position (Fig 5.2 (i)). NRG1α induced an increase in tyrosine phosphorylation at this position by 15min. The strength of signal had increased by more than 2-fold at 1h and a further increase was observed at 8h (Fig 5.3). The phosphotyrosine signal was sustained at this level at 24h. A small increase in tyrosine phosphorylation was observed between control cells at the start of the experiment and at 24h.

NRG1β increased tyrosine phosphorylation of p185 compared to control cells at 15min (Fig5.2(ii)). The strength of signal obtained at 15min with NRG1β was more than 10-fold greater than the maximum phosphotyrosine signal produced by NRG1α (Fig 5.3). The level of tyrosine phosphorylation induced by NRG1β had more than halved at 1h and was further reduced at 8h and 24h. The level of receptor tyrosine phosphorylation in the control cells at 24h was similar to that observed at the start of the experiment.

Two bands with approximate molecular weights of 170kDa and 185kDa were detected in response to treatment with TGFα at 15min (Fig 5.2(iii)) and are consistent with tyrosine phosphorylation of the EGF receptor and erbB2 (Fig 5.1). The level of tyrosine phosphorylation detected at these positions increased over the period from 15min to 1h (Fig 5.3). Bands were not detected at 8h but were apparent at 24h and were equivalent to those detected in control cells at 24h.



Lanes:
1 0h Control
2 15min
3 1h
4 8h
5 24h
6 24h Control
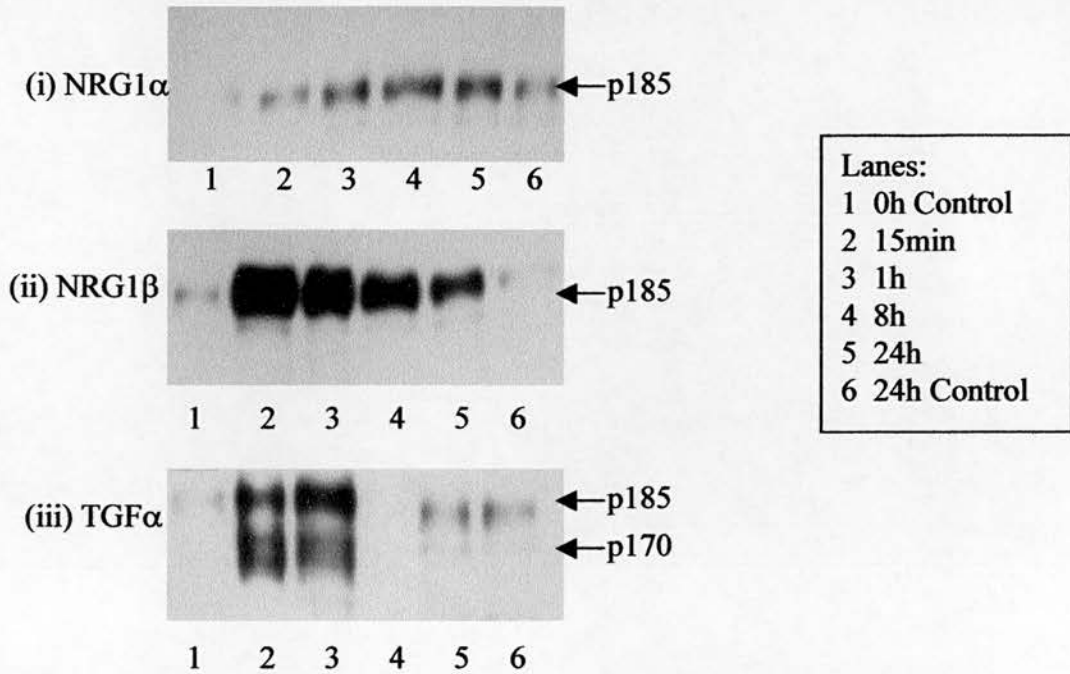
Fig 5.2 Tyrosine phosphorylation induced at the erbB receptor positions in the PEO1 cell line by (i) NRG1α which exerted a weak but sustained signal at the p185 position throughout the 24h timecourse (ii) NRG1β produced a strong signal around the p185 position at 15min that was decreased at 1h and further reduced at 8h and 24h (iii) TGFα increased tyrosine phosphorylation of the p170 and p185 positions at 15min. The signal density increased at 1h but was not detected at 8h. A weak signal was apparent at 24h and was comparable to that observed in control cells at 24h
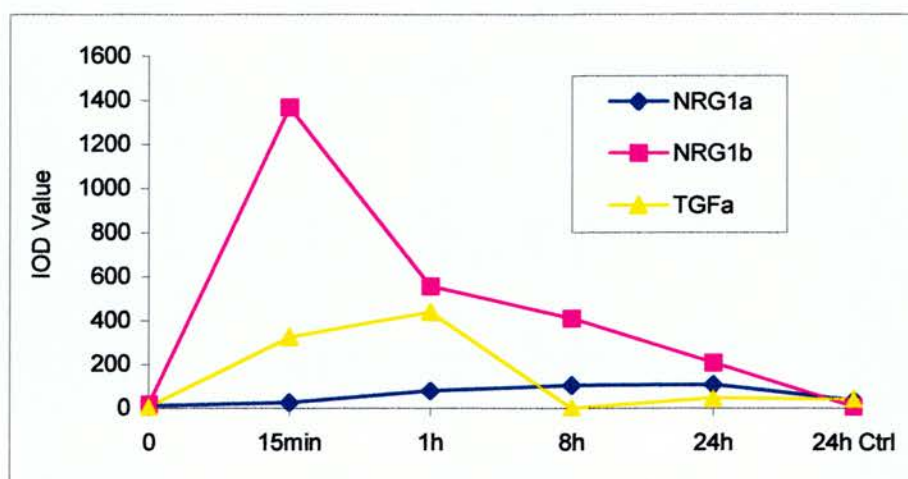
Fig 5.3 Graph of integrated optical density vs time for the tyrosine phosphorylation induced at the erbB receptor positions in response to NRG1α, NRG1β and TGFα in the PEO1 cell line. NRG1β and TGFα produced the greatest level of tyrosine phosphorylation which was most pronounced at the early time points of 15min and 1h. NRG1α induced a low level of tyrosine phosphorylation at the erbB receptor positions. The cumulative IOD value for phosphorylation of both the EGF receptor and erbB2 is shown in response to TGFα.

## 5.1.3 ErbB receptor tyrosine phosphorylation in the PEO6 cell line

Stimulation of the PEO6 cell line with NRG1α resulted in an induction of a weak phosphotyrosine signal at the p185 position at 15min (Fig 5.4(i) and Fig 5.5). The strength of the signal was reduced at 1h and was decreased further at 8h and 24h. Tyrosine phosphorylation at the erbB receptor level was not detected in control cells either at the start of the experiment or at 24h.

NRG1β induced strong tyrosine phosphorylations at the erbB receptor level at 15min (Fig 5.4 (ii) and Fig 5.5). The strength of the signal decreased slightly at 1h, was significantly reduced at 8h and was undetectable at 24h. Tyrosine phosphorylation was not observed in control cells at the start of the experiment although a very weak signal was detected at 24h.

Treatment of the PEO6 cell line with TGFα induced tyrosine phosphorylation of bands at the p170 and p185 positions at 15min (Fig 5.4(iii) and Fig 5.5), which are consistent with tyrosine phosphorylation of the EGF receptor and erbB2 respectively. The signal density of the bands had significantly reduced at 1h and only weak bands were observed at 8h and 24h. Tyrosine phosphorylation at the erbB receptor positions was not apparent in control cells at the start of the experiment but a very weak signal was detected at the p185 position at 24h.

CH5 Intracellular responses to Neuregulin and TGF alpha
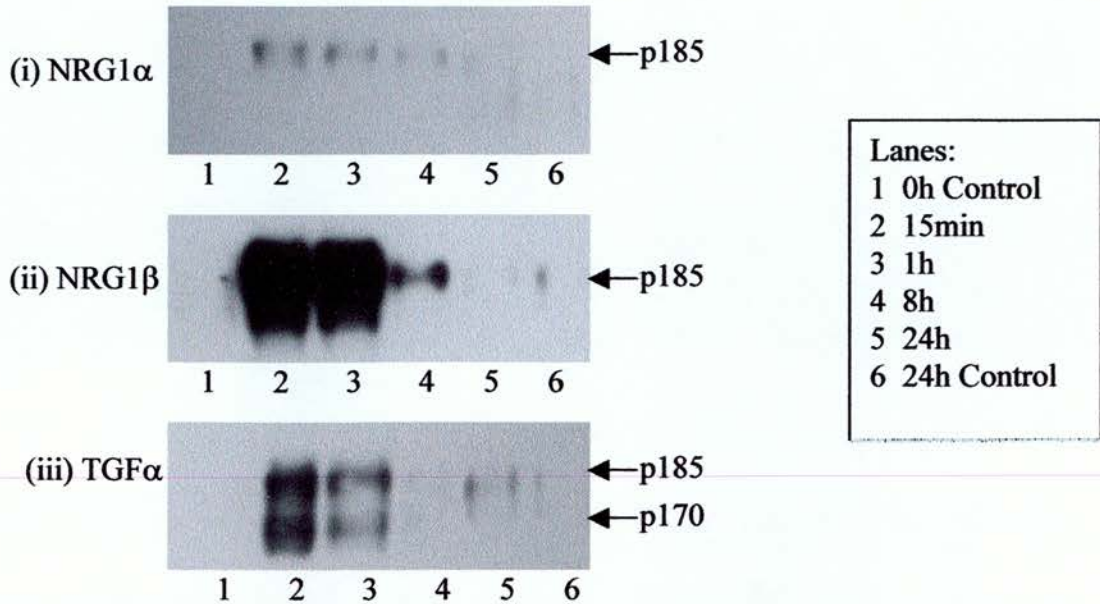
Fig 5.4 Western blot showing tyrosine phosphorylation induced at the erbB receptor positions in the PEO6 cell line by (i) NRG1α which produced a weak signal at the p185 position at 15min,1h and 8h, which was undetected at 24h. (ii) NRG1β which produced a strong tyrosine phosphorylation signal at the p185 position at 15min and 1h and was then significantly reduced at 8h and 24h. (iii) TGFα which resulted in tyrosine phosphorylation of bands at p170 and p185 at 15min and 1h, while only weak bands were detected at 8h and 24h.
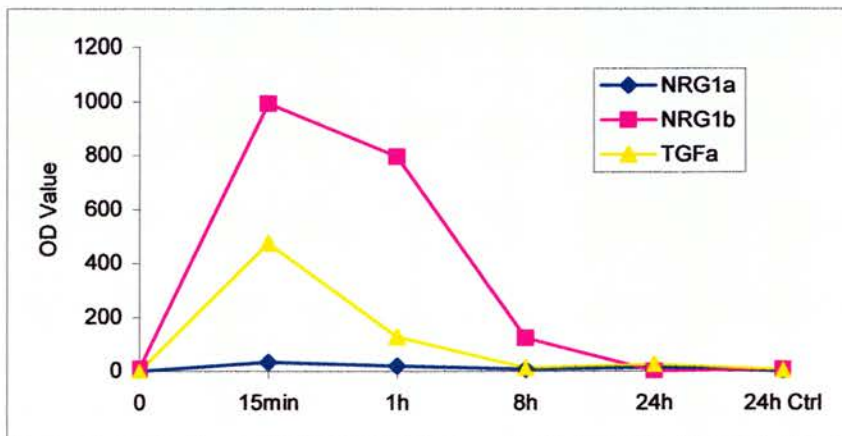


Fig 5.5 Graph of optical density vs time for tyrosine phosphorylation induced at the erbB receptor positions in response to NRG1α, NRG1β and TGFα in the PEO6 cell line. The magnitude of tyrosine phosphorylation induced at the erbB receptor level was greatest in response to NRG1β followed by TGFα. In contrast, only a weak phosphotyrosine signal was detected in response to NRG1α.

5.1.4 ErbB receptor tyrosine phosphorylation in the PEO1$^{CDDP}$ cell line

NRG1$\alpha$ produced weak tyrosine phosphorylation of a single band at the p185 position at 15min and 1h in the PEO1$^{CDDP}$ cell line (Fig 5.6(i) and Fig 5.7). The signal was not detected at 8h but reappeared as a weak band at 24h. ErbB receptor tyrosine phosphorylation was not detected in control cells at the start of the experiment but a weak signal was present at the p185 position at 24h.

Treatment with NRG1$\beta$ induced a strong tyrosine phosphorylation signal around the p185 position at 15min (Fig 5.6 (ii) and Fig 5.7). The strength of the signal had increased at 1h before a reduction in signal intensity was observed at 8h and again at 24h. Tyrosine phosphorylation was not detected in control cells either at the start of the experiment or at 24h.

Exposure of the PEO1$^{CDDP}$ cell line to TGF$\alpha$ resulted in tyrosine phosphorylation of bands at the p170 and p185 positions at 15min (Fig 5.6(iii) and Fig 5.7) which is consistent with tyrosine phosphorylation of the EGF receptor and erbB2 receptor respectively. Tyrosine phosphorylation had decreased by more than half at 1h and was not detected at 8h or 24h. ErbB receptor tyrosine phosphorylation was not detected in control cells at the start of the experiment or at 24h
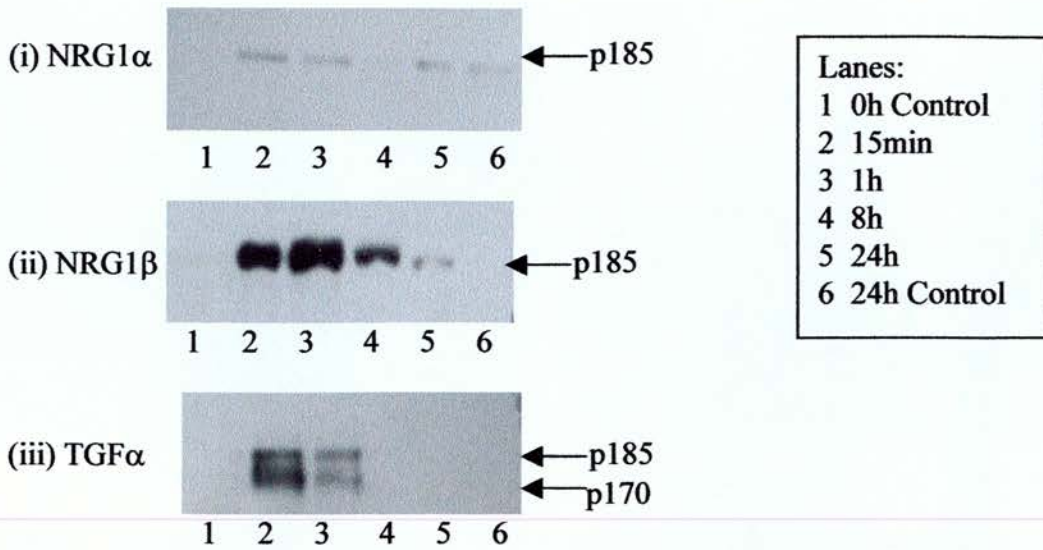
Fig 5.6 Western blot showing tyrosine phosphorylation produced at the erbB receptor level in the PEO1$^{CDDP}$ cell line by the ligands over 24h. (i) NRG1α produced weak tyrosine phosphorylation at the p185 position at 15min and 1h. A phosphotyrosine signal was not detected at 8h but a weak band was present at 24h. (ii) NRG1β induced a strong tyrosine phosphorylation signal at the p185 position at 15min, the strength of which increased at 1h and was reduced at 8h and again at 24h. (iii) TGFα resulted in tyrosine phosphorylation at both the p170 and p185 positions at 15min and 1h, signal was not detected at 8h and 24h.
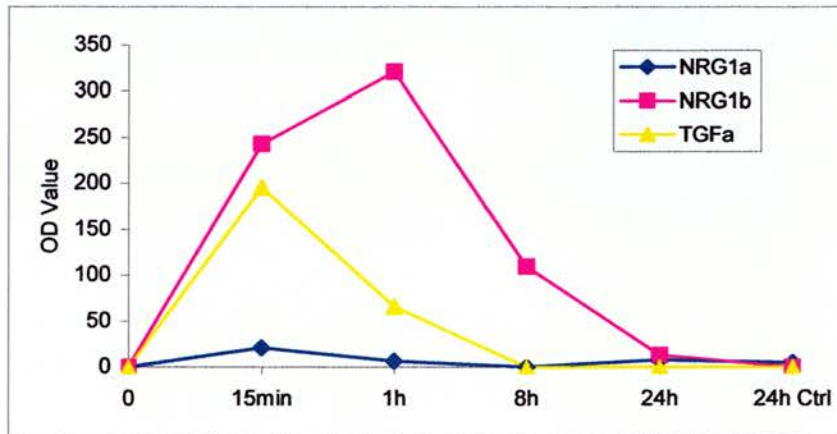


Fig 5.7 Graph of optical density vs time for tyrosine phosphorylation induced at the erbB receptor positions in response to NRG1α, NRG1β and TGFα in the PEO1$^{CDDP}$ cell line. NRG1β stimulated a high level of tyrosine phosphorylation at the erbB receptor positions at 15min which increased at 1h and was reduced at 8h and 24h. TGFα induced a strong tyrosine phosphorylation signal, the magnitude of which was greatest at 15min. In contrast, NRG1α stimulated weak tyrosine phosphorylation at the p185 erbB receptor position, the duration of which was transient.

CH5  Intracellular responses to Neuregulin and TGF alpha

5.1.4 ErbB receptor tyrosine phosphorylation in the SKOV3 cell line

Tyrosine phosphorylation was detected as a band at the p185 position in SKOV3 control cells at the start of the experiment (Fig 5.8).

Treatment with NRG1α produced a slight increase in tyrosine phosphorylation at the p185 position at 15min that gradually increased in intensity with time (Fig 5.8 (i) and Fig 5.9). The magnitude of the signal had increased 6-fold from 15min to 24h. However, tyrosine phosphorylation at the p185 position had increased 10-fold in control cells at 24h (Fig 5.9).

Treatment with NRG1β resulted in a tyrosine phosphorylation signal at the p185 position at 15min and was similar to that observed in control cells at the start of the experiment (Fig 5.8 (ii)). The signal intensity was increased at 1h and sustained to this level at 8h. Tyrosine phosphorylation had increased at 24h and the signal intensity was greater than that observed in control cells at 24h (Fig 5.9).

TGFα induced tyrosine phosphorylation of a band at the p170 position that was not apparent in control cells (Fig 5.8 (iii)). The intensity of the phosphotyrosine signal had doubled by 15min and was maintained to this level at 1h, before a reduction was observed at 8h. A significant increase was detected again at 24h, although tyrosine phosphorylation had also increased in control cells at 24h.

The increase in tyrosine phosphorylation observed from control cells at the start of the experiment to 24h is indicative of a rising level of tyrosine phosphorylation at the p185 erbB2 position in control cells. This suggests that the SKOV3 cell line may be growth regulated by erbB receptor ligands and these may have been present in the medium or produced in an autocrine manner.
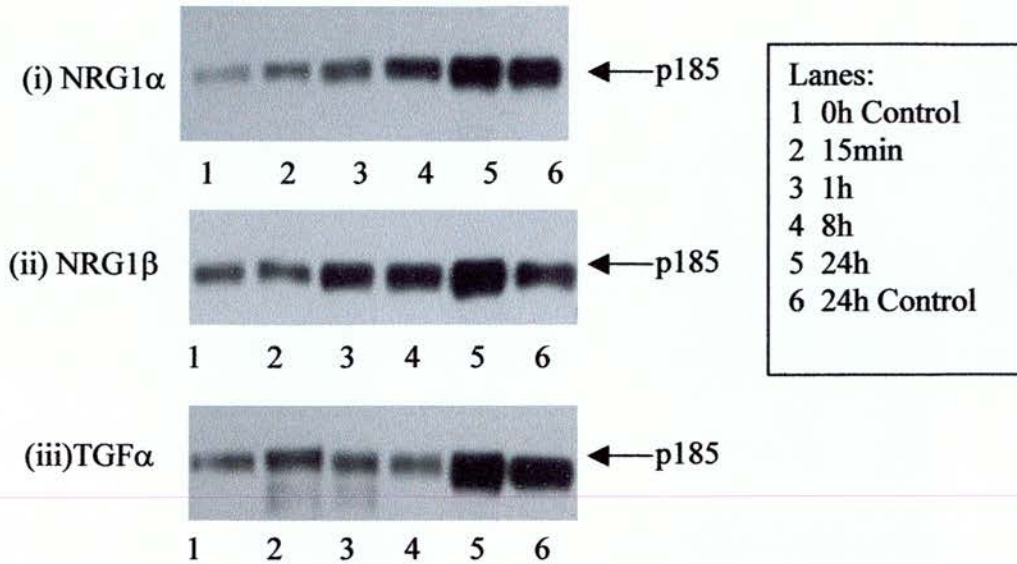
Fig 5.8 Western blot of tyrosine phosphorylation at the erbB receptor level induced by the ligands in the SKOV3 cell line. (i) NRG1α; tyrosine phosphorylation at the p185 position gradually increased over the time course with the greatest signal intensity observed at 24h, however this was comparable to the signal observed in control cells at 24h. (ii) NRG1β; tyrosine phosphorylation at the erbB receptor positions at 15min was similar to that observed in control cells. An increase in signal intensity was observed at 1h and maintained at this level at 8h before a further increase in signal intensity was observed at 24h which was above that detected in control cells at 24h. (iii)TGFα; induced phosphorylation at the p170 position at 15min and 1h, a significant increase in the level of tyrosine phosphorylation was observed at 24h.
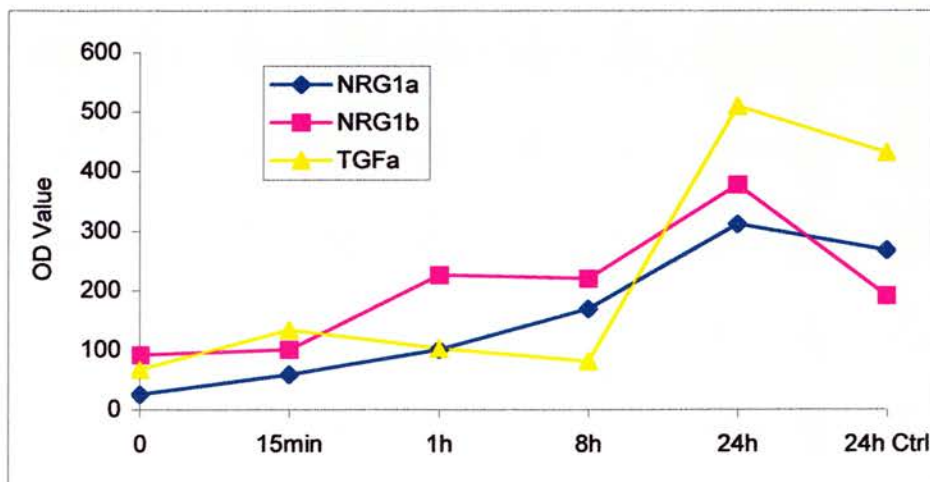


Fig 5.9 Graph of optical density vs time for tyrosine phosphorylation induced at the erbB receptor level in response to NRG1α, NRG1β and TGFα in the SKOV3 cell line. A gradual increase in tyrosine phosphorylation with time was observed in response to NRG1α. NRG1β induced an increase in tyrosine phosphorylation at 1h which was maintained at 8h before a further increase was observed at 24h. Treatment with TGFα resulted in an increase in tyrosine phosphorylation at the p170 and p185 erbB receptor positions at 15min, followed by a reduction at both 1h and 8h, before a further increase in tyrosine phosphorylation at 24h.

## 5.2 Band shifts associated with increased phosphorylation in the adapter molecule Shc

The secondary signalling molecule Shc may bind to all activated erbB receptors to initiate intracellular signalling in response to ligand. There are 3 Shc isoforms that are expressed in all tissues; p46, p52, p66 and are all subclassed as ShcA molecules. The highly related molecules p47, p52 (both ShcB) and p54 (ShcC) are expressed in brain tissues only (Pelicci G, 1996). Growth factor activated receptors induce an increase in Shc tyrosine phosphorylation at the principle sites Y239 and Y240. Phosphorylation of the third site Y317 is present without stimulation by addition of exogenous ligand (Van Der Geer P, 1996). EGF stimulates increased tyrosine phosphorylation as well as a serine / threonine phosphorylation in the p66 isoform (Okada S, 1997) resulting in a band shift to a position with increased molecular weight. Investigation of Shc band shifts in response to growth factor was evaluated by Western blot analysis using the anti-Shc antibody S14630 (Transduction laboratories) at a dilution of 1 / 1000. This antibody was known to detect the ShcA isoforms p46, p52, p66 and was specific for a sequence spanning the SH2 domain and part of the CH1 region of the molecule.

### 5.2.1 Investigation of Shc band shifts

The PEO1 cell line was investigated for band shifts to positions with increased molecular weight for the Shc isoforms in response to NRG1β (15 min). Immune-precipitation with the anti-phosphotyrosine antibody (PY20) was used to detect phosphorylation induced upon treatment with growth factor in comparison to phosphorylation in control cells. The anti-Shc antibody was used to probe for expression of the Shc isoforms.

PEO1 control cells clearly expressed the p46 and p52 isoforms and a weak signal was detected at the p66 position (Fig 5.10 lane 1). Another weak signal was detected at a position of approximately 54 kDa, which corresponds to the expected molecular weight for the ShcC isoform. The antibody was known to detect ShcA and cross-reactivity with the highly related ShcB and ShcC molecules was not specified in the literature. Since the antibody was raised to a region of the Shc molecule which is highly homologus in ShcB and ShcC, it is likely to be able to detect these related molecules. Treatment with NRG1β resulted in a band shift to a position with

CH5 Intracellular responses to Neuregulin and TGF alpha

increased molecular weight in both the p46 and p52 isoforms (Fig 5.10 lane 4). It is unclear if a band shift was present for the p66 isoform. Immune-precipitation showed that Shc isoforms in PEO1 control cells were tyrosine phosphorylated (Fig 5.10,lane2). Treatment with NRG1β induced a band shift in the p52 and p66 isoforms which were also tyrosine phosphorylated (Fig 5.10 lane 3).

These results are consistent with Shc undergoing additional phosphorylation in response to ligand which translates into reduced migration by gel electrophoresis. This was investigated for the panel of four cell lines (PEO1, PEO6, PEO1$^{CDDP}$ and SKOV3), in response to NRG1α, NRG1β and TGFα.
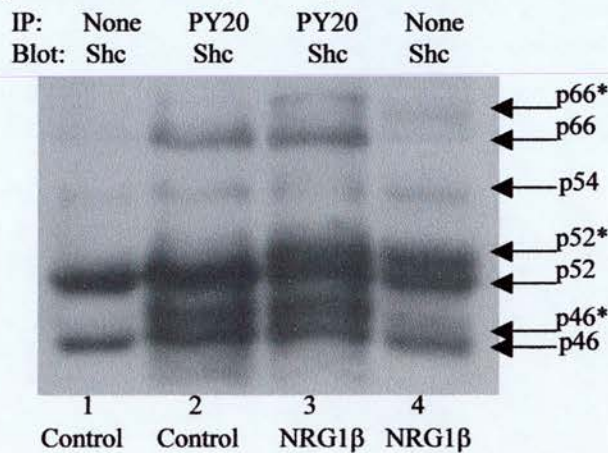


Fig 5.10 Western blot analysis of the PEO1 cell line indicating Shc band shifts in response to NRG1β. Treatment of PEO1 cells with NRG1β stimulated band shifts in the p46 and p52 isoforms (lane 4) to a position with increased molecular weight (*) that is not apparent in control cells (lane 1). Immune-precipitation with anti-phosphotyrosine antibody shows that p46, p52 and p66 are tyrosine phosphorylated in control cells (lane 2) and that treatment with NRG1β induces a band shift to a position with increased molecular weight that is also tyrosine phosphorylated. A band was detected at a position that would be expected for expression of p54 ShcC.

5.2.2    Increased phosphorylation of Shc isoforms in the PEO1 cell line

The PEO1 cell line clearly expressed the p46, p52 and p66 isoforms (Fig 5.11 lane 1). Treatment with NRG1α resulted in a band shift in the p52 isoform at 15min (Fig 5.11 lane 2). Band shifts were not detected in either the p46 or p66 isoforms at this time point in response to NRG1α.

NRG1β induced band shifts in all three isoforms p46, p52 and p66 at 15min (Fig 5.11 lane3). The p66 isoform had totally displaced to the position with increased molecular weight. In contrast, only a weak signal was detected at the higher molecular weight position for the p46 isoform, the amount of p52 at the anticipated molecular weight was equivalent to that observed at the position with increased molecular weight.

Similarly, TGFα induced band shifts in all three Shc isoforms at the 15min time point (Fig 5.11 lane 4). The p66 isoform had completely displaced to the position with increased molecular weight. Both the p46 and p52 isoforms had equivalent levels of protein at the anticipated molecular weight and at the position with increased molecular weight.
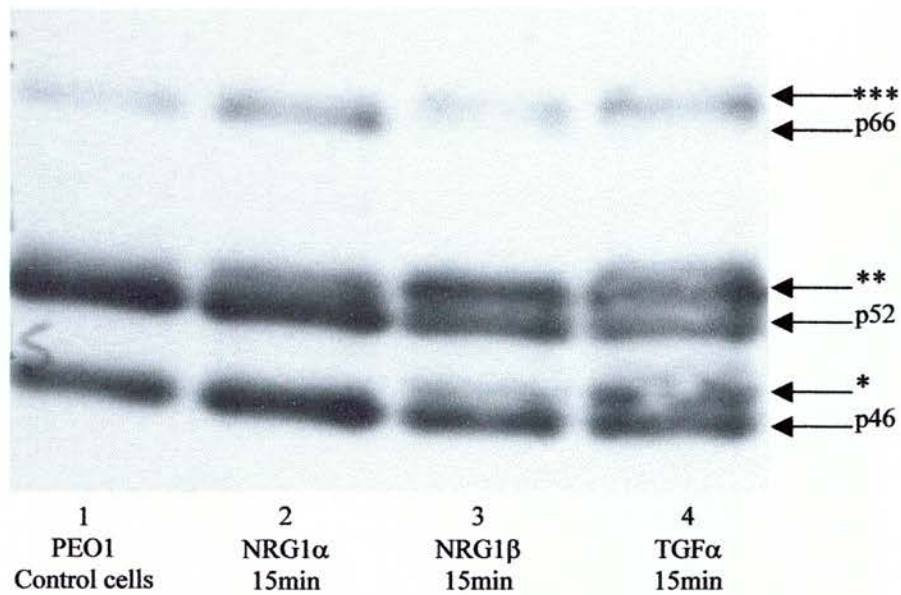
Fig 5.11 Shc isoform band shifts in response to ligand in the PEO1 cell line. NRG1α induced a band shift to a position with increased molecular weight in the p52 isoform at 15min. Treatment with NRG1β resulted in a band shift to increased molecular weight for the p46 and p52 isoforms. The p66 isoform was displaced to the higher molecular weight position. Similarly, TGFα induced band shifts to positions with increased molecular weight for the p46 and p52 isoforms, with complete displacement of the p66 isoform to the position with increased molecular weight. Band shifts to higher molecular weight positions are represented as follows p46(*), p52(**) and p66(***).

### 5.2.3 Enhanced phosphorylation of Shc in the PEO6 cell line

The PEO6 cell line clearly expressed the p46, p52 and p66 Shc isoforms (Fig 5.12 lane 1). NRG1α induced a weak band shift in the p46 isoform to a position with increased molecular weight (Fig 5.12 lane 2). The band shift observed for p52 suggests equivalent levels of p52 Shc at the expected molecular weight and at a position with increased molecular weight. It is unclear if a band shift was present for the p66 isoform in response to NRG1α.

PEO6 cells stimulated with NRG1β induced band shifts in all three Shc isoforms where equivalent levels of protein were detected at the expected position and at the position with increased molecular weight (Fig 5.12 lane 3).

PEO6 cells treated with TGFα resulted in band shifts in the p46 and p52 isoforms to positions with increased molecular weight. It is unclear if there was a band shift present for the p66 isoform (Fig 5.12 lane 4).

|   | 1 | 2 | 3 | 4 |
| --- | --- | --- | --- | --- |
|   | PEO6 | NRG1α | NRG1β | TGFα |
|   | Control cells | 15min | 15min | 15min |
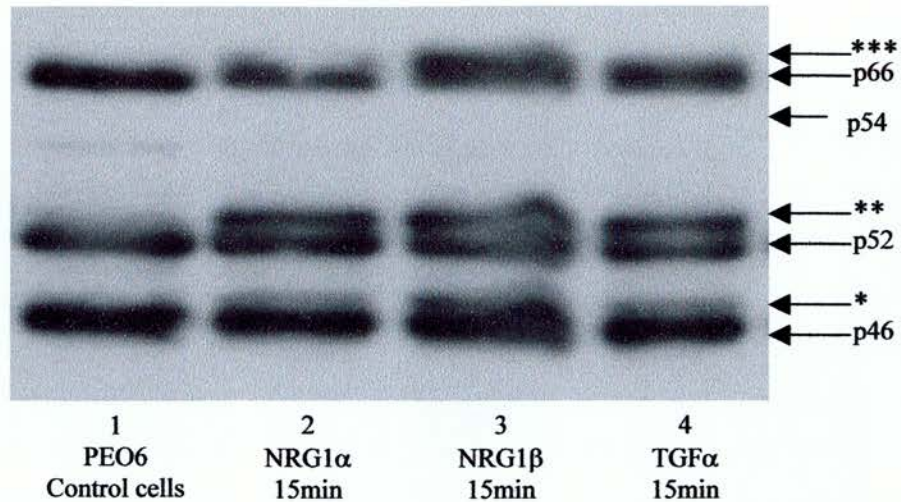
Fig 5.12 Shc isoform band shifts in response to ligand in the PEO6 cell line. Treatment with NRG1α resulted in a band shift to a position with increased molecular weight for p46 and p52. NRG1β induced a band shift in all three Shc isoforms p46, p52 and p66. TGFα induced a band shift to a position with increased molecular weight for the p46 and p52 isoforms.

### 5.2.4 Phosphorylation of Shc in the PEO1$^{CDDP}$ cell line

The PEO1$^{CDDP}$ cell line clearly expressed the p46 and p52 Shc isoforms. p66 was detected on a longer exposure but the level to which it was expressed was much less than that observed for the p46 and p52 isoforms (Fig 5.13 lane 1). Stimulation of PEO1$^{CDDP}$ cells with NRG1α did not affect the molecular weight of p46 and p52 and was directly comparable to that observed in control cells (Fig 5.13 lane 2). Treatment with NRG1β induced a band shift to a position of higher molecular weight for the p52 isoform (Fig 5.13 lane 3). Stimulation with TGFα resulted in a band shift to a position with increased molecular weight for the p52 isoform       (Fig 5.13 lane 4). A band shift was detected for the p46 isoform, but required longer exposure and is not observed in Fig 5.13.
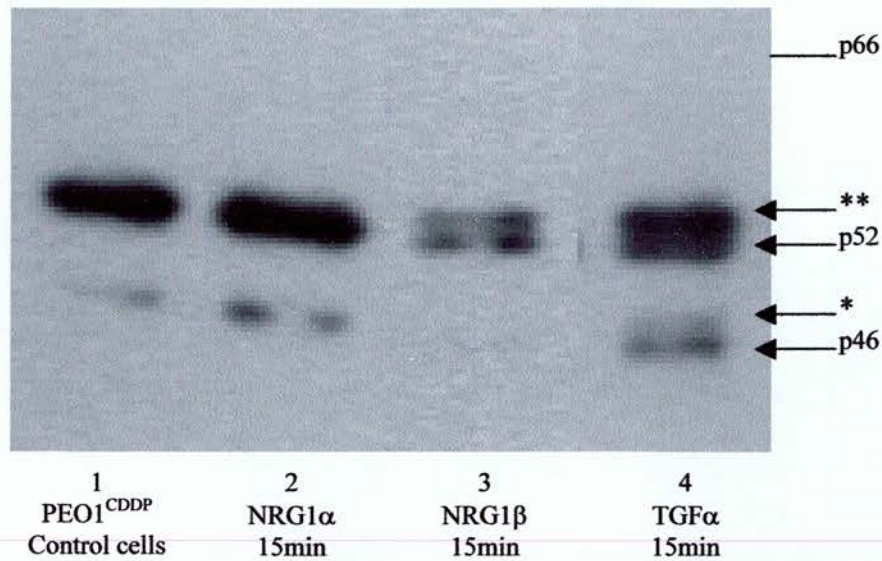
Fig 5.13 Shc isoform band shifts in response to ligand in the PEO1$^{CDDP}$ cell line. Treatment with NRG1$\alpha$ did not induce band shifts in the p46 and p52 isoforms at 15min. NRG1$\beta$ induced a band shift to a position of increased molecular weight for the p52 isoform at 15min. TGF$\alpha$ induced a band shift in both the p52 and p46 isoforms.

### 5.2.5    Enhanced phosphorylation of Shc in the SKOV3 cell line.

The SKOV3 cell line expressed the p46, p52 and p66 Shc isoforms (Fig 5.14 lane1). Cells that had been treated with NRG1$\alpha$ or NRG1$\beta$, displayed similar banding to that observed in control cells, a slight band shift of the p52 isoform was detected but this was also apparent in control cells (Fig 5.14 lanes 2 & 3 respectively).

In contrast, SKOV3 cells which had been exposed to TGF$\alpha$, had a band shift at a position with higher molecular weight in all three isoforms. A weak band shift was detected in the p46 isoform, whereas the band shift for the p52 isoform to the higher molecular weight had greater signal intensity than that at the original p52 position. The p66 isoform was displaced to the higher molecular weight position.
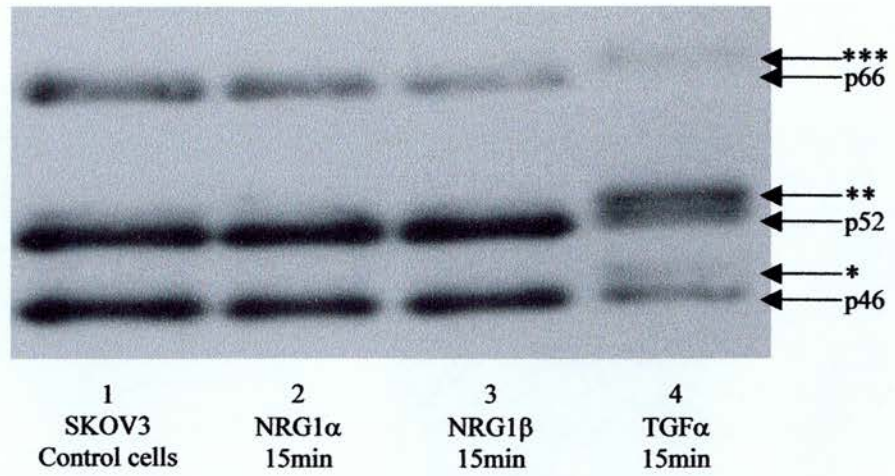
Fig 5.14 Shc isoform band shifts in response to ligand in the SKOV3 cell line. Treatment with NRG1α and NRG1β did not affect the positions of the Shc isoform bands in comparison to control cells. Treatment with TGFα resulted in a band shift to a position with increased molecular weight for all three isoforms, where the p66 isoform was completely displaced to the position with increased molecular weight.

CH5  Intracellular responses to Neuregulin and TGF alpha

5.3   Phosphorylation of Erk1 and Erk2 in response to ligand

This section describes the phosphorylation of p44 Erk1 and p42 Erk2 in response to the NRG's and TGFα ($10^{-9}$M) in the four cell lines. Phosphorylated Erk was detected by Western blot analysis using the antibody 9101S (New England Biolabs) which specifically detects dual-phosphorylated Erk ie: Erk that is phosphorylated on both the residues threonine 202 and tyrosine 204. The antibody was used at a dilution of 1 / 1000.

### 5.3.1 Ligand induced Erk phosphorylation in the PEO1 cell line

A weak signal corresponding to dual-phosphorylated p42 Erk2 was detected in PEO1 control cells (Fig 5.15(i)). Stimulation with NRG1α increased the signal density for phosphorylated p42 at 15min, however phosphorylated p42 was not detected at 1h or 6h, but appeared as a weak band at 24h. Phosphorylated p44 was not detected in control cells or in response to NRG1α.

Treatment of PEO1 cells with NRG1β resulted in a significant increase of more than 15-fold in the band density corresponding to the amount of phosphorylated p42 at 15min (Fig 5.15 (ii)). The signal density had reduced at 1h and was reduced again at 8h and 24h. NRG1β also induced phosphorylation of p44 by 15min, the signal was still apparent at 1h but the density had significantly decreased. Phosphorylated p44 was not detected at 8h or 24h.

In response to TGFα, the level of phosphorylated p42 at 15 min was significantly increased more than 12-fold above that observed in control cells (Fig 5.15(iii)). This level of p42 phosphorylation was maintained throughout the time course of 24h. TGFα also induced phosphorylation of p44. The amount of phosphorylated p44 induced by 15min had reduced by half at 1h and maintained at this level at 8h. A small increase in the amount of phosphorylated p44 was observed at 24h.

CH5  Intracellular responses to Neuregulin and TGF alpha
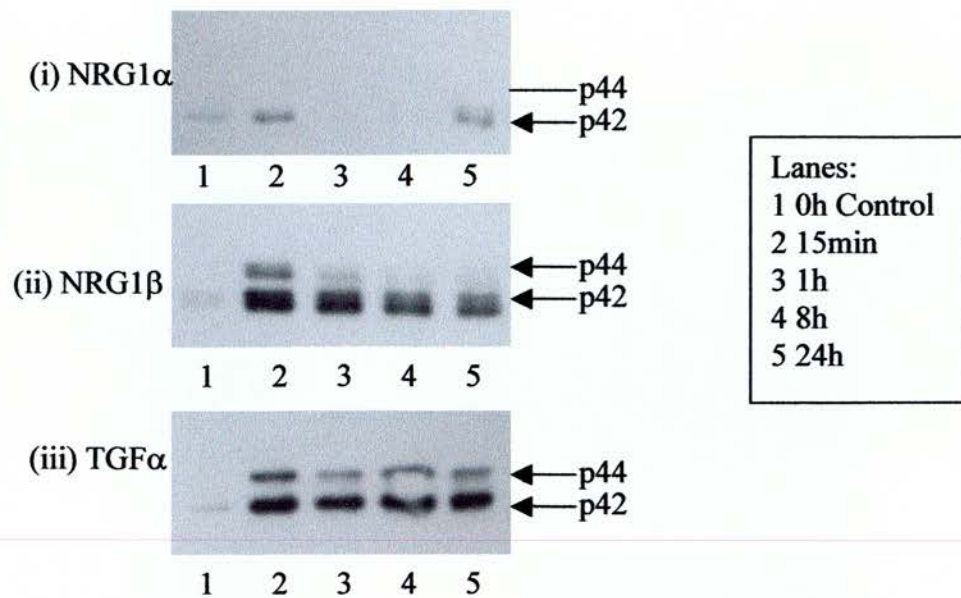
Fig 5.15 Ligand induced Erk phosphorylation in the PEO1 cell line. Phosphorylation was observed in response to (i) NRG1α, as a weak signal corresponding to phosphorylation of p42 at 15 min and 24h; (ii) NRG1β, where phosphorylation of p42 was apparent through the time points whilst p44 phosphorylation was detected at 15 min and 1h; (iii) TGFα, which induced phosphorylation of both p44 and p42 through the time points indicated.

### 5.2.3 Ligand induced Erk phosphorylation in the PEO6 cell line

Phosphorylated p44 Erk1 and p42 Erk2 were detected in PEO6 control cells (Fig 5.16). The amount of phosphorylated p44 was approximately equivalent to that observed for phosphorylated p42.

Stimulation of PEO6 cells with NRG1α resulted in an increase of more than 10-fold in the amount of both phosphorylated p44 and p42 at 15min (Fig 5.16(i)). The density of the signals corresponding to phosphorylated p44 and p42, simultaneously decreased at 1h and again at 8h. At 24h, the signal density for phosphorylated p44 was greater than that observed for phosphorylated p42. Signal intensity corresponding to phosphorylated p44 and p42 in control cells at 24h was reduced to less than half of that observed for control cells at the start of the experiment and was decreased in comparison to NRG1α treated cells at 24h.

NRG1β induced a 6-fold increase in the amount of phosphorylated p44 at 15min and this was equivalent to the increase observed for phosphorylated p42 (Fig 5.16(ii)). The intensity of the signals for phosphorylated p44 and p42 had reduced at 1h and again at 8h. At 24h, phosphorylated p44 and p42 had reduced to a barely

CH5 Intracellular responses to Neuregulin and TGF alpha

detectable level. Similarly, in control cells at 24h, the amount of phosphorylated p44 and p42 had reduced to barely detectable levels.

Treatment with TGFα stimulated a 10-fold increase in the amount of phosphorylated p44 and p42 at 15min (Fig 5.16(iii)). The density of signal corresponding to phosphorylated p44 was more intense than that observed for p42. The level of phosphorylated p44 was maintained at 1h and a reduction was observed at 8h. A further reduction in the amount of phosphorylated p44 was detected at 24h, although this level was greater than that observed in control cells at 24h. Conversely, the amount of phosphorylated p42 had increased at 1h, before a reduction was observed at 8h. At 24h, the level of phosphorylated p42 had decreased but was still greater than that observed for the control cells at 24h.
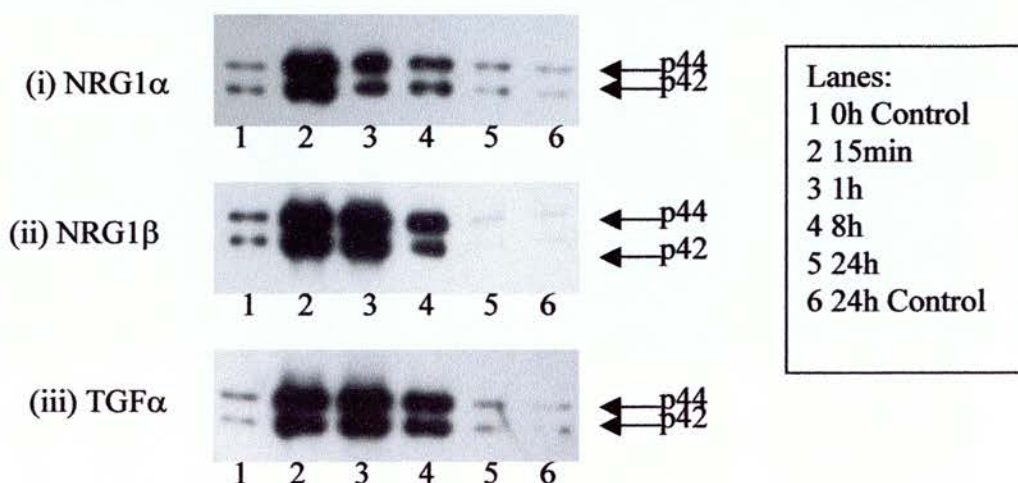


Fig 5.16 Ligand induced Erk phosphorylation in the PEO6 cell line. Increased phosphorylation was detected for both p44 and p42 in response to NRG1a, NRG1b and TGFa. The magnitude of p44 phosphorylation was approximately equivalent to that of the p42 isoform. The magnitude of Erk phosphorylation decreased with increasing time.

CH5  Intracellular responses to Neuregulin and TGF alpha

### 5.3.3 Ligand induced Erk phosphorylation in the PEO1$^{CDDP}$ cell line

Both p44 and p42 were phosphorylated in PEO1$^{CDDP}$ control cells but the signal corresponding to phosphorylated p42 was more intense than that observed for phosphorylated p44.

Treatment with NRG1α, resulted in a 2-fold increase in the amount of phosphorylated p44 and a 3-fold increase in the amount of phosphorylated p42 at 15min (Fig 5.17(i)). At 1h, the level of both phosphorylated p44 and p42 had decreased below that observed for control cells at the start of the experiment. The density of the signal corresponding to the amount of both phosphorylated p44 and p42 at 1h was maintained at 8h and 24h. The levels of phosphorylated p44 and p42 in control cells at 24h was greater than that observed for NRG1α treated cells at 24h, but this was reduced in comparison to control cells at the start of the experiment.

NRG1β induced a 3-fold increase in the amount of both phosphorylated p44 and p42 at 15min, the signal density for the amount of phosphorylated p44 was comparable to that of p42 (Fig 5.17(ii)). The level of phosphorylated p44 increased while that of p42 decreased at 1h. At 8h, the amount of both phosphorylated p44 and p42 had decreased, although the level of phosphorylated p44 was 3-fold greater than that of p42. By 24h, the signal densities for both phosphorylated p44 and p42 had decreased however, the amount of phosphorylated p44 was still 2-fold greater than that observed for phosphorylated p42. The signal intensity of phosphorylated p44 and p42 in control cells at 24h, was reduced in comparison to NRG1β treated cells at the same time point.

TGFα induced an increase in the amount of phosphorylated p44 and p42 of more than 12-fold at 15 min (Fig 5.17(iii)), the signal density for each was similar. Phosphorylation of both p44 and p42 gradually and simultaneously decreased at 1h, 8h and again at 24h. The signal intensity corresponding to phosphorylated p44 and p42 at 24h in response to TGFα, was similar to that observed in control cells at the same time point.

CH5 Intracellular responses to Neuregulin and TGF alpha
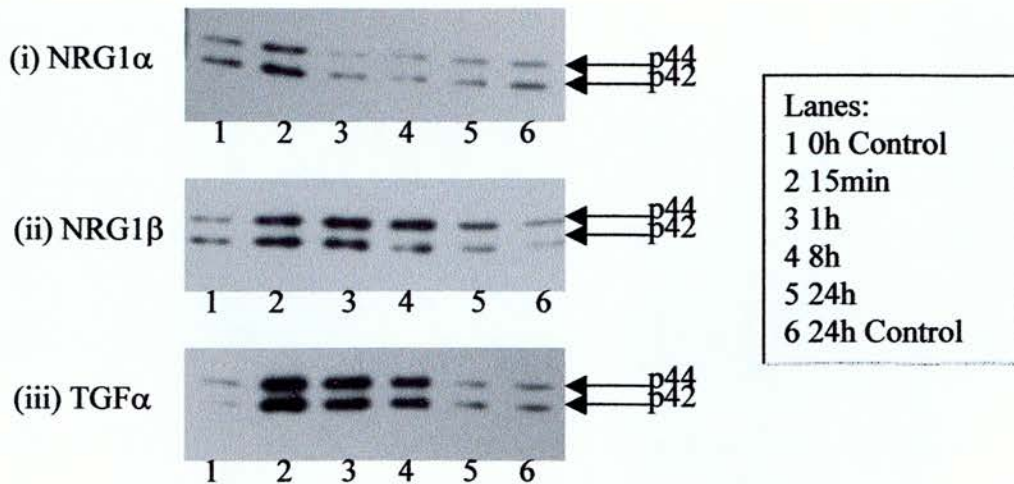
Fig 5.17 Ligand induced phosphorylation in p44 Erk1 and p42 Erk2 in the PEO1$^{CDDP}$ cell line. (i) NRG1α stimulated an increase in the amount of both phosphorylated p44 and p42 at 15min, which decreased to levels comparable with the control cells thereafter. (ii) NRG1β stimulated an increase in the amount of phosphorylated p44 and p42 at 15min, which was sustained at 1h and then decreased with increasing time. (iii) TGFα induced an increase in the amount of phosphorylated p44 and p42 at 15min, 1h, 8h and was then reduced to levels comparable with the control cells at 24h.

5.3.3 Ligand induced Erk phosphorylation in the SKOV3 cell line

A weak signal was detected in SKOV3 control cells corresponding to phosphorylated p42 Erk2, phosphorylation of p44 Erk1 was not apparent.

Treatment with NRG1α resulted in a slight increase (4-fold) in the band density for phosphorylated p42 at 15min (Fig 5.18(i)). The extent of p42 phosphorylation was sustained at 1h, 8h and 24h, although the magnitude of phosphorylation was comparable with that observed for control cells at 24h. Phosphorylation of p44 in response to NRG1α was not detected.

Similarly, NRG1β induced an increase in the amount of phosphorylated p42 at 15 min and was sustained to this level at 1h, 8h and 24h (Fig 5.18(ii)). Phosphorylated p44 was not detected in response to NRG1β.

In contrast, stimulation of SKOV3 cells with TGFα resulted in a significant increase of more than 10-fold in the amount of phosphorylated p42 at 15min and induced phosphorylation of p44 (Fig 5.18(iii)). The amount of phosphorylated p42 was 2 fold greater than that observed for phosphorylated p44. The signals corresponding to phosphorylated p44 and p42 simultaneously reduced at 1h. At 8h, a dramatic reduction was observed in the amount of phosphorylated p44, with only a

gradual decrease in the amount of phosphorylated p42. At 24h, the signal corresponding to phosphorylated p42 was similar to that observed at 8h, although only a weak signal was detected for phosphorylated p44. Similarly a strong band of phosphorylated p42 was observed in control cells at 24h, while only a weak signal was detected for phosphorylated p44. The density of the band corresponding to phosphorylated p42 had increased 5-fold from that observed in control cells at the start of the experiment.
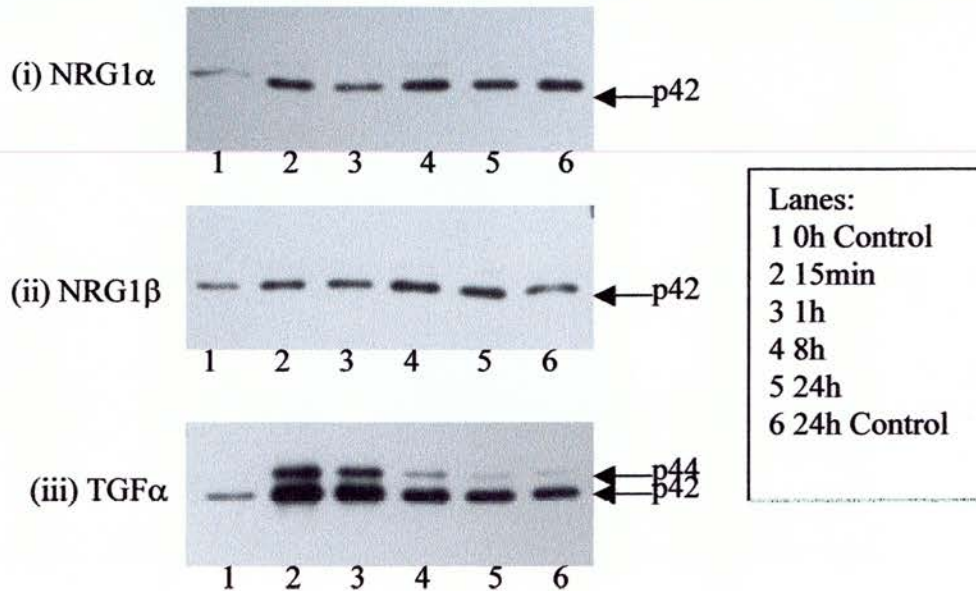


Fig 5.18 Ligand induced Erk phosphorylation in the SKOV3 cell line. Phosphorylated p42 Erk2 was present in SKOV3 control cells while phosphorylated p44 Erk1 was not detected. NRG1α and NRG1β induced an increase in the level of phosphorylated p42 at 15min, which was sustained at 1h, 8h and 24h although this was comparable with that observed in the control cells. In contrast, TGFα stimulated an increase in the amount of both phosphorylated p44 and p42 at 15min by 10-fold. The levels of phosphorylated p44 rapidly decreased with increasing time whilst phosphorylation of p42 decreased at 8h and was sustained to this level at 24h.

135

Ch 6 Anti-receptor antibodies to the erbB3 and erbB4 receptors influence cellular

## Ch 6 Anti-receptor antibodies to the erbB3 and erbB4 receptors influence cellular growth.

This section describes an investigation of the roles of the erbB3 and erbB4 receptors in mediating regulation of cellular growth in response to NRG1β. Anti-receptor antibodies that prevent ligand binding to receptor were used to test the receptor function through growth assays in the following panel of cell lines; PEO1, PEO6, PEO1$^{CDDP}$ and SKOV3. Growth assays were performed in 24 well trays; incubation of antibody was prior to replenishment of media with or without addition of NRG1β.

6.1 Effect of the anti-erbB3 receptor antibody on regulation of cellular growth

The anti-erbB3 receptor antibody H3.105.5 / Ab105 (Neomarkers) was used to evaluate the influence of the erbB3 receptor on cellular growth in cells which had or had not been stimulated with NRG1β. Cell number was evaluated on day 5 using a Coulter Counter and is expressed as a percentage in comparison to the control cell number assigned 100%. Cell counts were compared using the Student t test to determine statistical significance.

6.1.1 Growth regulation by the anti-erbB3 receptor antibody in the PEO1 cell line

PEO1 cells were growth stimulated by NRG1β, which resulted in an increase in cell number of 278% (± 5%) above the control cell count (Fig 6.1). Incubation with anti-erbB3 receptor antibody prior to treatment with NRG1β resulted in the growth stimulation being reduced from 278% to only 91% (± 8%) above the control cell count. This was a reduction to 1/3 of the NRG1β stimulated growth. Pre-treatment of cells with anti-erbB3 receptor antibody in the absence of NRG1β, reduced cell number by 19% (± 2%), in comparison to the control cell count (81% vs 100% control cell number).

Ch 6 Anti-receptor antibodies to the erbB3 and erbB4 receptors influence cellular
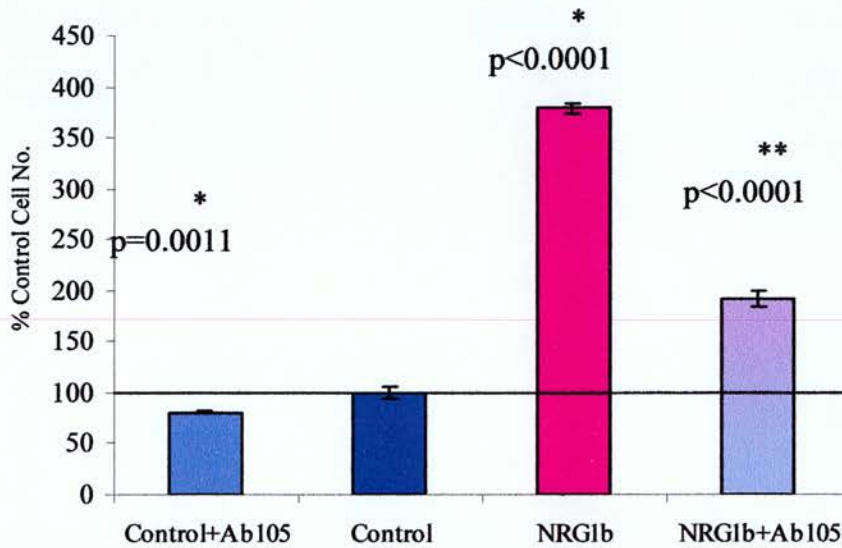
Fig 6.1 Growth regulation by the anti-erbB3 receptor antibody (Ab105) in the PEO1 cell line. NRG1β stimulated an increase in cellular growth of 278% above the control cell number. Treatment with anti-erbB3 receptor antibody reduced NRG1β stimulated growth to 91% above the control cell count. Anti-erbB3 receptor antibody in the absence of NRG1β reduced cell growth by 19% to 81% of the control cell number. p-values refer to statistical significance between cells treated with antibody or NRG1β, in comparison to cells grown under control conditions(*) and, cells treated with antibody and NRG1β in comparison to those treated with NRG1β(**).

137

Ch 6 Anti-receptor antibodies to the erbB3 and erbB4 receptors influence cellular growth.

6.1.2 Growth regulation by the anti-erbB3 receptor antibody in the PEO6 cell line.

The PEO6 cell line was growth stimulated by NRG1β to 215% (± 15%) above the control cell number (Fig 6.2). Treatment with anti-erbB3 receptor antibody reduced the NRG1β growth stimulation to 121% (± 9%) above the control cell number, corresponding to an approximate 45% inhibition of the growth stimulus. Anti-erbB3 receptor antibody in the absence of NRG1β, reduced cell growth to 82% (± 12%) in comparison to the control cell number, but this was not statistically significant.



Fig 6.2 Growth regulation by the anti-erbB3 receptor antibody (Ab105) in the PEO6 cell line. The PEO6 cell line was growth stimulated by NRG1β to 215% above the control cell count. The NRG1β growth stimulation was reduced by 94% by pre-incubation with anti-erbB3 receptor antibody. Pre-incubation with Ab105 in the absence of NRG1β, reduced cell growth to 82% in comparison to the control cell number assigned 100%, however this was not statistically significant. p-values refer to significance for cells treated with antibody or NRG1β, in comparison to cells grown under control conditions (*) and, cells treated with antibody and NRG1β in comparison to those treated with NRG1β (**).

Ch 6 Anti-receptor antibodies to the erbB3 and erbB4 receptors influence cellular growth.

6.1.3 Growth regulation by the anti-erbB3 receptor antibody in the PEO1$^{CDDP}$ cell line.

Treatment with NRG1$\beta$ in the PEO1$^{CDDP}$ cell line resulted in growth reduction to 62% ($\pm$ 18%) in comparison to the control cell number assigned 100%. However, analysis of the cell counts using the Student t test produced a p value only approaching significance (p=0.0632). Pre-incubation with anti-erbB3 receptor antibody resulted in restoration from the NRG1$\beta$ reduced growth to 110% ($\pm$ 10%) in comparison to the control cell count. Incubation of cells with anti-erbB3 receptor antibody in the absence of NRG1$\beta$, resulted in an overall increase in cellular growth of 28% ($\pm$ 2%) above the control cell number, but this was not significant (p=0.1018).
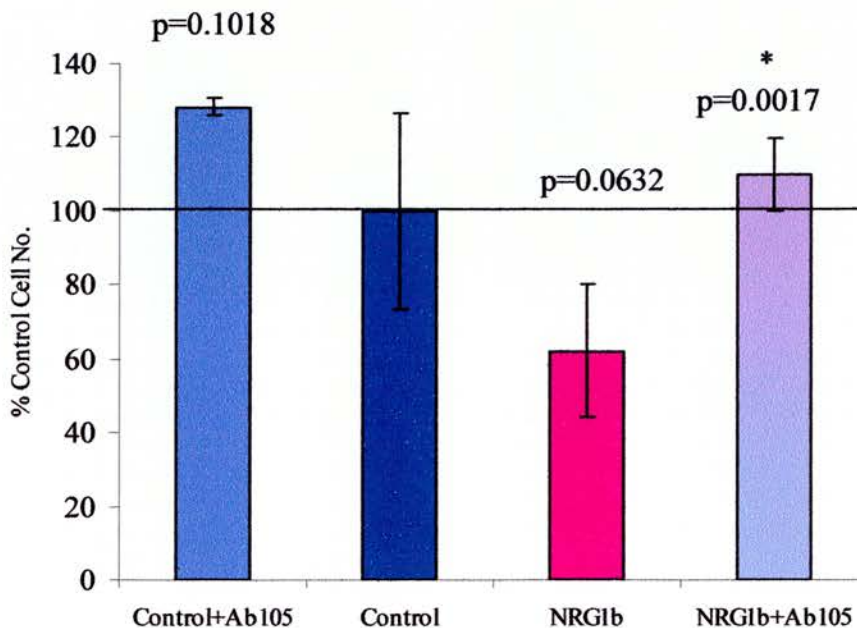


Fig 6.3 Growth regulation by the anti-erbB3 receptor antibody (Ab105) in the PEO1$^{CDDP}$ cell line. NRG1$\beta$ reduced cell growth to 62% in comparison to the control cell count assigned 100%, which approached significance. Pre-incubation with anti-erbB3 receptor stimulated growth by 10% above the control cell count. A significant change in cell growth was detected between NRG1$\beta$ treated cells and those that were incubated with antibody prior to the addition of NRG1$\beta$ (*). Incubation of cells with anti-erbB3 receptor antibody in the absence of NRG1$\beta$, resulted in an increase in cellular growth of 28% above the control cell number but this was not statistically significant.

139

Ch 6 Anti-receptor antibodies to the erbB3 and erbB4 receptors influence cellular growth.

### 6.1.4 Growth regulation by the anti-erbB3 receptor antibody in the SKOV3 cell line.

The SKOV3 cell line exhibited a small increase in cellular growth of 13% (± 5%) in response to NRG1β above the control cell number. Pre-incubation with anti-erbB3 receptor antibody prior to addition of medium and growth factor resulted in a reduction to 7% (± 1%) above the control cell number assigned 100%. Cells that had been pre-incubated with antibody and cultured in control conditions (100% ± 5%) did not vary from the control cell number 100% (± 4%). Statistical analysis of the cell counts did not detect significant changes in cell growth in response to NRG1β, incubation with antibody prior to the addition of NRG1β or incubation with antibody in cells that were maintained in control conditions.
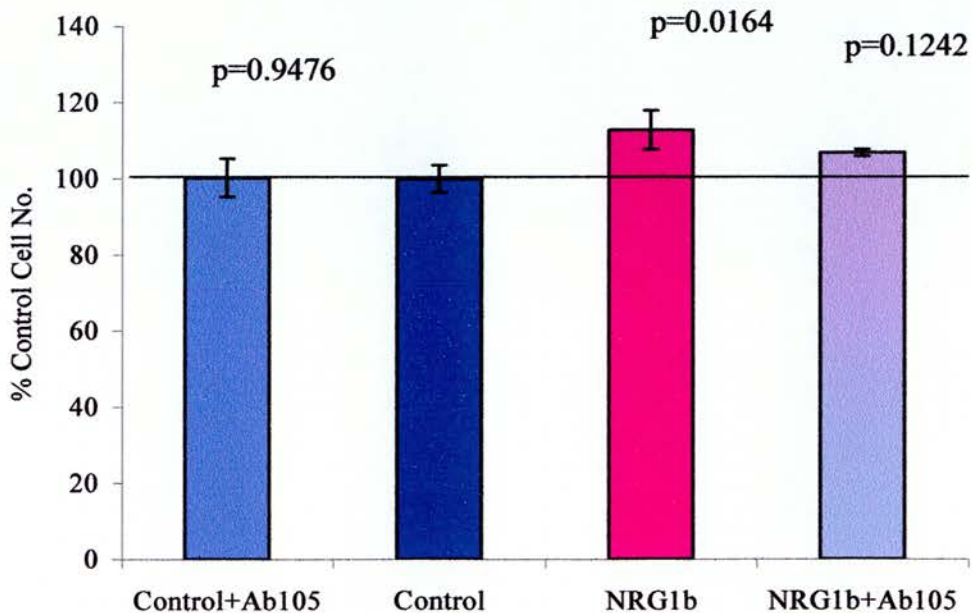


Fig 6.4 Growth regulation by the anti-erbB3 receptor antibody Ab105 in the SKOV3 cell line. NRG1β induced a small increase in cell number of 13% above the control cell count. Pre-incubation with anti-erbB3 receptor antibody reduced the NRG1β stimulated growth to 7% above the control cell count, whilst pre-incubation with anti-erbB3 receptor antibody in cells that were maintained in control conditions had no effect on cell number (100%) in comparison to the control cell count (100%).

Ch 6 Anti-receptor antibodies to the erbB3 and erbB4 receptors influence cellular growth.

6.2 Effect of the anti-erbB4 receptor antibody on regulation of cellular growth

The anti-erbB4 receptor antibody H4.72.8 / Ab72 (Neomarkers) was used to evaluate the involvement of the erbB4 receptor on cellular growth. Cells which had not been exposed to addition of NRG1β and cells which had been stimulated with NRG1β were studied. Cell number was evaluated on day 5 using a Coulter Counter. Comparisons were made using the Student t test.

6.2.1 Growth regulation by the anti-erbB4 receptor antibody in the PEO1 cell line.

The PEO1 cell line was growth stimulated by NRG1β to 285% (± 5%), above the control cell count. Pre-incubation with anti-erbB4 receptor antibody prior to addition of growth factor enhanced the NRG1β induced growth stimulus to 350% (± 4%) above the control cell number. Pre-incubation with anti-erbB4 receptor antibody increased PEO1 cell proliferation in response to NRG1β by an additional 65%. Similarly, pre-incubation with antibody in cells that were maintained in control conditions increased cellular growth by 193% (± 5%) above the control cell number.

Ch 6 Anti-receptor antibodies to the erbB3 and erbB4 receptors influence cellular growth.
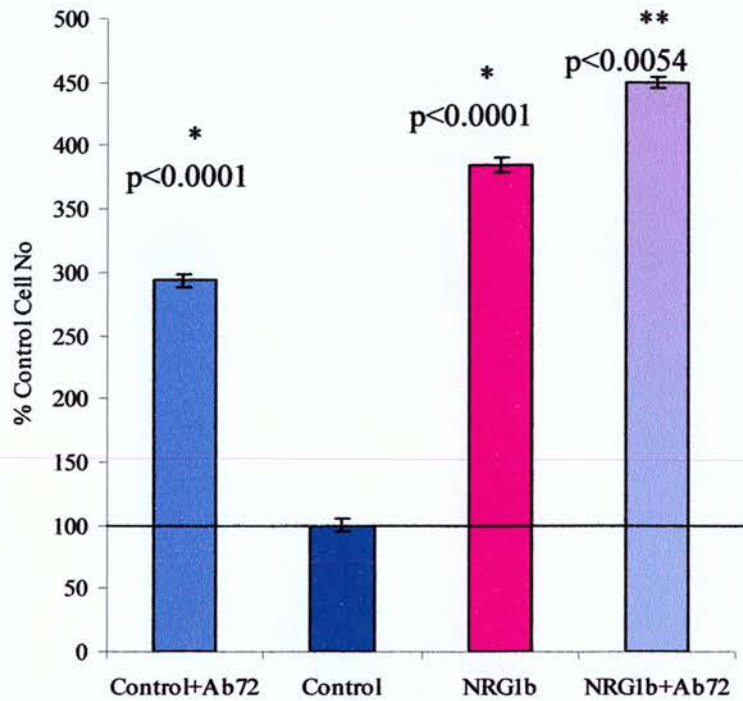
Fig 6.5 Growth regulation by the anti-erbB4 receptor antibody (Ab72) in the PEO1 cell line. NRG1β induced an increase in cell growth of 285% above the control cell count in PEO1 cells. Pre-incubation with Ab72 enhanced the NRG1β growth stimulation to 350% above the control cell count, an additional 65% above NRG1β stimulated cell growth. Treatment with Ab72 in cells that were maintained in control conditions resulted in an increase in cellular growth of 193% above the control cell number assigned 100%. p-values refer to statistical significance between cells treated with antibody or NRG1β, in comparison to cells grown under control conditions (*) and, cells treated with antibody and NRG1β in comparison to those treated with NRG1β (**).

Ch 6 Anti-receptor antibodies to the erbB3 and erbB4 receptors influence cellular growth.

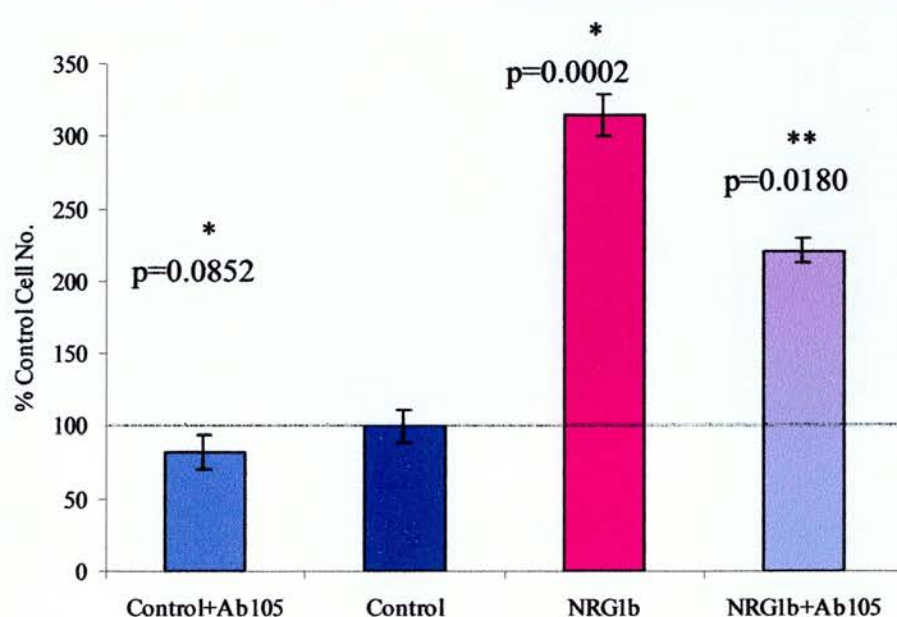6.2.2 Growth regulation by the anti-erbB4 receptor antibody in the PEO6 cell line.

The PEO6 cell line was growth stimulated in response to NRG1β by 203% (± 5%) above the control cell number assigned 100%. Pre-incubation with anti-erbB4 receptor antibody increased cell number by 64% in response to the NRG1β stimulation and resulted in a 267% (± 7%) increase above the control cell number. Pre-incubation of cells with antibody that were maintained in control conditions, resulted in a reduction in cellular growth to 84% in comparison to the control cell count. However, this reduction was accompanied by a large standard deviation of ± 27% and was not significant from the control cell number.
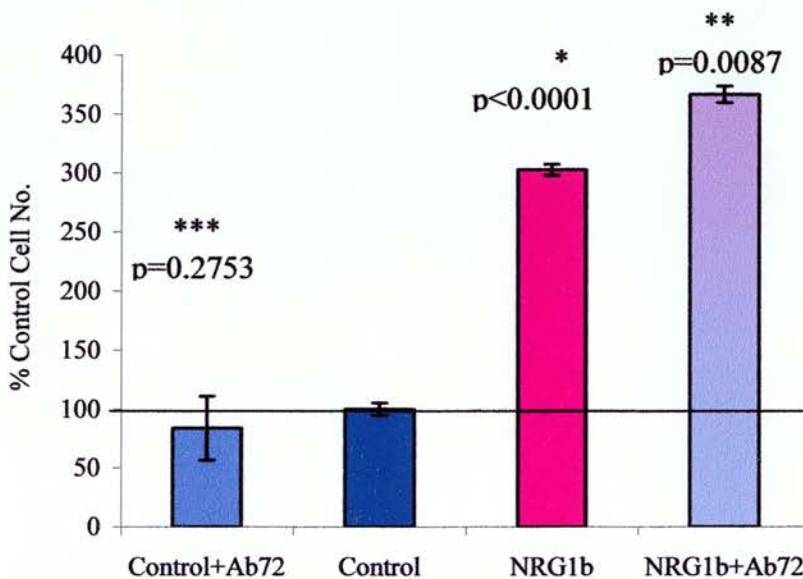


Fig 6.6 Growth regulation by the anti-erbB4 receptor antibody (Ab72) in the PEO6 cell line. NRG1β induced an increase in cell growth of 203% above the control cell number assigned 100% (*). Pre-incubation with Ab72 enhanced the NRG1β growth stimulation by an additional 64% to 267% above control the control cell count and this was statistically significant in comparison with cells treated with NRG1β alone (**). Pre-incubation with Ab72 in cells that were maintained in control conditions resulted in a reduction in cell number in comparison to the control cell count which was not significant (***).

Ch 6 Anti-receptor antibodies to the erbB3 and erbB4 receptors influence cellular growth.

6.2.3 Growth regulation by the anti-erbB4 receptor antibody in the PEO1$^{CDDP}$ cell line.

The PEO1$^{CDDP}$ cell line was growth inhibited by NRG1β to 40% (± 8%) in comparison to the control cell number assigned 100% (± 7%). Pre-incubation with anti-erbB4 receptor antibody enhanced the NRG1β induced inhibition of cellular growth by an additional 9% to 31% (± 6%). Pre-incubation of the antibody in cells that were maintained in control conditions also resulted in a reduction of cell growth to 88% (± 7%) in comparison to the control cell number (100%) which was not quite significant (p=0.0746).
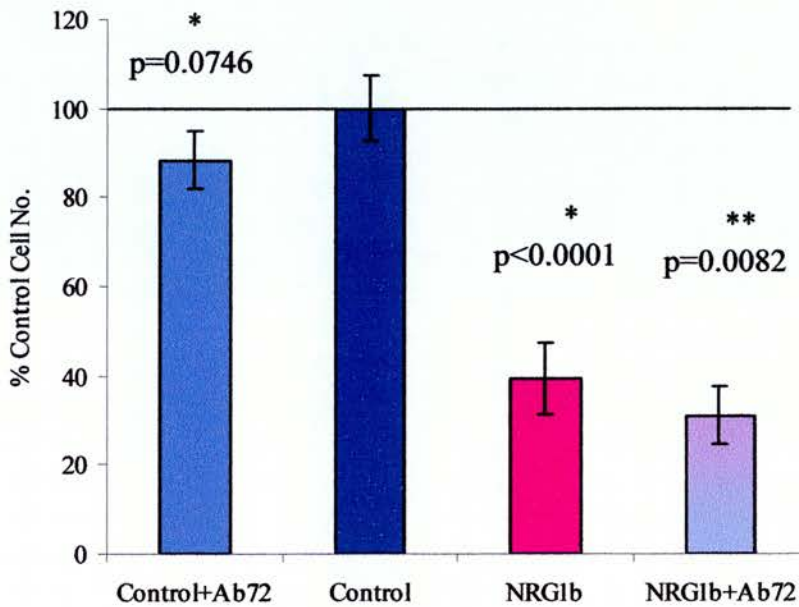


Fig 6.7 Growth regulation by the anti-erbB4 receptor antibody Ab72 in the PEO1$^{CDDP}$ cell line. NRG1β induced growth inhibition to 40% of control cell number (100%). Pre-incubation with Ab72 increased the NRG1β growth inhibition to 31%. Pre-treatment with Ab72 reduced cell growth in control conditions to 88% in comparison to the control cell count (100%), however this was not quite significant. p values refer to comparisons made between cells treated with antibody or NRG1β with cells grown under control conditions (*), whilst cells treated with antibody and NRG1β were compared to cells treated with NRG1β (**).

Ch 6 Anti-receptor antibodies to the erbB3 and erbB4 receptors influence cellular growth.

6.2.4 Growth regulation by the anti-erbB4 receptor antibody in the SKOV3 cell line.

Treatment with NRG1β in the SKOV3 cell line, did not have a clear effect on cell growth and resulted in a cell number of 104% (± 4%), in comparison to the control cell number of 100% (± 3%). Pre-incubation with anti-erbB4 receptor antibody did not affect cell number 102% (± 5%) in comparison to control cell number. Neither response was statistically significant, (p=0.6072 and 0.2758 respectively). However, incubation of antibody in cells that were maintained in control conditions resulted in a growth reduction to 92% (± 4%) in comparison to the control cell number (100%).
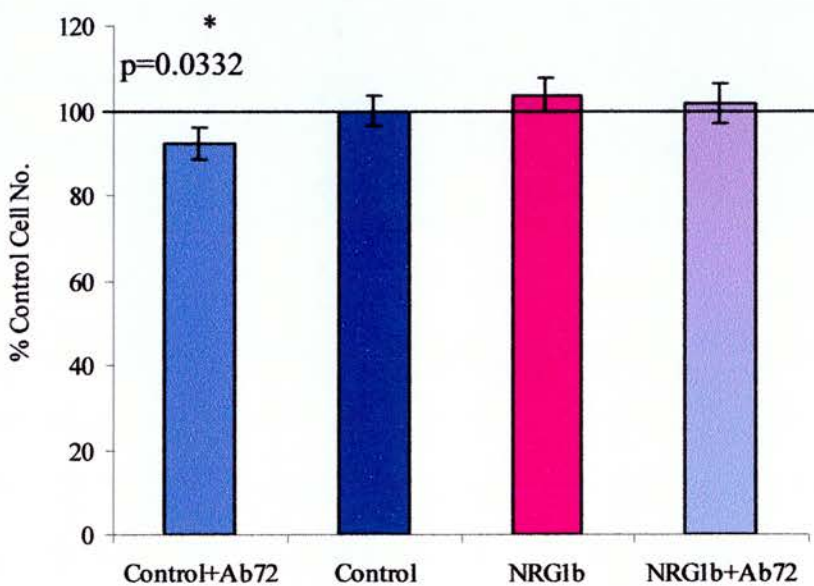


Fig 6.8 Growth regulation by the anti-erbB4 receptor antibody Ab72 in the SKOV3 cell line. Treatment with NRG1β did not affect cellular growth and similarly, pre-incubation with Ab72 had no effect on cell number. Pre-incubation with Ab72 in cells maintained in control conditions, produced a minor growth inhibition to 92% in comparison to the control cell number (100%) which was statistically significant (*).

Ch 6 Anti-receptor antibodies to the erbB3 and erbB4 receptors influence cellular growth.

6.4 Anti-receptor antibody effect on NRG1β induced intracellular signalling in the PEO1 cell line.

The effects of anti-receptor antibodies on NRG1β induced intracellular signalling in the PEO1 cell line were next explored. Western blot analysis was used to monitor tyrosine phosphorylation of the erbB receptors, band shifts of the Shc adapter molecule and phosphorylation of Erk in response to NRG1β. The anti-erbB3 receptor antibody Ab105 (10mgml$^{-1}$) or anti-erbB4 receptor antibody Ab72 (10mgml$^{-1}$), was incubated with PEO1 cells 30 min prior to the addition of NRG1β (10$^{-9}$M) or replenishment with medium. The antibodies used for detection in Western blotting were as follows: anti-phosphotyrosine PY20 (Santa Cruz Biotech.), anti-Shc S14630 (Transduction Laboratories) and the dual phospho-specific antibody to Erk1 and Erk2 9101S (New England Biolabs).

6.4.1 Anti-receptor antibody effects on NRG1β induced erbB receptor tyrosine phosphorylation.

Tyrosine phosphorylation was not detected in PEO1 control cells (Fig 6.9 & Table 6.1). Treatment with NRG1β induced tyrosine phosphorylation at the p185 position. Pre-incubation with the anti-erbB3 receptor antibody reduced the NRG1β stimulated tyrosine phosphorylation at the p185 position to a level that was unable to be measured by optical densitometry.

In another experiment, a small degree of tyrosine phosphorylation was detected in PEO1 control cells (Fig 6.9 & Table 6.2). NRG1β stimulated an increase in tyrosine phosphorylation at the p185 position which was reduced to almost a third of the strength by pre-incubation with anti-erbB4 receptor antibody.

Ch 6 Anti-receptor antibodies to the erbB3 and erbB4 receptors influence cellular growth.
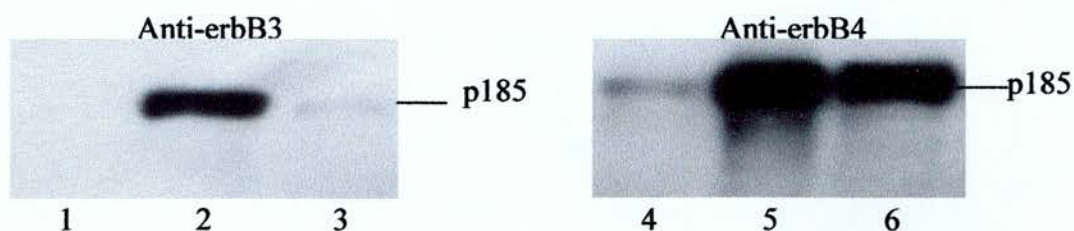
Fig 6.9 Anti-receptor antibody effects on NRG1β induced erbB receptor tyrosine phosphorylation. Tyrosine phosphorylation was not detected in PEO1 control cells (lane 1), NRG1β induced tyrosine phosphorylation at the p185 position at 15min (lane 2), pre-incubation with Ab105 reduced tyrosine phosphorylation to a level that was undetectable by Labworks 3.0 (lane 3). Tyrosine phosphorylation was detected in control cells (lane 4), NRG1β stimulated an increase in tyrosine phosphorylation at the p185 position (lane 5), pre-incubation with Ab72 decreased the NRG1β stimulated tyrosine phosphorylation (lane 6).

Table 6.1 IOD measurements for the strength of tyrosine phosphorylation signal in PEO1 control cells, NRG1β stimulated cells and cells that were pre-incubated with anti-erbB3 receptor antibody Ab105 prior to treatment with NRG1β.

|  | Control | NRG1β | NRG1β & Anti-erbB3 (Ab105) |
|---|---|---|---|
| IOD | 0.0 | 431 | 0.0 |
| % Change | 0.0 | 100.0 | 0.0 |

Table 6.2 IOD measurements for the strength of tyrosine phosphorylation signal in PEO1 control cells, NRG1β stimulated cells and cells that were pre-incubated with anti-erbB4 receptor antibody prior to the addition of NRG1β.

|  | Control | NRG1β | NRG1β & Anti-erbB4 (Ab72) |
|---|---|---|---|
| IOD | 30 | 2406 | 828 |
| % Change | 0.0 | 100.0 | 37 |

Ch 6 Anti-receptor antibodies to the erbB3 and erbB4 receptors influence cellular growth.

6.4.2 Anti-receptor antibody effect on NRG1β induced Shc band shifts.

This section describes the investigation of anti-receptor antibody influence on NRG1β induced band shifting of the Shc isoforms to positions with increased molecular weight.

The p52 and p46 Shc isoforms were detected in PEO1 cells (Fig 6.10 lane 1). Stimulation with NRG1β induced a band shift to a position with increased molecular weight for the p52 isoform (lane 2). The weak signal corresponding to the p46 isoform was also suggestive of a band shift to a position with reduced migration. Pre-incubation with the anti-erbB3 receptor antibody prior to the addition of NRG1β blocked the p52 band shift induced by the ligand and a band shift was not apparent for the p46 isoform (lane3). Similarly, in another experiment p52 and p46 isoforms were detected in PEO1 cells (lane 4). Band shifts to a position with increased molecular weight were not apparent in control cells although the intensity of the background in the lanes makes the analysis less clear. Treatment with NRG1β stimulated a clear band shift in the p52 isoform to a position with increased molecular weight, the band corresponding to the p46 isoform had also underwent a shift to a position with increased molecular weight, although the intensity is less than that observed for the p52 isoform. Pre-incubation with anti-erbB4 receptor antibody did not inhibit the band shift in the p52 isoform induced by NRG1β, it is unclear if a band shift was present for the p46 isoform. Although the intensity of banding in lane 6 was reduced in comparison to lanes 4 and 5, which may possibly reflect decreased protein loading, band shifts for the p52 isoform were clearly detected and suggest erbB4 receptor intracellular signalling does not act on this molecule.

Ch 6 Anti-receptor antibodies to the erbB3 and erbB4 receptors influence cellular growth.
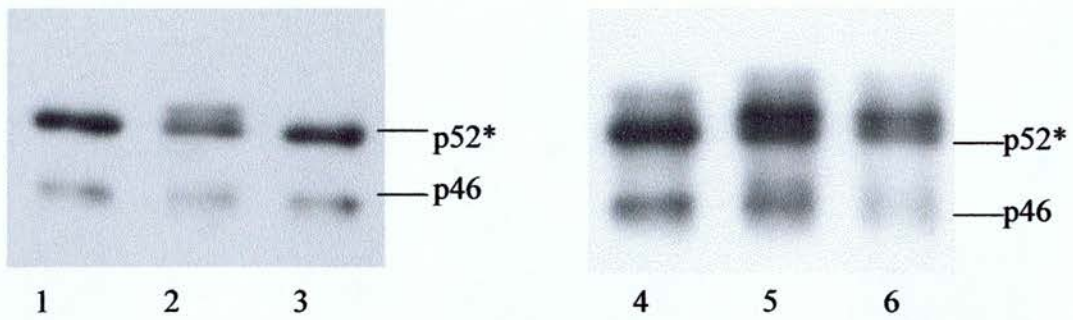
Fig 6.10 Anti-receptor antibody effect on NRG1β induced Shc band shifts in the PEO1 cell line. The p52 and p46 isoforms are present in PEO1 control cells (lane 1), NRG1β induced a band shift to a position with increased molecular weight in the p52 isoform (lane 2) which was inhibited by pre-incubation with anti-erbB3 receptor antibody (lane 3). The p52 and p46 isoforms are detected in PEO1 control cells (lane 4), treatment with NRG1β stimulated a band shift in both the p52 and p46 isoforms (lane 5). Pre-incubation with anti-erbB4 receptor antibody did not inhibit the NRG1β stimulated band shift in p52 (lane 6). The band shift in the p52 isoform is represented as *

Ch 6 Anti-receptor antibodies to the erbB3 and erbB4 receptors influence cellular growth.

6.4.3 Anti-receptor antibody effect on NRG1β induced phosphorylation of Erk

Phosphorylated p42 or p44 were not detected in PEO1 control cells (Fig 6.11 lane1). NRG1β stimulated phosphorylation of p42 and p44, although the signal intensity corresponding to phosphorylated p42 was superior to that of p44 (lane2). Pre-incubation with anti-erbB3 receptor antibody prior to the addition of NRG1β inhibited the ligand induced phosphorylation of both p42 and p44 (lane 3).

In a second experiment, phosphorylation of p42 and p44 were not detected in PEO1 control cells (lane 4). Treatment with NRG1β stimulated phosphorylation of both p42 and p44, the signal corresponding to phosphorylated p42 was of greater intensity than that observed for p44. Pre-incubation with anti-erbB4 receptor antibody prior to the addition of NRG1β, resulted in reduced phosphorylation of both p42 and p44. Pre-incubation with both anti-receptor antibodies decreased the NRG1β induced phosphorylation of p42 and p44.
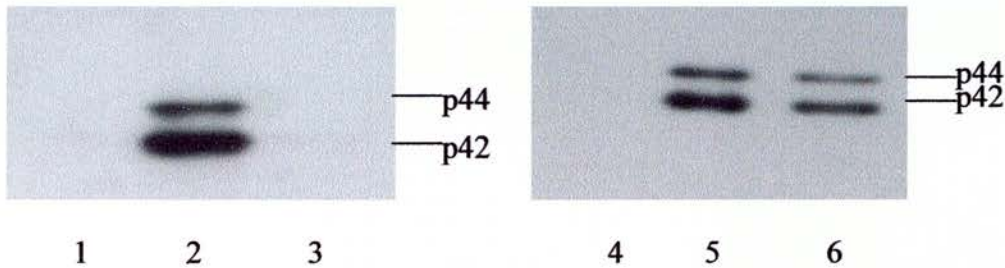


Fig 6.11 Anti-receptor antibody effect on NRG1β induced phosphorylation of Erk in the PEO1 cell line. Phosphorylation of p42 and p44 was not detected in PEO1 control cells (lane 1). NRG1β stimulated phosphorylation of both p42 and p44 (lane 2) and pre-incubation with anti-erbB3 receptor antibody inhibited the NRG1β induced Erk phosphorylation (lane 3). Similarly, Erk phosphorylation was not detected in PEO1 control cells (lane 4) and treatment with NRG1β stimulated phosphorylation of both p42 and p44 (lane 5). Pre-incubation with anti-erbB4 receptor antibody resulted in a reduction in the strength of NRG1β induced p42 and p44 phosphorylation (lane 6).

Ch 6 Anti-receptor antibodies to the erbB3 and erbB4 receptors influence cellular growth.

151
Ch 6 Anti-receptor antibodies to the erbB3 and erbB4 receptors influence cellular growth.

## Chapter 7 General discussion and suggestion for future studies

7.1 Introduction

Gene amplification and increased expression of the erbB family of receptors have been associated with neoplasia in many tissue types including the ovary (Berns EMJJ, 1992) (Simpson et al., 1995a) (Stromberg K, 1994) (Scoccia B, 1998). This is frequently in conjunction with expression of binding ligand (Jindal SK, 1994) (Bartlett et al., 1996) (Stromberg K, 1994) and is proposed to provide a selective growth advantage. In this study, expression of the erbB receptors was investigated in ovarian cancer cell line models. To complement expression of the erbB receptors, the presence or absence of transcripts for the ligand NRG was also investigated in human ovarian tumours as well as cancer cell lines. Cellular growth in a panel of cell lines in response to $NRG1\alpha$ and $NRG1\beta$ was monitored and compared to the changes in response to $TGF\alpha$. Growth responses were then evaluated with respect to receptor expression to determine receptors dominating the response to ligand.

7.2 Expression of EGF receptor protein

EGF receptor expression is reported to be present in between 50-98% of human ovarian carcinomas (Scambia G, 1992) (Stromberg K, 1994). Increased levels of EGF receptor expression have been detected in between 19 and 50% of ovarian adenocarcinomas and have been correlated with the more advanced stage tumours (Henzen-Longmans SC, 1992) (Stromberg K, 1994).

Co-expression of the EGF receptor with $TGF\alpha$ and also amphiregulin has been detected in ovarian tumours depicting a potential autocrine mechanism for cellular growth (Stromberg K, 1994). In earlier studies, constitutive tyrosine phosphorylation of the EGF receptor was not detected in ovarian cancer cell lines (Ottensmeier C, 1996) and in the same study, antibodies that prevented EGF binding to the EGF receptor did not have a significant effect on cell proliferation. Similarly, Rodrigez et al. 1991, reported comparable EGF receptor expression and EGF binding affinity in both normal human ovarian epithelial cells and cancer cell lines which would suggest that the EGF receptor has a lesser role in ovarian cancer. In direct contrast, a potential

152

autocrine growth promoting mechanism that involves secretion of TGFα, which binds to the EGF receptor has been detected in human ovarian adenocarcinomas (Morishige K, 1991). More recently, this co-expression model of both TGFα and EGF receptor has been confirmed and found to correlate with the promotion of abnormal growth in the onset and progression of ovarian cancer (Doraiswamy V, 2000). In addition, EGF receptor expression remains to be an independent prognostic indicator, with increasing levels of expression correlating with increasing tumour stage and increased expression is associated with reduced survival and poor response to chemotherapy (Scambia G, 1995) (Skirnisdottir I, 2001) (Niikura H, 1997).

In this study, protein expression of the EGF receptor was investigated by Western blot analysis and was detected in 15/16 ovarian cancer cell lines. Expression varied over a 300-fold range, from barely detectable levels (PEO16) to levels of comparatively high expression (OVCAR5 and 41M) and reflects expression of the EGF receptor in the majority of human ovarian tumours. The highest level of expression in 2 /16 cell lines is perhaps consistent with only a small proportion (19%) of ovarian tumours expressing increased levels of EGF receptor protein. Western blot analysis of whole cell lysates demonstrated banding other than that of 170kDa corresponding to molecular weights of approximately 110 kDa and 60 kDa. These bands may correspond to splice products of the EGF receptor gene, namely the constitutively active truncated EGF receptor VIII (100-140 kDa depending on additional glycosylation of the receptor) which is frequently expressed in ovarian tumours and yet not in the normal ovary (Moscatello DK, 1995) (Ekstrand et al., 1994), and the 60-70 kDa secreted product that is composed of the extra-cellular binding domain and is proposed to have growth regulatory properties (Flickinger TW, 1992) (Reiter JL, 1996). Alternatively, presence of the lower molecular weight bands may be due to receptor degradation either by ligand-induced down-regulation (Levkowitz G, 1998) or through enzymatic receptor cleavage during preparation of the cell lysates.

7.3 Expression of erbB2 receptor protein

Amplification of the erbB2 or HER2 gene is reported to occur in 25-30% of malignant ovarian neoplasms giving rise to increased-expression of the erbB2 receptor and a further 12% of cases giving rise to elevated levels of erbB2 receptor expression without gene amplification (Slamon DJ, 1989). Moreover, increased erbB2 receptor expression is now generally regarded as being a poor prognostic indicator in ovarian cancer despite earlier controversial reports questioning its significance in the disease (Hengstler JG, 1999) (Rubin SC, 1994) (Van Dam PA, 1994) (Singleton TP, 1994) (Hynes, 1993). In addition, erbB2 receptor expression is reported to be significantly increased in invasive ovarian cancer (Kim YT, 1998). More recently, findings that erbB2 acts as a pan-erbB receptor and is the preferential hetero-dimerization partner within the erbB receptor network as a whole(Graus-Porta D, 1997) (Klapper LN, 1999) (Huang GC, 1998) (Karunagaran D, 1996), support the importance of the role of this receptor. ErbB receptor hetero-dimerization diversifies intracellular signaling (Earp SH, 1995) (Riese DJ, 1998) (Alroy I, 1997) (Dougall WC, 1994) and thus has highlighted the importance of erbB2 receptor expression in carcinogenesis and disease progression. It was therefore important to determine erbB2 receptor expression in ovarian cancer cell lines.

The panel of 16 ovarian cancer cell lines was investigated for expression of the erbB2 receptor protein by Western blot analysis. All of the 16 cell lines were positive for erbB2 receptor expression and the protein expressed varied over a 400 fold range from a comparatively low level in the PEO16 cell line to the well-characterized over-expression in the SKOV3 cell line (Wiechen K, 1999). This is in agreement with Pegues JC et al (1999), where all five ovarian cancer cell lines tested expressed erbB2 receptor protein. These expression profiles indicate that erbB2 receptor expression is common in ovarian cancer cell lines which would be consistent with erbB2 having a potentially dominating role in growth of the disease since it has been directly linked to activation of Erk / MAP kinase (Ben-Levy et al., 1994).

More recently, Ouyang X et al (1999), have shown that measuring erbB2 phosphorylation-state in breast cancer, is a more sensitive technique and would be a more relevant parameter to measure for clinical diagnostics and prognosis. It would therefore be important to investigate erbB2 phosphorylation in ovarian cancer and

determine if this reflects poor response to therapy or reduced survival in a prospective study.

## 7.4 Expression of erbB3 receptor protein

Expression of the erbB3 receptor has been detected in 85% of human ovarian carcinomas by immunohistochemistry although expression has not been detected in normal ovarian surface epithelium, from which common epithelial malignancies are thought to originate (Simpson et al., 1995b) (Prigent et al., 1992). Immunohistochemical staining of erbB3 was predominantly cytoplasmic and may reflect the characteristic 'recycling' of this receptor to the membrane (Waterman et al., 1999) (Baulida J, 1996). The intensity of staining has been reported to be greatest in borderline tumours and malignant tumours displayed significantly more intense staining than benign ones. Similarly, increased intensity of staining was associated with early stage (I/II) tumours rather than late stage (III/IV), which may suggest erbB3 receptor expression is up-regulated in early invasive lesions. In addition, expression of multiple erbB3 receptor transcripts by Northern blot analysis has been detected in the majority of ovarian cancer cell lines tested (Lee H, 1998).

In this study, expression of erbB3 receptor protein was detected in 15/16 (94%) cell lines by Western blot analysis and is consistent with that previously found for ovarian tumours (85%). Only the 59M cell line did not display full length erbB3 receptor protein. The range of erbB3 receptor protein expressed varied over a range of 60-fold, from a barely detectable level in the PEO14 cell line to a comparatively high level of expression in the PEO1$^{CDDP}$ cell line. Lee H et al (1998), detected similar transcript expression levels for full length erbB3 receptor in the CAOV3, OVCAR3 and SW626 cell lines, however although both the CAOV3 and OVCAR3 cell lines expressed comparable levels of erbB3 receptor protein in this study, the SW626 cell line had exceptionally weak erbB3 receptor expression. This may in part be due to regulation of erbB3 receptor expression at the transcript level by alternate spliced erbB3 gene products or possibly an alternative mechanism that down-regulates receptor expression (Lee H, 1998). In addition, the erbB3 receptor protein was displayed as a doublet by Western blot analysis, which is consistent with other studies although recognition of this has provoked little comment (Carraway KL, 1994)(Pegues

JC, 1999). This has been proposed to be due to either increased phosphorylation or additional glycosylation of the erbB3 receptor (WJ Gullick, personal communication).

7.5 Expression of erbB4 receptor protein

The erbB4 receptor is the most recently identified member of the erbB family of receptors. To date, little is known of the role of erbB4 in neoplasia and publications have mostly focused on breast cancer which have implicated erbB4 receptor involvement in cell growth, differentiation and chemotaxis (Cohen BD, 1998)(Plowman GD, 1993)(Elenius et al., 1997b). Recently, expression of the erbB4 receptor was reported to be undetected in a panel of 17 serous ovarian adenocarcinomas (Scoccia B, 1998). In contrast, varying levels of expression of erbB4 and receptor phosphorylation were detected in a panel of 5 ovarian cancer cell lines [Pegues JC, 1999 #40].

In this study, the panel of 16 ovarian cancer cell lines was investigated for erbB4 receptor expression. Of the 16 cell lines, 8 tested positive for p180 erbB4 receptor protein and the level of protein expressed varied over a range of 90-fold; from a relatively low level of detection (PEO14) to a comparatively high level of expression (PEO6). These results are in agreement with those published by Pegues JC et al (1999), where expression of erbB4 receptor protein was detected in the SKOV3 cell line and an increased level of expression was detected in the OVCAR3 cell line. Srinivasan R et al (1998), have previously reported reduced expression in the majority of ovarian tumours compared to normal ovarian tissues, whereas increased expression of erbB4 in breast cancer has been associated with a differentiated phenotype (Kew TY, 2000). In ongoing studies in our laboratory, weak expression of erbB4 was detected by immunohistochemistry in 5 normal ovaries and 90% of tumours were positive for expression. Interestingly, increased levels of erbB4 receptor expression were evident at both the protein and mRNA level in serous tumours compared to endometrioid histology although there was no clear link with tumour grade or differentiation (McCaig, 1999). In this series of human ovarian tumours, expression of erbB4 alone was not obviously associated with survival however, co-expression with erbB2, the preferred heterodimerization partner for all the erbB receptors, did suggest a more favourable prognosis. Similarly in the panel of ovarian cancer cell lines, erbB4

receptor expression was detected in half of the cell lines and increased expression appeared to be associated with prior treatment / resistance to cisplatinum. For example, the PEO1, PEO4 and PEO6 cell lines were developed directly from material obtained at 3 different time-points from the same patient. The PEO4 and PEO6 cell lines were derived after clinical resistance to cisplatin had developed and possessed markedly higher levels of erbB4 receptor expression in comparison to that of the cisplatin sensitive PEO1 cell line. However, this increase in expression was not apparent for the *in vitro* derived PEO1$^{CDDP}$ cell line. Of the other 12 cell lines investigated, treatment data was available for 11 of the patients from which they were derived (no data for SW626). Only 3 cell lines had been obtained from patients after exposure to cisplatin and at a stage where patients had developed clinical resistance to this drug, these were the OVCAR3, OVCAR4 and OAW42 cell lines and were the highest expressors of the erbB4 receptor protein suggesting a link between expression and cisplatin treatment / resistance. Although increased expression of the EGF receptor, erbB2 and erbB3 has been previously detected in drug-resistant breast cancer cell lines (Wosikowski K, 1997), an association between erbB4 and drug-resistance has not been reported to date.

## 7.6 Expression of the erbB4 receptor isoforms

Expression of erbB4 receptor isoforms was investigated by the use of RT-PCR and arises by alternate splicing of 2 regions in the extracellular juxtamembrane domain (JM) and in the carboxyl terminal (CT) domains.

Alternate splicing of 2 sequences 'a' and 'b' in the JM region gives rise to 4 isoforms; JM-a which is comprised of the 'a' sequence only, JM-b which contains the 'b' sequence only, JM-c which has neither 'a' or 'b' sequence and JM-d which includes both sequences (Elenius et al., 1997a) (Sawyer et al., 1998) (Gilbertson RJ, 1999). Encompassed within the 'a' sequence is a region that is susceptible to cleavage by matrix metalloproteases and results in the release of a soluble ectodomain. This has been proposed to confer negative regulation of erbB4 JM-a receptor function by an inability to bind activating ligand and since the JM-d isoform also contains this sequence it is likely to be regulated in the same manner. Alternatively, JM-b and JM-c would not be subject to this type of regulation.

Similarly, alternate splicing of a region in the carboxyl terminal (CT) gives rise to 2 isoforms; CT-a and CT-b that contain and exclude the sequence respectively (Elenius et al., 1999). The sequence encodes the single erbB4 binding site for phosphatidyl inositol 3-kinase, a cytoplasmic signalling molecule that has been linked to promoting cell survival (Franke TF, 1997).

In this study, expression of the JM and CT isoforms was investigated in a panel of 10 ovarian cancer cell lines by RT-PCR. Confirmation of isoform expression was obtained by sequencing PCR products from the PEO6 cell line. Of the panel, 5 cell lines tested positive for JM-a expression including PEO6, SKOV3, OVCAR3, 41M and OAW42. In addition, JM-d expression was detected in 3 of these cell lines; PEO6, OVCAR3, OAW42. Expression of the JM-b or JM-c isoforms, if present was below the limit of detection by this methodology.

In the same 5 cell lines, expressing JM-a, both the CT-a and CT-b isoforms were detected. Of the 5, 4 cell lines PEO6, OVCAR3, 41M and OAW42, showed increased intensity in the band corresponding to the CT-a isoform over that of CT-b. In contrast, the SKOV3 cell line displayed a greater magnitude of intensity in the band corresponding to CT-b expression.

These results indicate that ovarian cancer cell lines that expressed mRNA for the erbB4 receptor, consist of the isoforms JM-a, CT-a and CT-b, with a smaller group that expressed mRNA for the JM-d isoform. Detection of only the JM-a and JM-d isoforms (and not JM-b or JM-c), which are proposed to be susceptible to cleavage by matrix metalloproteases, would suggest erbB4 receptor function could be regulated in these cell lines. Expression of the CT-a isoform increases the repertoire of secondary signalling molecules that can be recruited to the erbB4 receptor by inclusion of the phosphatidyl inositol-3-kinase binding site. In addition, co-expression with the CT-b isoform, that is unable to bind phosphatidyl inositol-3-kinase, is common in ovarian cancer cell lines. The majority of ovarian cancer cell lines expressing mRNA for erbB4 receptor CT isoforms displayed increased band intensity for the CT-a isoform. This may suggest a bias or predominance toward expression of the CT-a isoform over that of CT-b, suggesting erbB4 receptor expression may invoke cell survival by the ability to recruit the phosphatidyl inositol-3-kinase molecule.

Comparison of erbB4 receptor protein expression with mRNA expression indicated that 4/5 cell lines testing positive for erbB4 receptor mRNA (PEO6, OVCAR3, OAW42 and SKOV3) were also positive for expression of full length p180 erbB4 receptor protein. While erbB4 receptor mRNA was detected for the 41M cell line, protein expression appeared negative which may reflect the increased sensitivity of RT-PCR over Western blot analysis. Alternatively, this may suggest post-transcriptional regulation of erbB4 receptor expression in the 41M cell line.

Investigation of erbB4 receptor isoforms in a panel of 24 human ovarian tumours showed positive expression of JM-a in 18, JM-d in 6 and both CT-a and CT-b in 20 tumours. Consistent with the panel of ovarian cancer cell lines, neither JM-b nor JM-c isoform expression was detected. Tumours that expressed JM isoforms also expressed CT isoforms. However, the increased number of tumours positive for CT isoform expression most likely suggests increased sensitivity of this primer pair over those for the JM isoform. Although expression of a truncated erbB4 receptor isoform has not been reported to date, this could also compensate for the discrepancy in isoform expression.

Overall, the majority of ovarian tumours tested positive for erbB4 receptor mRNA expression and was consistent with data from the cell lines where JM-a, JM-d,

CT-a and CT-b isoform expression were detected. Expression of the JM-a isoform that is prone to cleavage by matrix metalloproteases and to a lesser extent the JM-d isoform that is likely to be regulated in the same manner, would confer regulation of erbB4 receptor function in both human ovarian tumours and cell lines. The inability to detect JM-b and JM-c isoform expression would suggest a preferential requirement to express erbB4 receptor isoforms that can be regulated by the cellular environment in ovarian cancer. Expression of the CT-a isoform alongside that of CT-b, confers the ability to recruit phosphatidyl inositol-3-kinase to the receptor. Expression of the CT-b isoform has been attributed to mediating cell proliferation in response to NRG1β, whereas the CT-a isoform has been shown to confer this and the additional properties of mediating cell chemotaxis and membrane ruffling (properties associated with cell motility), whilst also increasing cell survival by resisting apoptosis (Kainulainen V, 2000). This would suggest that NRG signalling in ovarian cancer cells expressing the erbB4 CT-a isoform, may confer a more aggressive phenotype, similar to that previously observed in breast cancer (Lupu R, 1996), where increased cell motility has been associated with NRG stimulated serine phosphorylation and transcriptional up-regulation of paxillin (Vadlamudi R, 1999b) (Vadlamudi R, 1999a).

In a parallel study in our laboratory, a panel of 53 ovarian tumours (including those tested in this study) was investigated for erbB4 receptor expression by immunohistochemistry. Positive staining was observed in 92% of all tumours being confined to the neoplastic epithelial cells and was of a diffuse cytoplasmic nature. Although erbB4 receptor staining did not correlate with clinical stage or degree of differentiation there was a trend for tumours of serous histology to display increased levels of erbB4 receptor expression over those of endometrioid histology. This high degree of erbB4 receptor expression 92%, correlates well with that found by RT-PCR where 18/24 (75%) and 20/24 (83%) of ovarian tumours expressed mRNA for the JM and CT isoforms respectively. This would suggest erbB4 receptor expression in ovarian cancer is more common than previously reported. Alternatively, the reduced proportion of ovarian cancer cell lines that displayed erbB4 receptor expression (50%), may suggest erbB4 receptor expression may be down-regulated as a consequence of *in vitro* culturing conditions.

7.7 Expression of Neuregulin (NRG)

In this study, investigation of NRG expression was carried out to determine if the ligand was present in human ovarian cancer cell lines and tumours. NRG expression in conjunction with the presence of NRG receptors, erbB3 and erbB4, may suggest a possible mechanism for the autocrine regulation of cellular growth.

Of the panel of 9 cell lines, 8 tested positive for NRG expression by RT-PCR. Interestingly, expression of erbB3 and /or erbB4 was detected was detected in 8 / 9 cell lines. The PEO1, PEO1$^{CDDP}$, PEO4, PEO6, 41M, SW626, 59M, and SKOV3 cell lines expressed NRG mRNA. Only in the case of the 59M cell line, neither erbB3 or erbB4 receptor protein was detected, although expression of the erbB4 receptor isoforms was identified by the increased sensitivity of RT-PCR.

Similarly in a panel of 24 human ovarian tumours, positivity for NRG expression was clearly detected in 22. Although expression of the erbB3 receptor was not investigated in this panel, expression of erbB4 was identified in at least 75% of these tumours by RT-PCR.

These results suggest that mRNA for NRG is expressed in the majority of human ovarian tumours and cancer cell lines. In addition, the majority of the ovarian cancer cell lines and tumours express at least one NRG receptor and may have the potential to regulate cellular growth by an autocrine mechanism. These findings are consistent with those previously reported for a number of neoplasms including cancer of the breast (Hijazi MM, 2000), head and neck (O-Charoenrat P, 2000), medulloblastoma (Gilbertson RJ, 1998), endometrial cancer (Srinivasan R, 1999) and support the role of the erbB receptor network and NRG in the pathogenesis and progression of disease.

Chapter 7 General discussion and suggestion for future studies

7.8 Growth response to the ligands NRG1α, NRG1β and TGFα in a panel of 14 ovarian cancer cell lines

A panel of 14 ovarian cancer cell lines was investigated for changes in cellular growth in response to the 3 ligands NRG1α, NRG1β and TGFα ($10^{-9}$M) over a period of 5 days. Significant changes in cellular growth were regarded as an increase or decrease in cell growth of more than 15% in comparison to the control cell number.

Of the panel of 14 cell lines, growth stimulation was observed for 5 in response to NRG1α, 7 in response to NRG1β and 8 in response to TGFα. Growth inhibition was produced in the PEO1$^{CDDP}$ cell line by both NRG1β and TGFα. Growth stimulation to each of the three ligands was consistent in 4 of the cell lines (PEO1, PEO4, PEO6 and 41M). In addition, growth response to both NRG1β and TGFα was common in another 2 cell lines (OVCAR3 and CAOV3). In contrast, cell growth in the PEO14 and OAW42 cell lines was unaffected by treatment with any of the ligands tested. Lack of response to the ligands in the 2 cell lines would suggest that either the level of erbB receptor expressed was below that required to produce a growth response or that functional erbB receptors were not expressed. It is feasible that a higher concentration of ligand might produce a response although this may not reflect physiological conditions. The growth responses were then evaluated with respect to receptor expression (as detected by Western blot analysis) to identify trends in receptor expression that determine growth response to ligand. Analyses were conducted including and excluding the SKOV3 data since this cell line is known to markedly over-express the erbB2 receptor (Peles E, 1993) which could possibly bias the results.

A positive association was detected for the magnitude of growth response to NRG1α and the level of expression of erbB2 using the Spearman rank test ($p=0.022$ including SKOV3 data, $p=0.0009$ excluding SKOV3 data). Whilst erbB2 receptor expression appears to be associated with a growth response to NRG, the presence of erbB3 and/or erbB4 is apparent in all situations where this was detected. This is consistent with the finding that erbB2 is the preferential heterodimerization partner of all the erbB receptors (Graus-Porta D, 1997) and similarly, erbB2 has been directly associated to activation of the MAP kinase cascade resulting in mitogenesis (Klapper LN, 1999). Moreover, these results reflect previous findings of NRG1α activating

erbB2/erbB3 high-affinity heterodimers (Weis FU, 1997) (Slikowski MX, 1994) and indicate that this predominant interaction mediates a growth response.

In response to NRG1β, a similar trend was observed where increased expression of erbB2 produced a greater magnitude of response (p=0.0795 including SKOV3 data), which was significant when the SKOV3 data was excluded (p=0.0047) using the Spearman rank test. Expression of the EGF receptor, erbB3, or erbB4 alone or in combination was not significant in determining response to ligand. However, it was apparent that the growth response to NRG that was associated with the level of erbB2 expression, also required erbB3 or erbB4 to be present. These findings are consistent with NRG1β activating erbB2 and erbB3 (Slikowski MX, 1994) and also activate erbB4 (Weis FU, 1997) (Fitzpatrick VD, 1998).

Patterns in erbB receptor expression were not detected for determining response to TGFα. This ligand has been proposed to bind primarily to EGF receptor homodimers (Gullick, 1998), although heterodimerisation of EGF receptor and erbB2 and also EGF receptor and erbB4 have also been reported (Alroy I, 1997). 15 of the 16 cell lines expressed various levels of EGF receptor protein but not all of the cell lines were growth responsive to TGFα. Similarly, patterns of EGF receptor co-expression with erbB2 or erbB4 were not detected and indicate that determining growth response to TGFα is more complex than simply evaluating receptor expression. Interestingly, the cell line that produced the greatest magnitude of growth response upon treatment with TGFα, was the PEO6 cell line that possessed only a very low level of EGF receptor protein.

7.9 Summary: ErbB receptor expression and growth responses in ovarian cancer cell lines

In this study, expression of the EGF receptor was detected in 15/16 cell lines, erbB2 in 16/16, erbB3 in 15/16 and erbB4 in 8/16 by Western blot analysis. These findings are consistent with observations of multiple expression of erbB receptors in human ovarian tumours (Simpson et al., 1995a). This is proposed to diversify the nature of intracellular signalling (Pinkas-Kramarski R, 1996) and may translate into cells having a selective growth advantage and possibly increased motility or cell survival. Since expression of the EGF receptor and erbB2 has been associated with a poor prognosis in ovarian cancer (Skirnisdottir I, 2001) (Slamon DJ, 1989), co-expression of erbB2 and erbB3, which are proposed to form the superior heterodimeric signalling complex mediating cell mitogenesis, this would similarly confer an unfavourable prognosis. In contrast, the most recently identified member of the family, erbB4, was detected in only half of the cell lines although the incidence of expression was greater in human ovarian tumours. So far, the erbB4 receptor is poorly characterized and is surrounded by conflicting reports which suggest its function varies from increased cell proliferation (Kainulainen V, 2000) to association with cells of a differentiated phenotype (Chausovsky A, 1998). This study is the first to identify erbB4 receptor isoforms in ovarian cancer. Expression of the matrix metalloprotease regulated JM-a isoform and to a lesser extent JM-d, but not that of JM-b or JM-c would suggest this receptor is under tight regulation in ovarian cancer. Expression of the CT-a isoform which can bind phosphatidyl inositol-3-kinase would implicate erbB4 increasing cell survival, although co-expression with the CT-b isoform does not suggest preferential expression in ovarian cancer. Moreover, with a greater number of ovarian tumours expressing erbB4 mRNA than the cell lines would suggest expression of erbB4 is more common than previously reported.

The majority of ovarian cancer cell lines were growth responsive to NRG1β and TGFα. Less than half of the cell lines were affected by treatment with NRG1α which may reflect its lower binding affinity for the neuregulin receptors than that of NRG1β. Similarly, an increase in cell growth in response to ligand was more common than growth inhibition; the CAOV3 cell line was growth inhibited by NRG1α and the PEO1[CDDP] cell line was growth inhibited by both NRG1β and TGFα. Since the *in vitro*

derived PEO1$^{CDDP}$ cell line has increased resistance to cisplatinum and growth inhibition was observed in response to NRG1β and TGFα whereas the parent cell line PEO1, displayed growth stimulation, this may infer that the reversed growth response may be a result of changes produced by treatment with cisplatinum. Moreover, the magnitude of growth change in response to the NRGs was associated with increased expression of the erbB2 receptor, which may be a direct consequence of its ability to activate the MAP kinase cascade (Reese DM, 1997).

### 7.10 ErbB activated signalling

Four cell lines were then chosen for further analysis, PEO1, PEO1$^{CDDP}$, PEO6 and SKOV3. The PEO1, PEO1$^{CDDP}$ and PEO6 cell lines were derived from material taken from the same patient, PEO1 taken from cell ascites during the initial treatment with cisplatin when the tumour was still responsive, PEO1$^{CDDP}$ was derived from the PEO1 cell line after exposure to increasing concentrations of cisplatin *in vitro*, PEO6 was derived from material taken from the patient after clinical resistance to cisplatin was diagnosed. Both PEO1 and PEO6 were growth stimulated by NRG1α, NRG1β and TGFα, and whilst the PEO1 cell line expressed EGF receptor, erbB2 and erbB3, the PEO6 cell line also expressed the erbB4 receptor. These 2 model systems were chosen to investigate differences in function of the erbB3 and erbB4 receptors in response to NRG. In contrast, the PEO1$^{CDDP}$ cell line was chosen since it expressed EGF receptor, erbB2 and erbB3 (similar to the PEO1 cell line) yet it was growth inhibited by NRG1β and TGFα. The SKOV3 cell line model, characterized by over-expression of erbB2 was chosen as an interesting model since although expressing all 4 erbB receptors, growth stimulation was only observed in response to TGFα.

Response to ligand was investigated by monitoring tyrosine phosphorylation of the erbB receptors and stimulation of components of the MAP kinase cascade, namely Shc and Erk1 and Erk2. Further characterization of erbB3 and erbB4 receptor function was investigated using antibodies that block ligand and receptor interaction. The following sections discuss these results illustrating the key mediators of the erbB receptor family that determine response to NRG and also identify the novel finding of antagonism between erbB3 and erbB4.

Chapter 7 General discussion and suggestion for future studies

7.11 ErbB receptor tyrosine phosphorylation in response to ligand

Tyrosine phosphorylation at the erbB receptor level was observed in response to NRG1$\alpha$, NRG1$\beta$ and TGF$\alpha$ in all 4 cell lines. However, the strength of tyrosine phosphorylation and duration of the signal varied. The PEO1 cell line was growth stimulated by all 3 ligands and expressed the following patterns of tyrosine phosphorylation: NRG1$\alpha$ induced a weak tyrosine phosphorylation signal at the erbB2 receptor position which increased in intensity with time; NRG1$\beta$ stimulated tyrosine phosphorylation at the erbB2 receptor position that was initially10-fold greater than the maximal signal produced by NRG1$\alpha$; the strength of signal then gradually decreased with time but was still greater than that produced by NRG1$\alpha$. TGF$\alpha$ increased tyrosine phosphorylation at the erbB2 receptor and induced tyrosine phosphorylation of the EGF receptor at the early timepoints of 15 min and 1h, however the signal dramatically reduced thereafter.

The strength and duration of tyrosine phosphorylation produced at the erbB receptor positions suggests NRG1$\beta$ as the most effective of the 3 ligands for activating erbB receptor phosphorylation, followed by TGF$\alpha$ and NRG1$\alpha$. This is consistent with the growth stimulation produced by each ligand in the PEO1 cell line where the magnitude of growth response was in the order NRG1$\beta$ > TGF$\alpha$ > NRG1$\alpha$. Treatment with the NRGs, that bind to the erbB3 and erbB4 receptors resulted in tyrosine phosphorylation of the erbB2 receptor which is indicative of receptor hetero-dimerization. Similarly, hetero-dimerization was detected in response to TGF$\alpha$ which binds to the EGF receptor, where both the EGF receptor and erbB2 were tyrosine phosphorylated. These results are consistent with those found for erbB2 being the preferential hetero-dimerization partner for the erbB receptors (Graus-Porta D, 1997) and by this suggest diversification of erbB receptor signalling (Alroy I, 1997) within this cell line. In addition, the erbB2 receptor has been directly linked to activation of the MAP kinase cascade (Klapper LN, 1999) that may account for the analogous degree of growth stimulation produced by the ligands. A background level of erbB2 receptor tyrosine phosphorylation was observed in PEO1 control cells and suggests

either presence of growth factor in the medium or production of growth factor in an autocrine manner.

Similarly, growth stimulation in response to the growth factors, NRG1α, NRG1β and TGFα was observed in the PEO6 cell line where the magnitude of growth was of the order NRG1β > TGFα > NRG1α. However, in contrast to the PEO1 cell line that expressed EGF receptor, erbB2 and erbB3, the PEO6 cell line expressed also expressed the erbB4 receptor. Although erbB2 and erbB3 were common to the 2 cell lines and expressed at similar levels, a greater magnitude of growth response to each ligand was achieved in the PEO6 cell line. This would suggest that the presence of erbB4 in the PEO6 cell line might be responsible for increasing cellular growth in response to the NRGs, however investigation of cell growth by treatment with anti-erbB4 receptor antibody suggested this receptor has a negative growth regulatory effect. Although the PEO6 cell line was growth stimulated by TGFα and expression of the EGF receptor was barely detectable by Western blot analysis and undetected by RT-PCR, phosphorylated EGF receptor was more easily detected by Western blot analysis (Fig 5.4). These findings suggest that a low level of EGF receptor must be present to relay receptor signalling in response to TGFα and also implicate alternate signalling mechanisms that generate a greater mitogenic response in this cell line. This in part may be a consequence to treatment with cisplatin since this cell line was derived from ascites fluid from the same patient as the PEO1 cell line, but at a point where the tumour had been classified as being cisplatin resistant.

The subsequent receptor tyrosine phosphorylation in response to ligand in the PEO6 cell line was as follows: NRG1α stimulated weak tyrosine phosphorylation at the erbB2 position at 15 min which decreased with time; NRG1β stimulated a strong tyrosine phosphorylation signal at 15 min and 1h and rapidly decreased thereafter; TGFα induced tyrosine phosphorylation of both EGF receptor and erbB2 at 15 min and 1h. Similar to the growth responses achieved, optical densitometry of the tyrosine phosphorylation signal indicated the magnitude of stimulus was greatest in response to NRG1β, followed by TGFα and then NRG1α. The gross difference between the NRG isoforms, either by growth response or receptor tyrosine phosphorylation, reflects the 8-10 fold higher affinity of NRG1β over NRG1α for binding the NRG receptors (Lu HS, 1995) (Wen D, 1994).

167

Chapter 7 General discussion and suggestion for future studies

In direct contrast, the PEO1<sup>CDDP</sup> cell line, which was made more cisplatin-resistant *in vitro*, was not growth responsive to the lower affinity NRG1α, yet growth inhibited by both NRG1β and TGFα. Although this cell line expressed EGF receptor, erbB2 and erbB3, treatment with the higher affinity ligands NRG1β and TGFα had the converse effect of decreasing cellular growth. This would suggest that treatment with cisplatin has modified the intracellular signalling pathways that lead to growth stimulation.

Tyrosine phosphorylation of the erbB receptors in response to ligand were as follows; NRG1α stimulated weak tyrosine phosphorylation at the erbB2 receptor position through the timepoints tested; NRG1β stimulated a greater intensity of tyrosine phosphorylation at the erbB2 position at 15 min which had increased at 1h and decreased thereafter; TGFα induced tyrosine phosphorylation of the EGF receptor and erbB2 at 15 min and 1h and was undetected thereafter. These findings suggest that the weak erbB receptor tyrosine phosphorylation induced by NRG1α was below a threshold level required to invoke a cell growth regulatory response. Since stimulation with NRG1β and TGFα resulted in receptor activation through tyrosine phosphorylation, yet overall the ligands induced growth inhibition suggests that at some point, activation of intracellular signalling that would characteristically lead to a growth response has been altered to an extent that produces the opposite effect of growth inhibition.

Growth of the highly erbB2 expressing cell line, SKOV3, was increased by treatment with TGFα and unaffected by treatment with NRG1α and NRG1β. This cell line expressed all 4 of the erbB receptors. In response to NRG1α, tyrosine phosphorylation of the erbB2 receptor was detected at 15 min and increased throughout the timepoints tested. However, erbB2 receptor tyrosine phosphorylation was detected in control cells at the start of the experiment and had increased to a similar level for that observed in response to NRG1α at 24h. ErbB2 receptor tyrosine phosphorylation was detected in response to NRG1β which was maximal at 24h and similarly, receptor tyrosine phosphorylation was also detected in control cells at the start and end of the experiment. In contrast, EGF receptor tyrosine phosphorylation was induced in response to TGFα and accompanied by an increase in the strength of

erbB2 receptor phosphorylation at 15 min. The phosphorylation signals then gradually decreased with time until an increase in erbB2 receptor phosphorylation was detected at 24h; again erbB2 receptor phosphorylation was detected in control cells.

To date, growth response to the NRGs in the SKOV3 cell line have been conflicting in that both growth stimulation (Pegues JC, 1999) and inhibition (Xu F, 1999) have been reported. In agreement with Campiglio M. et al,1999 #8, a growth response was not detected upon treatment with NRG although erbB2 receptor tyrosine phosphorylation was identified. This may be due to the significant expression of NRG mRNA transcripts that have been detected from the SKOV3 cell line suggesting a potential autocrine growth pathway and similarly hetero-dimerization of erbB3 and erbB4 with erbB2, without exogenous addition of NRG (Pegues JC, 1999). This may account for lack of response to treatment with NRG and for the constitutive tyrosine phosphorylation of erbB2 that was detected in cells maintained in control growth conditions in this and other studies. In addition, Campiglio M. et al,1999, detected activation of MAP kinase in response to NRG which did not result in a mitogenic response which further suggests that a 'threshold level' of activation must occur to have an overall growth regulatory effect. Similarly, the increase in erbB2 receptor tyrosine phosphorylation in control cells from the start of the experiment to 24h would infer that receptor tyrosine phosphorylation in response to treatment with the NRGs did not augment/enhance that of cells in control growth conditions in this study. Alternatively, due to the high level of erbB2, spontaneous erbB2 receptor dimerization may give rise to an intrinsic erbB2 receptor tyrosine kinase activity which has been previously reported for cell lines that over express the receptor (Lonardo F, 1990) (Akiyama T, 1991) (Ben-Levy et al., 1994). In contrast, treatment with TGFα induced EGF receptor phosphorylation that may suggest the secondary signalling molecules recruited to the EGF receptor are more efficient in producing a mitogenic response. Alternatively, TGFα stimulated a more intense erbB2 receptor phosphorylation signal than that observed for the NRGs, again perhaps suggesting a 'threshold level' of stimulus to produce a growth regulatory response. Whether this is due to the production of autocrine growth factors from the cell line, or presence of ligand in the medium, that competes for receptor binding with added growth factor remains to be elucidated.

169

Chapter 7 General discussion and suggestion for future studies

7.12 Increased phosphorylation of secondary signalling molecules in response to ligand

Further characterization of the ligand induced growth regulatory responses in the four cell lines was aided by monitoring the intracellular signalling events following receptor tyrosine phosphorylation. Activation of the classical MAP kinase cascade is associated with a mitogenic response and may be initiated by the molecule Shc binding to the carboxyl-terminal of the phosphorylated receptor. Shc binds to all of the erbB receptors (Alroy I, 1997) and may then activate Grb2-mSos, which results in sequential activation through the cascade comprising of Raf, MEKK and MAP kinase which translocates to the nucleus to invoke a mitogenic response (Brunet A, 1999a). This study investigated both the early event of Shc activation and the latter event of MAP kinase phosphorylation in response to ligand to determine if the differences in ligand induced growth regulation were evident and could be explained by intracellular signalling events.

Of the 3 Shc isoforms that are expressed in all mammalian tissues, the p46 and p52 (ShcA) isoforms are associated with a mitogenic response, whereas the p66 isoform is thought to be a negative regulator of erbB receptor signalling by inhibiting downstream activation of the MAP kinase cascade (Okada S, 1997). Band shifts of the p66 isoform have previously been described (Okada S, 1997) (Mahmoud YM, 1997b) and are attributed to serine/threonine phosphorylation subsequent to tyrosine phosphorylation and are associated with complex formation of Shc with Grb2 (Kannan S, 1997). In this study, band shifts of the p46 and p52 isoforms were also detected and are likely to be attributed to a similar phosphorylation event that reduces gel migration. The band shifts detected for the p46 and p56 isoforms are likely due to increased phosphorylations that ultimately induce regulation of cell growth since band shifts were not detected in cells maintained in control conditions, but were observed in response to growth factor that produced a growth regulatory effect. This would also suggest that the Shc molecule may be a valuable indicator for monitoring signal transduction from the tyrosine phosphorylated receptor.

In this study, expression of the p46, p52 and p66 molecules was common to all four cell lines. Expression of the p54 isoform which has previously only been detected

170

Chapter 7 General discussion and suggestion for future studies

in the brain, was also detected in the PEO1, PEO1$^{CDDP}$ and PEO6 cell lines, although the significance of this in ovarian cancer cells has yet to be determined. Increased tyrosine phosphorylation resulting in band shifts for the ShcA molecules was indicative of the growth responses obtained for the PEO1, PEO6 and SKOV3 cell lines upon treatment with growth factor. Similarly, where treatment with ligand did not result in a significant alteration of cell growth, band shifts for the Shc isoforms were not detected eg the PEO1$^{CDDP}$ cell line treated with NRG1α and SKOV3 cells with NRG1α and NRG1β. In contrast, band shifts were detected in PEO1$^{CDDP}$ in response to NRG1β and TGFα, both of which inhibited cellular growth of this cell line. This suggests that signal transduction normally associated with a growth response through ligand induced receptor phosphorylation has occurred and that at some latter point or by an alternate signalling mechanism, the overall response has been altered to induce growth inhibition.

Interestingly, a band shift for the p66 isoform was only detected in response to the ligands with higher proliferative properties, NRG1β and TGFα, rather than the lower affinity ligand NRG1α. Since increased phosphorylation of the p66 isoform is involved in down-regulation of receptor induced Erk activation by competing with p46 and p52 for a limited cellular pool of Grb2, it is likely that the p66 molecule is only activated in response to a strong stimulus to prevent over-signalling within the cytoplasmic compartment (Okada S, 1997).

Signal transduction was then monitored at the latter end of the cascade by assessing phosphorylation of Erk1 and Erk2, which are proposed to be the effector molecules in the classical MAP kinase cascade that regulate cellular processes such as cell proliferation and differentiation (Marshall, 1995). So far, conflicting characterizations have been proposed in that either sustained or transient phosphorylation of Erk results in either cell proliferation or differentiation, which seem to be governed by cellular context. Similarly, translocation of Erk to the nucleus has been shown to induce either differentiation or entry into cell cycle inducing proliferation in different systems (Brunet A, 1999a) (Shapiro PS, 1998). This study investigated if Erk phosphorylation could be used as a predictor for growth response to ligand and if the bands shifts observed for Shc isoforms were reflected in the phosphorylation of Erk1 and Erk2.

The PEO1 cell line showed a weak but sustained increase in tyrosine phosphorylation of the erbB receptors in response to NRG1α and only a band shift for p52 Shc, which was reflected in a weak increase in phosphorylation of p42 Erk. In contrast the high level of erbB receptor tyrosine phosphorylation in response to NRG1β, resulted in band shifts for all 3 Shc isoforms; p46, p52 and p66, and consequently a strong signal corresponding to p42 Erk2 phosphorylation that was sustained through the timepoints over 24h. Additionally, NRG1β produced a transient increase in p44 Erk1 phosphorylation at 15min and 1h. Similarly, treatment with TGFα resulted in a strong signal although transient which corresponded to EGF receptor and erbB2 receptor tyrosine phosphorylation, band shifts for the p46, p52 and p66 Shc molecules and was reflected in sustained phosphorylation of both the p42 and p44 Erk isoforms. This suggests that tyrosine phosphorylation of the EGF receptor recruits a subset of secondary signalling molecules that have the propensity to maintain signal transduction or at least phosphorylation of Erk long after the initiation of receptor activation. This is consistent with the results found for EGF, in a manner similar to TGFα which binds to the EGF receptor (Campiglio M, 1999). Both EGF and NRG were found to have equivalent capacities to stimulate DNA synthesis even though the EGF receptor was rapidly internalized and down-regulated upon ligand stimulation, which is a property of the EGF receptor whereas erbB2, erbB3 and erbB4 undergo receptor recycling to the membrane (Baulida J, 1996).

It was evident that in the PEO1 cell line that the strength and duration of receptor tyrosine kinase activity was indicative of the intracellular response, in that it reflected the extent and longevity of Erk phosphorylation. However, it was also apparent that stimulation with TGFα could maintain both phosphorylated p44 Erk1 and p42 Erk2 whereas stimulation with NRG1β could only maintain phosphorylation of p42 Erk2 through the time-points investigated. This may reflect the different secondary signalling molecules that can be recruited by each of the erbB receptors; these molecules may act in a variety of signalling pathways which may lead directly to Erk phosphorylation or in an indirect manner through intracellular crosstalk. For instance both Shc and phosphatidyl inositol-3-kinase (PI3K) may be recruited to erbB3 and erbB4, leading to activation of the MAP kinase cascade. Such differences in

intracellular signalling may preferentially phosphorylate one or other of the Erk isoforms.

Similarly the PEO6 cell line, which was also growth stimulated by the NRG's and TGFα, showed similar trends to those observed in the PEO1 cell line for Erk phosphorylation following receptor activation. NRG1α produced weak tyrosine phosphorylation of the erbB receptors which was detected up to 8h and resulted in band shifts of the p46 and p52 Shc isoforms. Subsequently, increased phosphorylation of the p44 Erk1 and p42 Erk2 was detected up to 8h. Likewise, receptor tyrosine phosphorylation was detected in response to NRG1β up to the 8h time-point although the strength of the signal was of increased intensity than that detected for the PEO1 cell line. Band shifts were detected for not only the p46 and p52 Shc isoforms, but also for the p66 isoform that is proposed to attenuate receptor signal transduction to prevent over-signalling. In contrast to the PEO1 cell line, increased phosphorylation of both p44 Erk1 and p42 Erk2 was detected up to the 8h time-point for NRG1β and similarly for NRG1α. Since both the PEO1 and PEO6 cell lines express similar levels of erbB2 and erbB3, expression of erbB4 in the PEO6 cell line may have necessitated recruitment of the p66 Shc isoform and also maintained phosphorylation of p44 Erk1 simultaneously with phosphorylation of Erk2. The carboxyl tail of the erbB4 receptor possesses sites for Shc and PI3K binding, similar to the erbB3 receptor. The availability of additional sites may serve to increase the rate or flux of signalling within the cell to an end where the cellular pool of Erk is phosphorylated. Alternatively expression of the erbB4 receptor would invoke a variety of hetero-dimerizations and recruitment of a different repertoire of signalling molecules that may be responsible for sustained phosphorylation of p44 Erk1.

Directly comparable with that found for the PEO1 cell line, treatment with TGFα in the PEO6 cell line resulted in transient phosphorylation of the EGF receptor and erbB2 producing phosphorylation of p44 Erk1 and p42 Erk2 over an extended period. This further suggests that the repertoire of signalling molecules recruited to the EGF receptor (which is expressed at a barely detectable level in this cell line) are responsible for maintaining prolonged phosphorylation of Erk.

Phosphorylation of Erk was detected in the PEO1[CDDP] cell line in response to each ligand. Treatment with NRG1α resulted in weak tyrosine phosphorylation of the

Chapter 7 General discussion and suggestion for future studies

p185 erbB2 receptor at the early time-points of 15min and 1h, which consequently stimulated phosphorylation of both Erk1 and Erk2 although this was only detected at the15min timepoint. Surprisingly, band shifts for the Shc isoforms were not detected. Since only trivial effects were seen in response to NRG1$\alpha$, this would suggest this ligand has little effect on the PEO1$^{CDDP}$ cell line and is consistent with the cell line having no change in growth upon treatment with NRG1$\alpha$.

In response to NRG1$\beta$, increased tyrosine phosphorylation of the p185 erbB2 receptor was detected at 15min and 1h and was reduced at 8h. A band shift corresponding to the p52 Shc isoform was detected and Erk phosphorylation followed that of receptor tyrosine phosphorylation with elevated levels detected at 15min,1h and 8h.

Similar to the previous findings, TGF$\alpha$ induced tyrosine phosphorylation of the EGF receptor and erbB2 at 15min, which was reduced at 1h and undetected at 8h. This resulted in band shifts for the p46 and p52 Shc isoforms and an increase in phosphorylation of Erk1 and Erk2 at 15min, 1h and 8h before returning to control levels. Interestingly, the levels of Erk phosphorylation following TGF$\alpha$ induced receptor activation were greatest in this cell line in comparison to the NRGs and consistent with that found for the other cell lines, the transient tyrosine phosphorylation of the EGF receptor and erbB2 resulted in a more prolonged phosphorylation of Erk.

Cellular growth of the PEO1$^{CDDP}$ cell line was not affected by treatment with NRG1$\alpha$, yet growth inhibited by NRG1$\beta$ and more so by TGF$\alpha$. Since similar receptor tyrosine kinase and Erk phosphorylation profiles have been observed for the PEO1 and PEO6 cell lines which are growth stimlulated by these ligands, as has been for the PEO1$^{CDDP}$ cell line. This suggests that the difference observed between the intracellular signalling and biological growth effect in the PEO1$^{CDDP}$ cell line, lies downstream of Erk phosphorylation and may possibly reside at the level of gene transcription. It would also suggest that this is a direct consequence of exposure to cisplatin *in vitro* ,although this is not reflected by cell lines that were exposed to cisplatin *in vivo*.

In direct contrast, growth of the SKOV3 cell line was not affected by treatment with either NRG1$\alpha$ or NRG1$\beta$, yet growth stimulated upon treatment with TGF$\alpha$.

These responses were mirrored by the resulting phosphorylation observed for both the erbB receptors and Erk. ErbB receptor tyrosine phosphorylation was observed in control cells at the start of the experiments and had increased by 24h. The tyrosine kinase profiles observed in response to NRG were consistent with that expected for autocrine regulation of cell growth and was reflected in the significant increase in control cell number from the start to the end of the experiment. Similarly, band shifts for the Shc molecules were not detected in response to the NRGs. Although levels of phosphorylated p42 Erk2 increased through the time-points evaluated, these were similar to those observed for cells maintained in control conditions. This may suggest that either an autocrine production of growth factor prevents exogenous addition of NRG having a growth regulatory effect or that treatment with NRG has no significant effect upon the growth regulatory pathways in this cell line under the conditions used.

In contrast, TGFα induced tyrosine phosphorylation of the EGF receptor at 15min and 1h that resulted in band shifts for the p46, p52 and p66 Shc isoforms. In addition, TGFα induced phosphorylation of p44 Erk1 in conjunction with a dramatic increase in p42 Erk2 phosphorylation, the levels of both decreased with time and were consistent with that previously found for growth increases in response to TGFα.

These results indicate that growth regulation upon treatment with ligand can be monitored in the four ovarian cancer cell lines. Significant deviation from control cellular growth was reflected in increased receptor tyrosine phosphorylation, band shifts corresponding to increased phosphorylation of the Shc molecules and increased phosphorylation of Erk1 and Erk2. This data is summarized in Table 7.1

Table 7.1 ErbB receptor phosphorylation and intracellular signalling detected in ovarian cancer cell lines upon treatment with the ligands NRG1α, NRG1β and TGFα.

| Cell Line | Ligand | ErbB Receptor Phosphorylation | Shc Band Shifts | Erk Phosphorylation | Growth Response |
|---|---|---|---|---|---|
| PEO1 | NRG1α | + | + | ± | ↑ |
| | NRG1β | + | + | + | ↑ |
| | TGFα | + | + | + | ↑ |
| PEO6 | NRG1α | ± | + | + | ↑ |
| | NRG1β | + | + | + | ↑ |
| | TGFα | + | + | + | ↑ |
| PEO1$^{CDDP}$ | NRG1α | ± | − | + | − |
| | NRG1β | + | + | + | ↓ |
| | TGFα | + | + | + | ↓ |
| SKOV3 | NRG1α | ± | − | ± | − |
| | NRG1β | ± | − | ± | − |
| | TGFα | + | + | + | ↑ |

+ Detected                                        ↑ Increase in cell growth

- Not detected                                    ↓ Decrease in cell growth

± Weak / comparable to control cells              - Change in cell growth not detected

7.13 Effect of anti-erbB3 and anti-erbB4 receptor antibody on cell growth and intracellular signalling

In order to further investigate the roles of erbB3 and erbB4, and their influence on cell growth regulation, anti-receptor antibodies were employed to prevent NRG1β binding with receptor.

In the panel of four cell lines, the PEO1 cell line which was growth stimulated by NRG1β, had its growth increase reduced to one third upon pre-treatment with anti-erbB3 receptor antibody. Similarly, cells that were pre-incubated with anti-erbB3 receptor antibody and maintained in control conditions were also growth retarded. These results would suggest that the majority of the NRG stimulated growth was mediated by the erbB3 receptor and indicates that erbB3 receptor ligands are present in the medium. This was reinforced by the observation that pre-incubation with antibody almost completely abolished erbB receptor tyrosine phosphorylation, Shc band shifts and phosphorylation of Erk. This is consistent with erbB3 hetero-dimerization with erbB2, which is proposed to be the most potent mitogenic signalling complex within the erbB receptor family and is in agreement with expression of both receptors in this cell line. However, treatment with anti-erbB3 receptor antibody did not eradicate NRG induced growth and suggested involvement of another NRG receptor, namely erbB4. Although erbB4 has not been detected in this study either by RT-PCR or Western blot analysis, a low level of erbB4 receptor transcripts have been identified in our lab using another set of primers. Similarly, treatment with anti-erbB4 receptor antibody also suggests expression of erbB4 receptor protein, since incubation of cells with antibody prior to the addition of NRG1β resulted in an increase in NRG stimulated proliferation. In addition, pre-incubation with anti-erbB4 receptor antibody in cells that were maintained in control conditions increased cell growth by almost 200% above the control cell number. Since investigation of the intracellular signalling events showed that pre-incubation with anti-erbB4 receptor antibody reduced NRG stimulated receptor tyrosine phosphorylation in conjunction with a decrease in Erk phosphorylation, this suggests that the antibody is binding to erbB4 and preventing ligand binding as opposed to antibody stimulating receptor phosphorylation.

Therefore, these results suggest that the erbB4 receptor has a negative effect on cell growth in that activation of the erbB4 receptor acts to reduce cell proliferation and such an observation would be consistent with erbB4 promoting cell differentiation (Kew TY, 2000) (Chausovsky A, 1998). This would also imply that prevention of ligand binding to erbB4 influences competition between the erbB3 and erbB4 receptors and simultaneously facilitates NRG signalling through the erbB3 and erbB2 receptors resulting in an enhanced growth effect above that previously observed for NRG.

Similar results were obtained for treatment of the PEO6 cell line with anti-receptor antibodies, whereby treatment with anti-erbB3 receptor antibody reduced the NRG stimulated growth by almost half and yet in contrast, pre-incubation with anti-erbB4 receptor antibody increased the NRG stimulated growth. These results further implicate erbB3 receptor as having a growth promoting role in response to NRG and the erbB4 receptor having a growth inhibitory role.

In contrast, the PEO1$^{CDDP}$ cell line was growth inhibited by treatment with NRG1$\beta$ and pre-incubation with anti-erbB3 receptor antibody resulted in restoration of cell growth from growth inhibition. This would suggest that the erbB3 receptor plays a predominant growth inhibitory role in this cell line. In contrast, incubation with anti-erbB4 receptor antibody prior to treatment with NRG1$\beta$ increased cell growth inhibition. Although the growth responses to NRG in the previous cell lines have been that of growth stimulation, in this cell line model growth inhibition was observed and similar trends for receptor function were apparent; erbB3 receptor is predominantly involved in mediating the NRG induced stimulus, yet the erbB4 receptor has an antagonistic role. This would suggest that if the PEO1$^{CDDP}$ cell line reflects that of tumours in vivo that have developed resistance to cisplatinum, presence of NRG would also confer cell growth regulation depending upon erbB3 / erbB4 ratio. Interestingly, higher levels of erbB4 receptor expression was associated with ovarian cancer cell lines that had been exposed to treatment with cisplatin and obtained from patients after clinical resistance to this drug had developed. These were the PEO4, PEO6, OVCAR3, OVCAR4 and OAW42 cell lines. It is noteworthy to mention that the PEO4 and PEO6 cell lines were sequentially derived from ascites of the same patient as the PEO1 cell line, but at a point after clinical resistance had developed.

Whilst, expression of erbB4 was not detected in the PEO1 cell line by Western blot analysis, increasing levels of expression were detected in the subsequent PEO4 and PEO6 cell lines and may suggest erbB4 is involved in the progression of the disease. This is consistent with the expression of NRG in conjunction with erbB2 and erbB4 being associated with clinical resistance and progression of disease in breast cancer (Lupu R, 1996). However, whilst the cell line data points to an association between increased erbB4 receptor expression and treatment with cisplatin, results from a certain subset of ovarian tumours suggest co-expression of erbB2 and erbB4 may relate to a better prognosis. Stage III human ovarian tumours of serous histology and moderate-poor differentiation that co-expressed moderate to high levels of erbB2 and erbB4 were found to have increased survival over those that did not (Gilmour LMR, 2001).

In direct contrast, the SKOV3 cell line, whose growth was unaffected by treatment with NRG, was also not growth regulated by treatment with either erbB3 or erbB4 receptor antibody. This indicates that both NRG receptors have little impact upon cellular growth in response to exogenous addition of NRG in the SKOV3 cell line. This is most likely due to over-expression of the erbB2 receptor regulating cellular growth and it would be interesting to evaluate erbB2 receptor involvement in cell growth within this cell line using an anti-erbB2 receptor antibody, such as herceptin. Interestingly, pre-incubation with anti-erbB4 receptor antibody with cells that were maintained in control conditions resulted in a small growth inhibition, which may suggest that erbB4 may be involved in regulating control cell growth. Since expression of NRG transcripts have been detected in this cell line, it may be reasonable to suggest that an autocrine production of NRG or that NRG present within the medium may bind to the higher affinity NRG receptor (erbB4).

This is the first study in ovarian cancer to directly compare erbB3 and erbB4 receptor function toward cell growth regulation and demonstrates the novel properties of antagonism between the two receptors. Therefore, the ratio of expression of the NRG receptors may well play a role in the growth response to NRG. Since NRG transcripts have been detected in the vast majority of human ovarian tumours co-expressed with the NRG receptors, would suggest that these findings are also consistent in vivo.

Chapter 7 General discussion and suggestion for future studies

180

Chapter 7 General discussion and suggestion for future studies

7.14   Suggestions for future studies

This study has assessed levels of erbB receptor expression in a panel of 16 human ovarian cancer cell lines. The level of expression was compared only within the cell lines investigated and not related directly to that found in normal ovarian tissue. It would be beneficial to obtain material from a small set of normal ovaries to assess erbB receptor expression and enable a direct comparison to normal tissue. It is likely that expression will vary even in normal ovaries, since like the endometrium, the ovary is regulated by the menstrual cycle. ErbB receptor expression, along with growth factor expression is variable through different phases of the menstrual cycle and also in endometrial cancer (Srinivasan R, 1999).

In addition, receptor phosphorylation may be a more valuable parameter to measure and provide greater insight to the activity of the erbB receptors in a particular ovarian tumour. This is most clearly demonstrated in this study by the PEO6 cell line in which EGF receptor expression was unable to be detected by Western blot analysis (Fig 3.10) whilst EGF receptor phosphorylation was clearly evident in response to TGFα (Fig 5.4). It would be beneficial to obtain receptor phospho-specific antibodies and measure erbB receptor activity within a panel of human ovarian tumours.

Since erbB2 expression appears to be a determinant of response to NRG, it would be of interest to study an anti-erbB2 receptor antibody on cell growth and if possible, in comparison to the anti-receptor antibodies used in this study, to gain further insight into the role(s) of each receptor in the growth and progression of ovarian cancer. This might provide further support for using herceptin in clinical trials for the treatment of high erbB2 expressing tumours.

This study has focused on the involvement of erbB receptors regulating cell growth. Given that the erbB receptors may couple to a large repertoire of intracellular signalling molecules, it would be beneficial for future studies to investigate their role(s) in cell migration, apoptosis / survival, angiogenesis and chemotaxis. NRG has also been shown to be involved in regulating cell morphology and chemotaxis in addition to proliferation (Chausovsky A, 1998) (Hijazi MM, 2000) (Elenius et al., 1997b). This may suggest it could be involved in cell metastasis and the dissemination of the primary tumour to distant sites. Expression of both NRG mRNA and protein has

Chapter 7 General discussion and suggestion for future studies

been detected in human ovarian tumours (this study and also McCaig, 1999) and it would be beneficial to investigate if NRG has the potential to invoke invasion and chemotaxis in the ovarian cancer cell lines. This has previously been shown to involve RAFTK/Pyk2 tyrosine kinase, a cytoplasmic tyrosine kinase related to focal adhesion kinase and serves as a mediator between the GAP proteins associated with cell motility and activation of the MAP kinase cascade in response to NRG (Zrihan-Licht S, 2000). It would be useful to investigate the intracellular crosstalk between these signalling pathways and the effect of activation of the associated integrins in mediating cell motility.

7.15 Final conclusion

These studies have demonstrated that ovarian cancer cell lines express multiple erbB receptors and reflect the expression patterns found in primary ovarian cancers. Multiple erbB receptor expression permits the potential of multiple heterodimerizations which may be associated with a growth advantage. The level of erbB2 receptor expression has been associated with the magnitude of growth response and therefore suggests erbB2 is a critical component in determining response to NRG. NRG, appears to be as potent a mitogen as TGFα indicating that activation of this ligand-receptor network via erbB3 / erbB4 may be as significant as via the well established EGF receptor. The extent of growth stimulation by the ligands was reflected by activation of the intracellular signalling molecules Shc and Erk1/2. Multiple splice variants of erbB4 were detected and use of a blocking antibody suggested that this receptor programmes for growth inhibition. Conversely, erbB3 appears to be a major determinant in the mitogenic response to NRG and given the presence of erbB3 in the majority of human ovarian cancers, these data support the possibility of autocrine and paracrine regulation of cell growth via NRG / erbB3.

Chapter 7 General discussion and suggestion for future studies

Chapter 7 General discussion and suggestion for future studies

## References

Aguilar Z, A. R., Finn RS, Ramos BL, Pegram MD, Kabbinavar FF, Rietras RJ, Piscane P, Sliwkowski MD, Slamon DJ. (1999)Biologic effects of heregulin/neu differentiation factor on normal and malignant human breast and ovarian epithelial cells*Oncogene,* **18,** 6050-62.

Akiyama T, M. S., Namba Y. (1991)The transforming potential of the c-erbB2 protein is regulated by its autophosphorylation at the carboxyl-terminal domain*Mol Cell Biol,* **11,** 833-842.

Alroy I, Y. Y. (1997)The erbB signaling network in embryogenesis and oncogenesis: signal diversification through combinatorial ligand-receptor interactions*FEBS Letters,* **410,** 83-86.

Bacus SS, H. E., Chin D, Kiguchi K, Simpson S, Lippman M, Lupu R. (1992)*Cell Growth and Differentiation,* **3,** 401-11.

Bartlett, J. M., Langdon, S. P., Simpson, B. J., Stewart, M., Katsaros, D., Sismondi, P., Love, S., Scott, W. N., Williams, A. R., Lessells, A. M., Macleod, K. G., Smyth, J. F. and Miller, W. R. (1996)The prognostic value of epidermal growth factor receptor mRNA expression in primary ovarian cancer*Br J Cancer,* **73,** 301-6.

Bast R, K. T., St-John E, Jenison E, Niloff JM, Lazarus H, Berkowitz RS, Leavitt T, Griffiths CT, Parker L, Zurawski V, Knapp RC. (1983)A radioimmunoassay using a monoclonal antibody to monitor the course of epithelial ovarian cancer*N Engl J Med,* **309,** 883.

References

Bauknecht T, B. G., Kommoss F (1990)Clinical significance of oncogenes and growth factors in ovarian carcinomas*J Steroid Biochem Mol Biol*, **37**, 855-62.

Bauknecht T, J. I., Kohler M, Pfleiderer A. (1989)Human ovarian carcinomas: correlation of malignancy and survival with the expression of epidermal growth factor receptors (EGF-R) and EGF-like factors (EGF-F)*Med Oncol Tumor Pharmacother*, **6**, 121-7.

Bauknecht T, K. F., Birmelin G, von Kleist S, Kohler M, Pfleiderer A. (1991)Expression analysis of EGF-R and TGFa in human ovarian carcinomas*Anticancer Res*, **11**, 1523-8.

Bauknecht T, K. M., Janz I, Pfleiderer A. (1989)The occurence of epidermal growth factor receptors and the characterization of EGF-like factors in human ovarian, endometrial, cervical and breast cancer. EGF receptors and factors in gynaecological carcinomas.*J Cancer Res Clin Oncol*, **115**, 193-9.

Bauknecht T, R. M., Schwall M, Pfleiderer A. (1988)Occurence of epidermal growth factor receptors in human adnexal tumours and their prognostic value in advanced ovarian carcinomas*Gynaecologic Oncology*, **29**, 147-57.

Baulida J, K. M., Alimandi M, Di Fiore PP, Carpenter G. (1996)All erbB receptors other than the epidermal growth factor receptor are endocytosis impaired *J Biol Chem*, **271**, 5251-5257.

Beerli, R. R., Graus-Porta, D., Woods-Cook, K., Chen, X., Yarden, Y. and Hynes, N. E. (1995)Neu differentiation factor activation of ErbB-3 and ErbB-4 is cell specific and displays a differential requirement for ErbB-2*Mol Cell Biol*, **15**, 6496-505.

186

References

Ben-Levy, R., Paterson, H. F., Marshall, C. J. and Yarden, Y. (1994)A single autophosphorylation site confers oncogenicity to the Neu/ErbB- 2 receptor and enables coupling to the MAP kinase pathway. *Embo J,* **13,** 3302-11.

Berns EMJJ, K. J., Henzen-Logmans, Rodenberg CJ, Van der Burg MEL, Foekens JA. (1992)Receptors for hormones and growth factors and onco-gene amplification in human ovarian cancer. *Int J Cancer,* **52,** 218-24.

Beuzeboc P, S. S., Garau XS, Vincent-Salomon A, Cremoux PD, CourturierJ, Palangie T, Pouillart P. (1999)Herceptin, a monoclonal humanized antibody anti-her2: a major therapeutic progress in breast cancers overexpressing this oncogene. *Bull Cancer,* **86,** 544-9.

Branch P, M. M., Aquilina G, Bignami M, Karran P. (2000)Spontaneous development of drug resistance: mismatch repair and p53 defects in resistance to cisplatin in human tumour cells*Oncogene,* **19,** 3138-45.

Brunet A, R. D., Lenormand P, Dowd S, Keyse S, Pouyssegur J. (1999)Nuclear translocation of p42/p44 mitogen-activated protein kinase is required for growth factor-induced gene expression and cell cycle entry. *EMBO J,* **18,** 664-674.

Burden S, Y. Y. (1997)Neuregulins and their receptors: a versatile signalling module in organogenesis and oncogenesis. *Neuron,* **18,** 847-855.

Burris, H. (2000)Docetaxel (Taxotere) in her-2-positive patients and in combination with trastuzumab (herceptin). *Semin Oncol,* **27,** 19-23.

Byers T, M. J., Graham S, Mettlin C, Swanson M. (1983)A case control study of dietary and non-dietary factors in ovarian cancer. *J Natl. Cancer Inst.,* **71,** 681.

References

Campiglio M, A. S., Knyazev PG, Ullrich A. (1999)Characteristics of EGFR family-mediated HRG signals in human ovarian cancer. *Journal of cellular biochemistry,* **73,** 522-532.

Carraway KL, S. C. (2001)Localization and modulation of erbB receptor tyrosine kinases. *Curr Opin Cell Biol,* **13,** 125-30.

Carraway KL, S. M., Akita R, PLatko JV, Guy PM, Nuijens A, Diamonti J, Vandlen RL, Cantley LC, Cerione RA. (1994)The erbB3 gene product is a receptor for heregulin. *J Biol Chem,* **269,** 14303-6.

Carraway KL, W. J., Unger MJ, Ledesma J, Yu N, Gassmann M, Lai C. (1997)Neuregulin-2, a new ligand of erbB3/erbB4 receptor tyrosine kinases. *Nature,* **387,** 512-516.

Chang H, R. D., Gilbert W, Stern DF, McMahan UJ. (1997)Ligands for erbB-family receptors encoded by a neyreulin-like gene. *Nature,* **387,** 509-512.

Chausovsky A, T. I., Kam Z, Yarden Y, Geiger B, Berhadsky AD. (1998)Morphogenetic effects of neuregulin (neu differentiation factor) in cultured epithelial cells. *Mol Biol of the Cell,* **9,** 3195-3209.

Chen X, L. G., Tzahar E, Karunagaran D, Lavi S, Ben-Baruch N, Leitner O, Ratzkin BJ, Bacus SS, Yarden Y. (1996)An immunological approach reveals biological differences between the two NDF/heregulin receptors, erbB-3 and erbB-4. *The Journal of Biological Chemistry,* **271,** 7620-7629.

Cohen BD, S. C., Bacus S, Foy L, Green JM, Hellstrom I, Hellstrom KE, Fell HP. (1998)Role of epidermal growth factor receptor family members in growth and differentiation of breast carcinoma. *Biochem. Soc. Symp,* **63,** 199-210.

References

Committee, I. F. o. G. a. O. F. C. (1979) Stockholm, , pp. pp17.

Cramer DW, H. G., Welch WR, Scully RE, Knapp RC. (1982)Factors affecting the association of oral contraceptives and ovarian cancer. *N. Engl. J. Med.,* **307,** 1047.

Cramer DW, H. G., Welch WR, Scully RE, Ryan KJ. (1983)Determinants of ovarian cancer risk I. Reproductive experiences and family history.*J Natl. Canc. Inst.,* **71,** 711.

Cramer DW, W. W., Hutchison GB, Willet W, Scully RE. (1984)Dietary animal fat in relation to ovarian cancer risk. *Obstet. Gynaecol.,* **63,** 833.

Crew AJ, L. S., Miller EP, Miller WR. (1992)Mitogenic effects of epidermal growth factor and transforming growth factor alpha on EGF-receptor positive human ovarian carcinoma cell lines. *Eur J Cancer,* **28,** 337-41.

Daly JM, J. C., Beerli RR, Graus-porta D, Maurer FG, Hynes NE (1997)Neu differentiation factor induces erbB2 down-regulation and apoptosis of erbB2-overexpressing breast tumour cells.*Cancer Research,* **57,** 3804-3811.

Daly JM, O. M., Wong AML, Neve R, Lane HA, Maurer FG, Hynes NE. (1999)NDF/Heregulin-induced cell cycle changes and apoptosis in breast tumour cells: role of PI3 kinase and p38 MAP kinase pathways. *Oncogene,* **18,** 3440-3451.

DiGiovanna MP, S. D. (1995)Activation state-specific monoclonal antibody detects tyrosine phosphorylated p185neu/erbB2 in a subset of human breast tumours overexpressing this receptor. *Cancer Res,* **55,** 1946-1955.

Doraiswamy V, P. J., Skinner MK. (2000)Expression and action of transforming growth factor alpha in normal ovarian surface epithelium and ovarian cancer. *Biol Reprod,* **63,** 789-96.

189

References

Dougall WC, Q. X., Peterson NC, Miller MJ, Samanta A, Greene MI. (1994)The neu-oncogene: signal transduction pathways, transformation mechanisms and evolving therapies. *Oncogene, 9,* 2109-2123.

Earp SH, D. T., Li X, Yu H. (1995) Heterodimerization and functional interaction between EGF receptor family members: a new signaling paradigm with implications for breast cancer research. *Breast cancer research and treatment, 35,* 115-132.

Einzig AI, W. P., Sasloff J, Runowicz CD, Goldberg GL. (1992)Phase II study and long-term follow-up of patients treated with taxol for advanced ovarian adenocarcinoma. *J Clin Oncol, 10,* 1748.

Ekstrand, A. J., Longo, N., Hamid, M. L., Olson, J. J., Liu, L., Collins, V. P. and James, C. D. (1994) Functional characterization of an EGF receptor with a truncated extracellular domain expressed in glioblastomas with EGFR gene amplification. *Oncogene, 9,* 2313-20.

Elenius, K., Choi, C. J., Paul, S., Santiestevan, E., Nishi, E. and Klagsbrun, M. (1999) Characterization of a naturally occurring ErbB4 isoform that does not bind or activate phosphatidyl inositol 3-kinase. *Oncogene, 18,* 2607-15.

Elenius, K., Corfas, G., Paul, S., Choi, C. J., Rio, C., Plowman, G. D. and Klagsbrun, M. (1997) A novel juxtamembrane domain isoform of HER4/ErbB4. Isoform-specific tissue distribution and differential processing in response to phorbol ester. *J Biol Chem, 272,* 26761-8.

Elenius, K., Paul, S., Allison, G., Sun, J. and Klagsbrun, M. (1997) Activation of HER4 by heparin-binding EGF-like growth factor stimulates chemotaxis but not proliferation. *Embo J, 16,* 1268-78.

References

Fathalla, M. (1971) Incessant ovulation - a factor in ovarian neoplasia? *Lancet,* **II,** 163.

Feldman AM, L. B., Reis SE. (2000)Trastuzumab in the treatment of metastatic breast cancer: anticancer therapy versus cardiotoxicity. *Circulation,* **102,** 272-4.

Fitzpatrick VD, P. P., Vandlen RL, Sliwkowski MX. (1998)Formation of a high affinity heregulin binding site using the soluble extracellular domains of erbB2 with erbB3 or erbB4. *FEBS Letters,* **431,** 102-106.

Flickinger TW, M. N., Hsing-Jien Kung (1992) An alternatively processed mRNA from the avian c-erbB gene encodes a soluble , truncated form of the receptor that can block ligand-dependent transformation. *Mol Cell Biol,* **12,** 883-893.

Fracasso., P. (2001)Overcoming drug resistance in ovarian carcinoma. *Curr Oncol Rep,* **3,** 19-26.

Franke TF, K. D., Cantley LC. (1997)PI3K: downstream AKTion blocks apoptosis. *Cell,* **88,** 435-7.

Gabra H, S. J. (1997) In *Biology of female cancers.* CRC Press, Boca Raton, Florida, pp. Chapter 6.

Gamet DC, P. G., Cerione RA, Friedberg I. (1997) Secondary dimerization between members of the epidermal growth factor receptor family. *J. Biol. Chem.,* **272,** 12052-12056.

Gassmann M, C. F., Orioli D, Simon H, Lai C, Klein R, Lemke G. (1995) Aberrant neural and cardiac development in mice lacking the erbB4 neuregulin receptor. *Nature,* **378,** 390-394.

References

Gilbertson RJ, C. S., MacMeekin W, Meekin W, Wright C, Perry RH, Kelly P, Pearson AD, Lunec J. (1998) Expression of the erbB-neuregulin signalling network during human cerebellar development: implications for the biology of medulloblastoma. *Cancer Res,* **58,** 3932-41.

Gilbertson RJ, H. R., Scotting P, Walker D, Pearson ADJ, Lunec J. (1999) In *British cancer research meeting 1999*, Vol. 80 (Ed, Weiss, R.) British Journal of Cancer, Edinburgh, pp. 86 (P232).

Gilewski T, S. A., Norton L, Hudis C. (2000) An immunotherapeutic approach to treatment of breast cancer: focus on trastuzumab plus paclitaxel. Breast Cancer Medicine Service*Cancer Chemother Pharmacol,* **46 Suppl,** S23-6.

Gilmour LMR, M. K., McCaig A, Gullick WJ, Smyth JF, Langdon SP. (2001) Expression of erbB-4/HER-4 growth factor receptor isoforms on ovarian cancer. *Cancer Research,* **61**.

Goldenberg, M. (1999) Trastuzumab, a recombinant DNA-derived humanized monoclonal antibody, a novel agent for the treatment of metastatic breast cancer. *Clinical Therapeutics,* **21,** 309-318.

Graus-Porta, D., Beerli, R. R. and Hynes, N. E. (1995)Single-chain antibody-mediated intracellular retention of ErbB-2 impairs Neu differentiation factor and epidermal growth factor signaling. *Mol Cell Biol,* **15,** 1182-91.

Graus-Porta D, B. R., Daly JM, Hynes NE. (1997) ErbB2, the preferred heterodimerization partner of all erbB receptors is a mediator of lateral signalling. *EMBO Journal,* **16,** 1647-55.

Groenen LC, N. E., Burgess AW. (1994) Structure-function relationships for the EGF / TGFa family of mitogens. *Growth Factors,* **11,** 235-257.

References

Gullick, W. (1996) The erbB3/HER3 receptor in human cancer. *Cancer Surv, 27*, 339-49.

Gullick, W. J. (1998) Type I growth factor receptors: current status and future work. *Biochem Soc Symp, 63,* 193-198.

Guy PM, P. J., Cantley LC, Cerione RA, Carraway KL. (1994) Insect cell expressed p180 erbB3 possesses an impaired tyrosine kinase activity. *Proc Natl Acad Sci USA, 91,* 8132-8136.

Harari D, T. E., Romano J, Shelly M, Pierce JH, Yarden Y. (1999) Neuregulin-4: anovel growth factor that acts through the erbB4 receptor tyrosine kinase. *Oncogene, 18,* 2681-9.

Hengstler JG, L. J., Kett A, Dornhofer N, Meinert R, Arand M, Knapstein PG, Becker R, Oesch F, Tanner B. (1999). Contribution of c-erbB2 and topoisomerase IIalpha to chemoresistance in ovarian cancer. *Cancer Research, 59,* 3206-14.

Henzen-Longmans SC, B. E., Klijn JGM, Van der Burg MEL, Foekens JA. (1992) Epidermal growth factor receptor in ovarian tumours: correlation of immunohistochemistry with ligand binding assay. *Br J Cancer, 66,* 1015-21.

Hijazi MM, T. E., Tang C, Coopman P, Yang D, Mueller SC, Lupu R. (2000) Heregulin regulates the actin cytoskeleton and promotes invasive properties in breast cancer cell lines. *Int J Oncol, 17,* 629-41.

Hijazi MM, Y. P., Dougherty MK, Bressette DS, Cao TT, Pierce JH, Wong LM, Alimandi, King CR. (1998) NRG-3 in human breast cancers: activation of multiple erbB family proteins. *Int J Oncol, 13,* 1061-7.

References

Huang GC, O. X., Epstein RJ. (1998) Proxy activation of protein erbB2 by heterologus ligands implies a heterotetrameric mode of receptor tyrosine kinase interaction. *Biochem. J,* **331,** 113-119.

Hynes, N. (1993) Amplification and overexpression of the erbB2 gene in human tumours: its involvement in tumour development, significance as a prognostic factor and potential as a target for cancer therapy. *Semin Cancer Biol,* **4,** 19-26.

Jindal SK, S. D., Lobb DK, Dorrington JH. (1994) Transforming growth factor alpha localization and role in surface epithelium of normal human ovaries and in ovarian carcinoma cells. *Gynaecol Oncol,* **53,** 17-23.

Kabawat SE, B. R., Bhan AK, Welch WR, Knapp RC, Colvin RB. (1983) Tissue distribution of a coelomic-epithelium-related antigen recognized by the monoclonal antibody OC125. *Int J Gynecol Pathol,* **2,** 275.

Kainulainen V, S. M., Maatta JA, Santiestevan E, Klagsbrun M, Elenius K. (2000) A natural erbB4 isoform that does not activate phosphoinositide 3-kinase mediates proliferation but not survival or chemotaxis. *J Biol Chem,* **275,** 8641-9.

Kannan S, D. S. M., Lohmeyer M, Reise DJ, Smith GH, Hynes N, Seno M, Brandt R, Bianco C, Persico G, Kenney N, Normanno N, Martinez-Lacaci I, Ciardiello F, Stern DF, Gullick WJ, Salomon DS. (1997) Cripto enhances the tyrosine phosphorylation of Shc and activates mitogen-activated protein kinase (MAPK) in mammary epithelial cells. *J Biol Chem,* **272,** 3330-3335.

Karunagaran D, T. E., Beerli RR, Chen X, Graus-Porta D, Ratzkin BJ, Seger R, Hynes NE, Yarden Y. (1996) ErbB2 is a common auxiliary subunit of NDF and EGF receptors: implications for breast cancer. *EMBO Journal,* **15,** 254-64.

References

Kavanagh JJ, K. A., Freedman RS, Edwards CL, Pazdur R, Bellet R, Bayssas M, Finnegan MB, Newman BM. (1993) A Phase II trial of taxotere (RP56976) in ovarian cancer patients (pts) refractory to cisplatin/carboplatin therapy. *Proc Ann Meet Am Soc Clin Oncol,* **12.**

Kerbel RS, V.-P. A., Klement G, Rak J. (2000)'Accidental' anti-angiogenic drugs. anti-oncogene directed signal transduction inhibitors and conventional chemotherapeutic agents as examples. *Eur J Cancer,* **36,** 1248-57.

Kew TY, B. J., Pinder SE, Denley H, Srinivasan R, Gullick WJ, Nicholson RI, Blamey RW, Ellis IO. (2000) C-erbB4 protein expression in human breast cancer. *Br J Cancer,* **82,** 1163-70.

Kim YT, K. J., Lee JW. (1998) c-erbB-2 oncoprotein assay in ovarian carcinoma and its clinical correlation with prognostic factors. *Cancer Letters,* **132,** 91-97.

Klapper LN, G. S., Vaisman N, Hynes NE, Andrews GC, Sela M, Yarden Y. (1999) The erbB2/Her2 oncoprotein of human carcinomas may function solely as a shared coreceptor for multiple stroma-derived growth factors. *PNAS,* **96,** 4995-5000.

Klapper LN, K. M., Sela M, Yarden Y. (2000) Biochemical and clinical implications of the erbB/HER signalling network of growth factor receptors. *Adv Cancer Res,* **77,** 25-79.

Klapper LN, K. M., Sela M, Yarden Y. (2000) Biochemical and clinical implications of the erbB/her signalling network of growth factor receptors. *Adv Cancer Res,* **77,** 25-79.

Knowlden JM, G. J., Seery LT, Farrow L, Gullick WJ, Ellis IO, Blamey RW, Robertson JF, Nicholson RI. (1998) c-erbB3 and c-erbB4 expression is a feature of the endocrine responsive phenotype in clinical breast cancer. *Oncogene,* **17,** 1949-57.

195

References

Krane IM, L. P. (1996) NDF/heregulin induces persistence of terminal end buds and adenocarcinomas in the mammary glands of transgenic mice. *Oncogene,* **12,** 1781-8.

Kurachi H, M. K., Amemiya K, Adachi H, Hirota K, Miyake A, Tanizawa O. (1991) Importance of transforming growth factor alpha / epideraml growth factor receptor autocrine mechanism in an ovarian cancer cell line *in vivo. Cancer Research,* **51,** 5956-5961.

Langdon SP, M. W., Berchuck A. (1997) In *Biology of Female Cancers.* CRC Press, Boca Raton, Florida.

Lee H, M. N. (1998) Isolation and characterization of four alternate transcripts expressed in ovarian carcinoma-derived cell lines and normal human tissues. *Oncogene,* **16,** 3243-3252.

Lenferink, A. E., Pinkas-Kramarski, R., van de Poll, M. L., van Vugt, M. J., Klapper, L. N., Tzahar, E., Waterman, H., Sela, M., van Zoelen, E. J. and Yarden, Y. (1998) Differential endocytic routing of homo- and hetero-dimeric ErbB tyrosine kinases confers signaling superiority to receptor heterodimers. *Embo J,* **17,** 3385-97.

Lessor TJ, Y. J., Xia X, Woodford N, Hamburger AW. (2000) Ectopic expression of the erbB3 binding protein ebp1 inhibits growth and induces differntiation of human breast cancer cell lines. *J Cell Physiol,* **183,** 321-9.

Levkowitz G, W. H., Zamir E, Kam Z, Oved S, Langdon WY, Beguinot L, Geiger B, Yarden Y. (1998)c-cbl / sli-1 regulates endocytic sorting and ubiquitination of the epidermal growth factor receptor. *Genes and Development,* **12,** 3663-3674.

References

Lewis GD, L. J., McMurtrey AE, Nuijens A, Fendly BM, Bauer KD, Slikowski MX. (1996) Growth regulation of human breast and ovarian tumour cells by heregulin: Evidence for the requirement of erbB2 as the critical component in mediating heregulin responsiveness. *Cancer Research,* **56,** 1457-1465.

Lonardo F, D. M. E., King CR, Pierce JH, Segatto O, Aaronson SA, Di Fiore PP. (1990) The normal erbB2 product is an atypical receptor-like tyrosine kinase with constitutive activity in the absence of ligand. *New Biol,* **2,** 992-1003.

Lu HS, C. D., Philo JS, Zhang K, Narhi LO, Liu N, Zhang M, Sun J, Wen J, Yanagihara D, Karunagaran D, Yarden Y, Ratzkin B. (1995) Studies on the structure and function of glycosylated and nonglycosylated neu differentiation factors. *The Journal of Biological Chemistry,* **270,** 4784-4791.

Lupu R, C. M., Cho C, Harris L, Hijazi M, Perez C, Rosenberg K, Yang D, Tang C. (1996) The significance of heregulin in breast cancer tumour progression and drug resistance. *Breast Cancer Res. Treat.,* **38,** 57-66.

Lynch HT, K. W., Albano WA, Lynch JF, Biscone K, Schuelke GS, Sanberg AA, Lipkin M, Deschner EE, Mikol YB. (1985) Hereditary nonpolyposis colorectal cancer (Lynch syndromes I and II). Clinical description of resource. *Cancer,* **56,** 934-938.

Mahmoud YM, E.-S., Besser D, Nagasawa M, Nagamine Y. (1997) 12-O-Tretradecanoylphorbol-13-acetate activates the ras/extracellular signal-related kinase(Erk) signalling pathway upstream of Sos involving serine phosphorylation of Shc in NIH3T3 cells. *J Biol Chem,* **272,** 30599-30602.

Marshall, C. (1995) Specificity of receptor tyrosine kinase signalling: transient versus sustained extracellular-signal regulated kinase activation. *Cell,* **80,** 179-185.

197

References

Maurer CA, F. H., Kretschmann B, Zimmermann A, Stauffer A, Baer HU, Korc M, Buchler MW. (1998) Increased expression of erbB3 in colorectal cancer is associated with concommitant increase in the level of erbB2. *Hum Pathol, 29*, 771-7.

Mayr D, P. U., Baretton GB, Gropp M, Flens MJ, Scheper R, Diebold J. (2000) Immunohistochemical analysis of drug resistance-associated proteins in ovarian carcinomas. *Pathol Res Pract, 196*, 469-75.

McCaig, A. (1999) Expression of the erbB4 and erbB2 growth factor receptors and heregulin isoforms in ovarian cancer: correlation with clinical and pathological parameters. *unpublished data.*

McGuire WP, H. W., Brady MF, Kucera PR, Partridge EE, Look KY, Davidson M. (1995) Taxol and cisplatin (TP) improves outcome in advanced ovarian cancer (AOC) as compared to cytoxan and cisplatin (CP) (Meeting Abstract). *Proc Annu Meet Am Soc Clin Oncol, 14*, 275.

Meiners S, B. V., Naundorf H, Birchmeier W. (1998) Role of morphogenetic growth factors in metastasis of mammary carcinoma cells. *Oncogene, 16*, 9-20.

Meyer D, B. C. (1995) Multiple essential functions of neuregulin in development. *Nature, 378*, 386-390.

Miki Y, S. J., Shattuck-Eidens D, Futreal PA, Harshman K, Tavtigian S, Liu Q, Cochran C, Bennett LM, Ding W. (1994) A strong candidate for the breast and ovarian cancer susceptibility gene BRCA1. *Science, 266*, 66.

Morishige K, K. H., Amemiya K, Fujita Y, Yamamoto T, Miyake A, Tanizawa o. (1991) Evidence for the involvement of transforming growth factor alpha and epidermal growth factor receptor autocrine growth mechanism in primary human ovarian cancers in vitro. *Cancer Res, 51*, 5322-8.

198

References

Moscatello DK, H.-M. M., Godwin AK, Ramirez G, Gunn G, Zoltick, Biegel JA, Hayes RL, Wong AJ. (1995) Frequent expression of a mutant epidermal growth factor receptor in multiple human tumours. *Cancer research,* **55,** 5536-5539.

Mudge., A. (1993) New ligands for neu? The neuregulin gene encodes multiple trophic factors for neural development. *Current Biology,* **3,** 361-364.

Neijt, J. (1990) *Advanced ovarian cancer,* Gardiner-Caldwell Communications Ltd, Macclesfield, Cheshire, UK.

Niikura H, S. H., Sato S, Yajima A. (1997) Expression of epidermal growth factor-related proteins and epidermal growth factor receptor in common epithelial ovarian tumours. *Int J Gynaecol Pathol,* **16,** 60-8.

Niloff JM, K. R., Schaetzl E, Reynolds C, Bast R. (1984) CA125 antigen levels in obstetric and gynaecologic patients. *Obstet Gynaecol,* **64,** 703.

Niloff JM, K. R., Lavin PT, Malkasian GD, Berek JS, Mortel R.Whitney C, Zurawski V, Bast R. (1986) The CA125 assay as a predictor of clinical recuurence in epithelial ovarian cancer. *Am J Obstet Gynecol,* **155,** 56.

Niloff JM, K. T., Schaetzl E, Zurawski V, Knapp RC, Bast R. (1984) Elevation of serum CA125 in carcinomas of the fallopian tube, endometrium and endocervix. *Am J Obstet Gynecol,* **148,** 1057.

O-Charoenrat P, R.-E. R., Eccles S. (2000) Expression and regulation of c-erbB ligands in human head and neck squamous carcinoma cells. *Int J Cancer,* **88,** 759-65.

Okada S, K. A., Ceresa BP, Blaike P, Margolis B, Pessin JE. (1997) The 66-kDa Shc isoform is a negative regulator of the epidermal growth factor stimulated mitogen activated protein kinase pathway. *J Biol Chem,* **272,** 28042-28049.

References

Ottensmeier C, S. L., Strobel T, Druker B, Niloff J, Cannistra SA. (1996) Absence of constitutive EGF receptor activation in ovarian cancer cell lines. *Br J Cancer,* **74,** 446-52.

Ouyang X, G. T., Doherty A, Huang GC, Epstein RJ. (1999) Detection of erbB2 oversignalling in a majority of breast cancers with phosphorylation-state-specific antibodies. *The Lancet,* **353,** 1591.

Owens OJ, S. C., Leake RE, McNIchol AM. (1992) A comparison of biochemical and immunohistochemical assessment of EGFR expression in ovarian cancer. *Anticancer Research,* **12,** 1455-1458.

Ozols, R. (2000) Paclitaxel (Taxol)/carboplatin combination chemotherapy in the treatment of advanced ovarian cancer. *Semin Oncol,* **27,** 3-7.

Pegues JC, K. B., Stromberg K. (1999) ErbB receptor expression and growth response to heregulin β1 in five ovarian carcinoma cell lines. *Int J Oncology,* **14,** 1169-1176.

Peles E, B.-L. R., Tzahar E, Liu N, Wen D, Yarden Y. (1993) Cell-type specific interaction of neu differentiation factor (NDF/heregulin) with neu/her2 suggests complex ligand-receptor realtionships. *EMBO J,* **12,** 961-971.

Pinkas-Kramarski R, A. I., Yarden Y. (1997) ErbB receptors and EGF-like ligands: cell lineage determination and oncogenesis through combinatorial signalling. *J Mammary Gland Biol Neoplasia,* **2,** 97-107.

Pinkas-Kramarski R, E. R., Alroy I, Levkowitz, Lonai P, Yarden Y. (1997) Differential expression of NDF/neuregulin receptors erbB3 and erbB4 and involvement in inhibition of neuronal differentiation. *Oncogene,* **15,** 2803-2815.

200

References

Pinkas-Kramarski R, S. L., Waterman H, Levkowitz G, Alroy I, Klapper L, Lavi S, Seger R, Ratzkin BJ, Sela M, Yarden Y. (1996) Diversification of Neu differentiation factor and epidermal growth factor signalling by combinatorial receptor interactions. *EMBO J,* **15,** 2452-2467.

Pinkas-Kramarski R, S. M., Guarino BC, Wang LM, Lyass L, Alroy I, Alamandi M, Kuo A, Moyer JD, Lavi S, Eisenstein M, Ratzkin BJ, Seger T, Bacus SS, Pierce JH, Andrews GC, Yarden Y. (1998) ErbB tyrosine kinases and the two neuregulin families constitute a ligand-receptor network. *Mol. Cell. Biol.,* **18,** 6090-6101.

Plowman GD, C. J., Whitney GS, Green JM, Carlton GW, Foy L, Neubauer MG, Shoyab M. (1993) Ligand-specific activation of HER4/p180erbB4, a fourth member of the epidermal growth factor receptor family. *Proc. Natl. Acad. USA,* **90,** 1746-1750.

Prigent, S. A., Lemoine, N. R., Hughes, C. M., Plowman, G. D., Selden, C. and Gullick, W. J. (1992) Expression of the c-erbB-3 protein in normal human adult and fetal tissues. *Oncogene,* **7,** 1273-8.

Prigent SA, L. N. (1992) The type I (EGFR-related) family of growth factor receptors and their ligands. *Progress in Growth Factor Research,* **4,** 1-24.

Rajkumar T, G. W. (1994) A monoclonal antibody to the human c-erbB3 protein stimulates the anchorage-independent growth of breast cancer cell lines.*Br J Cancer,* **70,** 459-465.

Reese DM, S. D. (1997) Her2/neu signal transduction in human breast and ovarian cancer. *Stem Cells,* **15,** 1-8.

Reiter JL, M. N. (1996)A 1.8kb alternative transcript from the human epidermal growth factor receptor gene encodes a truncated form of the receptor, 4050-4057.

References

Riese DJ, S. D. (1998) Specificity within the EGF family/ErbB receptor family signaling network. *BioEssays,* **20,** 41-48.

Risch HA, J. M., Marrett LD, Howe GR. (1994) Dietary fat intake and risk of epithelial ovarian cancer. *J Natl. Canc. Inst.,* **86,** 1409.

Rossing MA, D. J., Weiss NS, Moore DE, Self SG. (1994) Ovarian tumours in a cohort of infertile women. *N. Engl. J. Med.,* **331,** 771.

Rubin SC, F. C., Federici MG, Scheiner L, Lloyd KO, Hoskins WJ. (1994) Prevalence and significance of her2/neu expression in early epithelial ovarian cancer. *Cancer,* **73,** 1456-59.

Sainsbury JRC, F. J., Needham GK, Malcolm AJ, Harris AL. (1987) Epidermal growth factor receptor status as predictor of early recurrence of and death from breast cancer. *Lancet,* **1,** 1398-1402.

Sawyer, C., Hiles, I., Page, M., Crompton, M. and Dean, C. (1998) Two erbB-4 transcripts are expressed in normal breast and in most breast cancers. *Oncogene,* **17,** 919-24.

Scambia G, B.-P. P., Ferrandina G, Distefano M, Salerno G, Romanini ME, Fagotti A, Mancuso S. (1995) Epidermal growth factor, oestrogen and progesterone receptor expression in primary ovarian cancer: correlation with clinical outcome and response to chemotherapy. *Br J Cancer,* **72,** 361-6.

Scambia G, B. P. P., Battaglia F, Ferrandina G, Baiocchi G, Greggi S, De Vincenzo R, Mancuso S. (1992). Significance of epidermal growth factor receptor in advanced ovarian cancer. *J Clin Oncol,* **10,** 529-35.

References

Scoccia B, M. L. Y., Neiderberger C, Ilekis J. (1998) Expression of the erbB family of receptors in ovarian cancer. *J Soc Gynaecol Invest*, **5**, 161-65.

Sepp-Lorenzino L, E. I., Ma Z, Cho C, Serve H, Liu F, Rosen N, Lupu R. (1996) Signal transduction pathways induced by heregulin in MDA-MB-453 breast cancer cells. *Oncogene*, **12**, 1679-1687.

Shapiro PS, V. E., Hunt AJ, Tolwinski NS, Whalen AM, McIntosh JR, Ahn NG. (1998) Activation of the MKK/ERK pathway during somatic cell mitosis: direct interactions of active ERK with kinetochores and regulation of the mitotic 3F3/2 phosphoantigen. *J Cell Biol*, **142**, 1533-1545.

Simpson, B. J., Phillips, H. A., Lessells, A. M., Langdon, S. P. and Miller, W. R. (1995) c-erbB growth-factor-receptor proteins in ovarian tumours. *Int J Cancer*, **64**, 202-6.

Simpson, B. J., Weatherill, J., Miller, E. P., Lessells, A. M., Langdon, S. P. and Miller, W. R. (1995) c-erbB-3 protein expression in ovarian tumours. *Br J Cancer*, **71**, 758-62.

Singleton TP, P. T., Oakley G, Niehans GA, Carson L, Cha SS, Strickler JG. (1994) Activation of c-erbB2 and prognosis in ovarian carcinoma. *Cancer*, **73**, 1460-66.

Skirnisdottir I, S. B., Seidal T. (2001) The growth factor receptors HER-2/neu and EGFR, their relationship and their effects on the prognosis in early stage (FIGO I-II) epithelial ovarian carcinoma. *Int J Gynaecol Cancer*, **11**, 119-29.

Slamon DJ, G. W., Jones LA, Wong SG, Keith DE, Levin WJ, Stuart SG, Udove J, Ullrich A, Press MF. (1989) Studies of the her2/neu proto-oncogene in human breast and ovarian cancer. *Science*, **244**, 707-12.

References

Slikowski MX, S. G., Akita RW, Lofgren JA, Fitzpatrick VD, Nuijens A, Fendly BM, Cerione RA, Vandlen RL, Carraway KL. (1994) Coexpression of erbB2 and erbB3 proteins reconstitutes a high affinity receptor for heregulin. *J Biol Chem,* **269,** 14661-14665.

Soltoff SP, C. K., Prigent SA, Gullick WG, Cantley LC. (1994) ErbB3 is involved in activation of phosphatidylinositol 3-kinase by epidermal growth factor. *Mol Cell Biol,* **14,** 3550-3558.

Srinivasan R, B. E., McCormick F, Thomas H, Gullick WJ. (1999) Expression of the c-erbB3/HER3 and c-erbB4/HER4 growth factor receptors and their ligands, neuregulin1 alpha, neuregulin1beta and betacellulin, in normal endometrium and endometrial cancer. *Clin Cancer Res,* **5,** 2877-83.

Srinivasan R, P. R., Hurst HC, Gullick WJ. (1998) Expression of the c-erbB4/HER4 protein and mRNA in normal human fetal and adult tissues and in a survey of nine solid tumour types. *J. Pathol.,* **185,** 236-245.

Stebbing J, C. E., O'Reilly S. (2000) Herceptin (trastuzumab) in advanced breast cancer. *Cancer Treat Rev,* **26,** 287-90.

Stromberg K, J. G., O'Connor DM, Sorensen CM, Gullick WJ, Kannan B. (1994) Frequent immunohistochemical detection of EGF supergene family members in ovarian carcinogenesis. *International Journal of Gynaecological Pathology,* **13,** 342-47.

Sundaresan, S., Roberts, P. E., King, K. L., Sliwkowski, M. X. and Mather, J. P. (1998) Biological response to ErbB ligands in nontransformed cell lines correlates with a specific pattern of receptor expression. *Endocrinology,* **139,** 4756-64.

204

References

Sweeney C, C. K. (2000) Ligand discrimination by erbB receptors: differential signalling through differential phosphorylation site usage. *Oncogene,* **19,** 5568-73.

Tai, H. (2000) Technological evaluation: Valspodar, Norvartis AG. *Curr Opin Mol Ther,* **2,** 459-67.

Tang, C. K., Goldstein, D. J., Payne, J., Czubayko, F., Alimandi, M., Wang, L. M., Pierce, J. H. and Lippman, M. E. (1998) ErbB-4 ribozymes abolish neuregulin-induced mitogenesis. *Cancer Res,* **58,** 3415-22.

Thigpen, J. (2000) Chemotherapy for advanced ovarian cancer: overview of randomized trials. *Semin Oncol,* **27,** 11-6.

Thigpen JT, B. J., Ball H, Hummel SJ, Barrett RJ. (1994) Phase II trial of paclitaxel in patients with progressive ovarian carcinoma after platinum-based chemotherapy: a gynecologic oncology group study. *J Clin Oncol,* **12,** 1748.

Tzahar E, W. H., Chen X, Levkowitz G, Karunagaran D, Lavi S, Ratzkin BJ, Yarden Y. (1996) A hierarchical network of interreceptor interactions determines signal transduction by Neu differentiation factor / neuregulin and epidermal growth factor. *Mol. Cell. Biol.,* **16,** 5276-5287.

Vadlamudi R, A. L., Talukder A, Mendelsohn J, Kumar R. (1999) Serine phosphorylation of paxillin by heregulin-beta1: role of p38 mitogen activated protein kinase. *Oncogene,* **18,** 7253-64.

Vadlamudi R, A. L., Tseng B, Costa L, Kumar R.; (1999) Transcriptional up-regulation of paxillin by heregulin in human breast cancer cells. *Cancer Research,* **15,** 2843-6.

References

Van Dam PA, L. D., Watson JV, Van Damme P, Van der Auwera JC, Shepherd JH. (1994) Expression of c-erbB2, c-myc and c-ras oncoproteins, insulin-like growth factor receptor I and epidermal growth factor receptor in ovarian carcinoma. *J Clin Pathol,* **47,** 914-19.

Van der Burg ME, H.-L. S., Foekens JA, Berns EM, Rodenburg CJ, van Putten WL, Klijn JG. (1993) The prognostic value of epidermal growth factor receptors, determined by both immunohistochemistry and ligand binding assays in primary epithelial ovarian cancer: a pilot study. *Eur J Cancer,* **29A,** 1951-7.

Van Hattum AH, P. H., Schluper HM, Hausheer FH, Boven E. (2000) New highly lipophilic camptothecin BNP1350 is an effective drug in experimental human cancer.*Int J Cancer,* **88,** 260-6.

Vecchi M, B. J., Carpenter G. (1996) Selective cleavage of the heregulin receptor erbB4 by protein kinase C activation. *J Biol Chem,* **271,** 18989-18995.

Vecchi M, C. G. (1997) Constitutive proteolysis of the erbB4 receptor tyrosine kinase by a unique and sequential mechanism. *J Cell Biology,* **139,** 995-1003.

Waterman, H., Alroy, I., Strano, S., Seger, R. and Yarden, Y. (1999) The C-terminus of the kinase-defective neuregulin receptor ErbB-3 confers mitogenic superiority and dictates endocytic routing .*Embo J,* **18,** 3348-58.

Weis FU, W. C., Campiglio M, Issing W, Ullrich A. (1997) Distinct characteristics of heregulin signals mediated by her3 or her4. *J Cell Physiology,* **173,** 187-195.

Weiss NS, L. J., Liff JM, Vollamer WM, Daling JR. (1981) Incidence of ovarian cancer in relation to the use of oral contraceptives. *Int. J. Cancer,* **28,** 669.

References

Wen D, P. E., Cupples R, Suggs SV, Bacus SS, Luo Y, Trail G, Hu S, Silbiger SN, Ben Levy R, Koski RA, Lu HS, Yarden Y. (1992) Neu differentiation factor: a transmembrane glycoprotein containing an EGF domain and an immunoglobulin homology unit. *Cell,* **69,** 559-572.

Wen D, S. S., Karunagaran D, Liu N, Cupples RL, Luo L, Janssen AM,Ben-Baruch N, Trollinger DB, Jacobsen VL, Meng S, Lu HS, Hu S, Chang D, Yang W, Yanigahara D, Koski RA, Yarden Y. (1994) Structural and functional aspects of the multiplicity of neu differentiation factors. *Molecular and Cellular Biology,* **14,** 1909-1919.

Whittemore AS, W. M., Paffenbarger R, Sarles DL, Kampert JB, Grosser S, Jung DL, Ballon S, Hendrikson M. (1988) Personal and environmental characteristics related to epithelial ovarian cancer. II Exposures to talcum powder, tobacco, alcohol and coffee. *Am. J. Epidemiology,* **128,** 1288.

Wiechen K, K. S., Dietel M. (1999) Involvement of the c-erbB2 oncogene product in the EGF-induced cell motility of SKOV3 ovarian cancer cells. *Int. J Cancer,* **83,** 409-14.

Wooster R, N. S., Mangion J, Quirk Y, Ford D, Collins N, Nguyen K, Seal S, Tran T, Averill D, Fields P, Marshall G, Narod S, Lenoir G, Lynch H, Feunteun J, Devilee P, Cornelisse C, Menko F, Daly P, Ormiston W, McManus R, Pye C, Lewis C, Cannon-Albright L, Peto J, Ponder B, (1994) Localization of a breast cancer susceptibility gene, BRCA2, to chromosome 13q12-13.*Science,* **265,** 2088.

Wosikowski K, S. D., Kops GJPL, Saceda M, Bates SE. (1997) Altered gene expression in drug-resistant human breast cancer cells*Clin. Cancer Res.,* **3,** 2405-2414.

Wrann MM, F. C. (1979) Identification of epidermal growth factor receptors in a hyperproducing epideral carcinoma cell line. *J Biol Chem,* **254,** 8083-8086.

References

Xu F, Y. Y., Fe XF, Boyer c, Mills GB, Bast RC. (1999) The outcome of heregulin-induced activation of ovarian cancer cells depends on the relative levels of her-2 and her-3 expression. *Clin Cancer Res,* **5,** 3653-60.

Xu FJ, S. S., Boyer C, O'Briant K, Whitaker R, Mills GB, Yu YH, Bast RC. (1997) Heregulin and antagonistic anti-p185(c-erbB2) antibodies inhibit proliferation but increase invasiveness of breast cancer cells that over-express p185(c-erbB2): increased invasiveness may contribute to poor prognosis. *Clin Cancer Res,* **3,** 1629-34.

YamamotoT, I. S., Akiyama T, Semba K, Nomura N, Miyajima N, Saito T, Toyoshima K. (1986) Similarity of protein encoded by the human c-erb-B2 gene to epidermal growth factor receptor. *Nature,* **319,** 230-234.

Yazlovitskaya EM, D. R., Persons DL. (2001) Prolonged wild-type p53 protein accumulation and cisplatinum resistance. *Biochem Biophys Res Commun,* **283,** 732-7.

Zhang D, S. M., Mark M, Frantz G, Akita R, Sun Y, Hillan K, Crowley C, Brush J, Godowski PJ. (1997) Neuregulin-3 (NRG3): anovel neural tissue-enriched protein that binds and activates erbB4. *Proc. Natl. Acad. Sci. USA.,* **94,** 9562-9567.

Zrihan-Licht S, F. Y., Settleman J, Schinkmann K, Shaw L, Keydar I, Avraham S, Avraham H. (2000) RAKTK/Pyk2 tyrosine kinase mediates the association of p190 RhoGAP with RasGAP and is involved in breast cancer cell invasion. *Oncogene,* **19,** 1318-28.

References